JOURNAL OF BIOLOGICAL REGULATORS & HOMEOSTATIC AGENTS Vol. 26, no. 2, 165-170 (2012)

*EDITORIAL*

# NEW INSIGHTS INTO THE PATHOGENESIS OF CUTANEOUS AUTOIMMUNE DISORDERS

A. CHIRICOZZI[1,2], S. ZHANG[3], A. DATTOLA[1], M.V. CANNIZZARO[1], M. GABELLINI[1], S. CHIMENTI[1] and S.P. NISTICÒ[1]

*[1]Department of Dermatology, University of Rome Tor Vergata, Rome, Italy; [2]Laboratory for Investigative Dermatology, The Rockefeller University, New York, USA; [3]Ronald O. Perelman Department of Dermatology, New York University Langone Medical Center, New York, NY, USA*

*Received February 13, 2012 – Accepted April 5, 2012*

The first two authors contributed equally to this work

**T helper 17 (Th17) cells are characterized by the secretion of IL-17, a proinflammatory cytokine. They represent a newly described T helper subpopulation that is distinct from Th1 and Th2 lineages. Because of their pleiotropic activity on fibroblasts, keratinocytes, endothelial cells, neutrophils and memory T cells, Th17 cells are thought to be crucial in mediating tissue inflammation and autoimmunity. Autoimmune diseases were classically considered as Th1-mediated disorders such as rheumatoid arthritis or 'mixed' Th1/Th2 diseases such as inflammatory bowel diseases, systemic lupus erythematosus, bullous diseases, but new evidence suggests the deep involvement of Th17 cells in their pathogenesis that, potentially, may address a selective therapeutic approach targeting the IL23/Th17 pathway. This review summarizes the current knowledge of the pathogenic contribution of Th17 cells in select cutaneous autoimmune disorders, including lupus erythematosus, scleroderma, dermatomyositis, bullous pemphigoid and *pemphigus vulgaris*.**

*Involvement of Th17 in immune-mediated diseases*

IL-17A-producing CD4 T cells (Th17) have been classified as distinct from Th1 and Th2 subpopulations (1). Although they are considered part of the adaptive arm of the immune system, Th17 cells also regulate the innate immune system in the skin by, (i) promoting anti-microbial peptides (AMPs) production by keratinocytes, (ii) increasing memory T cells trafficking, infiltration and activation (iii) inducing keratinocyte production of CCL20, and (iv) enhancing neutrophil recruitment and survival by inducing the production of CXCL8 (IL-8) and granulocyte- macrophage colony-stimulating factor (GM-CSF) (2-6).

Moreover, IL-17 stimulates the expression of intercellular adhesion molecules (ICAM-1) in epithelial cells and of chemokines and cytokines such as tumor necrosis factor α (TNF α), IL1β, IL6, CXC chemokine family, monocyte chemoattractant protein-1 (MCP-1), granulocyte colony-stimulating factor (G-CSF) and granulocyte macrophage colony-stimulating factor (GM-CSF) by innate immune cells (7, 8).

Due to these broad effects on various immune

*Key words: Th17, IL-17, scleroderma, lupus erythematosus, pemphigus, pemphigoid*

*Mailing address:* Dr. Andrea Chiricozzi,
Department of Dermatology,
University of Rome Tor Vergata,
Viale Oxford 81,
00133 Rome, Italy
Tel.: +39 06 20902743 Fax: +39 06 20902742
e-mail: chiricozziandrea@gmail.com



0393-974X (2012)

**DISCLOSURE: ALL AUTHORS REPORT NO CONFLICTS OF INTEREST RELEVANT TO THIS ARTICLE.**

cell types, the IL-23/Th17 axis plays a critical protective role in the resolution of extracellular bacteria (*Klebsiella pneumoniae*, *Streptococcus pneumoniae*), parasitic (*Toxoplasma gondii*) and fungi (*Candida albicans*) infections (9-11).

Because of their pleiotropic activity on fibroblasts, keratinocytes, endothelial cells, neutrophils and memory T cells, Th17 cells are thought to be crucial in mediating tissue inflammation.

Interestingly, the development of many immune disorders may be attributed to IL-17-producing T cells. Experimental models of inflammatory and autoimmune diseases show Th17 cells are likely involved in multiple sclerosis, Crohn's disease, ulcerative colitis, cystic fibrosis, rheumatoid arthritis and autoimmune encephalomyelitis (6, 12-14). For instance, Th17 cells seem to be responsible for autoimmune encephalomyelitis pathology, since IL-17-deficient mice as well as IL-23p19 knockout mice do not develop the disease (13). Moreover, the adoptive transfer of Th17 cells into naïve mice induced the development of autoimmune encephalomyelitis (14). Experimental rheumatoid arthritis showed IL-17 as key mediator of bone erosion and cartilage degradation as demonstrated by the cartilage damage induced by a single injection of IL-17 in healthy mice knee. Supporting this observation, IL-17A antibodies decreased the experimental, collagen-induced arthritis inducing a reduction of joint damage and histologic destruction of cartilage and bone (15). Clinical studies found increased IL-17 levels in sera and inflamed mucosae of patients with inflammatory bowel diseases (16). Animal models support a role for the IL-23/IL-17 axis, since IL-10/IL23p19-knockout mouse does not develop spontaneous colitis (selective lack of Th17 cells), whereas it occurs in IL-10/IL12p35-knockout mouse (selective lack of Th1 cells) (17).

Genetic studies found polymorphisms in the IL-23R that have been associated with the development of the disease (18). Polymorphisms within the IL-23R gene sequence are also associated with disease susceptibility to psoriasis and multiple sclerosis (19-21). Moreover, in psoriasis, sequence variants of both IL-23p40 and IL-23p19 subunits have also been shown to correlate with the development of disease (20, 21).

Further studies detected high expression levels of IL-17 and IL-17-expressing CD4+ T cells in lesional tissue, fluids and serum from patients with multiple sclerosis, rheumatoid arthritis, systemic lupus erythematosus, Behcet's disease, psoriasis, scleroderma and lupus erythematosus (22-25).

In addition to autoimmune diseases, Th17 cells also seem to mediate a typical Th2-related disease, asthma, since high expression levels of IL-17A were detected in the peripheral blood, sputum, and airways of asthmatic patients, which correlate with the degree of bronchial hyper-reactivity. These observations made on humans are supported by experimental models for asthma, wherein, inflammation and destruction in lung epithelium is mediated by IL-17, which induces recruitment and activation of neutrophils (26).

These findings do not find confirmation in other mouse models of asthma, in which IL-17 seems to be protective, reducing eosinophilia and bronchial hyper-reactivity in the chronic phase.

This review briefly reports new insights in the pathogenesis of select skin autoimmune diseases, with particular focus on the pathogenic role of Th17 cells.

*Systemic lupus erythematosus*

Lupus erythematosus is an autoimmune condition of unclear etiology comprising a broad clinical spectrum from exclusively cutaneous manifestations (discoid lupus erythematosus, DLE), to subacute lupus erythematosus (SCLE), to multi-organ involvement in systemic lupus erythematosus (SLE). The diagnostic criteria for SLE include a number of muco-cutaneous manifestations such as photosensitivity, malar rash, discoid lesions, and oral ulcers (27).

Pathogenically, SLE is characterized by autoreactive CD4+ T cells that recognize self-antigens as "non-self" and mount both a humoral and a cytotoxic response. Autoantibody production and subsequent deposition of immune complexes caused by a deficient clearance of apoptotic bodies lead to widespread inflammation and tissue injury. Current thoughts suggest a shared role among Th1, Th2, and Th17 (28).

These theories derive from recent studies that investigated the cytokine profile of patients with SLE and detected high serum levels of IL-17 in their

plasma (29, 30). Tanasescu et al. observed IL-17A expression in the DLE, SCLE and SLE skin, similar to the high levels observed in psoriatic skin (30).

However, the role of Th17/IL-17 in SLE remains controversial as suggested by some authors who did not detect an upregulation of Th17 pathway (31, 32). Furthermore, Th17 cells have not been reported to be involved in the clearance of apoptotic bodies. Nonetheless, both experimental and clinical studies strongly suggest Th17 cells have a role in autoimmune disease pathogenesis. Therefore, the correlation between Th17 cells and lupus warrants further investigation.

*Scleroderma*

Since Th17 cells appear to play a role in autoimmune diseases, their involvement has also been proposed in scleroderma. Scleroderma is a chronic, systemic disorder characterized by an inflammatory process that promotes connective fibrosis with consequent stiffening of the skin, blood vessels, and internal organs.

Although the exact pathogenesis of the disease is unknown, it is thought that autoantibodies trigger an inflammatory cascade resulting in fibroblast deposition of collagen fibers and extracellular matrix. This fibrotic process is likely induced by various cytokines including TGF-β, connective tissue growth factor (CTGF), IL13 and IL-4 (33).

The production of antibodies directed against self-antigens is driven by autoreactive T cells showing a Th2-predominant profile. However, the Th17 cells have been postulated as key-players in the pathogenic inflammatory circuits because increased IL-17 expression levels were discovered in the peripheral blood, and the sclerotic lesions of the skin and lungs of scleroderma patients (34, 35). IL-17 may contribute to the pathogenic picture by inducing fibroblast proliferation and synthesis of cytokines IL-6, IL-8, CXCL1 and TNFα in scleroderma fibroblasts (36).

Additionally, IL-17 acts on endothelial cells and stimulates neutrophil recruitment, which is an important feature of pulmonary manifestations in scleroderma. Thus, IL-17 may play a prominent role in the early stages of disease.

*Dermatomyositis*

Dermatomyositis is an autoimmune myopathy featured by the presence of autoantibodies, T-cell myocytotoxicity, and the upregulation of major histocompatibility complex (MHC) class I antigens in muscle cells. Tissue inflammation is mainly driven by TNF-α, IL-1, IL-6, IFN-γ, but also IL17-producing T cells have been detected in muscle biopsy. Indeed, IL-17 has been reported to act on muscle cells in synergy with other proinflammatory cytokines including IL-1 and TNF-α, inducing muscle tissue damage and dysfunction (37).

Relevant infiltrates of IFN-γ–producing cells and scattered presence of IL-17–producing T cells in inflamed muscle tissue suggest a crucial role of Th1 with a minor contribution of the Th17 pathway (38).

*Pemphigus vulgaris*

In recent years, Th17 cells were reportedly associated with other bullous diseases such as *Pemphigus vulgaris* (PV), *Pemphigus foliaceum* (PF) and bullous pemphigoid (BP) (39-40) characterized by the presence of autoantibodies directed against various adhesion molecules localized on the cell surface of keratinocytes.

PV is a rare muco-cutaneous bullous disease characterized by high titers of antibodies anti-Desmoglein 1 and 3, and dermal infiltration of both CD4+ and CD8+ T cells. PF is considered a variant of PV, caused by anti-Desmoglein 1 antibodies and characterized by blister formation within the granular layer. Th17 infiltration was found in lesional skin of patients affected by PV and PF, although detection of Th17 did not correlate with either auto-Ig titers or disease severity (39).

While the presence of Th17/IL23 axis in blood and skin of patients suffering from PV, PF or BP has been reported anecdotally, clear evidence implicating Th17 in the pathogenesis of bullous diseases is lacking. Thus, further studies may be needed to fully clarify their pathogenic role.

*Bullous pemphigoid*

Bullous pemphigoid is a blistering autoimmune disorder characterized by the presence of autoantibodies directed against two major self-antigens: the BP antigen 180 (BP180) and the BP antigen 230 (BP230), representing two components of the hemidesmosomes. BP is currently believed to be Th1/Th2 cell mediated disease with Th2

dominance as the humoral response is sustained by Th2 cells, although, the presence of IL-17–producing T cells in lesional skin and blood of BP patients suggests an additional involvement of the Th17 subset. Nevertheless, the presence of Th17 did not correlate with either auto-Ig titers or disease severity (39).

IL-17 is also thought to be involved in the pathogenesis of BP because of (i) its proinflammatory effects, (ii) its capability to recruit and activate neutrophils (which are a major component of the infiltrate in the skin lesions of BP), (iii) and its contribution to Th2 cell activation, eosinophil accumulation and IgE production, which are all features that are characteristic of this disease.

## CONCLUSION

Although future research evaluating the role of Th17 pathway in autoimmune disorders is still necessary, mounting evidence does suggest that Th17 cells play an important role in the pathogenesis of a variety of diseases. Thus, targeting the IL23/Th17 pathway may represent an important therapeutic strategy for many autoimmune diseases.

## REFERENCES

1. Harrington LE, Mangan PR, Weaver CT. Expanding the effector CD4 T-cell repertoire: the Th17 lineage. Curr Opin Immunol 2006; 18:349-56.
2. Chiricozzi A, Guttman-Yassky E, Suárez-Fariñas M, Nograles KE, Tian S, Cardinale I, Chimenti S, Krueger JG. Integrative responses to IL-17 and TNF-α in human keratinocytes account for key inflammatory pathogenic circuits in psoriasis. J Invest Dermatol 2011; 131(3):677-87.
3. Nograles KE, Zaba LC, Guttman-Yassky E, et al. Th17 cytokines interleukin (IL)-17 and IL-22 modulate distinct inflammatory and keratinocyte-response pathways. Br J Dermatol 2008; 159(5):1092-102.
4. Laan M, Cui ZH, Hoshino H, Lötvall J, Sjöstrand M, Gruenert DC, Skoogh BE, Lindén A. Neutrophil recruitment by human IL-17 via C-X-C chemokine release in the airways. J Immunol 1999; 162 (4):2347-52.
5. Iwakura Y, Nakae S, Saijo S, Ishigame H. The roles of IL-17A in inflammatory immune responses and host defense against pathogens. Immunol Rev 2008; 226:57-79.
6. McAllister F, Henry A, Kreindler JL, et al. Role of IL-17A, IL-17F, and the IL-17 receptor in regulating growth-related oncogene-alpha and granulocyte colony-stimulating factor in bronchial epithelium: implications for airway inflammation in cystic fibrosis. J Immunol 2005; 175(1):404-12.
7. Albanesi C, Cavani A, Girolomoni G. IL-17 is produced by nickel-specific T lymphocytes and regulates ICAM-1 expression and chemokine production in human keratinocytes: synergistic or antagonist effects with IFN-gamma and TNF-alpha. J Immunol 1999; 162:494-502.
8. Fossiez F, Djossou O, Chomarat P, et al. T cell interleukin-17 induces stromal cells to produce proinflammatory and hematopoietic cytokines. J Exp Med 1996; 183(6):2593-603.
9. Kelly MN, Kolls JK, Happel K, Schwartzman JD, Schwarzenberger P, Combe C, Moretto M, Khan IA. Interleukin-17/interleukin-17 receptor-mediated signaling is important for generation of an optimal polymorphonuclear response against Toxoplasma gondii infection. Infect Immun 2005; 73:617-21.
10. Ye P, Rodriguez FH, Kanaly S, et al. Requirement of interleukin 17 receptor signaling for lung CXC chemokine and granulocyte colony-stimulating factor expression, neutrophil recruitment, and host defense. J Exp Med 2001; 194 (4):519-27.
11. Huang W, Na L, Fidel PL, Schwarzenberger P. Requirement of interleukin-17A for systemic anti-Candida albicans host defense in mice. J Infect Dis 2004; 190(3):624-31.
12. Chao CC, Chen SJ, Adamopoulos IE, et al. Anti-IL-17A therapy protects against bone erosion in experimental models of rheumatoid arthritis. Autoimmunity 2011; 44(3):243-52.
13. Cua DJ, Sherlock J, Chen Y, et al. Interleukin-23 rather than interleukin-12 is the critical cytokine for autoimmune inflammation of the brain. Nature 2003; 421(6924):744-8.
14. Langrish CL, Chen Y, Blumenschein WM, et al. IL-23 drives a pathogenic T cell population that induces autoimmune inflammation. J Exp Med 2005; 201(2):233-40.
15. Lubberts E, Koenders MI, Oppers-Walgreen B,

van den Bersselaar L, Coenen-de Roo CJ, Joosten LA and van den Berg WB. Treatment with a neutralizing anti-murine interleukin-17 antibody after the onset of collagen- induced arthritis reduces joint inflammation, cartilage destruction, and bone erosion. Arthritis Rheum 2004; 50: 650-59.

16. Fujino S, Andoh A, Bamba S, Ogawa A, Hata K, Araki Y, Bamba T, Fujiyama Y. Increased expression of interleukin 17 in inflammatory bowel disease. Gut 2003; 52(1):65-70.
17. Yen D, Cheung J, Scheerens H et al. IL-23 is essential for T cell-mediated colitis and promotes inflammation via IL-17 and IL-6. J Clin Invest 2006; 116:1310-6.
18. Cho JH. The genetics and immunopathogenesis of inflammatory bowel disease. Nat Rev Immunol 2008; 8(6):458-66.
19. Begovich AB, Chang M, Caillier SJ, Lew D, Catanese JJ, Wang J, Hauser SL, Oksenberg JR. The autoimmune disease-associated IL12B and IL23R polymorphisms in multiple sclerosis. Hum Immunol 2007; 68(11):934-7.
20. Ca M, Schrodi SJ, Chang M, et al. A large-scale genetic association study confirms IL12B and leads to the identification of IL23R as psoriasis-risk genes. Am J Hum Genet 2007; 80 (2):273-90.
21. Nair RP, Duffin KC, Helms C, et al. Genome-wide scan reveals association of psoriasis with IL-23 and NF-kappaB pathways. Nat Genet 2009; 41(2):199-204.
22. Wong CK, Ho CY, Li EK, Lam CW. Elevation of proinflammatory cytokine (IL-18, IL-17, IL-12) and Th2 cytokine (IL-4) concentrations in patients with systemic lupus erythematosus. Lupus 2000; 9(8):589-93.
23. Matusevicius D, Kivisäkk P, He B, Kostulas N, Ozenci V, Fredrikson S, Link H. Interleukin-17 mRNA expression in blood and CSF mononuclear cells is augmented in multiple sclerosis. Mult Scler 1999; 5(2):101-4.
24. Hamzaoui K, Hamzaoui A, Guemira F, Bessioud M, Hamza M, Ayed K. Cytokine profile in Behcet's disease patients. Relationship with disease activity. Scand J Rheumatol 2002; 31:205-10.
25. Lowes MA, Kikuchi T, Fuentes-Duculan J, Cardinale I, Zaba LC, Haider AS, Bowman EP, Krueger JG. Psoriasis vulgaris lesions contain discrete populations of Th1 and Th17 T cells. J Invest Dermatol 2008; 128 (5):1207-11.
26. Holgate ST.Pathogenesis of asthma. Clin Exp Allergy 2008; 38(6):872-97.
27. Ruiz-Irastorza G, Khamashta MA, Castellino G, Hughes GR. Systemic lupus erythematosus. Lancet 2001; 357:1027-32.
28. Dolff S, Bijl M, Huitema MG, Limburg PC, Kallenberg CG, Abdulahad WH. Disturbed Th1, Th2, Th17 and T (reg) balance in patients with systemic lupus erythematosus. Clin Immunol 2011; 141(2):197-204.
29. Doreau A, Belot A, Bastid J, et al. Interleukin 17 acts in synergy with B cell-activating factor to influence B cell biology and the pathophysiology of systemic lupus erythematosus. Nat Immunol 2009; 10(7):778-85.
30. Tanasescu C, Balanescu E, Balanescu P, et al. IL-17 in cutaneous lupus erythematosus. Eur J Intern Med 2010; 21 (3):202-7.
31. Kurasawa K, Hirose K, Sano H, Endo H, Shinkai H, Nawata Y, Takabayashi K, Iwamoto I. Increased interleukin-17 production in patients with systemic sclerosis. Arthritis Rheum 2000; 43 (11):2455-63.
32. Cheng F, Guo Z, Xu H, Yan D, Li Q. Decreased plasma IL22 levels, but not increased IL17 and IL23 levels, correlate with disease activity in patients with systemic lupus erythematosus. Ann Rheum Dis 2009; 68 (4):604-6.
33. Connolly MK. Systemic Sclerosis (Scleroderma) and Related Disorders. Chapter 44 in Dermatology 2nd Edition, Bolognia JL, Jorizzo JL, Rapini RP. 1998; p. 1319-44.
34. Rodríguez-Reyna TS, Furuzawa-Carballeda J, Cabiedes J, Fajardo-Hermosillo LD, Martínez-Reyes C, Díaz-Zamudio M, Llorente L. Th17 peripheral cells are increased in diffuse cutaneous systemic sclerosis compared with limited illness: a cross-sectional study. Rheumatol Int 2011 Jul 26. [Epub ahead of print]
35. Deleuran B, Abraham DJ. Possible implication of the effector CD4+ T-cell subpopulation TH17 in the pathogenesis of systemic scleroderma. Nat Clin Pract Rheumatol 2007; 3(12):682-3.
36. Katz Y, Nadiv O, Beer Y. Interleukin-17 enhances tumor necrosis factor alpha-induced synthesis of interleukins 1,6, and 8 in skin and synovial

fibroblasts: a possible role as a “fine-tuning cytokine” in inflammation processes. Arthritis Rheum 2001; 44 (9):2176-84.
37. Tournadre A, Miossec P. Interleukin-17 in Inflammatory Myopathies. Curr Rheumatol Rep 2012; 14(3):252-6.
38. Tournadre A, Porcherot M, Chérin P, Marie I, Hachulla E, Miossec P. Th1 and Th17 balance in inflammatory myopathies: interaction with dendritic cells and possible link with response to high-dose immunoglobulins. Cytokine 2009; 46(3):297-301.
39. Arakawa M, Dainichi T, Ishii N, et al. Lesional Th17 cells and regulatory T cells in bullous pemphigoid. Exp Dermatol 2011; 20(12):1022-4.
40. Arakawa M, Dainichi T, Yasumoto S, Hashimoto T. Lesional Th17 cells in pemphigus vulgaris and pemphigus foliaceus. J Dermatol Sci 2009; 53 (3):228-31.

JOURNAL OF BIOLOGICAL REGULATORS & HOMEOSTATIC AGENTS Vol. 26, no. 2, 171-179 (2012)

*EDITORIAL*

# NEW INSIGHTS ON THE ROLE OF T CELLS IN THE PATHOGENESIS OF CELIAC DISEASE

R. CIANCI, D. PAGLIARI, R. LANDOLFI, S. FROSALI, A. COLAGIOVANNI, G. CAMMAROTA and F. PANDOLFI

*Department of Internal Medicine, Catholic University, Rome, Italy*

*Received January 12, 2012 – Accepted March 26, 2012*

**Despite intense investigation, the pathogenetic mechanisms leading to villous atrophy in Celiac disease (CD) remain not completely understood. The traditional interpretation is that CD4 cells recognize gliadin and develop an inflammatory reaction by production of Th1 cytokines at the mucosa level inducing CD8 cells to kill mucosal cells by a direct cytotoxic mechanism or by Fas-mediated apoptosis. Recent data, however, have shown that novel CD4 T-cells subpopulations, CD4+ CD25+ Regulatory T cells (Tregs) and Th17 cells also play a role in the ongoing inflammatory process. Both Tregs and Th17 cells are increased in active CD. However, because Tregs have a suppressive activity on inflammation, their role is controversial. In this editorial we discuss these recent findings and the hypothesis formulated to explain the increase of Tregs. To understand the pathogenesis of tissue damage of CD, we have focused on the duodenal micro-environment, introducing the new concept of "immunological niche" that in CD summarizes cellular and cytokine interactions in duodenal mucosa, where a high plasticity of T-cell subsets is present. CD is often complicated by T-cell lymphomas, especially in cases of refractory CD.**

Celiac disease (CD) is an enteropathy resulting in villous atrophy. CD is induced by an abnormal response to gliadin in genetically susceptible individuals expressing HLA-DQ2 or HLA-DQ8 (1) and other non-HLA genes (2). Although approximately 1% of the population is affected by CD, most affected individuals remain undiagnosed. This probably reflects the fact that patients with CD can manifest a spectrum of intestinal and/or extraintestinal symptoms and, in some cases, they can be relatively asymptomatic.

Despite intensive investigation, the mechanisms leading to villous atrophy remain not completely understood. To date, several studies have pointed to the role of activated CD8 cells expressing either the alpha-beta TCR or NK-associated markers. The activation of these cells induces expression of Fas (CD95), a potent inducer of apoptosis (3).

Pro-inflammatory Th1 cytokines, such as IFN-gamma, IL-12, IL-15, IL-18, IL-21 and IL-23, are also involved in the ongoing inflammatory process. Perforin-mediated killing by CD8 cells has also been reported (4). As Kagnoff put it, following activation, intraepithelial lymphocytes (IELs) from patients change from being typical antigen-specific T cells to being NK-like cells able to mediate epithelial cell damage. Upregulation of IL-15 contributes to altered signaling properties of CD8+ IEL-cells (5). Others have proposed that IL-15 mediates inflammation because CD patients present a hypersensitivity to IL-15 (6). In 2002, Sollid commented that our knowledge of the effector mechanisms that produce the celiac

*Key words: celiac disease, T lymphocytes, Treg, Th17, cytokines, immunological niche*

*Mailing address:* Prof. Franco Pandolfi,
Institute of Internal Medicine,
Catholic University,
Largo Francesco Vito, 1
00168, Rome, Italy
Tel: +39 0630154914 Fax: +39 063386446
e-mail: pandolfi@rm.unicatt.it



0393-974X (2012)

lesion is rather limited, although mostly CD8 cells are expanded in CD (3). In healthy individuals, intraepithelial CTLs express the inhibitory receptor CD161 and low levels of the activating receptors NKG2D and CD94–NKG2C89,91,92. By contrast, intraepithelial CTLs from patients with CD lose their expression of the inhibitory receptor CD94–NKG2A92 and acquire high levels of expression of the activating receptors NKG2D90 and CD94–NKG2C92 (3). Whatever cells may be involved in the delivery of the final tissue damage, the initial recognition of gliadin peptide is performed by CD4 cells. More in detail, Qiao et al. have shown that post-translational modification of the antigen is a key element in the pathogenesis and functional testing of the residue in the DQ2-alpha-II peptide poses constrains on the TCR structure in which the conserved Arg residue is a critical element. These data suggest that a non-germline encoded part of TCR is central in recognition of a post-translationally modified residue (7).

The present model suggests gliadin recognition by CD4 cells. This is followed by a leading role of activated CD8 cells in the pathogenesis of tissue damage in CD. CD8 cells may induce inflammation and villous atrophy by several mechanisms, including cytokines production or cell killing by both Fas mediated apoptosis (8) or perforin (9). Though T-cells are the key elements in the induction and progression of CD, their activation must be preceded by an engagement/activation of the innate immune system. The role of resident professional antigen-presenting cells is indeed essential for antigen recognition and T cell activation in CD. This function is operated by tissue myeloid-derived cells (usually dendritic cells) which process antigen and deliver the appropriate co-stimulatory signal to T-cells.

*Tregs and Th17cells: new CD4 agonists in CD pathogenesis*

CD4 cells have been considered for a long time as T cells involved in providing help in antibody production or CD8-mediated functions. Heterogeneity among CD4 cells was reported years ago (10, 11). Later, heterogeneity among CD4 cell was described when it was shown that CD4 cells can secrete different patterns of cytokines: pro-inflammatory cytokines and anti-inflammatory cytokines. The Th1 pattern is increased in CD (3). More recently two novel CD4 subpopulations were described: Tregs and Th17 cells (12). In brief, Tregs are suppressive, while Th17 cells have strong pro-inflammatory activities (13).

Data on Tregs and Th17 cells in CD are still limited. Both Tregs (14) and Th17 cells appear to be increased in active CD (15-16) while others have shown upregulation of IL-17A in active CD (17). Localization of these new populations is still poorly understood. Anecdotal reports show the localization of both Tregs and Th17 cells is in the lamina propria (LP) where most of the Th1 activity is also reported (18, 19).

CTLA-4 is an important negative regulator of T-cell activation and proliferation and is constitutively expressed on Tregs (13), interacting with B7 molecules on antigen-presenting cells. It is therefore a plausible candidate as a susceptibility gene in diseases with T-cell-mediated pathogenesis. The study by Simone et al. provides the first evidence that serum CTLA-4 levels are elevated in CD patients and correlate with disease activity and may be involved in the pathogenesis (20). A common CTLA-4 haplotype is associated with CD because of the key role of CTLA-4 in regulating T-cell-mediated inflammatory responses (21). Moreover, linkage and association of CD with CTLA4-ICOS is well documented (22).

Increased numbers of Tregs are intriguing because of their anti-inflammatory activity. To explain this paradox, several mechanisms have been proposed: it has been proposed that effector T lymphocytes from active CD become resistant to suppression by Tregs. This resistance might cause loss of tolerance to gluten (23). On the other hand, Peluso et al. suggested that IL-21 may render CD4+/CD25-negative T cells resistant to Tregs-mediated suppression (24). This result questions the role of IL-21 in disease pathogenesis since it is not clear whether this generally pro-inflammatory cytokine plays such role in CD or rather, as suggested by Peluso et al., in CD it results in down regulation of Tregs.

Others suggest that Tregs are induced *in situ* by gliadin, but their suppressor activity may be impaired by IL-15 (19). Recently, it has been shown that IL-15 not only has a pleiotropic role at the interface

between innate and adaptive immunity in CD, but also exerts effects interfering with anti-inflammatory pathways that are normally activated in the small intestinal mucosa by the cytokine TGF- beta1. Impairment of TGF-beta-mediated signalling by IL-15 might promote and sustain intestinal inflammation in celiac disease (25).

It has been previously shown that IL-15 is the major mediator of the innate immune response and cooperates with active epidermal growth factor (EGF) to alter vescicular trafficking. Concluding that both IL-15 and EGFR have a role in the gliadin-induced proliferation of epithelial cells one of the hallmarks of CD (26).

In conclusion, the role of two pro-inflammatory cytokines (IL-15 and IL-21) is still poorly defined in CD pathogenesis. These cytokines, initially thought to participate in augmenting the ongoing inflammatory process, were later proposed to impair T-reg suppressor activity.

The functional role of Th17 cells is still ill-defined as well. The study by Monteleone et al. showed increased numbers of Th17 cells, but, as pointed out by the authors, it was not designed to measure their function (16). Therefore, the role of these cells is not clarified. Several studies have shown the role of Th17 cells in increasing inflammatory responses in diseases. However, these authors also suggest that IL-17A may act as counter-regulatory molecules that limit the detrimental effects of Th1 cytokines. They also reported that IL-17A is regulated by IL-21, since IL-21 blockade by neutralizing anti IL-21 antibodies reduced IL17A expression of active CD biopsy. However, these data need to be confirmed because of a conflicting report by Sollid's group showing that HLA-Q2-restricted gluten reactive T cells produce IL-21 but not IL-17 or IL-22 (27). One possible explanation for these controversial data may be that IL-17A was found by Monteleone et al. on CD4+ CD8+ cells, suggesting a more immature T-cell subset, while gluten reactive T cells described by Sollid's group belonged to the more mature CD4+ phenotype (16).

On the other hand, production of IL-17 and IL-23 has been reported by IL-15-differentiated dendritic cells (CD14+ APC ) in response to pepsin-trypsin digested gliadin and supports Th17 responses to gliadin (6).

*Immunological niche*

We can consider CD as a model, in which several actors play a role in the immunopathogenetic mechanisms of damage. These include Tregs, Th17 cells, others CD4+ cells, CD8+ CTLs and other inflammatory cells present at tissue level, furthermore the cytokines play a crucial and sometimes inconsistent role in modulation of T-cell function.

Therefore the CD model may also be used to understand the complex regulatory stimuli that modulate the overall immune response at the tissue level in other autoimmune disorders.

Cytokines and inflammatory processes have been studied widely in peripheral blood, but the most important pathogenetic events occur at the tissue level, therefore, studies of Tissue-infiltrating lymphocytes (TILs) are of foremost importance (28).

The differentiation of naïve CD4 T cells into lineages with distinct effector functions was considered to be an irreversible event. However, the discovery of other T-cell subpopulations than Th1 and Th2, such as Tregs and Th17 cells, has led to a rethinking of the notion that helper T-cell subsets represent irreversibly differentiated endpoints. Accumulating evidence suggests that CD4 T cells are more plastic than previously appreciated. It appears that expression of FoxP3 by Tregs or IL-17 by Th17 cells may not be stable and that there is a great degree of flexibility in their differentiation options (29).

The possibility of peripheral plasticity of immune cells into several subpopulations, further underlines the key importance of tissue micro-environment, in which the cytokine-cocktails can modulate and regulate T-cell proliferation and differentiation. According to its important role in the physiology of the immune system, tissue micro-environment, characterized by the presence of T cells, B cells, APCs, other inflammatory cells and cytokines, can be considered as a specific anatomo-physiologic location that orchestrates the differentiation of the immune system, regulating inflammatory and anti-inflammatory processes.

In accordance with the distribution of T cells discussed above, we propose to consider the duodenal mucosa as an "immunological niche", i.e., a definite anatomo-functional region that hosts

the components of a complex immune functional tissue. Immunological niche plays a direct role in the homeostasis of local immune system, regulating inflammation, apoptosis, immune T-cell differentiation, peripheral tolerance and anergy.

The concept of "niche" was first formulated by Schofield, in the 1970s, defining the "haematopoietic stem cell niche" as a region within the bone marrow containing functional cell types that can maintain haematopoietic stem cell potency throughout life (30). Haematopoietic stem cell niche, such as immunological niche just described, is a specialized microenvironment composed by numerous cell types and a plethora of signals that dictate their behaviour in respect to homeostatic requirements and exogenous stresses in a complicated picture, with functional crosstalk between cells (31). It constitutes a basic unit of tissue physiology, integrating signals that mediate the balanced cellular response to the needs of organisms (32). Specific microenvironmental cues delivered from tissues are likely to determine the commitment to either lineage and to affect the balance between regulation and inflammation in the intestine (33).

The complex functional and cellular structure of the immunological niche of duodenal mucosa in CD includes pro-inflammatory cytokines, anti-inflammatory cytokines, gluten-specific naïve and memory T cells, Tregs and Th17 cells. The inflammatory environment in the intestinal mucosa of patients with CD is characterized by several distinct types of T cells. However, herein we focus our attention mainly on Tregs and Th17 cells.

Tregs perform immunosuppressive functions. Cytokines involved in Tregs' activity are: IL-10, TGF-beta and IL-35. IL-35 is a novel member of the IL-12 family, that comprises also IL-27 (34).

The role of antigen trigger is also present at tissue level. Gliadin antigens are involved in generating local inflammation and in naïve and memory T-cell recruitment. This complex cascade of events starts the immunopathogenetic mechanisms of tissue damage.

Gliadin-specific Th17 cells are present in the mucosa of CD patients. Th17 cells are generally believed to be proinflammatory cells. However, in CD mucosa, Th17 cells play a more complex role. In fact, they produce proinflammatory cytokines (IL-17, IFN-gamma, IL-21) but also mucosa-protective IL-22, IL-27 and regulatory TGF-beta. This last cytokine actively modulates IL-17A production by T cells in the celiac mucosa (18).

There is a close relationship between Tregs and Th17 cells. TGF-beta is essential for the generation of both cells. TGF-beta orchestrates Tregs and Th17 cell differentiation in a concentration-depended manner. At low concentration, TGF-beta synergizes with IL-6 and IL-21 to promote IL-23R expression, favouring Th17 cell differentiation. On the other hand, high concentrations of TGF-beta represses IL-23R expression and favours FoxP3+ Tregs. There is also an inverse correlation with the transcription factors that identify each of these two T-cell subpopulations. In fact, in the presence of TGF-beta, CD4+ T-cells express both ROR-gammat and FoxP3, but ROR-gammat function is antagonized by FoxP3. Rather in the presence of proinflammatory cytokines and low concentration of TGF-beta, ROR-gammat expression is further upregulated, whereas FoxP3 expression and function are inhibited. This evidence shows the importance of cytokines' environment in the differentiation of CD4+ T-cell subsets, depending upon the balance of expression of the transcriptional factors ROR-gammat and FoxP3 (13).

Recently, a strong link was reported between IL-23 and IL-17 defined as the IL-23/IL-17 axis. It has been shown that the absence of IL-17A or its receptor (IL-17R) in T cells led to an accelerated and severe wasting disease accompanied by higher expression of genes encoding for Th1-type of cytokines. IL-17A can also modulate the Th1 polarization *in vitro* in an inhibitory sense, suppressing the induction of the transcriptional factor T-bet, the "master regulator" of Th1 differentiation of T cells (35).

Tregs and Th17 cells are involved in the production of cytokines that lead to Th1-mediated tissue damage. Thus, inflammation in CD is the result of the complex interaction of many factors.

Upon activation, gluten-reactive CD4-positive T cells produce IFN-gamma, which is a major contributor to the development of the celiac lesion. IFN-gamma is also produced by intra-epithelial T-cells (36).

The precise molecular mechanism involved in the differentiation of Th1 secreting cells in duodenal mucosa remains not completely understood. A

possible mechanism is that naïve T cells recruited by gluten at tissue level from the blood are induced *in situ* to produce Th1 cytokines. Moreover, it is likely that Th1 cells primed in the Peyer's patches seed the lamina propria of CD patients where locally induced factors may contribute to maintain and expand the gluten specific Th1 response (37).

The majority of gliadin-specific T cells has a Th0 cytokine production profile with secretion of IL-2, IL-4, IFN-gamma, and IL-10. These cells proliferate in response to gliadin. Tr1-cytokine profile secreting cells are also present in intestinal mucosa of CD patients. Tr1-cells are anergic, restricted by DQ2, and produce IL-10 and IFN-gamma, but little or no IL-2 or IL-4 upon activation with gliadin or polyclonal stimuli. Gliadin-specific Tr1-cell clones suppressed proliferation of pathogenic Th0-cells (38).

Both Th0-cells that Tr1-cells are antigen-specific and differentiated at tissue level after gluten trigger activity. Several cytokines contribute to peripheral differentiation of gluten-specific naïve T-cells, into gluten-specific pro-inflammatory Th1 and Th17 cells (38).

In this context, IL-18, that is mainly produced by macrophages, dendritic, and epithelial cells, may play a significant role, enhancing IFN-gamma synthesis and favouring Th1 cell polarisation induced by either IL-12 or IFN-alpha (37).

Several studies have demonstrated that IL-15 production is highly increased in intestinal mucosa of CD patients. The greater sensitivity to IL-15 of CD patients is augmented by the increased expression of IL-15 receptor. IL-15, produced by many cell types and playing pleiotropic functions at the interface between innate and adaptive immunity, is involved with modulation of Treg function (3). IL-15, produced by either mononuclear cells in the lamina propria or by enterocytes, attracts T-cells with the capacity to kill enterocytes. IL-15 production is stimulated by gluten in the intestine in CD (36).

IL-12 produced by APC is also involved in Th1 differentiation and IFN-gamma secretion.

IFN-gamma is produced at high levels in celiac lesions and its secretion is IL-12 mediated. However, mRNA encoding the p40 subunity of IL-12 (IL-12p40) is not present in celiac lesions, suggesting that IL-12 expression might be implicated in T-cell priming in the mesenteric lymph nodes (3).

Lack of suppression activity by increased Tregs in mucosa of CD patients is intriguing. Recent data have shown that IL-15 interferes with suppressor activity of intestinal Tregs, and this is probably related to enhanced expression of IL-15 receptor (19). Moreover, IL-15 was involved in the local downregulation of TGF-beta signalling, which is required to maintain the regulatory function of Tregs (25). In addition, an alternative explanation for lack of Treg activity, may be found in the data by Hmida et al., who demonstrated that IL-15 could make human T-cells resistant to Tregs suppression (23).

IL-27, a recently described cytokine, member of the IL-12 family of cytokines, antagonizes tissue damaging Th17 effector cell responses (39). Initial studies on the biology of IL-27 provided evidence for its role in the initiation of Th1 responses (40). However, subsequent evidences have revealed that IL-27 has important immunoregulatory functions *in vivo* (41). IL-27 suppresses the development of human Th17 cells by downregulating ROR-gammat expression (42). Despite these relevant functions of IL-27 in immuno-regulations, data on IL-27 in CD are missing and no clear cut conclusions can be drawn.

IL-10 is an immunosuppressive cytokine, produced by Tregs, that can downregulate Th1 immune responses. IL-10 suppresses gliadin-specific T-cell activation. It may interfere with the antigen presenting capacity of lamina propria mononuclear cells as it reduces the expression of CD80. Interestingly, IL-10 also induces a long term hyporesponsiveness of gliadin specific mucosal T-cells.

*Refractory Celiac disease (RCD) and Enteropathy-associated T-cell lymphoma (EATL)*

CD is associated with an increased risk of malignant lymphomas. In particular, it has consistently been reported that the relative risk of intestinal or T-cell lymphoma is higher than extraintestinal or B-cell lymphoma in CD patients (43).

Several mechanisms can be implicated in the increased risk of malignancies in CD. For example, as described above in this review, Tregs proportion and FoxP3 expression in circulating CD4+ CD25+ T-cells could justify the increased global risk of

malignancy in CD population and support the efficacy of lifelong gluten-free diet in the reduction of the cancer risk (14). However, other clinical data have revealed that compliance to a gluten-free diet did not significantly alter lymphoma risk, even if a moderate effect of the diet cannot be excluded and furthermore, weight loss, a potential marker of CD severity, may be associated with lymphoma risk (43).

As result of tissue chronic inflammation there is a continued antigen presentation at tissue level in duodenal mucosa of CD patients (3). This process consists in a communication between different cellular populations, including IELs, which are cytotoxic CD3+/CD8+ lymphocytes found in very high numbers in the intestinal epithelium of patients with CD, the intestinal epithelial cells (IECs), the dendritic cells and the macrophages (44). IL-15 plays a major role in these cellular interactions. IL-15, which is increased in the mucosa of patients with CD, acts not only on a physiological level in the development, differentiation and function of the intestinal IELs, NK and NKT cells, but also in the disease process since it increases the cytotoxic activity of the IELs and the expression of the cytotoxic IEL ligands on the IECs surface (45).

Chronic inflammation, with this constant and progressive mechanism of antigen presentation to several cellular populations, acts as a trigger factor in the pathogenesis of malignant transformation of T-cell clones into intra-epithelial T lymphoma.

Enteropathy-associated T-cell lymphoma (EATL) is a rare non-Hodgkin lymphoma of T-cell origin showing varying degrees of transformation but usually presenting as a tumor composed of a large lymphoid cell, often with an inflammatory background. The recent 2008 World Health Organization classification of hematologic malignancies distinguishes between two types of EATL (46).

EATL is uncommon in most parts of the world, but is seen with greater frequency in those areas with a high prevalence of CD, in particular Northern Europe (47).

EATL is associated with CD and also with other CD-related disease, such as dermatitis herpetiformis (48,49).

Approximately 5% of CD patients may have refractory celiac disease (3), that is defined by persistent or recurrent malabsorptive symptoms and villous atrophy despite strict adherence to a gluten-free diet for at least 6–12 months in the absence of other causes of non-responsive treated CD and overt malignancy. Symptoms are often severe and require additional therapeutic intervention besides dietary treatment (50). RCD can be classified as type 1, defined by normal (polyclonal) IEL phenotype, or type 2, defined by the emergence of a population of abnormal aberrant IELs within the epithelium, which are characterised by a clonal rearrangement of the TCR-gamma, by loss of surface expression of CD3 and CD8 and very stereotypical phenotype anomalies. Type 2 RCD is considered as an equivalent of intraepithelial T lymphoma known as low-grade (44). Although the cytological appearance is normal and the absence of active *in situ* proliferation, the presence of clonal rearrangements of the TCR-gamma, sometimes also chromosomic anomalies, as well as their potential dissemination in the chorion, blood or other extra-intestinal sites such as the skin and lung, are all highly suggestive factors of their malignant nature (44).

EATL may be preceded by refractory celiac disease (RCD) with or without ulceration. In some cases of RCD, the IELs are phenotypically aberrant showing down-regulation of CD8 similar to the IELs in mucosa adjacent to EATL (51).

## CONCLUSION

In recent years the focus on the role of T-cells in CD pathogenesis has shifted from CD8 cytotoxic cells and Th1-secreting cells to newly described CD4 T-cell subpopulations.

In summary, in the CD pathogenesis the pivotal role is played by the gluten-presentation by APC cells in genetically susceptible individuals. Gluten acts as a trigger factor for the recruitment of antigen-specific T cells from peripheral blood to duodenal mucosa. Several cytokines secreted from different T-cell subsets are involved in tissue damage and contribute to the T-cell subsets' differentiation themselves. In previous years, the mechanism of duodenal damage has been related to a Th1-reponse. Here we discuss the role of newly described pro-inflammatory cytokines (such as IL-15. IL-17 and lL-18) and novel CD4 cells (Tregs and Th17).

To understand the pathogenesis of tissue damage

of CD, we have focused on the duodenal micro-environment, in which modulation of the immune response takes place, depending on the cocktail of cytokines secreted by the T-cell subtypes that take part in this intricate puzzle.

We have introduced the new concept of "immunological niche" that in CD summarizes cellular and cytokine interactions in duodenal micro-environment, where a high plasticity of T-cell subsets is present. The immunological niche is defined as an anatomo-functional region that hosts the components of a complex immune response, playing a direct role in the homeostasis of local tissue immune system.

Thus, the study of the complexity of the immune system of the duodenal immunological niche may have diagnostic, prognostic and therapeutical impact for CD patients.

## ACKNOWLEDGEMENTS

This editorial was supported in part by linea D1 from Catholic University of Rome.

## REFERENCES

1. Sollid LM, Thorsby E. HLA susceptibility genes in celiac disease: genetic mapping and role in pathogenesis. Gastroenterology 1993; 105:910-22.
2. Frezza D, Giambra V, Cianci R, et al. Increased frequency of the immunoglobulin enhancer HS1,2 allele 2 in coeliac disease. Scand J Gastroenterol 2004; 39:1083-7.
3. Jabri B, Sollid LM. Tissue-mediated control of immunopathology in coeliac disease. Nat Rev Immunol 2009; 9:858-70.
4. Ebert EC. Interleukin 21 up-regulates perforin-mediated cytotoxic activity of human intra-epithelial lymphocytes. Immunology 2009; 127:206-15.
5. Kagnoff MF. Celiac disease: pathogenesis of a model immunogenetic disease. J Clin Invest 2007; 117:41-9.
6. Harris KM, Fasano A, Mann DL. Monocytes differentiated with IL-15 support Th17 and Th1 responses to wheat gliadin: implications for celiac disease. Clin Immunol 2010; 135:430-9.
7. Qiao SW, Raki M, Gunnarsen KS, Loset GA, Lundin KE, Sandlie I, Sollid LM. Posttranslational modification of gluten shapes TCR usage in celiac disease. J Immunol 2011; 187:3064-71.
8. Giovannetti A, Pierdominici M, Di Iorio A, Cianci R, Murdaca G, Puppo F, Pandolfi F, Paganelli R. Apoptosis in the homeostasis of the immune system and in human immune mediated diseases. Curr Pharm Des 2008; 14:253-68.
9. Buri C, Burri P, Bahler P, Straumann A, Muller-Schenker B, Birrer S, Mueller C. Cytotoxic T cells are preferentially activated in the duodenal epithelium from patients with florid coeliac disease. J Pathol 2005; 206:178-85.
10. Pandolfi F, Corte G, Quinti I, Fiorilli M, Frieligsdorf A, Bargellesi A, Aiuti F. Defect of T helper lymphocytes, as identified by the 5/9 monoclonal antibody, in patients with common variable hypogammaglobulinaemia. Clin Exp Immunol 1983; 51:470-4.
11. Hishii M, Kurnick JT, Ramirez-Montagut T, Pandolfi F. Studies of the mechanism of cytolysis by tumour-infiltrating lymphocytes. Clin Exp Immunol 1999; 116:388-94.
12. Sakaguchi S, Miyara M, Costantino CM, Hafler DA. FOXP3+ regulatory T cells in the human immune system. Nat Rev Immunol 2010; 10:490-500.
13. Pandolfi F, Cianci R, Pagliari D, Landolfi R, Cammarota G. Cellular mediators of inflammation: tregs and TH17 cells in gastrointestinal diseases. Mediators Inflamm 2009; 2009:132028.
14. Frisullo G, Nociti V, Iorio R, et al. Increased CD4+CD25+Foxp3+ T cells in peripheral blood of celiac disease patients: correlation with dietary treatment. Hum Immunol 2009; 70:430-5.
15. Brazowski E, Cohen S, Yaron A, Filip I, Eisenthal A. FOXP3 expression in duodenal mucosa in pediatric patients with celiac disease. Pathobiology 2010; 77:328-34.
16. Monteleone I, Sarra M, Del Vecchio Blanco G, et al. Characterization of IL-17A-producing cells in celiac disease mucosa. J Immunol 2010; 184:2211-8.
17. Castellanos-Rubio A, Santin I, Irastorza I, Castano L, Carlos Vitoria J, Ramon Bilbao J. TH17 (and TH1) signatures of intestinal biopsies of CD patients in response to gliadin. Autoimmunity 2009; 42:69-73.
18. Fernandez S, Molina IJ, Romero P, et al. Characterization of gliadin-specific Th17 cells

from the mucosa of celiac disease patients. Am J Gastroenterol 2011; 106:528-38.
19. Zanzi D, Stefanile R, Santagata S, et al. IL-15 interferes with suppressive activity of intestinal regulatory T cells expanded in Celiac disease. Am J Gastroenterol 2011; 106:1308-17.
20. Simone R, Brizzolara R, Chiappori A, et al. A functional soluble form of CTLA-4 is present in the serum of celiac patients and correlates with mucosal injury. Int Immunol 2009; 21:1037-45.
21. Hunt KA, McGovern DP, Kumar PJ, et al. A common CTLA4 haplotype associated with coeliac disease. Eur J Hum Genet 2005; 13:440-4.
22. Haimila K, Einarsdottir E, de Kauwe A, et al. The shared CTLA4-ICOS risk locus in celiac disease, IgA deficiency and common variable immunodeficiency. Genes Immun 2009; 10:151-61.
23. Hmida NB, Ahmed MB, Moussa A, et al. Impaired Control of Effector T Cells by Regulatory T Cells: A Clue to Loss of Oral Tolerance and Autoimmunity in Celiac Disease? Am J Gastroenterol 2011; doi: 10.1038/ajg.2011.397.
24. Peluso I, Fantini MC, Fina D, Caruso R, Boirivant M, MacDonald TT, Pallone F, Monteleone G. IL-21 counteracts the regulatory T cell-mediated suppression of human CD4+ T lymphocytes. J Immunol 2007; 178:732-9.
25. Benahmed M, Meresse B, Arnulf B, et al. Inhibition of TGF-beta signaling by IL-15: a new role for IL-15 in the loss of immune homeostasis in celiac disease. Gastroenterology 2007; 132:994-1008.
26. Barone MV, Zanzi D, Maglio M, et al. Gliadin-mediated proliferation and innate immune activation in celiac disease are due to alterations in vesicular trafficking. PLoS One 2011; 6:e17039.
27. Bodd M, Raki M, Tollefsen S, Fallang LE, Bergseng E, Lundin KE, Sollid LM. HLA-DQ2-restricted gluten-reactive T cells produce IL-21 but not IL-17 or IL-22. Mucosal Immunol 2010; 3:594-601.
28. Cianci R, Pagliari D, Pietroni V, Landolfi R, Pandolfi F. Tissue infiltrating lymphocytes: the role of cytokines in their growth and differentiation. J Biol Regul Homeost Agents 2010; 24:239-49.
29. Zhou L, Chong MM, Littman DR. Plasticity of CD4+ T cell lineage differentiation. Immunity 2009; 30:646-55.
30. Schofield R. The relationship between the spleen colony-forming cell and the haemopoietic stem cell. Blood Cells 1978; 4:7-25.
31. Park D, Sykes DB, Scadden DT. The hematopoietic stem cell niche. Front Biosci 2012; 17:30-9.
32. Scadden DT. The stem-cell niche as an entity of action. Nature 2006; 441:1075-9.
33. Hovhannisyan Z, Treatman J, Littman DR, Mayer L. Characterization of interleukin-17-producing regulatory T cells in inflamed intestinal mucosa from patients with inflammatory bowel diseases. Gastroenterology 2011; 140:957-65.
34. Wirtz S, Billmeier U, McHedlidze T, Blumberg RS, Neurath MF. Interleukin-35 mediates mucosal immune responses that protect against T-cell-dependent colitis. Gastroenterology 2011; 141:1875-86.
35. O'Connor W, Jr., Kamanaka M, Booth CJ, Town T, Nakae S, Iwakura Y, Kolls JK, Flavell RA. A protective function for interleukin 17A in T cell-mediated intestinal inflammation. Nat Immunol 2009; 10:603-9.
36. Sollid LM, Khosla C. Novel therapies for coeliac disease. J Intern Med 2011; 269:604-13.
37. Salvati VM, MacDonald TT, Bajaj-Elliott M, Borrelli M, Staiano A, Auricchio S, Troncone R, Monteleone G. Interleukin 18 and associated markers of T helper cell type 1 activity in coeliac disease. Gut 2002; 50:186-90.
38. Gianfrani C, Levings MK, Sartirana C, et al. Gliadin-specific type 1 regulatory T cells from the intestinal mucosa of treated celiac patients inhibit pathogenic T cells. J Immunol 2006; 177:4178-86.
39. Colgan J, Rothman P. All in the family: IL-27 suppression of T(H)-17 cells. Nat Immunol 2006; 7:899-901.
40. Jankowski M, Kopinski P, Goc A. Interleukin-27: biological properties and clinical application. Arch Immunol Ther Exp (Warsz) 2010; 58:417-25.
41. Batten M, Li J, Yi S, et al. Interleukin 27 limits autoimmune encephalomyelitis by suppressing the development of interleukin 17-producing T cells. Nat Immunol 2006; 7:929-36.
42. Liu H, Rohowsky-Kochan C. Interleukin-27-mediated suppression of human Th17 cells is associated with activation of STAT1 and suppressor of cytokine signaling protein 1. J Interferon Cytokine

Res 2011; 31:459-69.
43. Olen O, Askling J, Ludvigsson JF, Hildebrand H, Ekbom A, Smedby KE. Coeliac disease characteristics, compliance to a gluten free diet and risk of lymphoma by subtype. Dig Liver Dis 2011; 43:862-8.
44. Chandesris MO, Malamut G, Verkarre V, et al. Enteropathy-associated T-cell lymphoma: a review on clinical presentation, diagnosis, therapeutic strategies and perspectives. Gastroenterol Clin Biol 2010; 34:590-605.
45. Di Sabatino A, Ciccocioppo R, Cupelli F, et al. Epithelium derived interleukin 15 regulates intraepithelial lymphocyte Th1 cytokine production, cytotoxicity, and survival in coeliac disease. Gut 2006; 55:469-77.
46. Sieniawski MK, Lennard AL. Enteropathy-associated T-cell lymphoma: epidemiology, clinical features, and current treatment strategies. Curr Hematol Malig Rep 2011; 6:231-40.
47. Delabie J, Holte H, Vose JM, et al. Enteropathy-associated T-cell lymphoma: clinical and histological findings from the international peripheral T-cell lymphoma project. Blood 2011; 118:148-55.
48. Viljamaa M, Kaukinen K, Pukkala E, Hervonen K, Reunala T, Collin P. Malignancies and mortality in patients with coeliac disease and dermatitis herpetiformis: 30-year population-based study. Dig Liver Dis 2006; 38:374-80.
49. Holtmeier W, Pfander M, Zollner TM, Kaufmann R, Caspary WF. Distinct TCR delta repertoires are present in the cutaneous lesions and inflamed duodenum of patients with dermatitis herpetiformis. Exp Dermatol 2002; 11:527-31.
50. Rubio-Tapia A, Murray JA. Classification and management of refractory coeliac disease. Gut 2010; 59:547-57.
51. Bagdi E, Diss TC, Munson P, Isaacson PG. Mucosal intra-epithelial lymphocytes in enteropathy-associated T-cell lymphoma, ulcerative jejunitis, and refractory celiac disease constitute a neoplastic population. Blood 1999; 94:260-4.

JOURNAL OF BIOLOGICAL REGULATORS & HOMEOSTATIC AGENTS Vol. 26, no. 2, 181-192 (2012)

*EDITORIAL*

# IMMUNOHISTOCHEMICAL EXPRESSION AND LOCALIZATION OF SOMATOSTATIN RECEPTORS IN NORMAL PROSTATE, HIGH GRADE PROSTATIC INTRAEPITHELIAL NEOPLASIA AND PROSTATE CANCER AND ITS MANY FACES

R. MAZZUCCHELLI[1], M. SCARPELLI[1], A. LOPEZ-BELTRAN[2], L. CHENG[3], R. DI PRIMIO[4], A. BONO[1] and R. MONTIRONI[1]

*[1]Section of Pathological Anatomy, Polytechnic University of the Marche Region, School of Medicine, United Hospitals, Ancona, Italy; [2]Department of Pathology, Reina Sofia University Hospital and Faculty of Medicine, Cordoba, Spain; [3]Department of Pathology and Laboratory Medicine, Indiana University School of Medicine, Indianapolis, IN, USA; [4]Department of Clinical and Molecular Sciences, Polytechnic University of the Marche Region, School of Medicine, Ancona, Italy*

*Received January 30, 2012 – Accepted March 14, 2012*

The first two authors contributed equally to this work

**Data on the immunohistochemical expression and localization of the five somatostatin receptors (SSTRs) have been obtained by our group in separate studies concerning the many faces of prostate cancer (PCa), its precursor high grade prostatic intraepithelial neoplasia (HGPIN) and normal epithelium (Nep). This publication highlights the key findings, with special reference to: normal prostate epithelium; untreated HGPIN and PCa, both clinically and incidentally detected; PCa with NE differentiation; HGPIN and PCa following complete androgen ablation (CAA); and hormone refractory (HR) PCa. Taken together, the data obtained in these investigations demonstrate that SSTR profiling in individual patients with HGPIN and the multifaceted PCa is feasible and is of relevance to better tailor the somatostatin analogue-based treatment.**

Somatostatin (SST) is a 14- or 28-amino acid peptide that was originally described in 1973 as a hypothalamic NE hormone (1), whose role was to inhibit the secretion of growth hormone from the anterior pituitary gland. The presence of this peptide hormone was subsequently detected throughout the central and peripheral nervous systems, in the endocrine pancreas and in the gut, and to a lower extent in the thyroid, adrenal and sub-mandibular glands, kidney, liver, colon, rectum, small intestine, stomach, placenta, and prostate (2-9).

SST is known to inhibit the secretion of a wide range of hormones, exocrine glands, and gastrointestinal motility. SST has revealed an antiproliferative potential, reversing the impact of mitogenic signals delivered by substances such as epidermal growth factor and somatomedin C/insulin-like growth factor-1 (10). SST has been found to play a critical role in the negative control of cell growth and to act as a tumor-suppressor gene for pancreatic cancer and medullary thyroid carcinoma (11).

The actions of SST are mediated by a family of

*Key words: somatostatin receptors, prostate, prostate cancer, high-grade prostatic intraepithelial neoplasia, NE differentiation, complete androgen ablation, hormone refractory prostate cancer*

*Mailing address:* Prof. Rodolfo Montironi,
Pathological Anatomy,
Polytechnic University of the Marche Region,
School of Medicine, United Hospitals,
Via Conca 71, I−60126 Torrette, Ancona, Italy
Tel: +39 0715964830 Fax: +39 071889985
e-mail: r.montironi@univpm.it



0393-974X (2012)

transmembrane domain G-protein-coupled receptors that comprise five distinct subtypes (termed SSTR1 to 5). SSTRs are widely expressed in many organs, including the central nervous system (5), gastrointestinal tract (3), pancreas (6), kidney (2), and prostate (4, 7). Frequently, multiple subtypes coexist in the same cell. The five SSTRs share common signaling pathways such as the inhibition of adenylatecyclase, activation of phosphotyrosine phosphatase, and modulation of mitogen-activated protein kinase through G-protein-dependent mechanisms (11).

Cloning of five SSTRs has led to the development of subtype-selective agonists, among which SSTR2-specific SST analogues octreotide (OCT) and lanreotide have attracted significant attention in the past several years. They have been used as new diagnostic and treatment modalities for various endocrine disorders and as adjunctive treatment for a variety of benign and malignant tumours (12, 13). The antiproliferative and antiangiogenic properties of OCT have been exploited (14). Therefore, it is very important to determine cell expression and localization of the five SSTRs in prostate lesions. In particular, somatostatin receptor profiling in individual patients may be of relevance to better tailor a somatostatin analogue-based treatment.

Data on the immunohistochemical expression and localization of the five SSTRs have been obtained by our group in separate studies (15-19) concerning the many faces of prostate cancer, its precursor HGPIN and Nep (Table I). This publication highlights the key findings from the previous investigations, with special reference to:

1. SSTR expression in the epithelial component of the prostate tissues:
   a. Normal prostate epithelium
   b. Untreated HGPIN and PCa
   c. PCa with NE differentiation
   d. HGPIN and PCa following complete androgen ablation
   e. Hormone refractory prostate cancer
2. SSTR expression in nonepithelial components of the prostate:
   a. Endothelial cells
   b. Smooth muscle cells

This paper also includes an Appendix dedicated to the immunohistochemical approach adopted and used in such studies and assessment of antibody specificity to allow other groups to validate our findings.

*SSTR expression in the epithelial component of the prostate tissues*

*Normal prostate epithelium* (Figs. 1A and 2). The investigation was carried out on 14 surgical specimens of normal prostate epithelium from adenomectomy specimens from patients with bladder outlet obstruction (17).

*Luminal (secretory) cells.* A distinct positivity of moderate intensity in the cell membrane was seen only with SSTR3 (65.4% of cells) and SSTR4 (23.5% of cells). In all the cases and for all the receptor subtypes, close to 90% of cells showed a weak positivity in the cytoplasm. Strong immunoreactivity was present in a very small proportion of cells, ranging from 0.8% (SSTR3) to 3.2% (SSTR1). Weak nuclear staining was observed with subtypes 4 (26% of cells) and 5 (58.8% of cells).

*Basal cells.* Immunoreactivity was primarily detected in the cytoplasm in all SSTR subtypes. For the subtypes 1 and 3 the greatest proportion of cells showed a moderate intensity (42.5% and 41.4%, respectively), strong immunoreactivity being present in 18.1% and 15.8% of cells, respectively. For the subtypes 2, 4 and 5, the majority of cells showed a weak intensity (72.3%, 65.7%, and 65.1%, respectively), whereas a strong immunoreactivity was present in a small proportion of cells, ranging from 0.9% (SSTR2) to 3.2% (SSTR4).

*Highlights.* The study demonstrated the degree of expression as well as localization of the five SSTR subtypes in the luminal and basal cells of the transition zone (17). Similar results were obtained in the other investigations in which normal epithelium was selected from the peripheral zone (19).

When considering localization, although SSTRs are membrane-associated receptors, a significant amount of staining was seen in the cytoplasm within some nuclear staining in many immunoreactive cells. The interpretation, also based on molecular studies by others suggesting nuclear accumulation of SST analogs mediated by SSTRs (13, 20, 21), is that, after binding their ligand, SSTR-ligand complexes undergo cellular internalization with progressive intracytoplasmic and intranuclear translocation. This

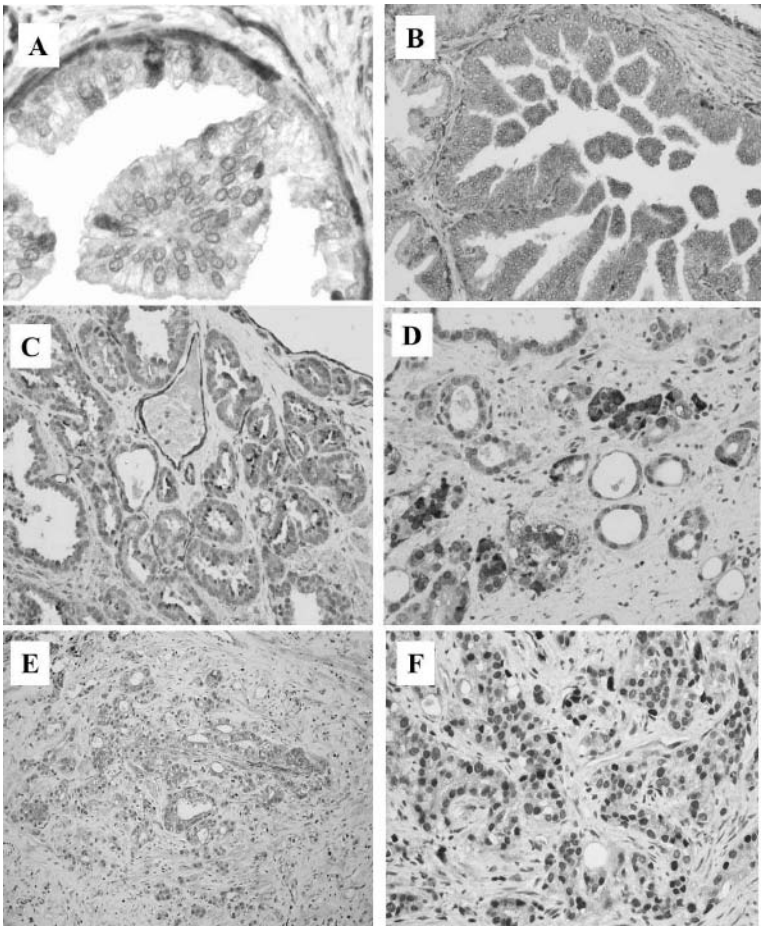


**Fig. 1.** *Immunoreactivity for SSTR4 in the luminal and basal cells in normal prostate (**A**); for SSTR3 in untreated HGPIN (**B**); for SSTR4 in untreated PCa (**C**); for SSTR4 in PCa with NE differentiation (**D**); for SSTR4 in complete androgen ablated PCa (**E**); and for SSTR4 in hormone refractory prostate cancer (**F**).*

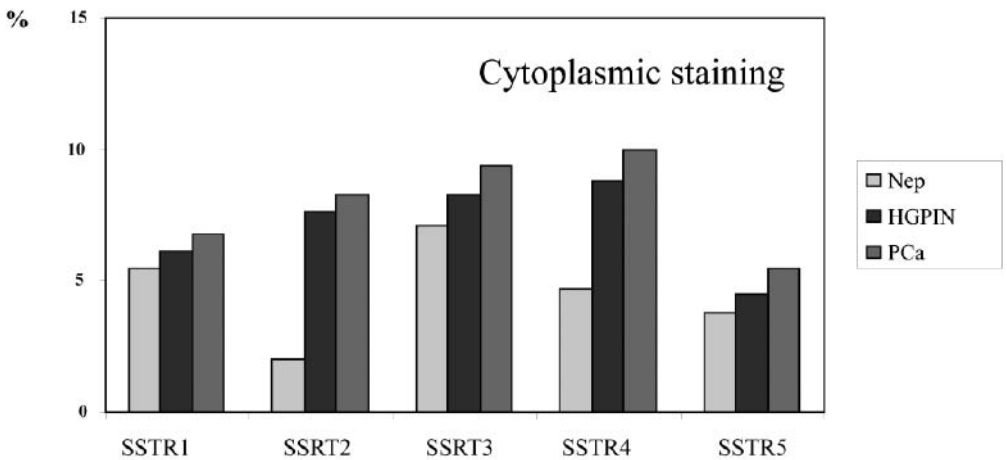


**Fig. 2.** *Mean percentages of intensely immunostained luminal (secretory) cells in the cytoplasm for the five SSTR subtypes in normal epithelium, HGPIN and PCa from untreated patients (The differences between NEp, HGPIN and PCa are statistically significant for the subtypes 2 and 4).*

hypothesis is not supported by the studies made by Le Romancer et al (22). This group suggested that the nuclear translocation of SST analogs is mediated by p86-Ku and not by SSTRs.

*Untreated HGPIN and prostate cancer (Figs. 1 B and C, and 2)*

The five SSTRs were evaluated in Nep, HGPIN and pT2a Gleason score 3+3=6 (GS6) PCa in 20 cystoprostatectomies (CyPs) with incidental PCa and in 20 radical prostatectomies (RPs) with clinically detected PCa. (19).

*Luminal (secretory) cells*. Membrane staining was seen with the subtypes 3 and 4. The mean percentages, higher in the subtype 3 than in the subtype 4, decreased from Nep to HGPIN and PCa. The differences between Nep, HGPIN and PCa were statistically significant for the subtype 3, both in the CyPs and in the RPs. The mean values in the CyPs were lower than in RP, the differences being not statistically significant.

The mean values of cells with strong cytoplasmic staining in the five subtypes increased from Nep to HGPIN and PCa. Both in the CyPs and RPs the highest expression of strong intensity was seen for the subtype 4 (in HGPIN and PCa) and the lowest for the subtype 5 (in Nep, HGPIN and PCa). In the CyPs, the differences between Nep, HGPIN and PCa were statistically significant for the subtypes 2 and 4. In the RPs, only the difference between Nep and HGPIN for the subtype 4 was statistically significant. Even though the mean values in CyP were lower than in RP, the differences were statistically significant in Nep only and for two out of five SSTRs.

Nuclear staining was seen in the subtypes 4 and 5. For the subtype 4, the mean percentages in Nep, HGPIN and PCa were similar. For the subtype 5, the mean percentages decreased from Nep to PCa. The differences between Nep, HGPIN and PCa were statistically significant for the subtype 5, both in the CyPs and in the RPs. Even though the mean values in the CyPs were lower than in the RPs, the differences were not statistically significant.

*Basal cells in HGPIN*. Immunoreactivity was primarily detected in the cytoplasm in all the five subtypes. In the subtypes 1 and 3 the mean proportions of positive cells were higher than in the other three subtypes. The proportions were higher in Nep compared with HGPIN. In the CyPs the differences between Nep and HGPIN were statistically significant for the subtypes 1, 3, 4, and 5, whereas, in the RPs, the differences were statistically significant for the subtypes 3 and 4. When considering strong expression in the CyPs, the differences between Nep and HGPIN were statistically significant for the subtypes 1 and 2, whereas in the RPs for the subtype 1 only. The mean values in CyP were lower than in RP, with statistically significant differences in the subtype 1 and only for the percentages of positive cells in HGPIN.

Individual cells in Nep, HGPIN and PCa showed very strong SSTR subtype expression. The cells in the same location proved to be Chromogranin A positive in adjacent sections (See below under: *PCa with neuroendocrine differentiation*).

*Highlights.* The investigation showed differences in the expression and localization of SSTRs between normal and preneoplastic and neoplastic tissues, and between incidentally-detected and clinically-detected PCa, therefore between insignificant or indolent and significant or aggressive cancers (19, 23-27).

The immunohistochemical expression at the cell level of the five SSTRs in normal and pathological prostate tissue was also investigated by Dizeyi et al (28). There are differences between our investigation and that by Dizeyi et al. They observed the presence of SSTR1 and SSTR3 in tumoral and non-tumoral epithelial cells as well as in the stromal compartment (See below), whereas SSTR4 was found to be confined to epithelial cells, and SSTR5 was not detectable. The differences are probably due to the types of antibodies used (in Dizeyi's investigation the antibodies were a private source and not commercially available). The investigation also differs in that we collected information on the differential localization of the five SSTR subtypes in the luminal cells but also in the basal cells both as well as in CyPs with incidental cancer and RPs with clinical cancer.

*PCa with Neuroendocrine Differentiation (Figs. 1D and 3)*

The five SSTR subtypes were evaluated in Nep, HGPIN and PCa with neuroendocrine (NE) differentiation in 20 RPs (18). The study also included

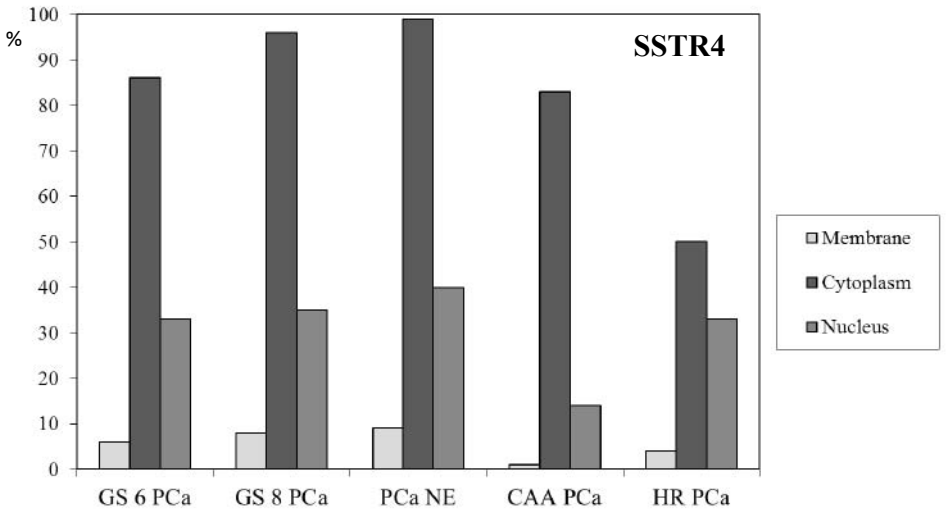


**Fig. 3.** *Mean percentages of immunostained luminal cells for SSTR4 in PCa, separately for cell membrane, cytoplasm and nucleus from all groups (See text for abbreviations). The mean values of SSTR expression in the cytoplasm, membrane and nuclei of the epithelial cells of HR PCa are lower than in the cancer areas of the PCa of the other two groups. The highest values are seen in the cytoplasm, the difference being significant.*

20 RPs with GS6 PCa and 20 RPs with GS 4+4=8 (GS8) and 4+5=9 (GS9) PCa the results of which were identical to those shown in the investigation related HR PCa (See also below). NE differentiation was determined with Chromogranin A immunostaining and the SSTRS expression was evaluated only in the tumor areas with NE differentiation.

*NE and luminal (secretory) cells.* Membrane staining was seen with the subtypes 3 and 4. The mean percentages of positive cells, higher in the subtype 3 than in the subtype 4, decreased from Nep to HGPIN and PCa in all three RP groups. For the subtype 3 but not for the subtype 4, the differences between Nep and HGPIN and PCa were statistically significant for the three RP groups. For PCa there were no statistically significant differences between the three RP groups. The greatest mean proportions of cells with strong cytoplasmic staining in PCa were seen for SSTR2, mainly in the group of RP with NE differentiation, and for SSTR4 in all three groups; the mean values in HGPIN were intermediate between Nep and PCa. Nuclear staining was seen with SSTR4 and SSTR5. For SSTR4, the mean percentages in the PCa of the three groups were higher than in HGPIN and Nep, the highest proportion being with PCa with NE differentiation. For the subtype 5, there were few nuclei with strong staining intensity in the PCa in the RP with NE differentiation group.

*Basal cells.* Immunoreactivity for the five SSTRs was similar in terms of expression and localization to that seen in the group of *"Untreated HGPIN and Prostate Cancer"* (See above).

*Highlights.* Almost all prostate cancers have focal NE differentiation, although the majority show only rare or sparse single NE cells. In 5-10% of prostatic carcinomas there are zones with a large number of single or clustered NE cells detected by Chromogranin A immunostaining. Scant information was available on SSTR subtype expression and localization in PCa with NE differentiation, in comparison to conventional PCa.

This study (18) expanded our knowledge on immunohistochemical the expression and localization of five SSTRs in the various tissue components in prostates with PCa with NE differentiation, compared with those with conventional PCa. Typing somatostatin receptor expression in NE tumours could be of relevance to target somatostatin

analogue-based diagnostic approach and treatment.

*HGPIN and PCa Following Complete Androgen Ablation (Figs. 1E and 3)*

The five SSTRs were evaluated in Nep, HGPIN and PCa in 20 RPs with clinically detected PCa from patients under CAA. 20 RPs with clinically detected GS6 PCa from hormonally untreated patients were used as control group (15).

*Luminal (secretory) cells.* Membrane staining was seen for SSTR3 and SSTR4. The mean percentages of positive cells in the androgen ablated group, higher in SSTR3 than in SSTR4 and 30 to 90% lower than in the untreated, decreased in HGPIN and PCa compared with Nep. Cytoplasmic staining was seen for all 5 SSTRs. In the treated group, the Nep values were similar to those in the untreated, whereas the values in HGPIN and PCa were lower for SSTR1, 3 and 5, with a decrease of 30% for SSTR1. Treatment reduced the percentages of intensely stained cells for all 5 SSTRs in Nep, HGPIN and PCa. Nuclear staining was seen with SSTR4 and SSTR5. The mean percentages for the former being much lower than for the latter. Treatment affected both HGPIN and PCa, whose proportions of stained cells were 30 to 55% lower than in the untreated group. SSTR expression in Nep was no affected.

*Basal cells.* Cytoplasmic staining was seen for all 5 SSTRs, both in Nep and HGPIN. The values in the treated group were lower than in the other, the difference between the two group being in general comprised between 10 and 40%.

*Highlights.* The study showed that the five SSTRs were detectable in prostate tissue from patients under CAA, even though there was reduction of their level in HGPIN and PCa in comparison with untreated ones (15).

This was the first investigation that documented

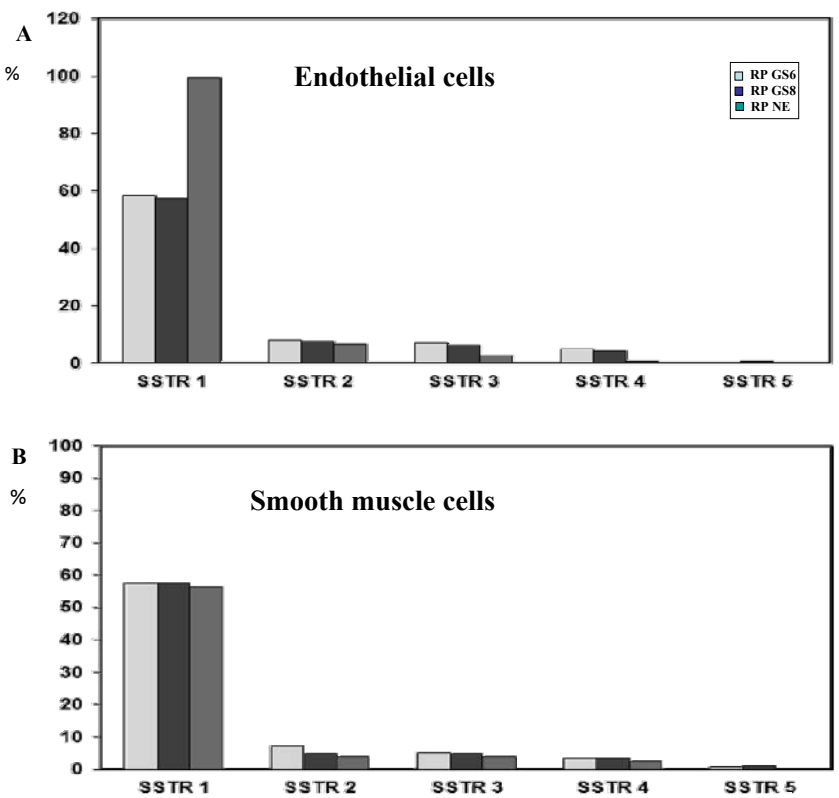


**Fig. 4.** *Mean percentages of intensely immunostained cells in the cytoplasm for the five SSTR subtypes in the endothelial (**A**) and smooth muscle cells (**B**). For the endothelial cells the highest proportion of positive cells is seen in the subtype 1 and the lowest in the subtype 5. For the former subtype the highest proportion of cells with strong intensity is seen with the RP NE group, the difference being statistically significant between RP NE and RP GS6, and between RP NE and RP GS8. For the smoth muscle cells, the proportions are similar in the three RP subgroups, the differences being the three RP groups being not statistically significant.*

**Table I.** *Investigations on the expression and localization of the SSTRs in human prostate tissue the results of which are summarized in this publication.*

| Authors, reference and publication year | No of cases investigated | Technique | Receptors | Localization | Type of tissue |
|---|---|---|---|---|---|
| Montironi R, et al. (17) 2008 | 14 | IHC | SSTR1<br>SSTR2<br>SSTR3<br>SSTR4<br>SSTR5 | Luminal (secretory) cells, basal cells, smooth muscle stromal cells, endothelial cells | Benign prostatic hyperplasia |
| Morichetti D, et al. (19) 2010 | 40 | IHC | SSTR1<br>SSTR2<br>SSTR3<br>SSTR4<br>SSTR5 | Luminal (secretory) cells, basal cells, smooth muscle stromal cells, endothelial cells | Normal,<br>HGPIN and incidentally- and clinically-detected PCa |
| Morichetti D, et al. (18) 2010 | 60 | IHC | SSTR1<br>SSTR2<br>SSTR3<br>SSTR4<br>SSTR5 | Luminal (secretory) cells, basal cells, smooth muscle stromal cells, endothelial cells | PCa with NE differentiation |
| Mazzucchelli, et al. (15) 2010 | 40 | IHC | SSTR1<br>SSTR2<br>SSTR3<br>SSTR4<br>SSTR5 | Luminal (secretory) cells, basal cells, smooth muscle stromal cells, endothelial cells | Complete androgen ablated PCa |
| Mazzucchelli, et al. (16) 2011 | 60 | IHC | SSTR1<br>SSTR2<br>SSTR3<br>SSTR4<br>SSTR5 | Luminal (secretory) cells, smooth muscle stromal cells, endothelial cells | Hormone refractory PCa |

*(See text for abbreviations)*

a pattern of SSTR expression and localization in the prostate lesions following androgen ablation. There was only one previous investigation with some similarities with this investigation, in which the effect of chemotherapy on SSTR expression was evaluated. It was found that chemotherapy seemed to reduce the cellular receptors for SST analogues.

This information could be of paramount importance in therapeutic approaches in which SST analogues are combined with other drugs, including those that reduce the effect of androgens on PCa.

*Hormone Refractory Prostate Cancer (Figs. 1F and 3)*

The five SSTR subtypes were evaluated in 20 transurethral resection of the prostate (TURP) specimens with locally recurrent HR PCa. The study also included 20 RPs with GS6 PCa and 20 RPs with GS8 and GS9 PCa.

**Table II.** *Investigations on the SSTRs in human prostate tissue from groups other than ours.*

| Authors and reference | Publication year | Technique | Receptors | Localization | Type of tissue |
|---|---|---|---|---|---|
| Reubi JC, et al. (7) | 1995 | Autoradiography, in situ hybridization | SSTR1 SSTR2 SSTR3 | Smooth muscle, endothelium | Benign prostatic hyperplasia and prostate cancer |
| Halmos G, et al. (39) | 2000 | RT-PCR | SSTR1 SSTR2 SSTR5 | Epithelial cells | Prostate cancer |
| Dizeyi N, et al. (28) | 2002 | IHC, RT-PCR, Western blot | SSTR1 SSTR2 SSTR3 SSTR4 SSTR5 | Epithelial cells, stromal cells, endothelium | Normal, benign prostatic hyperplasia, prostate cancer |
| Hansson J, et al. (4) | 2002 | In situ hybridization | SSTR2 SSTR4 | Epithelial cells, stromal cells | Benign prostatic hyperplasia, PIN, prostate cancer |
| Volante M, et al. (40) | 2007 | IHC | SSTR2A SSTR3 SSTR5 | Epithelial cells | Cancer |
| Cariaga-Martinez AE, et al. (38) | 2009 | IHC | SSTR2 | Luminal side of duct and acinar cells | Normal, benign hyperplasia and prostate cancer |

*(See text for abbreviations)*

*Luminal (secretory) cells*. The mean values of SSTR expression in the cytoplasm, membrane and nuclei of the epithelial cells of HR PCa were 20 to 70% lower than in the cancer areas of the PCa of the other two groups. Membrane staining was observed for SSTR3 and SSTR4. The mean percentage of the former in HR PCa was lower than in the other two PCa groups, the differences being statistically significant in the comparison with RP with GS8 and GS9 PCa. The mean value for the latter was intermediate between those of the two cancer groups, the differences being not statistically significant. When considering cytoplasm staining, the differences between the HR PCa and RP with GS6 PCa groups were statistically significant for all SSTRs. Statistically significant differences were also present in the comparison between HR PCa and RP with GS8 and GS9 PCa groups. Nuclear staining was seen for SSTR4 and in SSTR5. The mean percentage of the former in the HR group was higher than in the other two cancer groups, the differences being not statistically significant. The mean value for the latter in the HR group was lower than those of the other two cancer groups, the differences being statistically significant.

Concerning the HR group, the results obtained

in Nep and PCa in the five TURP where the initial diagnosis of PCa was made were comparable to those seen in the untreated PCa investigation.

*Highlights.* Conventional chemotherapy for prostate cancer that is no longer responsive to androgen deprivation, i.e., HR PCa, was initially found to produce only marginal responses (29), but others re-evaluated with interest as new agents and better supportive care become available (30). Nevertheless, palliation still remains the primary goal of current chemotherapy, and overall response rates are low and are associated with general toxicity. To overcome the problem of toxicity, attempts have been made to achieve site-specific drug delivery and improve the therapeutic index. Targeted chemotherapy using potent cytotoxic radicals conjugated to carrier molecules, such as antibodies (31,32) or analogues of peptide hormones (33), that can be specifically recognized by tumour cells, improves therapy of HR PCa.

*SSTR expression in the nonepithelial components of the prostate*

*Endothelial cells* (Figs. 1C and 4A). There were no cases with a distinct positivity in the cell membrane. Subtype 1 showed a strong immunoreactivity in the cytoplasm in 98.6% of the cells. With subtypes 3 and 4 the greatest proportion of cells showed a weak intensity (73.5% and 56.4%, respectively). With the subtype 2 and 5 the majority of cells were negative (59.1% and 50.7%, respectively). Nuclear staining was not seen.

*Highlights.* This type of information confirms that provided previously by Curtis et al. (34) and Badway et al. (35) who independently demonstrated SSTR1 and SSTR 2 expression in endothelial cells. The presence of the SSTR subtypes in endothelial cells in prostate tissue was also reported by Dizeyi et al. (28). This group mentioned that peritumoral vessels were intensely stained by the SSTR2 antiserum. In their molecular study in prostate cancer, Reubi et al. (7, 36) observed that many peritumoral vessels, in particular veins, contain a high density of SSTRs. SSTR-positive veins were also occasionally identified in samples of prostate tissue distant from the prostate tumour as well as in the prostate of the patient with bladder cancer. Precise actions of somatostatin in endothelial cells have not yet been clarified, but somatostatin may be involved in regulating endothelial cell homeostasis and anti-inflammatory effects (37).

*Smooth Muscle Cells* (Figs. 1C and 4B). There were no cases with a distinct positivity in the cell membrane. Subtype 1 showed a strong immunoreactivity in the cytoplasm in 60% of the cells. With subtypes 2, 3 and 4 the greatest proportion of cells showed a weak intensity (63.4%, 89.8%, and 81.7%, respectively). With the subtype 5 the majority of cells (59.8%) were negative. Nuclear staining was seen only with subtypes 4 and 5, it was always weak and was observed in a minority of cells (27.1% and 45.2%, respectively).

NE differentiation in PCa well as CAA did not affect SSTR expression and localization in the in the endothelial and smooth muscle cells.

*Highlights.* A possible role of the SSTRs in the smooth muscle could be to influence the release of various growth factors (i.e., nerve growth factor) known to be synthesized in the stroma. As several of these growth factors act in a paracrine manner on the glandular part of the prostate to regulate prostate growth (28), somatostatin could indirectly regulate biological events in the prostatic gland through a stromal action. Another possible role would be a regulatory mechanism dependent on the SSTR action on the prostate mediated by the pituitary.

## SSTR INVESTIGATIONS WITH MOLECULAR TECHNIQUES

Molecular techniques such as *in situ* hybridization histochemistry and autoradiography have been used in a limited number of studies (4, 7, 20, 28, 38-40). The former basically investigates SSTR mRNA expression in cryostat sections. The latter also utilizes cryostat sections and is based on radioligands, i.e., $^{125}$I-labeled somatostatin ligands, such as octreotide. The studies often dealt with only some of the subtypes, therefore information is only partial. For instance, Reubi et al investigated SSTRl, SSTR2, and SSTR3 only (41) (Table II). The type of information that these two techniques can give is not always comparable to that obtained with immunohistochemical analysis in formalin-fixed and paraffin-embedded tissue in which the architecture and the cytology in the background is well preserved.

In addition, the immunohistochemical technique is much easier to apply than *in situ* hybridization histochemistry and autoradiography.

## CONCLUSIONS

Data on the expression and localization of the SSTRs have been obtained in separate studies concerning the many faces of PCa, HGPIN and Nep. This publication highlights the key findings, with special reference to: normal prostate epithelium; untreated HGPIN and PCa, both clinically and incidentally detected; PCa with NE differentiation; HGPIN and PCa following CAA; and HR PCa. The data demonstrate that SSTR profiling in individual patients with HGPIN and the multifaceted PCa is feasible and of relevance to better tailor the somatostatin analogue-based treatment.

## ACKNOWLEDGEMENTS

This study was supported by a grant from Novartis Oncology, Italy.

## REFERENCES

1. Brazeau P, Vale W, Burgus R, Ling N, Butcher M, Rivier J, Guillemin R. Hypothalamic polypeptide that inhibits the secretion of immunoreactive pituitary growth hormone. Science 1973; 179**:**77-9.
2. Balster DA, O'Dorisio MS, Summers MA, Turman MA. Segmental expression of somatostatin receptor subtypes sst(1) and sst(2) in tubules and glomeruli of human kidney. Am J Physiol Renal Physiol 2001; 280:F457-65.
3. Casini Raggi C, Calabro A, Renzi D, et al. Quantitative evaluation of somatostatin receptor subtype 2 expression in sporadic colorectal tumor and in the corresponding normal mucosa. Clin Cancer Res 2002; 8:419-27.
4. Hansson J, Bjartell A, Gadaleanu V, Dizeyi N, Abrahamsson PA. Expression of somatostatin receptor subtypes 2 and 4 in human benign prostatic hyperplasia and prostatic cancer. Prostate 2002; 53:50-9.
5. Kumar U. Expression of somatostatin receptor subtypes (SSTR1–5) in Alzheimer's disease brain: an immunohistochemical analysis. Neuroscience 2005; 134:525-38.
6. Portela-Gomes MG, Stridsberg M, Grimelius L, Oberg K, Janson ET. Expression of the five different somatostatin receptor subtypes in endocrine cells of the pancreas. Appl Immunohistochem Mol Morph 2000; 8:126-32.
7. Reubi JC, Waser B, Schaer JC, Markwalder R. Somatostatin receptors in human prostate and prostate cancer. J Clin Endocrinol Metab 1995; 80:2806-14.
8. Reynaert H, Rombouts K, Vandermonde A, Urbain D, Kumar U, Bioulac-Sage P, Pinzani M, Rosenbaum J, Geerts A. Expression of somatostatin receptors in normal and cirrhotic human liver and in hepatocellular carcinoma. Gut 2004; 53:1180-9.
9. Zatelli MC, degli Uberti EC. Somatostatin receptors: from basic science to clinical approach--thyroid. Dig Liver Dis 2004; 36(S):86-92.
10. Epelbaum J, Dournaud P, Fodor M, Viollet C. The neurobiology of somatostatin. Crit Rev Neurobiol 1994; 8:25-44.
11. Patel YC**.** Somatostatin and its receptor family. Front Neuroendocrinol 1999; 20:157-98.
12. Hofland LJ, van der Hoek J, Feelders R, van der Lely AJ, de Herder W, Lamberts SW. Pre-clinical and clinical experiences with novel somatostatin ligands: advantages, disadvantages and new prospects. J Endocrinol Invest 2005; 28:36-42.
13. Klisovic DD, O'Dorisio MS, Katz SE, Sall JW, Balster D, O'Dorisio TM, Craig E, Lubow M. Somatostatin receptor gene expression in human ocular tissues: RT-PCR and immunohistochemical study. Invest Ophthalmol Vis Sci 2001; 42:2193-201.
14. Verset G, Verslype C, Reynaert H, et al. Efficacy of the combination of long-acting release octreotide and tamoxifen in patients with advanced hepatocellular carcinoma: a randomised multicentre phase III study. Br J Cancer 2007; 97:582-8.
15. Mazzucchelli R, Morichetti D, Santinelli A, Scarpelli M, Bono AV, Lopez-Beltran A, Cheng L, Montironi R. Immunohistochemical expression and localization of somatostatin receptor subtypes in androgen ablated prostate cancer. Cell Oncol (Dordr) 2011; 34:235-43.
16. Mazzucchelli R, Morichetti D, Scarpelli M, Bono

AV, Lopez-Beltran A, Cheng L, Kirkali Z, Montironi R. Somatostatin receptor subtypes in hormone-refractory (castration-resistant) prostatic carcinoma. Asian J Androl 2011; 13:242-7.

17. Montironi R, Cheng L, Mazzucchelli R, et al. Immunohistochemical detection and localization of somatostatin receptor subtypes in prostate tissue from patients with bladder outlet obstruction. Cell Oncol 2008; 30:473-82.
18. Morichetti D, Mazzucchelli R, Santinelli A, Stramazzotti D, Lopez-Beltran A, Scarpelli M, Bono AV, Cheng L, Montironi R. Immunohistochemical expression and localization of somatostatin receptor subtypes in prostate cancer with neuroendocrine differentiation. Int J Immunopathol Pharmacol 2010; 23:511-22.
19. Morichetti D, Mazzucchelli R, Stramazzotti D, Santinelli A, Lopez-Beltran A, Scarpelli M, Bono AV, Cheng L, Montironi R. Immunohistochemical expression of somatostatin receptor subtypes in prostate tissue from cystoprostatectomies with incidental prostate cancer. BJU Int 2010; 106:1072-80.
20. Reubi JC, Waser B, Schaer JC, Laissue JA. Somatostatin receptor sst1-sst5 expression in normal and neoplastic human tissues using receptor autoradiography with subtype-selective ligands. Eur J Nucl Med 2001; 28:836-46.
21. Hornick CA, Anthony CT, Hughey S, Gebhardt BM, Espenan GD, Woltering EA. Progressive nuclear translocation of somatostatin analogs. J Nucl Med 2000; 41:1256-63.
22. Le Romancer M, Reyl-Desmars F, Cherifi Y, Pigeon C, Bottari S, Meyer O, Lewin MJ. The 86-kDa subunit of autoantigen Ku is a somatostatin receptor regulating protein phosphatase-2A activity. J Biol Chem 1994; 269:17464-8.
23. Barbisan F, Mazzucchelli R, Santinelli A, Lopez-Beltran A, Cheng L, Scarpelli M, Montorsi F, Montironi R. Overexpression of ELAV-like protein HuR is associated with increased COX-2 expression in atrophy, high-grade prostatic intraepithelial neoplasia, and incidental prostate cancer in cystoprostatectomies. Eur Urol 2009; 56:105-12.
24. Mazzucchelli R, Barbisan F, Santinelli A, Lopez-Beltran A, Cheng L, Scarpelli M, Montironi R. Immunohistochemical expression of prostate stem cell antigen in cystoprostatectomies with incidental prostate cancer. Int J Immunopathol Pharmacol 2009; 22:755-62.
25. Montironi R, Mazzucchelli R, Barbisan F, Stramazzotti D, Santinelli A, Scarpelli M, Lòpez Beltran A. HER2 expression and gene amplification in pT2a Gleason score 6 prostate cancer incidentally detected incystoprostatectomies: comparison with clinically detected androgen-dependent and androgen-independent cancer. Hum Pathol 2006; 37:1137-44.
26. Montironi R, Mazzucchelli R, Santinelli A, Scarpelli M, Lopez-Beltran A, Bostwick DG. Incidentally detected prostate cancer in cystoprostatectomies: pathological and morphometric comparison with clinically detected cancer in totally embedded specimens. Hum Pathol 2005; 36:646-54.
27. Santinelli A, Mazzucchelli R, Barbisan F, Lopez-Beltran A, Cheng L, Scarpelli M, Montironi R. alpha-Methylacyl coenzyme A racemase, Ki-67, and topoisomerase IIalpha in cystoprostatectomies with incidental prostate cancer. Am J Clin Pathol 2007; 128:657-66.
28. Dizeyi N, Konrad L, Bjartell A, Wu H, Gadaleanu V, Hansson J, Helboe L, Abrahamsson PA. Localization and mRNA expression of somatostatin receptor subtypes in human prostatic tissue and prostate cancer cell lines. Urol Oncol 2002; 7:91-8.
29. Yagoda A, Petrylak D. Cytotoxic chemotherapy for advanced hormone-resistant prostate cancer. Cancer 1993; 71:1098-109.
30. Oh WK, Kantoff PW. Management of hormone refractory prostate cancer: current standards and future prospects. J Urol 1998; 160:1220-9.
31. Fu W, Madan E, Yee M, Zhang H. Progress of molecular targeted therapies for prostate cancers. Biochim Biophys Acta 2011; 1825:140-52.
32. Sciarra A, Innocenzi M, Ravaziol M, Minisola F, Alfarone A, Cattarino S, Monti G, Gentile V, Di Silverio F. Neuroendocrine target therapies for prostate cancer. Urologia 2011; 78:137-41.
33. Song HZ, Chen LB. Targeted therapies for hormone-refractory prostate cancer. Zhonghua Nan Ke Xue 2010; 16:1108-12
34. Curtis SB, Hewitt J, Yakubovitz S, Anzarut A, Hsiang

YN, Buchan AM. Somatostatin receptor subtype expression and function in human vascular tissue. Am J Physiol Heart Circ Physiol 2000; 278:H1815-22.

35. Badway AC, West FM, Tente SM, Blake AD. Somatostatin regulates intracellular signaling in human carotid endothelial cells. Biochem Biophys Res Commun 2004; 319:1222-7.
36. Reubi JC, Schaer JC, Markwalder R, Waser B, Horisberger U, Laissue J. Distribution of somatostatin receptors in normal and neoplastic human tissues: recent advances and potential relevance. Yale J Biol Med 1997; 70:471-9.
37. Reubi JC, Schaer JC, Laissue JA, Waser B. Somatostatin receptors and their subtypes in human tumors and in peritumoral vessels. Metabolism 1996; 45:39-41.
38. Cariaga-Martinez AE, Lorenzati MA, Riera MA, et al. Tumoral prostate shows different expression pattern of somatostatin receptor 2 (SSTR2) and phosphotyrosine phosphatase SHP-1 (PTPN6) according to tumor progression. Adv Urol (Epub 2009).
39. Halmos G, Schally AV, Sun B, Davis R, Bostwick DG, Plonowski A. High expression of somatostatin receptors and messenger ribonucleic acid for its receptor subtypes in organ-confined and locally advanced human prostate cancers. J Clin Endocrinol Metab 2000; 85:2564-71.
40. Volante M, Brizzi MP, Faggiano A, et al. Somatostatin receptor type 2A immunohistochemistry in neuroendocrine tumors: a proposal of scoring system correlated with somatostatin receptor scintigraphy. Mod Pathol 2007; 20:1172-82.
41. Reubi JC, Schaer JC, Waser B, Mengod G. Expression and localization of somatostatin receptor SSTR1, SSTR2, and SSTR3 messenger RNAs in primary human tumors using in situ hybridization. Cancer Res 1994; 54:3455-9.

JOURNAL OF BIOLOGICAL REGULATORS & HOMEOSTATIC AGENTS Vol. 26, no. 2, 193-201 (2012)

*EDITORIAL*

# ROLE OF MAST CELLS IN INNATE AND ADAPTIVE IMMUNITY

S. TETÈ[1], D. TRIPODI[1], M. ROSATI[2], F. CONTI[2], G. MACCAURO[3], A. SAGGINI[4], V. SALINI[5], E. CIANCHETTI[6], A. CARAFFA[7], P. ANTINOLFI[7], E. TONIATO[8], M.L. CASTELLANI[8], F. PANDOLFI[9], S. FRYDAS[10], P. CONTI[8] and T.C. THEOHARIDES[11]

*[1]Dental School, University of Chieti-Pescara, Italy; [2]Gynecology Division, Pescara Hospital, Pescara, Italy; [3]Department of Orthopedics, Catholic University of Rome, Rome, Italy; [4]Department of Dermatology, University of Rome Tor Vergata, Rome, Italy; [5]Department of Orthopedics, University of Chieti-Pescara, Chieti, Italy; [6]Ortona Hospital, University of Chieti-Pescara, Italy; [7]Department of Orthopedics, University of Perugia, Perugia, Italy; [8]Immunology Division, University of Chieti-Pescara, Italy; [9]Department of Medicine, Catholic University of Rome, Italy; [10]Department of Parassitology, Thessaloniki University, Greece; [11]Department of Physiology and Pharmacology, Tufts University School of Medicine, New England Medical Center, Boston, MA, USA*

*Received March 11, 2012 – Accepted June 10, 2012*

**Mast cells play a central role in inflammatory and immediate allergic reactions and are necessary for allergic reactions. Mast cells play a role in the pathophysiology of autoimmune diseases and appear to be especially important in inflamed tissues, because they infiltrate tissues and produce a variety of cytokines. Mast cells are important for both innate and adaptive immunity in tissues that are in close contact with the environment, i.e. the skin, the airways and the lung, and the lining of the intestine. However, there are still many unsolved issues of mast cell functions, including their regulatory mechanism on cell differentiation in bone marrow; for example, the cytokines and transcription factors necessary for their differentiation and expansion, as well as the molecular mechanism underlying basophil migration from the bloodstream to peripheral tissues such as lymph nodes still need to be clarified.**

Mast cells (MCs) are granulated hematopoietic cells derived from stem cells that reside in nearly all tissues and are considered to be part of the immune system. Mast cells were first described by Ehrlich in his 1878 doctoral thesis on the basis of their unique staining characteristics and large granules, that gave them their name, "Mastzellen" which means well-fed cells, because their cytoplasm was stuffed with granular material. MCs are involved in immediate, as well as chronic inflammatory reactions and are characterized by their biphasic response to stimuli which involves rapid degranulation and a slower secretion of a variety of pharmacological compounds and cytokines (1-4). Mast cells play a central role in inflammatory and immediate allergic reactions and are necessary for allergic reactions, but also in innate and acquired immunity (5-9). It has been reported that mast cells play a role in the pathophysiology of autoimmune diseases and appear to be especially important in inflamed tissues, because they infiltrate

*Key words: mast cells; innate and adaptive immunity, interleukins, inflammation*

*Mailing address:* Prof. S. Tetè,
Dipartimento di Scienze Orali,
Università "G. d'Annunzio" Chieti- Pescara",
Via dei Vestini, 31
Chieti, Italy
Tel/Fax: +39 0871 3554095
e-mail: tete@unich.it



0393-974X (2012)

**DISCLOSURE: ALL AUTHORS REPORT NO CONFLICTS OF INTEREST RELEVANT TO THIS ARTICLE.**

the tissues and produce a variety of cytokines (10-14). MCs have a large repertoire of cell surface receptors and respond to a wide variety of exogenous and endogenous stimuli (15-19). Mast cells arise in the bone marrow where maturation is influenced by stem cell factors binding to the *c-kit* receptor and by other cytokines such as interleukin (IL)-3, -4, -9, and -10 and are traditionally considered to be inflammatory (20-24). These cytokines promote differentiation and proliferation of mast cells (25-28). The strength and nature of the response of mast cells to many activating stimuli, includes aggregation of high affinity IgE receptors by IgE and specific antigens (29-32). MCs are located close to blood vessels and nerve ending and their mediators can play an important role in innate and adaptive immunity. In humoral immune responses FcεR1 receptors facilitate allergen uptake and processing, with IgE occupancy the FcεRI receptor positively regulates the level of receptor expression (33-35). IgE can also bind the low-affinity FcεRII (CD23) receptor on B cells, where it serves to enhance both allergen-specific B and T cell recall functions (36-39). Mast cells secrete pre-stored mediators such as histamine and tryptase through rapid degranulation, as well as delay newly synthesized cytokines such as IL-4, IL-6, IL-8, IL-13, TNF alpha and IL-33, in response to allergic or neuropeptide triggers. Accessory cells, especially mast cells and basophils also produce IL-4 (40-41).

Histamine was synthesized in 1907 and later isolated from mammalian tissue. The bound form of histamine is biologically inactive, but many stimuli can trigger the release of mast cell histamine. Mast cells are especially rich at sites of potential tissue injury: nose, mouth, and feet; internal body surface; and blood vessels (42-43). However, the exact basis of mast cell-mediated activation of inflammation and immune responses is not clear.

*Role of mast cells in innate immunity*

Mast cells are involved in protection of the host from bacterial infection and have protective and pathogenic activity. They express a variety of pattern-recognition receptors, which have important roles in the activation of the innate immune response (44-46). In the body, antigenic compounds provide the initial danger signal and activate innate signaling receptors, leading to cytokine and chemokine secretion (47-50). Cross-linking of receptor-bound IgE by an allergen initiates cell activation and the release of preformed and newly generated mediators, cytokines, chemokines and growth factors. Many growth factors, chemokines and cytokines can influence the number and mediator content of mast cells and other aspects of their phenotype, including IL-3, which is especially important in mice, $T_H2$-associated cytokines (such as IL-4 and IL-9), and TGF-$b_1$ (51-53).

Dysregulated expression of pro-inflammatory cytokines is sufficient to produce tissue injury. The inflammatory reaction is triggered in response to infection and allergy. $T_H2$-type cytokines orchestrate the allergic inflammatory cascade that occurs in many inflammatory diseases. Tissue-derived cytokines and chemokines such as IL-33, IL-25, CCL17 and CCL22 influence antigen presenting cell (APC) activation and $T_H2$ maturation and migration. In chronic allergic diseases there is an elevated concentration of IL-33 in circulation (54-56). IL-33 is expressed by human synovial fibroblasts and induced by inflammatory cytokines (57-59). IL-33 plays a significant role in cytokine and chemokine production, which contribute to innate and antigen-induced tissue inflammation (60-61). IL-33 is a critical proinflammatory cytokine and promotes cellular and humoral immune responses, as well as mast cell activities. Inflammatory APC have been suggested to be necessary and sufficient for the development of $T_H2$ immunity to antigen stimulation (62-65). $T_{reg}$ cell development and suppression is fundamental in protecting normal tissue against antigen activation; while $T_H17$ cells are a distinct T cell lineage that does not share developmental pathways with either $T_H1$ or $T_H2$ cells and are inhibited by IFN-γ and IL-4 (66-68). $T_H17$ cells are characterized by the production of IL-17A, IL-17F and IL-22. IL-17A and IL-17F both induce IL-6, GM-CSF, CXCL10 and CXCL8 in several cell types (69-71). Different leukocyte subsets generate cytokines that influence different cell types and the attendant inflammatory response, driving tissue hyper-reactivity and inflammation (72-73). The important question that remains to be addressed is whether or not it will be possible to modulate the inappropriate or maladaptive consequences of innate

immune activation and pro-inflammatory cytokine expression in the mammalian tissue.

Mast cells can be categorized into populations defined by anatomical location and/or mediator content (such as proteoglycans (heparin versus chondroitin sulfates) or proteases (tryptases, chymases. Mast cell activation via cross-linking of IgE bound to high-affinity receptors for IgE (FceRI) on the cell surface by antigens result in rapid exocytosis of cytoplasmic granules (degranulation) and the production of leukotrienes, prostaglandins, growth factors, chemokines, and many cytokines (74). Many of these mediators have proinflammatory effects, promote tissue remodeling and contribute to tissue repair; while others can have an anti-inflammatory effect (75-78).

Human mast cells have been categorized on the basis of their protease content into those that contain predominantly tryptase or (more rarely) chymase or both major proteases (79). MCP-6 a mast-cell protease, contributes to the recruitment of neutrophils to sites of bacterial infection (80-82). In humans mast cells contain tryptase but little or no chymase and are maintained in SCF-containing media which can induce more chymase after incubation with IL-4, IL-6 or IL-1b, TGF-b1, or some bacteria products (83-84). Mechanisms of tryptase-induced inflammation include leukocyte recruitment mediated indirectly by stimulating chemokine release from epithelial and endothelial cells (85-87). Recombinant human tryptase, introduced in the airway provokes production of the allergic cytokine IL-13, and bronchial irritability (88). In a histochemical study of human bronchi, it was demonstrated that chymase-positive mast cells are locally enriched in the immediate vicinity of sub-mucosal glands, where secreted chymase might be positioned to fulfill its potential as a secretagogue (89-90). Chymase augments the size of skin wheals (91) and chymase inhibitors decrease wheals induced by allergen. Therefore, chymase can worsen allergic inflammation by acting in conjunction with other inflammatory products of mast cells and contributes to matrix destruction directly by cleaving fibronectin and collagens.

*Role of mast cells in adaptive immunity*

Mast cells are important for both innate and adaptive immunity in tissues that are in close contact with the environment, i.e. the skin, the airways and the lung, and the lining of the intestine (92). Mast cells are commonly found at sites exposed to the external environment, namely the skin, the airways and the gastrointestinal tract (93). The crucial role of mast cells in the defense against parasites was defined thirty years ago and for many years the protective function of mast cells was only correlated with parasitic infections. Parasite infected tissue is associated with considerable increases in mast-cell numbers. This effect confirms that MCs are involved in adaptive immunity where they secrete protease for MC functions and inflammatory cytokines. In addition, Th2 cells are the major actors in the response against parasites and play a central role in allergic inflammation where high concentrations of circulating IgE result in high surface expression of FceRI by tissue mast cells (94).

In certain conditions mast cells have the ability to secrete IL-10 via an FcgRIII-dependent mechanism. In addition to producing IL-10, mast cells can

**Table I.** *Mast cells release: cytokines, growth factors and phospholipids.*

| |
|---|
| ***Cytokines:*** |
| - Interleukins (IL)-1, 2, 3, 4, 5, 6, 8, 9, 10, 13, 16, 18, IL-33 |
| - IFN-α, IFN-β, IFN-γ; MIF; TGFβ; TNF-α, MIP-1α, MCP-1 |
| ***Growth factors:*** |
| - SCF, GM-CSF, β-FGF, neurotrophin 3, NGF, PDGF, TGFβ, VEGF |
| ***Phospholipid metabolites:*** |
| - Leukotriene $B_4$ |
| - Leukotriene $C_4$ |

produce a large spectrum of cytokines, chemokines and growth factors, as well as histamine and other mediators, many of which can participate in innate immunity and adaptive immunity. For instance, mast cells represent a potential source of IL-33, IL-9, and TNF alpha which can have an influence on white blood cells such as macrophages, neutrophils and lymphocytes. Addition of IL-5 to human umbilical cord blood-derived cultured mast cells augment IgE-induced production of distinct cytokines, such as tumor necrosis factor-α (TNF-α), macrophage inflammatory protein-1α (MIP-1α) and granulocyte–macrophage-colony stimulating factor (GM-CSF), without histamine release.

In cancer, mast-cell accumulation has also been noted repeatedly around melanomas, especially invasive melanoma (95). In fact, mast-cell accumulation was correlated with increased neovascularization, mast-cell overexpression of VEGF, tumor aggressiveness and poor prognosis. In spite of their small number, mast cells are critically involved in the development of immunological abnormalities such as allergic and autoimmune disorders.

Recent technological and conceptual advances have ushered in an exciting new era in mast cell research. However, there are still many unsolved issues, including the regulatory mechanism of mast cell differentiation in the bone marrow; for example, the cytokines and transcription factors necessary for their differentiation and expansion, as well as the molecular mechanism underlying basophil migration

**Table II.** *Mast cell mediators.*

| |
|---|
| ***Mast Cell Preformed Mediators :*** |
| Histamine |
| Proteases |
| Serotonin |
| Heparin |
| IL-4, TNF, GM-CSF, IL-33 |
| |
| ***Mast Cell Newly Synthesized Mediators:*** |
| Lipid Derived Prostaglandin (D2) |
| Leukotrienes |
| PAF |
| Cytokines |
| Chemokines |
| Growth Factors |
| Free Radicals |
| Substance P |

**Table III.** *Mast cells are involved in many pathophysiological diseases, such as:*

| |
|---|
| immunology of allergic contact dermatitis and allergic asthma and skin barrier function and mechanisms in allergic airway inflammation |
| allergic and non-allergic immune responses |
| atherosclerosis |
| systemic sclerosis |
| renal injury and progressive renal diseases. |
| cannabinomimetic control in chronic inflammation. |
| psoriasis |
| Systemic sclerosis; multiple sclerosis |
| pathophysiology of atopic eczema |
| bacteria, and intestinal immunity |
| molecular basis of contact allergy |
| immune responses of the dental pulp |
| acute graft rejection |
| modulation of the immune response. |
| angiogenesis, tissue remodelling and immune-modulation. |
| gastrointestinal diseases |
| nematode infection |
| regulation of allergic sensitization |
| ischemia/reperfusion injury |
| cancer: in the pathogenesis of non-small cell lung cancer; colorectal cancer development; prostate cancer |

from the bloodstream to peripheral tissues such as lymph nodes.

In conclusion, mast cells contribute to:

- airway inflammatory response
- remodeling
- symptomatology
- initiation of the allergic immune response
- provide signals inducing IgE synthesis by B-lymphocytes
- induce Th2 lymphocyte differentiation.

## REFERENCES


1. Mekori YA, Metcalfe DD. Mast cells in innate immunity. Immunol Rev 2000; 173:131-40.
2. Di Muzio G, Perricone C, Ballanti E, et al. Complement system and rheumatoid arthritis: relationships with autoantibodies, serological, clinical features, and anti-TNF treatment. Int J Immunopathol Pharmacol 2011; 24:357-66.
3. Colombo C, Faelli N, Tirelli AS, et al. Analysis of inflammatory and immune response biomarkers in sputum and exhaled breath condensate by a multi-parametric biochip array in cystic fibrosis. Int J Immunopathol Pharmacol 2011; 24:423-32.
4. Belizário JE. Pathogens and dead cells cooperate with cytokines in activating the innate and adaptive response. Eur J Inflamm 2011; 9:1-11.
5. Amin K. The role of mast cells in allergic inflammation. Respiratory Medicine 2012: 106:9-14.
6. Guillén D, Millán O, Brunet M. *In vitro* studies of the immunomodulatory effects of statins alone and in combination with immunosuppressive drugs. Eur J Inflamm 2011; 9:117-24.
7. Losi M, Bocchino M, Matarese A, et al. Role of the quantiferon-TB test in ruling out pleural tuberculosis: a multi-centre study. Int J Immunopathol Pharmacol 2011; 24:159-65.
8. Iezzi M, Quaglino E, Cappello P, Toto V, Sabatini F, Curcio C, Garotta G, Musiani P, Cavallo F. HCG hastens both the development of mammary carcinoma and the metastatization of HCG/LH and ERBB-2 receptor-positive cells in mice. Int J Immunopathol Pharmacol 2011; 24:621-30.
9. Sancilio S, Di Giacomo V, Quaglietta AM, et al. TRAIL promotes a pro-survival signal in erythropoietin-deprived human erythroblasts through the activation of an NF-κB/IκBα pathway. J Biol Regul Homeost Agents 2011; 25:375-86.
10. Borish L, Joseph BZ. Inflammation and the allergic response. Med Clin North Am 1992; 76:765-87.
11. Cantarini L, Iacoponi F, Lucherini OM, et al. Validation of a diagnostic score for the diagnosis of autoinflammatory diseases in adults. Int J Immunopathol Pharmacol 2011; 24:695-702.
12. Wu KG, Li TH, Chen CJ, Cheng HI, Wang TY. Correlations of serum Interleukin-16, total IgE, eosinophil cationic protein and total eosinophil counts with disease activity in children with atopic dermatitis. Int J Immunopathol Pharmacol 2011; 24:15-23.
13. Berardi D, De Benedittis S, Scoccia A, Perfetti G. Evaluation of neridronate on the osseointegration process of endeous titanium implants in animal models. Eur J Inflamm 2011; 9:141-49.
14. Belloli L, Carlo-Stella N, Ughi N, Marasini B. Cancer in Italian patients with systemic sclerosis. Eur J Inflamm 2011; 9:151-56.
15. Kunder CA, St John AL, Abraham SN. Mast cell modulation of vascular and lymphatic endothelium. Blood 2011; 118(20):5383-93.
16. Li XF, Guo YJ, Wang ML, Zhang DM, Li YH, Wang YF, Tao JY, Zhang SL, Dong JH, Li LL, Zhao L. Inducing-apoptotic activity of the ethanol extract of Duchesnea indica Focke on treatment of herpes simplex encephalitis. Int J Immunopathol Pharmacol 2011; 24:631-8.
17. Gallenga PE, Del Boccio M, Rapinese M, Di Iorio A, Toniato E, Martinotti S. Molecular approach by PCR is the best method to detect the presence of Chlamydia trachomatis and to define the true agent of ocular bacterial inflammation. Int J Immunopathol Pharmacol 2011; 24:285-96.
18. Mirzaei K, Hossein-Nezhad A, Mokhtari F, Najmafshar A, Khoshniat Nikoo M. VISFATIN/NAMPT/PBCEF and cytokine concentration in multiple sclerosis patients compared to healthy subjects. Eur J Inflamm 2011; 9:31-37.
19. Kokkas A, Goulas A, Stavrianos C, Anogianakis G. The role of cytokines in pulp inflammation. J Biol Regul Homeost Agents 2011; 25:303-11.
20. Ishizaka T, Mitsui H, Yanagida M, Miura T, Dvorak AM. Development of human mast cells from their

progenitors. Curr Opin Immunol 1993; 5:937-43.
21. Nenna R, Papoff P, Moretti C, et al. Detection of respiratory viruses in the 2009 winter season in Rome: 2009 influenza A (H1N1) complications in children and concomitant type 1 diabetes onset. Int J Immunopathol Pharmacol 2011; 24:651-9.
22. Drago L, Vassena C, Dozio E, Corsi MM, De Vecchi E, Mattina R, Romanò C. Procalcitonin, C-reactive protein, interleukin-6, and soluble intercellular adhesion molecule-1 as markers of postoperative orthopaedic joint prosthesis infections. Int J Immunopathol Pharmacol 2011; 24:433-40.
23. Mazzoccoli G, Carughi S, Sperandeo M, Pazienza V, Giuliani F, Tarquini R. Neuro-endocrine correlations of hypothalamic-pituitary-thyroid axis in healthy humans. J Biol Regul Homeost Agents 2011; 25:249-57.
24. Pollice R, Bianchini V, Marola V, Verni L, Di Mauro S, Ussorio D, Cavicchio A, Ortenzi R, Roncone R, Casacchia M. Post-traumatic and psychiatric symptoms among young earthquake survivors in primary care camp hospital. Eur J Inflamm 2011; 9:39-44.
25. Okayama Y, Kawakami T. Development, migration, and survival of mast cells. Immunol Res 2006; 34:97-115.
26. Sharma JN, Kesavarao U. The effects of captopril on cardiac regression, blood pressure and bradykinin components in diabetic Wistar Kyoto rats. Int J Immunopathol Pharmacol 2011; 24:337-43.
27. De Amici M, Villani MA, Milanesi E, Rossini B, Barco S, Gerletti M, Ciprandi G. Adverse reactions to anaesthetics prevented by the use of specific laboratory tests Eur J Inflamm 2011; 9:79-81.
28. Tsoupras AB, Chini M, Tsogas N, Mangafas N, Demopoulos CA, Lazanas MC. *In vivo* effects of a *Ginkgo biloba* extract on platelet activating factor metabolism in two asymptomatic HIV-infected patients. Eur J Inflamm 2011; 9:107-16
29. Platzer B, Ruiter F, van der Mee J, Fiebiger E. Soluble IgE receptors--elements of the IgE network. Immunol Lett 2011; 141(1):36-44.
30. Rivetti S, Lauriola M, Voltattorni M, et al. Gene expression profile of human colon cancer cells treated with cross-reacting material 197, a diphtheria toxin non-toxic mutant. Int J Immunopathol Pharmacol 2011; 24:639-49.
31. Symeonidou I, Hatzistilianou M, Papadopoulos E, Dovas CI, Karagouni E, Pappa S, Pantzartzi CN, Kourelis A, Frydas S. Susceptibility and resistance to canine leishmaniosis is associated to polymorphisms of the canine TNF-α gene. Eur J Inflamm 2011; 9:23-29.
32. Zanna P, Maida I, Turpin Sevilla MC, et al. Molecular characterization of novel melanoma cell lines. J Biol Regul Homeost Agents 2011; 25:239-47.
33. Wu LC. Immunoglobulin E receptor signaling and asthma. J Biol Chem 2011; 286(38):32891-7.
34. Tammaro A, Narcisi A, Persechino S, De Marco G, Camplone G. Contact allergy to disperse blue dye in goggles for swimming-bath. Eur J Inflamm 2011; 9:83-84.
35. Veda P. Why are neutrophils polymorphonuclear? Eur J Inflamm 2011; 9:85-93.
36. Caughey GH. Mast cell proteases as protective and inflammatory mediators. Adv Exp Med Biol 2011; 716:212-34.
37. Romano G, Barbagli G, Lazzeri M. The use of topical hyaluronic acid and silver sulfadiazine (Altergen®) in patients undergoing two-stage anterior urethroplasty with oral mucosal graft. Eur J Inflamm 2011; 9:175-183.
38. Hossein-Nezhad A, Mirzaei K, Aslani S, Tootee A, Karimi F. MIF expression in induced peripheral blood mononuclear cells by vitamin D3 and its potential correlation with resting metabolic rate in obesity. Eur J Inflamm 2011; 9:125-34.
39. Naruishi K, Omori K, Maeda H, et al. Immune responses to *Porphyromonas gingivalis* infection suppress systemic inflammatory response in experimental murine model. J Biol Regul Homeost Agents 2011; 25:195-202.
40. Nakanishi K. Basophils are potent antigen-presenting cells that selectively induce Th2 cells. Eur J Immunol 2010; 40:1836-42.
41. Scaparrotta A, Verrotti A, Consilvio NP, Cingolani A, Di Pillo S, Di Gioacchino M, Verini M, Chiarelli F. Pathogenesis and clinical approaches to anticonvulsant hypersensitivity syndrome: current state of knowledge. Int J Immunopathol Pharmacol 2011; 24:277-84.
42. Church MK, Levi-Schaffer F. The human mast cell. J

Allergy Clin Immunol 1997; 99:155-60.
43. Pandolfi F, Cianci R, Casciano F, Pagliari D, De Pasquale T, Landolfi R, Di Sante G, Kurnick JT, Ria F. Skewed T-cell receptor repertoire: more than a marker of malignancy, a tool to dissect the immunopathology of inflammatory diseases. J Biol Regul Homeost Agents 2011; 25:153-161.
44. Galli SJ, Borregaard N, Wynn TA. Phenotypic and functional plasticity of cells of innate immunity: macrophages, mast cells and neutrophils. Nature Immunology 2011; 12:1035-44.
45. Altorjay I, Veréb Z, Serfozo Z, et al. Anti-TNF-alpha antibody (infliximab) therapy supports the recovery of eNOS and VEGFR2 protein expression in endothelial cells. Int J Immunopathol Pharmacol 2011; 24:323-35.
46. Wu KG, Li TH, Chen CJ, Cheng HI, Wang TY. A pilot study evaluating the clinical and immunomodulatory effects of an orally administered extract of Dendrobium huoshanense in children with moderate to severe recalcitrant atopic dermatitis. Int J Immunopathol Pharmacol 2011; 24:367-75.
47. 47. Chaly Y, Marinov AD, Oxburgh L, Bushnell DS, Hirsch R. FSTL1 promotes arthritis in mice by enhancing inflammatory cytokine/chemokine expression. Arthritis Rheum 2012; 64(4):1082-8.
48. Salini V, Conti P. Inflammatory markers: serum amyloid A, fibrinogen and C-reactive protein – a revisited study. Eur J Inflamm 2011; 9:95-102.
49. Failli A, Legitimo A, Mazzoni A, Urbani L, Scatena F, Mosca F, Consolini R. The combination of immunosuppressive drugs with 8-methoxypsoralen and ultraviolet a light modulates the myeloid-derived dendritic cell function. Int J Immunopathol Pharmacol 2011; 24:89-99.
50. Silambarasan G, Ramanathan T, Nabeel MA, Kalaichelvan VK, Kathiresan K, Balasubramanian T. Anti-inflammatory activity of the marine cyanobacterium *trichodesmium erythraeum* against carrageenan-induced paw oedema in wistar albino rats. Eur J Inflamm 2011; 9:53-56.
51. Hsu CL, Neilsen CV, Bryce PJ. IL-33 is produced by mast cells and regulates IgE-dependent inflammation. PLoS One 2010; 5(8):e11944.
52. Binici DN, Güneş N, Kayataş K, Pişkinpaşa N. The effects of interferon-α2b on intestinal flora in peritoneal fibrosis. Eur J Inflamm 2011; 9:135-39.
53. Ciprandi G, De Amici M, Berardi L, Vignini M, Marseglia G. Serum IgE for Bet v 1 in patients affected by atopic dermatitis. Eur J Inflamm 2011;9:205-207.
54. Hsu CL, Neilsen CV, Bryce PJ. IL-33 is produced by mast cells and regulates IgE-dependent inflammation. PLoS One 2010; 5(8):e11944.
55. Rigante D, Zampetti A, Bersani G, Candelli M, Piras A, Rendeli C, Antuzzi D, Feliciani C, Stabile A. Serum interleukin-18 in children with Henoch-Schönlein purpura: a promising marker of disease activity. Eur J Inflamm 2011; 9:157-68.
56. Nisticò R, Mehdawy B, Piccirilli S, Mercuri N. Paraquat- and rotenone-induced models of Parkinson's disease. Int J Immunopathol Pharmacol 2011; 24:313-22.
57. Kurokawa M, Matsukura S, Kawaguchi M, et al. Expression and effects of IL-33 and ST2 in allergic bronchial asthma: IL-33 induces eotaxin production in lung fibroblasts. Int Arch Allergy Immunol 2011; 155S1:12-20.
58. Marzano AV, Cugno M, Trevisan V, Lazzari R, Fanoni D, Berti E, Crosti C. Inflammatory cells, cytokines and matrix metalloproteinases in amicrobial pustulosis of the folds and other neutrophilic dermatoses. Int J Immunopathol Pharmacol 2011; 24:451-60.
59. Scaramuzzo L, Manicone PF, Graci C, Muratori F, Spinelli MS, Damis G, Raffaelli L, Maccauro G. Morphological modifications in osteoarthritis: a scanning electron microscopy study Eur J Inflamm 2011; 9:73-78.
60. Liew FY. IL-33: a Janus cytokine. Ann Rheum Dis 2012; 71 (S2): i101-4.
61. Shi Q, Gao ZY, Xie F, Wang LF, Gu YP, Yang TJ, Huang L, Qian QH, Qiu YH. A novel monoclonal antibody against human CD80 and its immune protection in a mouse lupus-like disease. Int J Immunopathol Pharmacol 2011; 24:583-93.
62. Mitsui H, Furitsu T, Dvorak AM, et al. Development of human mast cells from umbilical cord blood cells by recombinant human and murine c-kit ligand. Proc Natl Acad Sci USA 1993; 90:735-39.
63. Sakellaropoulou AV, Hatzistilianou MN, Emporiadou MN, Aivazis VT, Rousso I, Athanasiadou-Piperopoulou F. Evaluation of thyroid gland function

in children with obstructive apnea hypopnea syndrome. Int J Immunopathol Pharmacol 2011; 24:377-86.
64. Tsoucalas G, Karamanou M, Androutsos G. Travelling through time with aspirin, a healing companion. Eur J Inflamm 2011; 9:13-16.
65. Ciprandi G, De Amici M, Quaglini S, et al., Workgroup "Allergy Project". Prediction of allergy by total serum IgE measurements in infancy: a 10-year follow-up. Eur J Inflamm 2011; 9:199-203.
66. Hovhannisyan Z, Treatman J, Littman DR, Mayer L. Characterization of interleukin-17-producing regulatory T cells in inflamed intestinal mucosa from patients with inflammatory bowel diseases. Gastroenterology 2011; 140(3):957-65.
67. Zhang C-Y, Shao S-H, Chen X, Shi Y-L. Anti-frostbite effects of *prunus tomentosa thunb* total flavone Eur J Inflamm 2011; 9:65-71.
68. Artini M, Scoarughi GL, Papa R, et al. A new anti-infective strategy to reduce adhesion-mediated virulence in Staphylococcus aureus affecting surface proteins. Int J Immunopathol Pharmacol 2011; 24:661-72.
69. Penna G, Fibbi B, Amuchastegui S, et al. Human benign prostatic hyperplasia stromal cells as inducers and targets of chronic immuno-mediated inflammation. J Immunol 2009; 182(7):4056-64.
70. Palumbo P, Cinque B, Miconi G, et al. Biological effects of low frequency high intensity ultrasound application on ex vivo human adipose tissue. Int J Immunopathol Pharmacol 2011; 24:411-22.
71. Di Paola R, Mazzon E, Paterniti I, Impellizzeri D, Bramanti P, Cuzzocrea S. Apocynin, a plant-derived drug, might be useful in the treatment of myocardial ischemia reperfusion injury in rat hearts. Eur J Inflamm 2011; 9:169-74.
72. K. Amin, C. Janson, G. Boman, P. Venge. The extracellular deposition of mast cell products is increased in hypertrophic airways smooth muscles in allergic asthma but not in nonallergic asthma. Allergy 2005; 60:1241-47.
73. Zhu J-S, Xu Z-P, Song M-Q, Zhang Q. Effect of oxymatrine combined with low dose 5-FU on lymphatic vessel and microvascular endothelial cell growth of gastric cancer in a severe combined immunodeficient mouse orthotopic implantation model. Eur J Inflamm 2011; 9:45-51.
74. Klein LM, Lavker RM, Matis WL, Murphy GF. Degranulation of human mast cells induces an endothelial antigen central to leukocyte adhesion. Proc Natl Acad Sci USA 1989; 86:8972-76.
75. Tziakas DN, Chalikias GK, Kaski JC. Anti-inflammatory cytokines: a wolf in sheep's clothing? Am J Med 2012; 125(5):e19.
76. Conti CM, Maccauro G, Fulcheri M. Psychological stress and cancer. Int J Immunopathol Pharmacol 2011; 24:1-5.
77. Racciatti D, Gorgoretti V, Sepede G, Gambi F, Pizzigallo E. An Italian study on health-related quality of life and fatigue in patients with chronic fatigue syndrome and patients with chronic HCV virus infection: similarities and differences. Int J Immunopathol Pharmacol 2011; 24:673-81.
78. Tripodi D, D'Ercole S, Pasini M, Nastasio S, Bonini S, Giuca MR. Inflammatory and immunitary modifications in saliva of subjects with labial and tongue piercing. Eur J Inflamm 2011; 9:185-91.
79. Caughey GH. Mast cell proteases as protective and inflammatory mediators. Adv Exp Med Biol 2011; 716:212-34.
80. Shelburne CP, Nakano H, St John AL, Chan C, McLachlan JB, Gunn MD, Staats HF, Abraham SN. Mast cells augment adaptive immunity by orchestrating dendritic cell trafficking through infected tissues. Cell Host Microbe 2009; 6(4):331-42.
81. Saggini A, Anogeianaki A, Maccauro G, Teté S, Salini V, Caraffa A, Conti P, Shaik-Dasthagirisaheb YB. What you should know about *Escherichia coli* infection. Eur J Inflamm 2011; 9:103-106.
82. Marchisio P, Bianchini S, Galeone C, Baggi E, Rossi E, Albertario G, Torretta S, Pignataro L, Esposito S, Principi N. Use of complementary and alternative medicine in children with recurrent acute otitis media in Italy. Int J Immunopathol Pharmacol 2011; 24:441-9.
83. Khodoun MV, Orekhova T, Potter C, Morris S, Finkelman FD. Basophils initiate IL-4 production during a memory T-dependent response. J Exp Med 2004; 200(7):857-70.
84. Giganti MG, Minella D, Testa B, Zenobi R, Biancolella M, Isidori AM, Caprio M, Novelli G, Fabbri A. A pilot study on the transcriptional

response of androgen- and insulin-related genes in peripheral blood mononuclear cells induced by testosterone administration in hypogonadal men. J Biol Regul Homeost Agents 2011; 25:291-94.

85. Cromwell O, Hamid Q, Corrigan CJ, Barkans J, Meng Q, Collins PD, Kay AB. Expression and generation of interleukin-8, IL-6 and granulocyte-macrophage colony-stimulating factor by bronchial epithelial cells and enhancement by IL-1 beta and tumour necrosis factor-alpha. Immunology 1992; 77(3):330-7.
86. Re M, Magliulo G, Tarchini P, Mallardi V, Rubini C, Santarelli A, Lo Muzio L. p53 and BCL-2 over-expression inversely correlates with histological differentiation in occupational ethmoidal intestinal-type sinonasal adenocarcinoma. Int J Immunopathol Pharmacol 2011; 24:603-9.
87. Maghbooli Z, Hossein-Nezhad A, Shirzad M, Behzadi H. The role of osteoprotegrin/ nuclear factor kb ligand in coronary collateral development Eur J Inflamm 2011; 9:57-64.
88. Wong GW, Foster PS, Yasuda S, Qi JC, Mahalingam S, Mellor EA, Katsoulotos G, Li L, Boyce JA, Krilis SA, Stevens RL. Biochemical and functional characterization of human transmembrane tryptase (TMT)/tryptase gamma. TMT is an exocytosed mast cell protease that induces airway hyperresponsiveness in vivo via an interleukin-13/interleukin-4 receptor alpha/signal transducer and activator of transcription (STAT) 6-dependent pathway. J Biol Chem 2002; 277(44):41906-15.
89. Matin R, Tam EK, Nadel JA, Caughey GH. Distribution of chymase-containing mast cells in human bronchi. J Histochem Cytochem 1992; 40(6):781-6.
90. Migueres M, Fontaine JF, Haddad T, Grosclaude M, Saint-Martin F, Bem David D, Crestani B. Characteristics of patients with respiratory allergy in France and factors influencing immunotherapy prescription: a prospective observational study (REALIS). Int J Immunopathol Pharmacol 2011; 24:387-400.
91. Rubinstein I, Nadel JA, Graf PD, Caughey GH. Mast cell chymase potentiates histamine-induced wheal formation in the skin of ragweed-allergic dogs. J Clin Invest 1990; 86(2):555-9.
92. L. Enerback. Mast cells in rat gastrointestinal mucosa. 2. Dye-binding and metachromatic properties. Acta Pathol Microbiol Scand 1966; 66:303-12.
93. Saggini A, Tripodi D, Maccauro G, et al. Tumor necrosis factor-alpha and mast cells: revisited study. Eur J Inflamm 2011; 9:17-22.
94. Aslani S, Hossein-Nezhad A, Mirzaei K, Maghbooli Z, Asgarabad SN, Karimi F. Tandem repeats of the CATT element of macrophage migration inhibitory factor gene may predict gestational diabetes mellitus severity. Eur J Inflamm 2011; 9:193-97.
95. TC Theoharides, P Conti. Mast cells: the Jekyll and Hyde of tumor growth. Trends Immunol 2004; 25:235-41.

# THE ANTIOXIDANT EFFECT OF FERMENTED PAPAYA PREPARATION INVOLVES IRON CHELATION

E. PRUS and E. FIBACH

*Department of Hematology, Hadassah – Hebrew University Medical Center, Jerusalem, Israel*

*Received September 8, 2011 – Accepted February 27, 2012*

**Iron-overload is a major clinical problem in various diseases. Under this condition, serum iron which surpasses the binding capacity of transferrin is present as non-transferrin bound iron and cellular unbound Labile Iron Pool (LIP) is increased. LIP participates in the generation of free radicals, including reactive oxygen species (ROS). Increased ROS, with concomitant decrease in anti-oxidants, results in oxidative stress and toxicity to the liver, heart and other tissues, causing serious morbidity and eventually mortality. Therapeutic iron chelation reduces the LIP and thereby ameliorates oxidative stress-mediated toxicity. Many food-derived antioxidants have the capacities to scavenge ROS and chelate iron. We have reported that fermented papaya preparation (FPP) has ROS scavenging effect on blood cells in vitro or in vivo (in thalassemic patients and experimental animals). We now investigated FPP's iron chelating effect - its ability to prevent (and revert) LIP accumulation. Liver- and heart-derived cells, and RBCs were exposed to non-transferrin bound iron in the form of ferrous ammonium sulfate and the effect of FPP on their LIP content and ROS generation was measured by flow-cytometry. The results indicate that FPP reduces LIP and ROS, and suggests that its antioxidant mechanism is related, at least in part, to iron chelation.**

Iron overload is a major clinical problem associated with various diseases (1). In hereditary hemolytic anemias, such as thalassemia, it is caused by repeated blood transfusions and increased iron uptake in the gastrointestinal track (2). The latter is believed to be due to decreased hepcidin production associated with elevated erythropoiesis (3). In anemia of chronic disease, iron overload is due to increased production of hepcidin due to high levels of cytokines such as IL-6 (4). In other diseases such as in hereditary hemochromatosis it is caused by abnormalities in other iron-regulating proteins (5).

Normally, iron is transported in the circulation and transferred into cells through binding to transferrin (6). In iron overload, serum iron exceeds the binding capacity of transferrin, and it is present in the form of non-transferrin bound iron (NTBI) (7). In cells, iron is bound to various components such as hemoglobin, heme and cytochrome C; excess is stored in ferritin (8). In addition, all cells contain some unbound, chelatable iron, termed labile iron pool (LIP) or labile cellular iron (LCI) (9, 10). It was first suggested by Jacobs as a low molecular weight intermediate or transitory pool between extracellular iron and cellular firmly bound iron (9). This iron is redox active and it participates in the generation of free radicals, reactive oxygen species (ROS) (11). ROS have important physiological functions, but in excess they are cytotoxic due to their interaction with DNA, proteins and mainly with the membrane

*Key words: iron overload, iron chelation, oxidative stress*

*Mailing address:* Dr Eitan Fibach,
Department of Hematology,
Hadassah – Hebrew University Medical Center,
Ein-Kerem,
Jerusalem 91120, Israel
Tel: +972 26776751 Fax: +972 26423067
e-mail: Fibach@yahoo.com



0393-974X (2012)

**DISCLOSURE: ALL AUTHORS REPORT NO CONFLICTS OF INTEREST RELEVANT TO THIS ARTICLE.**

lipids (12). Normally, their level is tightly balanced by anti-oxidant systems that regulate the rate of ROS generation and scavenge excess ROS (13). In iron overload, increased ROS, with concomitant decrease in anti-oxidants, results in oxidative stress which affects vital organs such as the liver, heart and the endocrine system, causing serious morbidity and eventually mortality (14). In thalassemia it causes chronic anemia due to ineffective erythropoiesis (increased apoptosis of erythroid precursors in the bone marrow) and shortened survival of mature RBC in the circulation (13).

Many dietary antioxidants have the capacity to scavenge ROS (15); in addition, some of them, e.g., polyphenols, have been shown to possess iron chelating capacity (16). Fermented papaya preparation (FPP) is a product of yeast fermentation of *Carica papaya Linn*. Studies in chronic and degenerative disease conditions, such as thalassemia(11), cirrhosis (17), diabetes (18) and aging (19), and performance sports (20) have shown that FPP favorably modulates immunological, hematological, inflammatory, vascular and oxidative stress damage parameters (20). We have studied its anti-oxidant properties on blood cells in various hematological diseases, such as thalassemia, paroxysmal nocturnal hemoglobinuria and the myelodysplastic syndrome (21, 22). *In vitro* and *in vivo* (in patients and experimental animals) studies show that FPP ameliorates the oxidative stress of RBC, granulocytes and platelets. Some of these diseases are characterized by iron overload that requires chelation therapy (23). It has been shown that FPP protected against damage to DNA (induction of single and double strand breaks) and proteins (albumin) caused by combined treatment with ferric nitrilotriacetate and hydrogen peroxide, suggesting that the antioxidant properties of FPP are related to both hydroxyl scavenging, as well as iron chelating properties (24).

Since LIP is the major culprit in iron-mediated cytotoxicity, in the present study we investigated the ability of FPP to prevent (and revert) cellular accumulation of LIP and thereby reduce ROS generation. Liver- and heart-derived cells, as well as RBCs were exposed to NTBI in the form of ferrous ammonium sulfate (FAS) and the effects of FPP on their LIP and ROS were measured by flow cytometry. The results indicate that FPP reduces LIP, and suggests that the antioxidant mechanism of FPP is related, at least in part, to iron chelation.

## MATERIALS AND METHODS

*Blood cells and cell lines*

Normal human peripheral RBCs were obtained in heparin-containing tubes from normal blood donors who gave written informed consent. The research was approved by the Hadassah – Hebrew University Medical Center Human Experimentation Review Board. HEPG2 cells are human hepatoma-derived cell line (25); H9C2 cells are embryonic rat heart-derived cell line (26) (both from ATCC, Manassas, VA). The cells grew as monolayers in alpha medium supplemented with 10% fetal bovine serum, and were subcultured once a week with 0.25% (w/v) trypsin- 0.53 mM EDTA solution. Cells were incubated at 37°C in a humidified atmosphere of 5% $CO_2$ in air.

*FPP and iron*

FPP, a product of yeast fermentation of *Carica papaya Linn,* was supplied as sachets containing 3g powder, by Osato Research Institute, Gifu, Japan. The composition of its principal components was previously reported (27). FPP was dissolved in water and used at final concentration of 50 mg/ml, unless otherwise indicated. Ferrous ammonium sulfate (FAS) (Sigma, St. Louis, MO) was freshly dissolved for each experiment in water to 1 mM and used at final concentration of 20 mM, unless otherwise indicated.

*LIP and ROS*

Cytosolic LIP was determined by staining the cells with 0.25 mM calcein acetoxymethyl ester (CA-AM) (Sigma-Aldrich, St. Louis, MO). CA-AM enters viable cells and becomes fluorescent upon hydrolysis by esterases; its fluorescence is quenched by binding of LIP (28). Mitochondrial LIP was measured in HEPG2 and H9C2 cells by staining with 1 mM rhodamine B-[(1,10-phenanthrolin-5-yl)-aminocarbonyl] benzyl ester (RPA, Squarix biotechnology, Marl, Germany). It enters viable cells and specifically localized in the mitochondria; its fluorescence is quenched by binding of the mitochondrial LIP (29). The CA- and RPA-fluorescence is reversely proportional to the amount of cytosolic and mitochondrial LIP, respectively. ROS were measured by staining with 0.2 mM 2'-7'-dichlorofluorescin diacetate (DCF, Sigma). Upon crossing the membrane, this compound undergoes deacetylation by cellular esterases, producing a non-fluorescent compound that is trapped inside the cells. Its oxidation by ROS produces a fluorescent compound - 2'-7'-dichlorofluorescine (30). The DCF-fluorescence is

proportional to the amount ROS. Staining was done by incubating the cells with the reagents for 15-min at 37ºC.

*Flow cytometry*

Cell fluorescence was analyzed by a flow cytometer (FACS-calibur$^R$, Becton-Dickinson, Immunofluorometry systems, Mountain View, CA) as previously described (31). A 488-nm argon laser was used for excitation. At least 20,000 cells were analyzed using logarithmic amplification for the fluorescence signal height and linear amplification for forward light scatter and side light scatter. The arithmetic Mean Fluorescence Intensities (MFI) were calculated by the CellQuest$^R$ software (Becton-Dickinson). For each experiment, unstained cells served as controls; their MFI was <10. The results are expressed as the average ± standard deviation (SD) MFI and compared using the two-sample Student's *t*-test for differences in means of MFI; $p< 0.05$ was considered significant.

## RESULTS

The flow cytometry methodology for measuring the cellular and mitochondrial LIP contents and ROS generation is demonstrated in Fig. 1. Monolayers of HepG2 cells were trypsinized and the cell suspension incubated for 2 h in phosphate buffered saline (PBS) with FAS (20 mM) with and without FPP (50 mg/ml), or with none (Cont.). The cells were washed and stained for 15 min with either DCF (0.2 mM), CA-AM (0.25 mM) or RPA (1 mM). The cells were then washed, suspended in PBS and their fluorescence determined by flow cytometry. The results show that incubation with FAS increased the DCF-fluorescence indicating an 8.3-fold increase in ROS generation (Fig. 1B); decreased the CA- and RPA-fluorescence - indicating a 3.3-fold and 9.4-fold increases in the cytosolic and mitochondrial LIPs, respectively (Fig. IC-D). FPP ameliorated these effects of iron (Fig. 1, B-D).

Using this methodology, we studied the effects of FPP on ROS and LIP in HepG2 cells, H9C2 cells and in RBCs treated with or without FAS. In these

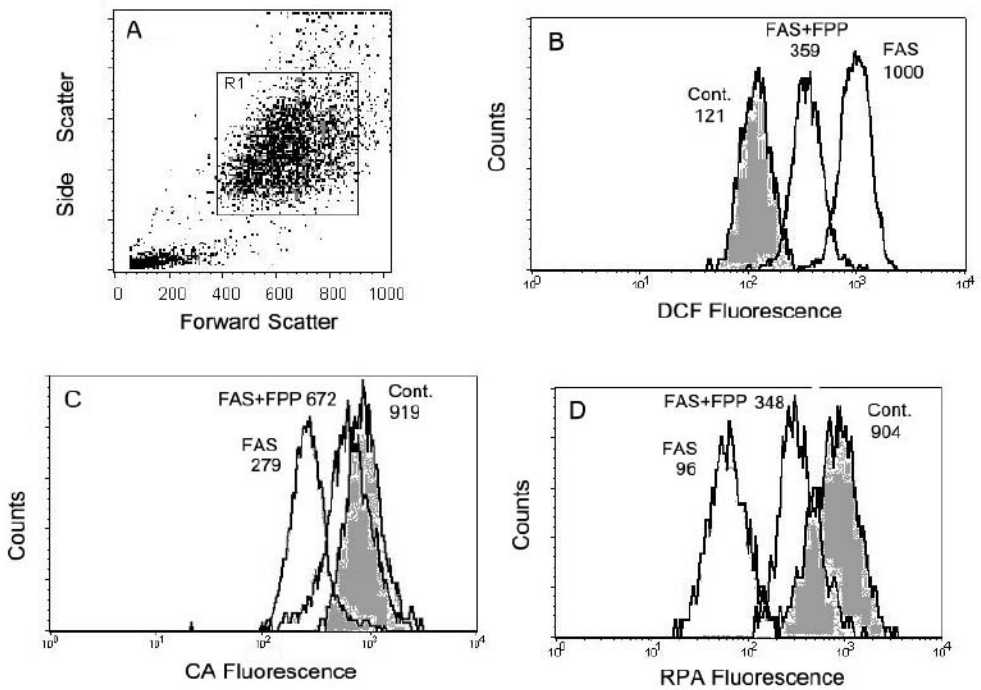


**Fig. 1.** *Flow cytometry analyses of LIP and ROS in cells treated with iron and FPP. Monolayers of HepG2 cells were trypsinized and the cell suspension in PBS was incubated for 1 h with FAS (20 mM) with and without FPP (50 mg/ml), or with none (Cont., grey). The cells were washed and diluted in PBS and labeled with for 15 min with either DCF (0.2 mM), CA-AM (0.25 mM) or RPA (1 mM). The cells were then washed and suspended in PBS and analyzed by flow cytometry.* ***A)*** *A forward light scatter x side light scatter dot-plot showing a gate (R1) on live cells.* ***B-D)*** *Distribution histograms of cells with respect to their DCF- (B), CA- (C) and RPA- (D) fluorescence. The mean fluorescence intensity of each histogram is shown. The results show that iron caused an increase in the DCF-fluorescence (1000 vs 121) – indicating an increase in ROS generation, and a decrease in CA- (279 vs 919) and RPA- (96 vs 904) fluorescence - indicating an increase in the cytosolic and mitochondrial LIP, respectively. FPP ameliorated these effects of iron (B-D).*

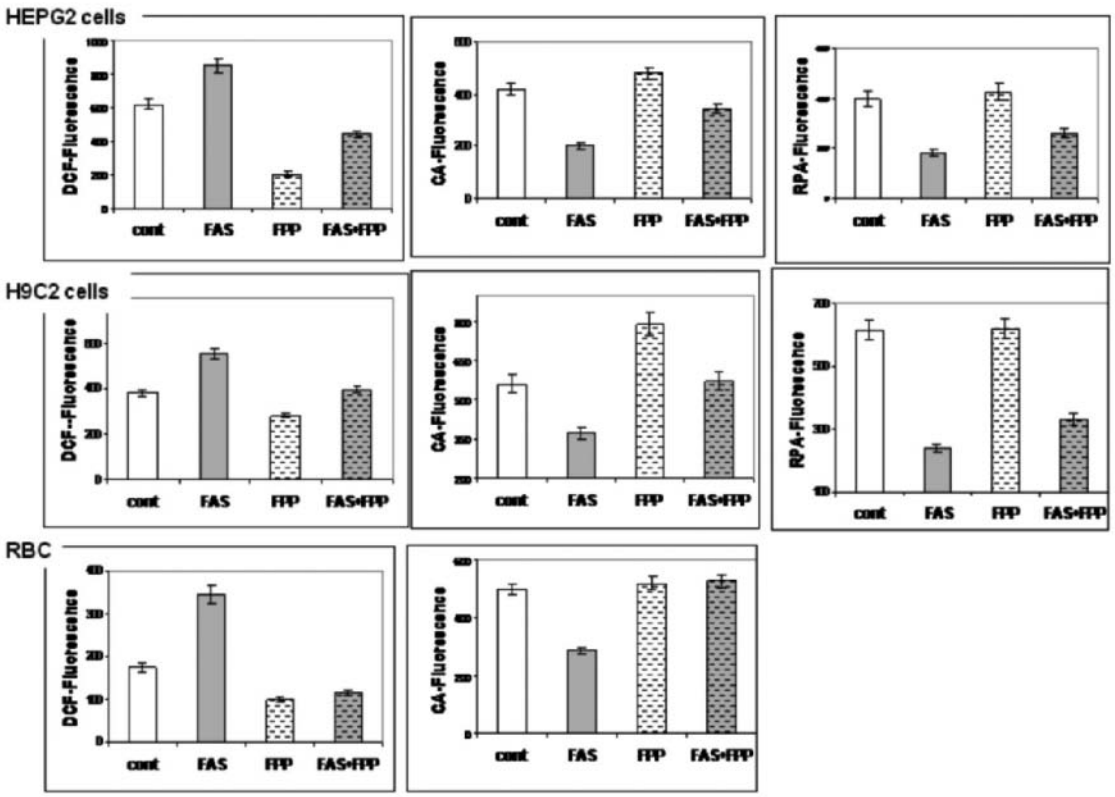


**Fig. 2.** *The effects of iron and FPP on cellular LIP and ROS. HEPG2 cells, H9C2 cells and RBCs were first stained for 15 min with DCF, CA-AM or RPA as indicated, washed and incubated for 1 h with FAS (20 mM), FPP (50 mg/ml), both, or none (cont). Cells were then washed with PBS and analyzed by flow cytometry. The data are presented as the MFI (mean ± SD) of 4 experiments. The results show that in all cells tested FAS increased the DCF-fluorescence, indicating an increase in ROS generation, and decreased the CA-fluorescence, indicating an increase in the cytosolic LIP. In HEPG2 and H9C2 cells, FAS also decreased the RPA-fluorescence, indicating an increase in the mitochondrial LIP. FPP had a significant ameliorating effect ROS generation and LIP accumulation in cells treated or untreated with iron.*

experiments (Fig. 2), cells were first stained with DCF, CA-AM or RPA as indicated, washed and incubated for 1 h with or without 20 mM FAS, FPP (50 mg/ml), both, or none (cont). Cells were then washed and analyzed by flow cytometry. The results show that in all cells tested FAS increased the DCF-fluorescence - indicating an increase in ROS generation, and decreased the CA-fluorescence - indicating an increase in the cytosolic LIP. In HEPG2 and H9C2 cells, FAS also decreased the RPA-fluorescence - indicating an increase in the mitochondrial LIP. FPP had a significant ameliorating effect on both ROS generation and LIP accumulation in cells treated or untreated with iron.

The dose-related effects of FAS and FPP on cytosolic LIP were studied by first staining HEPG2 cells with CA-AM (0.25 mM) for 15 min and then incubating the cells for 1 h with the different concentrations of FAS (A) or FPP (Fig. 3 A and B, respectively). A decrease in CA-fluorescence indicates an increase in LIP and vice versa. The results show that addition of FAS drastically increased the LIP (by 290% at 50 mM and 477% at 100 mM, Fig. 3A) while the addition of FPP moderately reduced the basal level of LIP (by 18% at 50 mg/ml, Fig. 3B). In Fig. 3, C and D, the difference in CA-fluorescence between each data point on the two lines indicate the effects of FPP; in Fig. 3C, the effect of 50mg/ml FPP in cells treated with the indicated concentrations of FAS, and in Fig. 3D, the effect of each concentration

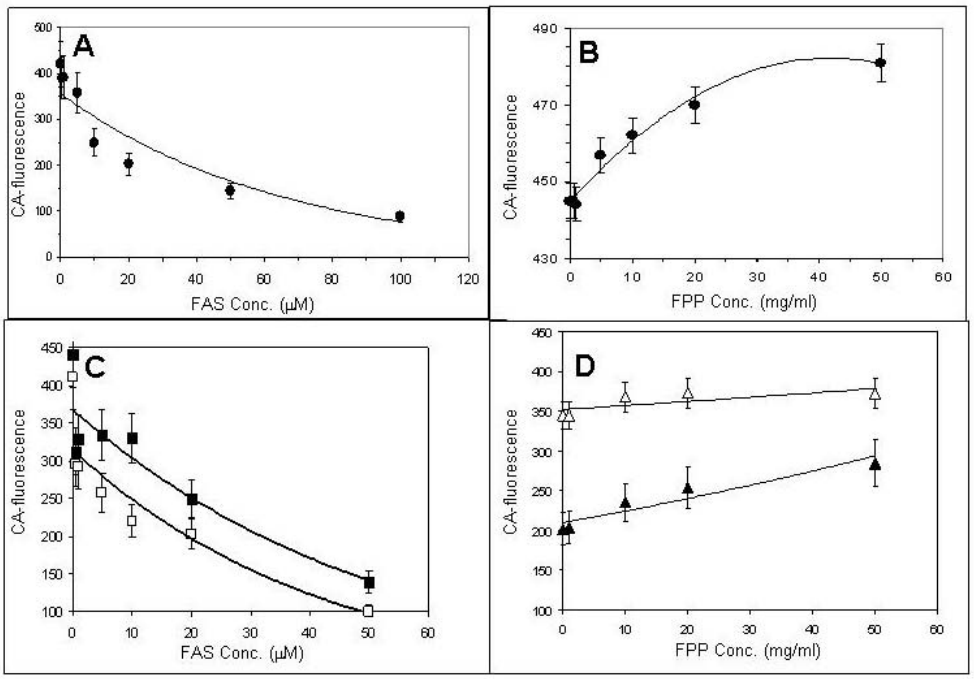


**Fig. 3.** *The dose-related effect of iron and FPP on cellular LIP. (**A-B**) HEPG2 cells were trypsinized, wash in PBS, loaded with CA-AM (0.25 mM) for 15 min, washed again and suspended in PBS. Then, the cells were incubated for 1 h with the indicated concentrations of FAS (A) or FPP (B). (**C-D**) Following trypsinization and washing, cells were incubated simultaneously with the indicated concentrations of FAS with (■) or without (□) 50 mg/ml of FPP (C), or with the indicated concentrations of FPP with (▲) or without (Δ) 20 mM of FAS (D). Following incubations, the cells were washed and analyzed by flow cytometry. The data are presented as the CA-MFI (mean ± SD) of 4 experiments. A decrease in CA-fluorescence indicates an increase in LIP and vice versa. The results in (A-B) show that upon separate incubation, LIP was drastically increased by FAS (by 290% at 50 mM) while moderately decreased by FPP (18% at 50 mg/ml) (differences in the Y-axis in A and B should be noted). The results in (C-D) show that FPP ameliorated the effect of FPP on LIP, but did not reduce it to normal levels of cells untreated with FAS.*

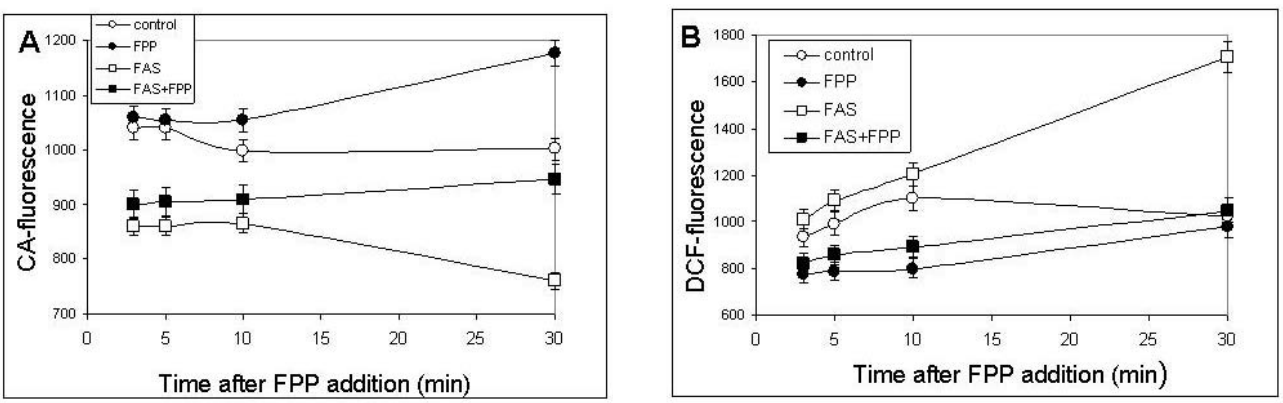


**Fig. 4**. *The short-term effects of FPP on LIP and ROS. H9C2 cells were incubated with or without 20 mM FAS for 1 h, then washed and loaded for 15 min with CA-AM (**A**) or DCF (**B**), washed again and incubated with or without 50 mg/ml FPP. At different time points the cells were analyzed by flow cytometry. The data are presented as the MFI (mean ± SD) of 4 experiments. The results show that FPP increased the CA-fluorescence (i.e., decreased LIP) and decreased the DCF-fluorescence (i.e., decreased ROS) in cells loaded or unloaded with FAS.*

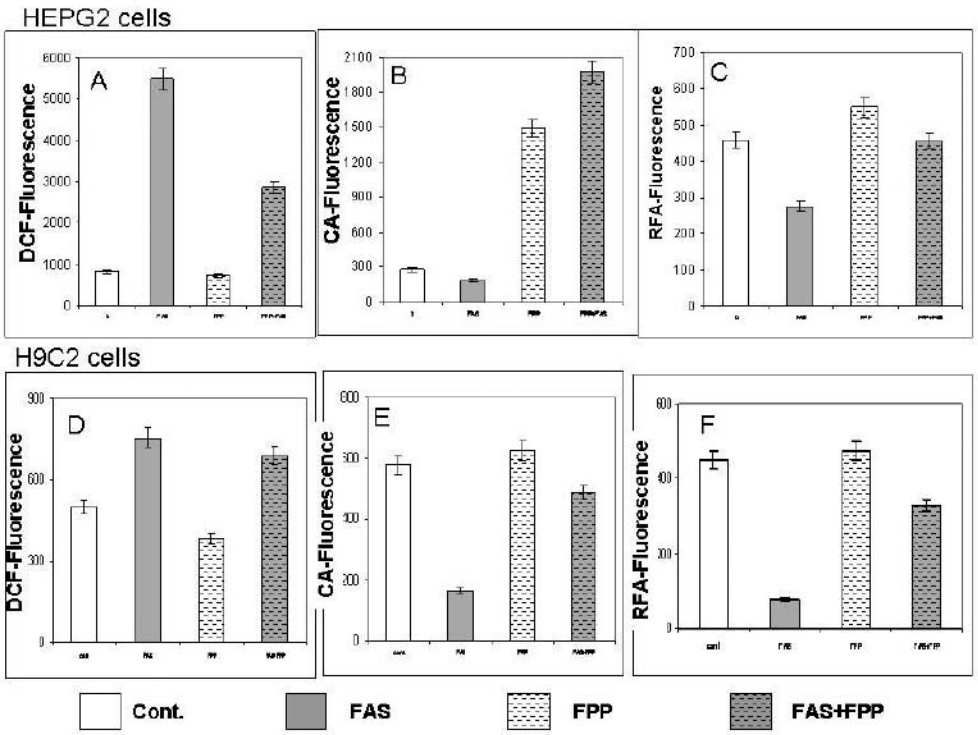


**Fig. 5.** *The long-term effects of iron and FPP on LIP and ROS. HepG2 (**A-C**) and H9C2 (**D-E**) cells were cultured for 3 days with FAS (20 mM), FPP (50 mg/ml), both, or none (Con.). The cells were then washed with PBS, trypsinized, washed again and resuspended in PBS and stained with DCF (A,D), CA-AM (B,E) or RPA (C,F) for 15 min, washed, and analyzed. The data are presented as the MFI (mean ± SD) of 4 experiments.*

of FPP in cells treated with 20 mM of FAS. The results of these experiments show that FPP ameliorated the effect of FAS on LIP, but did not reduce it to its basal level of cells untreated with FAS.

The time-related effect of FPP action is demonstrated in Fig. 4. H9C2 cells were incubated with or without 20 mM FAS for 1 h, then washed and stained for 15 min with CA-AM or DCF, washed again and incubated with or without 50 mg/ml FPP. The figure shows the changes in CA- and DCF-fluorescence at different time points after addition of FPP. The results also show that FPP ameliorated LIP and ROS starting 10 min after its addition to FAS-loaded and unloaded cells. The fact that these cells had been preloaded with FAS and washed prior to addition of FPP, suggests that components of FPP can enter the cells and chelate intra-cellular LIP.

The long-term effects of FPP were studied by culturing HepG2 and H9C2 cells for 3 days with FAS (20 mM), FPP (50 mg/ml), both, or none (control) (Fig. 5). The cells were then washed, trypsinized and stained by DCF, CA-AM or RPA. The results show that continuous presence of FPP during the growth of the cells had a significant reducing effect on their FAS-induced cytosolic and mitochondrial LIP and consequently – their ROS (FAS+FPP *vs* FAS).

## DISCUSSION

Iron-overload affects many organs including the liver and heart as well as erythroid cells (32-34). This toxicity is mediated by LIP-induced oxidative stress (11). In the present study, using flow cytometry methodology, we investigated the effect of FPP on the intracellular LIP, as well as on ROS, of normal RBCs and cell lines derived from heart (H9C2 cells) and liver (HepG2 cells) tissues. The results indicated that FPP reduced the cytosolic LIP in RBCs and both the cytosolic and mitochondrial LIPs in the heart- and liver-derived cells. The chelating effect was

noticed minutes after addition of FPP and it continued for several days when the cells were cultured in the presence of FPP. LIP could be reduced by chelation of extra-cellular iron, but the experiments presented in Fig. 4, where the cells had been preloaded with FAS and washed prior to addition of FPP, suggest that components of FPP can enter cells and chelate intra-cellular LIP. These results suggest that FPP treatment may be preventive as well as therapeutic in the sense of being able to actively reverse iron overloaded. We have already shown that administering FPP per os to patients with thalassemia is safe and effective in reducing their oxidative stress (21, 27). The present results suggest that the antioxidant mechanism of FPP may be related, at least in part, to its ability to chelate iron.

## ACKNOWLEDGEMENTS

EF is a consultant to the Osato Research Institute.

## REFERENCES

1. Weinberg ED. The hazards of iron loading. Metallomics 2010; 2:732-40.
2. Porter JB, Shah FT. Iron overload in thalassemia and related conditions: therapeutic goals and assessment of response to chelation therapies. Hematol Oncol Clin North Am 2010; 24:1109-30.
3. Gardenghi S, Grady RW, Rivella S. Anemia, ineffective erythropoiesis, and hepcidin: interacting factors in abnormal iron metabolism leading to iron overload in beta-thalassemia. Hematol Oncol Clin North Am 2010; 24:1089-107.
4. Ganz T, Nemeth E. Hepcidin and disorders of iron metabolism. Annu Rev Med 2011; 62:347-60.
5. Camaschella C, Poggiali E. Inherited disorders of iron metabolism. Curr Opin Pediatr 2011; 23:14-20.
6. Wang J, Pantopoulos K. Regulation of cellular iron metabolism. Biochem J 2011; 434:365-81.
7. Breuer W, Hershko C, Cabantchik ZI. The importance of non-transferrin bound iron in disorders of iron metabolism. Transfus Sci 2000; 23:185-92.
8. Konijn AM, Meyron-Holtz EG, Fibach E, Gelvan D. Cellular ferritin uptake: a highly regulated pathway for iron assimilation in human erythroid precursor cells. Adv Exp Med Biol 1994; 356:189-97.
9. Jacobs A. Low molecular weight intracellular iron transport compounds. Blood 1977; 50:433-9.
10. Prus E, Fibach E. The labile iron pool in human erythroid cells. Br J Haematol 2008; 142:301-7.
11. Fibach E, Rachmilewitz EA. The role of antioxidants and iron chelators in the treatment of oxidative stress in thalassemia. Ann NY Acad Sci 2010; 1202:10-16.
12. Avery SV. Molecular targets of oxidative stress. Biochem J 2011; 434:201-10.
13. Fibach E, Rachmilewitz E. The role of oxidative stress in hemolytic anemia. Curr Mol Med 2008; 8:609-19.
14. Kohgo Y, Ikuta K, Ohtake T, Torimoto Y, Kato J. Body iron metabolism and pathophysiology of iron overload. Int J Hematol 2008; 88:7-15.
15. Fraga CG, Galleano M, Verstraeten SV, Oteiza PI. Basic biochemical mechanisms behind the health benefits of polyphenols. Mol Aspects Med 2010; 31:435-45.
16. Perron NR, Brumaghim JL. A review of the antioxidant mechanisms of polyphenol compounds related to iron binding. Cell Biochem Biophys 2009; 53:75-100.
17. Marotta F, Chui DH, Jain S, Polimeni A, Koike K, Zhou L, Lorenzetti A, Shimizu H, Yang H. Effect of a fermented nutraceutical on thioredoxin level and TNF-alpha signalling in cirrhotic patients. J Biol Regul Homeost Agents 2011; 25:37-45.
18. Danese C, Esposito D, D'Alfonso V, Cirene M, Ambrosino M, Colotto M. Plasma glucose level decreases as collateral effect of fermented papaya preparation use. Clin Ter 2006; 157:195-8.
19. Marotta F, Koike K, Lorenzetti A, Naito Y, Fayet F, Shimizu H, Marandola P. Nutraceutical strategy in aging: targeting heat shock protein and inflammatory profile through understanding interleukin-6 polymorphism. Ann NY Acad Sci 2007; 1119:196-202.
20. Aruoma OI, Hayashi Y, Marotta F, Mantello P, Rachmilewitz E, Montagnier L. Applications and bioefficacy of the functional food supplement fermented papaya preparation. Toxicology 2010; 278:6-16.
21. Amer J, Goldfarb A, Rachmilewitz EA, Fibach E. Fermented papaya preparation as redox regulator in blood cells of beta-thalassemic mice and patients.

Phytother Res 2008; 22:820-8.
22. Ghoti H, Rosenbaum H, Fibach E, Rachmilewitz EA. Decreased hemolysis following administration of antioxidant-fermented papaya preparation (FPP) to a patient with PNH. Ann Hematol 2010; 89:429-430.
23. Brittenham GM. Iron-chelating therapy for transfusional iron overload. N Engl J Med 2011; 364:146-56.
24. Rimbach G, Guo Q, Akiyama T, Matsugo S, Moini H, Virgili F, Packer L. Ferric nitrilotriacetate induced DNA and protein damage: inhibitory effect of a fermented papaya preparation. Anticancer Res 2000; 20:2907-14.
25. Knowles BB, Howe CC, Aden DP. Human hepatocellular carcinoma cell lines secrete the major plasma proteins and hepatitis B surface antigen. Science 1980; 209:497-99.
26. Kimes BW, Brandt BL. Properties of a clonal muscle cell line from rat heart. Exp Cell Res 1976; 98:367-81.
27. Fibach E, Tan ES, Jamuar S, Ng I, Amer J, Rachmilewitz EA. Amelioration of oxidative stress in red blood cells from patients with beta-thalassemia major and intermedia and E-beta-thalassemia following administration of a fermented papaya preparation. Phytother Res 2010; 24:1334-8.
28. Weston SA, Parish CR. New fluorescent dyes for lymphocyte migration studies. Analysis by flow cytometry and fluorescence microscopy. J Immunol Meth 1990; 133:87-97.
29. Shvartsman M, Fibach E, Cabantchik ZI. Transferrin-iron routing to the cytosol and mitochondria as studied by live and real-time fluorescence. Biochem J 2010; 429:185-93.
30. Bass DA, Parce JW, Dechatelet LR, Szejda P, Seeds MC, Thomas M. Flow cytometric studies of oxidative product formation by neutrophils: a graded response to membrane stimulation. J Immunol 1983; 130:1910-17.
31. Prus E, Fibach E. Flow cytometry measurement of the labile iron pool in human hematopoietic cells. Cytometry A 2008; 73:22-7.
32. Murphy CJ, Oudit GY. Iron-overload cardiomyopathy: pathophysiology, diagnosis, and treatment. J Card Fail 2010; 16:888-900.
33. Ramm GA, Ruddell RG. Iron homeostasis, hepatocellular injury, and fibrogenesis in hemochromatosis: the role of inflammation in a noninflammatory liver disease. Semin Liver Dis 2010; 30:271-87.
34. Rivella S. Ineffective erythropoiesis and thalassemias. Curr Opin Hematol 2009; 16:187-94.

# LOW FREQUENCY OF $CD8^+CD25^+FOXP3^{BRIGHT}$ T CELLS AND FOXP3 mRNA EXPRESSION IN THE PERIPHERAL BLOOD OF ALLERGIC ASTHMA PATIENTS

M. EUSEBIO[1], L. KRASZULA[1], M. KUPCZYK[2], P. KUNA[2] and M. PIETRUCZUK[1]

*[1]Department of Laboratory Diagnostics, II Chair of Internal Medicine, Medical University of Lodz, Poland; [2]Department of Internal Medicine, II Chair of Internal Medicine, Medical University of Lodz, Poland*

*Received August 2, 2011 – Accepted March 14, 2012*

**The aim of this study is to determine whether frequencies of $CD8^+CD25^+$ T cells and FoxP3 messenger RNA (mRNA) expression levels in $CD8^+$ T cells isolated from peripheral blood are related to allergic asthma and disease severity. We enrolled 50 patients with allergic asthma (AA) and 25 healthy control subjects (NC) in our study. The frequencies of $CD8^+CD25^+FoxP3^{-/+}$ T cells were assessed with flow cytometry, and mRNA FoxP3 level in $CD8^+$ T cells was determined with real time polymerase chain reaction (RT-PCR). Asthma patients had fewer $CD8^+CD25^+FoxP3^{bright}$ T cells [SA (median = 3.4%, IQR = 3.1) *vs* MA (median = 7.5%, IQR = 4.7)] than controls NC [median = 12.1 %, IQR = 8, P < 0.0001] but more $CD8^+CD25^+FoxP3^-$ T cells [SA (median = 96 %, IQR = 3.1) *vs* MA (median = 92.5%, IQR = 4.7)] than controls NC [median = 87.9%, IQR = 9.2, P < 0.0001]. FoxP3 mRNA level was significantly decreased in $CD8^+$ T cells of severe asthma patients (median = 0.82, IQR = 0.54) than that of patients with mild to moderate asthma and controls [(median = 2.29, IQR = 4.40) *vs* (median = 2.11, IQR = 3.2)]. The percentage of $FoxP3^+$ T cells was correlated positively with the percentage of forced expiratory volume in 1 second ($FEV_1$) (r = 0.71, p< 0.01) in patients with severe asthma. The proportion of $CD8^+CD25^+FoxP3^{bright}$ T cells and the level of FOXP3 gene expression in $CD8^+$ T cells are relevant to allergic asthma and disease severity. The manipulation of $FoxP3^+CD25^+CD8^+$ T cells may prevent chronic allergic inflammation and improve lung function during an acute allergic asthma exacerbation.**

The dramatic increase in the prevalence of asthma over the past 20 years has created the need for a better understanding of the pathogenesis of the disease. Allergic diseases are caused by a greater abundance of $Th_2$ cells and their related cytokines, namely IL-4, IL-5, and IL-13. The precise mechanisms involved in the imbalance between $Th_1$ and $Th_2$ responses are still not fully elucidated. Increasing evidence suggests that dysregulation of the immune system may play a crucial role in the pathogenesis of allergic asthma. Regulatory T (Treg) cells, namely the naturally occurring subsets, can suppress the activation and proliferation of effector T cells (1) thus, their implication in the development of allergy or autoimmunity. Tregs control airway hyper responsiveness (AHR) and remodeling in chronic inflammatory T-cell response (2). The forkhead transcription factor family member named FOXP3 is required for the development and function of Treg cells. The lack of FOXP3 proteins causes

*Key words: allergic asthma, $CD8^+CD25^+$ T cells, FoxP3, real-time PCR, $FEV_1$*

*Mailing address:* Makandjou-Ola Eusebio, MD, PhD
Department of Laboratory Diagnostics,
II Chair of Internal Medicine,
Medical University of Lodz, Kopcinski 22 str.,
90-153 Lodz, Poland
Tel: +48 42 677 69 83 Fax: +48 42 678 28 33
e-mail: eusemak@yahoo.com / mak.eusebio@umed.lodz.pl



0393-974X (2012)

severe immune disorders in humans and mice. More precisely, humans with loss mutations in FOXP3 gene develop a severe and rapidly fatal autoimmune disorder known as Immune dysregulation, Polyendocrinopathy, Enteropathy X-linked (IPEX) syndrome. A similar disorder was described in mice. IPEX syndrome shares some clinical features with allergies and autoimmune disorders (3). These findings may provide clues to the role of regulatory T cells in maintaining immune tolerance. Most regulatory T cells belong to the $CD4^+$ or $CD8^+$ T cell compartment. Although $CD8^+$ Treg cells were the first identified suppressor cells, they have received less attention due to technical and methodological issues. Nevertheless, $CD8^+$ Tregs have been shown to protect against delayed type hypersensitivity T-cell responses (4). Most studies that evaluated human Treg cell functions have been carried out analyzing naturally occurring $CD4^+CD25^+$ T cells. Thymic derived $CD4^+CD25^+Foxp3^+$ T cells (nTregs) have been shown to control allergic airway hyper responsiveness (AHR) and inflammation in mice models (5). Our current knowledge on the role of $CD8^+$ Treg cells in immunity and tolerance is scarce. Nevertheless, $CD8^+$ T regulatory cells have been shown to control the suppressive function of other nTregs through IL-6 production (6). Although a plethoric number of phenotypic and functional markers including CD25 and FOXP3 were identified for Treg characterization, a classic marker specific and unique for Tregs was not described. Tregs were originally characterized by the expression of the α-chain of IL-2 receptor (CD25) and the transcription factor FOXP3. Nowadays, it is clear that the identification of Treg cells based solely on CD25 expression is controversial because this marker is also expressed on both human and murine $CD4^+$ and $CD8^+$ T cells (7), and dendritic cells (DC). In contrast to its murine counterpart, human FOXP3 gene expression is not restricted to the naturally occurring Treg cells and does not always confer suppressive capability (8). B and cytotoxic T cells secrete IL-2 and express the IL-2 receptor α chain (CD25) upon activation (9). Furthermore, expression of FOXP3 does not distinguish activated T cells from Treg subsets (10). Given that CD25 is transiently up-regulated in activated T cells, circulating $CD25^+$ T cells represent a heterogeneous population (11), in which not all cells express FoxP3.

In this paper, we have analyzed $CD8^+CD25^+FoxP3^{bright}$ T cells and $CD8^+CD25^+FoxP3^-$ T cells percentages on sorted circulatory $CD8^+$ T cells. Moreover, FoxP3 mRNA expression in $CD8^+$ T cells was compared between patients with allergic asthma and healthy subjects. We found marked decrease in $CD8^+CD25^+FoxP3^{bright}$ T cells and mRNA FoxP3 expression in $CD8^+$ T cells of severe asthma patients compared with those of the mild to moderate asthma and controls. Furthermore, the percentage of $FoxP3^+$ T cells was correlated positively with the percentage of forced expiratory volume in 1 second ($FEV_1$) in patients with severe asthma. We suggested that the manipulation of $FoxP3^+$ T cells may prevent chronic allergic inflammation and improve lung function during an acute allergic asthma exacerbation.

## MATERIALS AND METHODS

*Ethics approval*

The study was approved by the ethics committee, Medical University of Lodz, Poland (RNN/17/09/KE). All participants gave written informed consent before screening and enrolment. Venous blood was drawn from each patient and the study was performed according to the Helsinki Declaration.

*Questionnaires*

All participants underwent a standard check-up including a questionnaire related to their general health status. In addition, all subjects with clinical symptoms of asthma filled Asthma Control Questionnaire.

*Patients*

We studied 50 patients with allergic asthma (AA) as defined by the Global Initiative for Asthma (GINA) guidelines (12) and 25 gender and age-matched controls (NC). The diagnosis of asthma has been confirmed by pulmonologists based on evidence of variable airways obstruction according to The Global Initiative for Asthma (GINA 2008) guidelines. Patients were divided into severe asthma (SA) (n = 25) and mild-to-moderate asthma (MA) (n = 25) groups (Table I) and were treated based on European Network for Understanding Mechanisms of Severe Asthma (ENFUMOSA) guidelines (13). Atopy was evaluated based on skin prick tests or evidence of increase specific serum IgE. Patients with SA required treatment with either high dose of inhaled steroids, or long acting ß-agonists for at least a year. Patients with MA received inhaled steroids daily in combination

with symptomatic therapy. Subjects without evidence of allergic or infectious diseases served as controls.

*The assessment of asthma and its severity*

Pulmonary function tests were performed using a calibrated spirometer as recommended by the American Thoracic Society/European Respiratory Society guidelines (14). The best of three reproducible loops was recorded for the study. The forced expiratory volume in first second ($FEV_1$), forced vital capacity (FVC) and the ratio of $FEV_1$/FVC were recorded for the differential diagnosis of asthma. Patients also underwent skin-prick test to common allergens, methacholine test (15) and specific serum immunoglobulin E (IgE) was measured. Patients with initially impaired lung function values were banned from the challenge test. Bronchodilator and steroid drugs were discontinued 24 h before the challenge test.

*Isolation of peripheral blood mononuclear cells*

Peripheral blood mononuclear cells (PBMC) were isolated from heparinized venous blood of each participant using density gradient centrifugation (2500 g, 30 min) over Histopaque 1077 (Sigma-Aldrich Company, St. Louis, MO). PBMC were then harvested by pipetting cells from buffy coats located at the Histopaque/serum interface and washed twice in PBS.

*Sorting of $CD8^+$ T cells*

$CD8^+$ T cells were negatively selected according to the manufacturer's instructions (BD Bioscience) by incubating PBMCs with biotinylated human CD8 T lymphocyte enrichment cocktail directed against non-$CD8^+$ T cells: CD4, CD11, CD16, CD19, CD 36, CD41a, CD56, CD123, CD235a, and γδ TCR. Cells were incubated with saturating amounts of antibodies at a ratio of 5 µl per 1 x $10^6$ cells, for 15 min at 4°C. Thereafter, streptavidin particles were added at a concentration of 5 µl of particles for every 1 x $10^6$ total cells and incubated for 30 min at 4°C. Beads and contaminating cells were removed by running the mixture through BD™ IMagnet magnetic field. The remaining cells representing the purified $CD8^+$ T cells were collected. In order to evaluate the purity of the $CD8^+$ T cells enrichment fraction, we stained 100 µl of the suspension with anti-CD8 antibodies for 20 min on ice. Data were analyzed by flow cytometry. The purity of the enriched $CD8^+$ T cells ranges between 90 and 93%.

*Immunostaining*

For the detection of CD25 and Foxp3 expression, purified $CD8^+$ T cells (1x$10^6$ cells/100 µl) were stained with 10 µl of the following monoclonal antibodies: anti-human CD8- peridinin-chlorophyll protein-cyanine 5 conjugate (PerCp-Cy5.5) (clone SK1,Mouse IgG1, k), anti-Human CD25 fluorescein isothiocyanate conjugate (FITC) (clone M-A251, Mouse IgG1, k), anti-Human FoxP3 Alexa Fluor 647 (clone 259D/C7, Mouse IgG1). The monoclonal antibodies were purchased from BD Pharmingen, USA. In particular, purified $CD8^+$ T cells were washed twice in 2 ml of BD Pharmingen Stain Buffer (FBS) and incubated with both anti-human CD8-PerCp-Cy5.5 and anti-Human CD25 FITC for 30 mins at 4°C in the dark. After the cell-surface staining procedure, cells were fixed and permeabilized using a commercially available perm/wash kit (BD Pharmingen). Specifically, cells were re-suspended in wash buffer and then incubated with 2 ml of 1x Human FoxP3 Buffer A for 10 mins in the dark at 4°C. After incubation, cells were washed twice with 2 ml of BD Pharmingen Stain Buffer (FBS) and centrifuged. After removing the supernatant, cells were resuspended in wash buffer and incubated with 0.5 ml of 1x Human FoxP3 Buffer C for 10 mins. Thereafter, cells were once again washed with 2 ml of BD Pharmingen Stain Buffer (FBS) and incubated with anti-Human FoxP3 Alexa Fluor 647 for 30 mins in the dark at 4°C. After incubation, 500 µl staining buffer was added into each tube before flow cytometric analysis.

*Flow cytometry analysis*

Stained $CD8^+$ T cells were phenotypically analyzed by 8-color flow cytometry using a panel of directly conjugated antibodies described in the Immunostaining section. Phenotypic analysis was performed with FACS CANTO II flow cytometer (BD Biosciences, San Jose, CA, USA). Data were acquired using BD FACSDiva version 4.1.2 software. At least 50,000 gated viable lymphocytes were collected for each sample. FACSDiva and FCS softwares were used for the analysis. Lymphocyte gates were set according to forward and side-scatter parameters (forward scatter *vs* side scatter), excluding cell debris. To analyze CD25 and FOXP3 protein expression in circulatory $CD8^+$ T cells, cells were gated as $CD8^+CD25^+$ events and the expression of FOXP3 was quantified within $CD8^+CD25^+$ cells. Quadrants of dot-plots were set for each extracellular and intracellular antibody (Fig. 1). Automatic compensation for spectral overlap was performed electronically using antibody capture beads (BD Biosciences). Automatic compensation was applied to minimize fluorescence spillover. Fluorescence-minus-one (FMO) control was used to set positive/negative boundaries. Gating was standardized within individual samples to generate a fully comparative data. Data are representative flow cytometry plots for experiments performed with cells obtained from 50 patients with allergic asthma and 25 healthy controls. Experiments involving readouts at different days were run with the same instrument and compensation settings to ensure

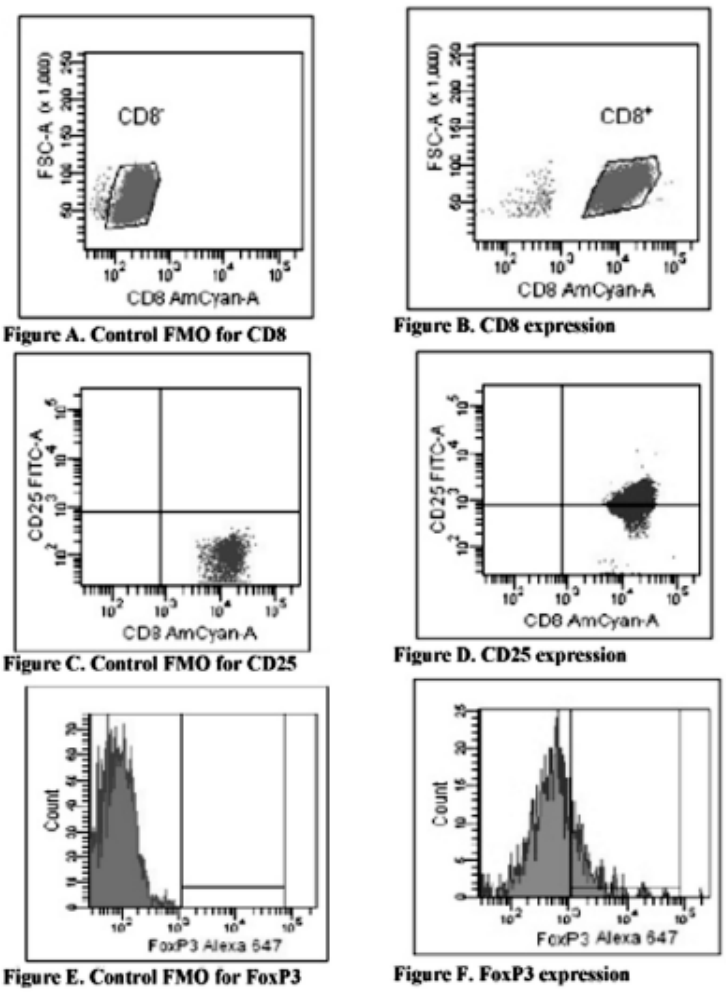


**Fig. 1.** *Phenotypic characterization of CD8$^+$ T cells based on the expression of CD8, CD25 and FOXP3. Percent positive cells were evaluated by common gating criteria with less than 1% of events within the positive gate.* ***A)*** *Control FMO for CD8,* ***(B)*** *CD8 expression,* ***(C)*** *Control FMO for CD25,* ***(D)*** *CD25 expression,* ***(E)*** *Control FMO for FoxP3 and* ***(F)*** *FOXP3 expression. Data are representative of 25 patients with severe allergic asthma, 25 with mild to moderate asthma and 25 controls groups.*

comparability of data.

*RNA Isolation and detection of FOXP3 mRNA in Tregs*

Total RNA was extracted from sorted CD8$^+$ T lymphocytes with a NucliSENS Magnetic Extraction Reagents kit, BioMerieux. TaqMan reverse transcription (RT)-polymerase chain reaction (PCR) was performed with 1 μg of total RNA for cDNA synthesis (16). Primers were used as follows: forward primer 18S rRNA 5'-AGT CCC TGC CCT TTG TAC ACA-3' reverse primer 18S rRNA 5'-GAT CCG AGG TCA CTA AAC-3'. For the generation of FOXP3 cDNA, a total of 41 cycles were run. The following conditions were used for FOXP3 RT-PCR: 10 min at 95°C, 30 sec at 95°C, and 1 min at 58°C. For quantitative real-time PCR analysis, 2 μM of isolated RNA was transcribed into cDNA using random hexamers. Polymerase chain reactions were performed in duplicates according to the Brilliant II QPCR Master Mix procedure, Stratagene, USA and run on the Smart Cycler Sequence Detector System. The amount of FOXP3 mRNA expression was normalized to the 18S rRNA standard (primer TTA GAA GAG ACT CGG TAT AAA AGC AAA GTT GTT TT) by calibration curve. Relative quantification and calculation of the range of confidence was performed by using the comparative threshold cycle (DDCT) method, as previously described in the real-time

Quantitative Nucleic Acid Sequence Based Amplification (real-time QT-NASBA) method (17). The concentration of the FoxP3 calibrator is expressed in pmol/µl in this technique.

*Statistical analyses*

The Mann-Whitney U test and the Kruskal-Wallis analysis were used to assess statistical differences between study and controls groups. A Spearman correlation test was performed to analyze the association between the forced expiratory volume in one second $FEV_1$ (% predicted) and the percentage of FoxP3 $^+$ T cells. Data were expressed as median and interquartile range (IQR) which is the difference between the third and first quartiles. A *p*-value less than 0.05 was considered significant. Calculations were performed by the statistical software package Statistica (Stat Soft, Polska).

## RESULTS

*Characteristics of study participants*

The characteristics of our study subjects are presented in Table I. Atopy was defined as at least one positive skin-prick test against the most common allergens and its degree was assessed based on total serum IgE levels as previously described (18). Allergen polysensitization was defined as sensitization to more than 2 allergens-specific IgE, regardless of allergen class.

*Decrease in the expression of $CD8^+CD25^+FoxP3^{bright}$ T cells but increase in $CD8^+CD25^+FoxP3^-$ T cells in severe asthma group compared with the mild asthma group*

We showed an inverse correlation between the numbers of $CD8^+CD25^+FoxP3^{bright}$ T cells and $CD8^+CD25^+FoxP3^-$ T cells in patients with allergic asthma at any level of severity. Asthma patients had fewer $CD8^+CD25^+FoxP3^{bright}$ T cells [SA (median = 3.4%, IQR = 3.1) *vs* MA (median = 7.5%, IQR = 4.7)] than controls NC [median = 12.1%, IQR = 8, $P < 0.0001$] but more $CD8^+CD25^+FoxP3^-$ T cells [SA (median = 96%, IQR = 3.1) *vs* MA (median = 92.5%, IQR = 4.7)] than controls NC [median = 87.9%, IQR = 9.2, $P < 0.0001$] (Fig. 2) (Table II). Individuals with severe allergic asthma had less $CD8^+CD25^+FoxP3^{bright}$ T cells (median = 3.4, IQR = 3.1) than did patients with mild to moderate allergic asthma (median = 7.5 and IQR = 4.7) $P < 0.001$). In contrast, individuals with severe asthma had more $CD8^+CD25^+FoxP3^-$ T cells than patients with mild to moderate asthma (median = 96.0, IQR = 3.1) *vs* (median = 92.50 and IQR = 4.7), $P < 0.01$) (Fig. 2) (Table II). We suggested that the low frequency of $CD8^+CD25^+FoxP3^{bright}$ T cells phenotype in AA patients and consequently the decrease in their suppressive capacity might play a role in the pathogenesis of allergic asthma and disease severity.

*Decrease in mRNA FoxP3 expression level by $CD8^+$ T cells in severe asthma*

Of interest, the transcription factor FOXP3 which has previously been shown to be absolutely critical for Treg development and function, is also transiently expressed by almost all activated T-cells. Therefore, FoxP3 mRNA expression was analyzed in healthy subjects, as well as in patients with moderate and severe asthma. We purified naïve human $CD8^+$

**Table I.** *Characteristics of the study population.*

| Population / Characteristic | SA | MA | NC |
|---|---|---|---|
| Age (years) | 48 ± 14 | 42 ± 13 | 48.5 ± 14.5 |
| Sex (female/male) | 13♀/ 12♂ | 12♀/ 13♂ | 12♀/ 13♂ |
| Mean $FEV_1$ ( % predicted values) | 67 ± 15.98% | 87.71 ± 16.12% | 96.6 ± 4% |
| ICS | 800-1600 µg | 200-800 µg | No |
| LABA | Yes | Yes | No |
| Hypersensitivity to ASA | 9 | 1 | 0 |

*SA: severe asthma; MA: middle to moderate asthma; NC: controls; $FEV_1$: forced expiratory volume in 1 second; ASA: acetylsalicylic acid; ICS: Inhaled corticosteroids; LABA: long acting beta agonists*

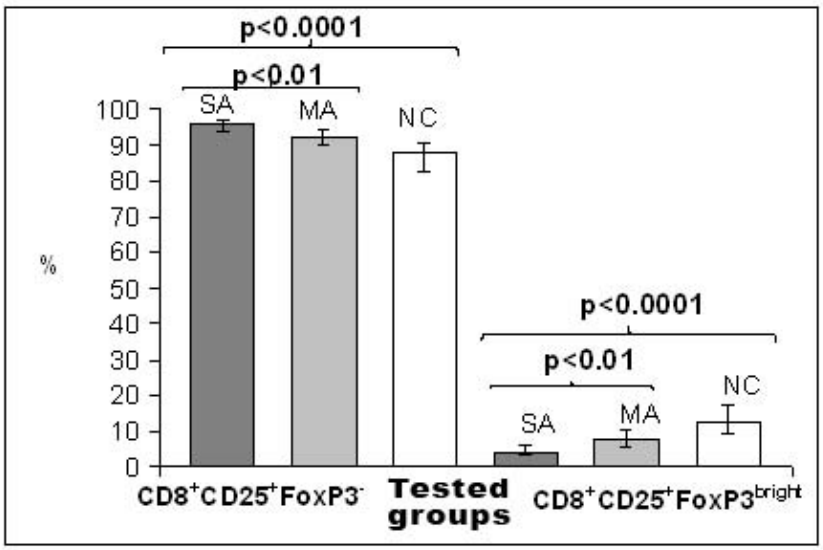


**Fig. 2.** *Decrease in the percentage of $CD8^+CD25^+FoxP3^{bright}$ T cells but increase in the percentage of $CD8^+CD25^+FoxP3^-$ T cells in patients with allergic asthma compared with controls. The percentage of $CD8^+CD25^+FoxP3^{bright}$ T cells was significantly lower in AA patients as compared with NC ($p < 0.0001$). In contrast, patients with allergic asthma had higher percentage of $CD8^+CD25^+FoxP3^-$ T cells than their controls.*

**Table II.** *Comparison of total counts and percentages (median ± interquartile range, minimum, maximum) $CD8^+CD25^+FoxP3^{-/bright}$ T cells subsets and the concentration of mRNA for the gene FOXP3 in $CD8^+$ T lymphocytes.*

| Tested parameters | Statistical parameters | Severe asthma (SA) | Mild to moderate asthma (MA) | Control (NC) |
|---|---|---|---|---|
| mRNA FOXP3 of purified $CD8^+$ T cells | Median | 0.82 | 2.29 | 2.11 |
| | interquartile | 0.31-0.85<br>IQR=0.54 | 0.09-4.49<br>IQR=4.40 | 0.9-4.1<br>IQR= 3.2 |
| $CD8^+CD25^+FoxP3^{bright}$ % | Median | 3.4 | 7.5 | 12.1 |
| | interquartile | 3.0-6.1<br>IQR=3.1 | 5.8-10.5<br>IQR=4.7 | 9.2-17.2<br>IQR=8 |
| $CD8^+CD25^+FoxP3^-$ % | Median | 96.0 | 92.5 | 87.9 |
| | interquartile | 93.9-97.0<br>IQR=3.1 | 89.5-94.2<br>IQR=4.7 | 82.8-91.0<br>IQR=9.2 |

*Cells were stained with either of the appropriate antibodies. To analyze FOXP3 protein expression in circulatory $CD8^+CD25^+$ T cells, T cells were gated as $CD8^+CD25^+$ events, and the expression of FOXP3 was quantified within $CD8^+CD25^+$ cells. Percentages are shown here of respective cells expressed as median and interquartile range (IQR) being equal to the difference between the third and first quartiles. Values are representative of 25 patients with severe allergic asthma,25 with mild to moderate asthma and 25 controls.*

T cells as described at the Methods section. The FOXP3 gene was sequenced; FOXP3 messenger RNA levels were evaluated by real-time polymerase chain reaction (PCR). The FOXP3 protein expression in $CD8^+$ T lymphocytes was also analyzed by flow cytometry after intracellular staining. We compared levels of mRNA expression for FOXP3 in twenty-five patients with severe allergic asthma, twenty-five patients with mild to moderate asthma and twenty-five healthy subjects. Patients with severe allergic

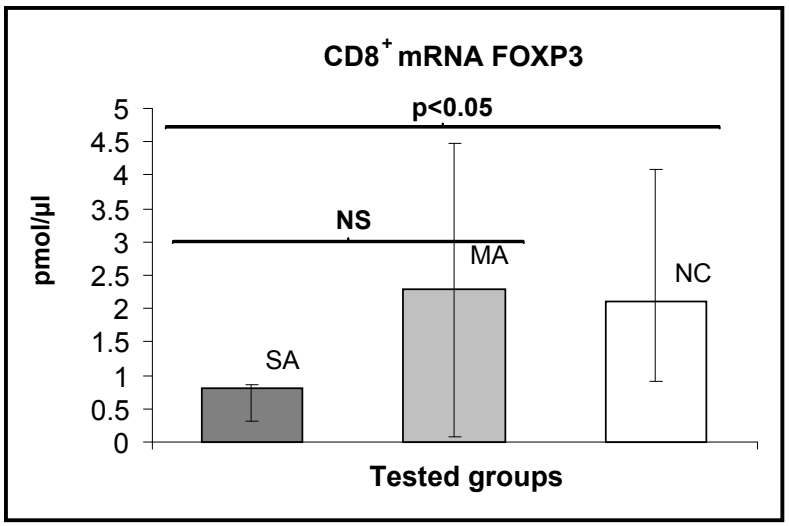


**Fig. 3.** *Decrease in the mRNA FoxP3 expression in purified CD8⁺ T cells of severe asthma patients compared with controls. There was no statistically significant difference in the level of mRNA FoxP3 expression in CD8⁺ T cells between patients with severe and mild asthma. However, there was a statistically significant difference ($p < 0.05$) between the mRNA FoxP3 expression in severe asthma (SA) patients and healthy subjects (NC). The severe asthma patients had lower mRNA FoxP3 than the healthy subjects.*

asthma had lower expression of FoxP3 mRNA in $CD8^+$ T cells (median = 0.82 and IQR = 0.54) than that of patients with mild to moderate bronchial asthma (median = 2.29 and IQR = 4.40) versus controls (median = 2.11 and IQR = 3.2) (Fig. 3) (Table II).

*Percentage of FoxP3⁺ T cells correlates with percentage predicted $FEV_1$ in severe allergic patients*

Reduced lung function is a feature of chronic lung disease especially asthma. There is a progressive loss of pulmonary function in persistent asthma phenotype. The $FEV_1$ is the volume exhaled during the first second of a forced expiratory maneuver started from the level of total lung capacity. We checked whether there was any correlation between lung function, as measured by $FEV_1$ and the percentage of $CD8^+CD25^+FoxP3^{bright}$ T cells. We found a positive Spearman Rank correlation between the percentage of $FoxP3^+$ cells and $FEV_1$ predicted values ($r = 0.71$, $p < 0.01$) in patients with severe allergic asthma (Fig. 4) (Table II).

## DISCUSSION

$CD4^+CD25^+$ regulatory T cells (Tregs) have the ability to potently suppress the proliferation of T cells (19) and thereby protect against allergy-induced asthma. It has been demonstrated that several other subsets of Tregs are implicated in maintaining immune homeostasis. $CD8^+$ Treg cells play a crucial role in Th2 mediated autoimmune diseases (20). $CD8^+$ Treg cells have not been extensively characterized due to methodological and technological limitations. Nevertheless, human $CD8^+CD25^+$ Treg cells are known to share phenotypic and functional features with $CD4^+CD25^+$ regulatory T cells (21). Naturally occurring $CD4^+CD25^+$ T cells were shown to play an important role in the pathogenesis of asthma. Several other subsets of naturally occurring Treg including $CD8^+CD25^+$ Treg cells were shown to inhibit the proliferation of effectors T cells. On the basis of previous findings that the synthetic TLR2 agonist Pam3CSK4 has the unique capacity to counteract allergies by increasing the proportion of $CD8^+CD25^+FoxP3^+$ T cells (22), it is reasonable to assume an imbalance of $CD8^+CD25^+FoxP3^+$T cells subsets in peripheral blood of asthmatic subjects.

In this study, allergic asthma patients had a significantly decreased proportion of $CD8^+CD25^+FoxP3^{bright}$ T cell population and a lower expression of FoxP3 mRNA in a population

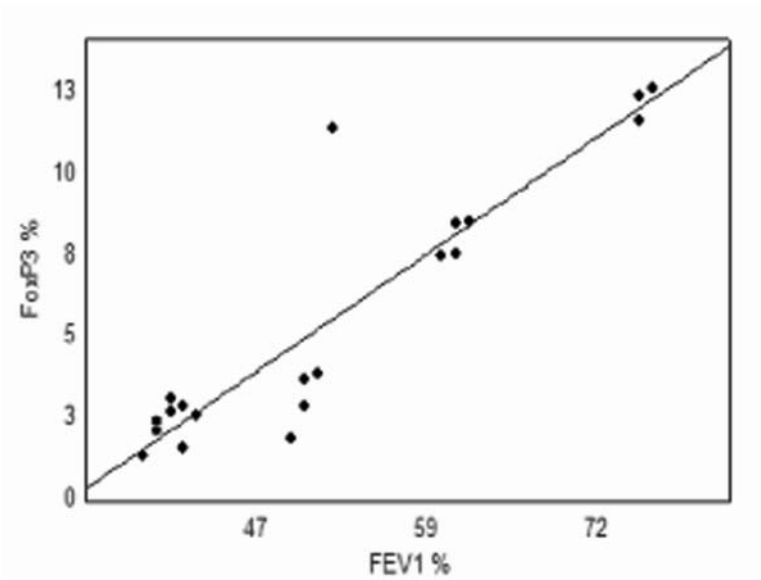


**Fig. 4.** *Correlation between % Foxp3$^+$ T cells and %FEV$_1$ in peripheral blood of patients with severe asthma. We found a positive Spearman rank correlation between the percentage of FOXP3$^+$ T cells and FEV$_1$% predicted values ($r = 0.71$, $p < 0.01$) in patients with severe allergic asthma.*

of circulatory CD8$^+$ T cells compared with healthy subjects.

Our study confirms previous research indicating that CD8$^+$ T cells expressing both CD25 and forkhead box P3 (FoxP3) markers play a role in the pathogenesis of T helper type 2 (Th2) mediated immune response (23). Another interesting observation from our study was that FOXP3 mRNA expression was decreased in CD8$^+$ T cells of severe asthmatic patients compared with those with mild asthma and the healthy groups. The decrease in the FoxP3 mRNA expression in CD8$^+$ T cells of allergic asthma patients suggests a defective FOXP3 expression in patients with allergic asthma. O'Sullivan and colleagues previously demonstrated that CD8$^+$ T lymphocytes accumulate in the airways during acute asthma exacerbations (24). The significant decrease of circulating CD8$^+$CD25$^+$FoxP3$^{bright}$ T cells in peripheral blood of allergic asthmatic individuals might therefore be driven as a direct consequence of the allergic inflammation in the airways. A possible explanation of our finding is that the decrease in the percentage of CD8$^+$CD25$^+$FoxP3$^{bright}$T cells might be caused by an accumulation of CD8$^+$ T cells through recruitment from the blood to the site of airways inflammation. Moreover, taking into account the down-regulatory effect of glucocorticosteroids on CD25 and FOXP3 expression, another explanation of our findings may also be of relevance to the effect of glucocorticosteroid therapy. The asthma patients were treated with corticosteroids. These anti-inflammatory drugs have been shown to alter T cell activation signals (25). Having said that, our investigation is in the same direction of quite a few others, which previously suggested a relationship between steroid therapy and reduced T-cell activation and cytokine mRNA expression in asthmatic patients after steroid treatment (26). O. Lourenc-o and colleagues claimed that there is no correlation between T cell proportion in the target organ and disease severity (27). However, another central finding of our study is the inverse correlation between severity of asthma and the percentage of CD8$^+$CD25$^+$FoxP3$^{bright}$ T cells. The percentage of CD8$^+$CD25$^+$FoxP3$^{bright}$ T cells was probably significantly lower in severe asthma than in mild to moderate asthma subjects due to the high dose of GCs and the extent of lung inflammation. Larger cohort studies are needed to confirm the contribution of CD8$^+$CD25$^+$FoxP3$^{bright}$ T cells and FoxP3 mRNA expression level in the pathogenesis of allergic asthma and their relevance to the severity of the disease. Existing studies of the association between the clinical asthma symptoms and the immune

biology of allergic asthma have generally examined lung function and the immune modulator capacity of Treg cells. However, few reported studies exist that directly investigated the relationship between these two parameters in humans. Nevertheless, one study has established a strong relationship between pulmonary function changes and proportions of regulatory T cells in mice (28). Similarly, other research groups have demonstrated a correlation between decreased FOXP3 expression and airflow limitation in smokers (29).

The present study reveals a link between the percentage of $CD8^+CD25^+FoxP3^{bright}$ T cells and the percentage predicted $FEV_1$ in patients with severe allergic asthma. Our data confirm without exception the previous findings that suggest that the deficiency and dysfunction of T cells in the lung cause chronic inflammatory responses (30). Unfortunately, our investigation has some limitations that need to be addressed in further studies. It did not divide the asthmatic populations into the atopic and the non-atopic subgroups. Another problem is that it did not take into account sensitivity to steroid, which limited our conclusion. Given that CD25 is also transiently up-regulated in T cells after activation, circulating $CD25^+$ T cells make a heterogeneous population. One of the limitations of our study is that we were not able to determine whether $CD8^+CD25^+$ cells are activated or regulatory T cells. Although this study is small, it has yielded promising results for the diagnostics and management of asthma. In particular, our data, if confirmed by future cohort studies, could be used to design clinical trials using $CD8^+$ T cells as cellular therapy for asthma

## ACKNOWLEDGEMENTS

This work was supported by Polish Academy of Sciences grant KBN nr N N402 517339.

## REFERENCES

1. McNally A, Hill GR, Sparwasser T, Thomas R, Steptoe RJ. CD4+CD25+ regulatory T cells control CD8+ T-cell effectors differentiation by modulating IL-2 homeostasis. Proc Natl Acad Sci USA 2011; 108:7529-34.
2. McGee HS, Agrawal DK. TH2 cells in the pathogenesis of airway remodeling: regulatory T cells a plausible panacea for asthma. Immunol Res 2006; 35:219-32.
3. Torgerson TR, Linane A, Moes N, et al. Severe food allergy as a variant of IPEX syndrome caused by a deletion in a noncoding region of the FOXP3 gene. Gastroenterology 2007; 132:1705-17.
4. Jarvis LB, Matyszak MK, Duggleby RC, Goodall JC, Hall FC, Gaston JS. Autoreactive human peripheral blood CD8+ T cells with a regulatory phenotype and function. Eur J Immunol 2005; 35:2896-908.
5. Joetham A, Takeda K, Miyahara N, Matsubara S, Ohnishi H, Koya T, Dakhama A, Gelfand EW. Activation of naturally occurring lung CD4 (+) CD25 (+) regulatory T cells requires CD8 and MHC I interaction. Proc Natl Acad Sci USA 2007; 104:15057-62.
6. Joetham A, Okamoto M, Takeda K, Schedel M, Ohnishi H, Dakhama A, Gelfand EW. CD8 regulates suppressive allergic airways disorder through the production of IL-6. J Immunol 2011; 186:113-20.
7. Stanzani M, Martins SL, Saliba RM, et al. CD25 expression on donor CD4+ or CD8+ T cells is associated with an increased risk for graft-versus-host disease after HLA-identical stem cell transplantation in humans. Blood 2004; 103:1140-6.
8. Morgan ME, van Bilsen JH, Bakker AM, et al. Expression of FOXP3 mRNA is not confined to CD4+CD25+ T regulatory cells in humans. Hum Immunol 2005; 66:13-20.
9. Yarkoni S, Sagiv Y, Kaminitz A, Askenasy N. Interleukin 2 targeted therapy in inflammatory bowel disease. Gut 2009; 58:1705-6.
10. Mayer CT, Floess S, Baru AM, Lahl K, Huehn J, Sparwasser T. CD8+ Foxp3+ T cells share developmental and phenotypic features with classical CD4+ Foxp3+ regulatory T cells but lack potent suppressive activity. Eur J Immunol 2011; 41:716-25.
11. Cao Q, Wang L, Du F, et al. Downregulation of CD4+CD25+ regulatory T cells may underlie enhanced Th1 immunity caused by immunization with activated autologous T cells. Cell Res 2007; 17(7):627-37.
12. Koya T, Hasegawa T, Tanaka J, Kawakami H, Hayashi M, Kagamu H, Narita I, Arakawa M,

Suzuki E. Effect of ciclesonide on bronchial asthma in athletes. J Asthma 2009; 46:1032-6.
13. Gaga M, Papageorgiou N, Yiourgioti G, Karydi P, Liapikou A, Bitsakou H, Zervas E, Koulouris NG, Holgate ST; ENFUMOSA Study Group. Risk factors and characteristics associated with severe and difficult to treat asthma phenotype: an analysis of the ENFUMOSA group of patients based on the ECRHS questionnaire. Clin Exp Allergy 2005; 35:954-9.
14. Hsia CC, Hyde DM, Ochs M, Weibel ER; ATS/ERS Joint Task Force on Quantitative Assessment of Lung Structure. An official research policy statement of the American Thoracic Society/European Respiratory Society: standards for quantitative assessment of lung structure. Am J Respir Crit Care Med 2010; 181:394-418.
15. Ekstrand Y, Ternesten-Hasséus E, Arvidsson M, Löfdahl K, Palmqvist M, Millqvist E. Sensitivity to environmental irritants and capsaicin cough reaction in patients with a positive methacholine provocation test before and after treatment with inhaled corticosteroids. J Asthma 2011; 48:482-9.
16. Kunzmann S, Wohlfahrt JG, Itoh S, Asao H, Komada M, Akdis CA. SARA and Hgs attenuate susceptibility to TGF-beta1-mediated T cell suppression. FASEB J 2003; 17:194-202.
17. Medhurst AD, Harrison DC, Read SJ, Campbell CA, Robbins MJ, Pangalos MN. The use of TaqMan RT-PCR assays for semi quantitative analysis of gene expression in CNS tissues and disease models. J Neurosci Methods 2000; 98:9-20.
18. Adams B, Dubois A, Delbauve S, Debock I, Lhommé F, Goldman M, Flamand V. Expansion of regulatory CD8+ CD25+ T cells after neonatal alloimmunization. Clin Exp Immunol 2011; 163:354-61.
19. Piccirillo CA, Shevach EM. Naturally-occurring CD4+CD25+ immunoregulatory T cells: central players in the arena of peripheral tolerance. Semin Immunol 2004; 16(2):81-8.
20. Field AC, Bloch MF, Bellon B. Neonatal tolerance to a Th2-mediated autoimmune disease generates CD8+ Tc1 regulatory cells. J Autoimmun 2003; 21:201-12.
21. Cosmi L, Liotta F, Lazzeri E, et al. Human CD8+CD25+ thymocytes share phenotypic and functional features with CD4+CD25+ regulatory thymocytes. Blood 2003; 102: 4107-14.
22. Tsai YG, Yang KD, Niu DM, Chien JW, Lin CY. TLR2 agonists enhance CD8+Foxp3+ regulatory T cells and suppress Th2 immune responses during allergen immunotherapy. J Immunol 2010; 184(12):7229-37.
23. Adams B, Dubois A, Delbauve S, Debock I, Lhommé F, Goldman M, Flamand V.Expansion of regulatory CD8+ CD25+ T cells after neonatal alloimmunization. Clin Exp Immunol 2011; 163(3):354-61
24. O'Sullivan SM. Asthma death, CD8+ T cells, and viruses. Proc Am Thorac Soc 2005; 2(2):162-5.
25. Corrigan CJ, Shiner R, Shakur BH, Ind PW. Methotrexate therapy in asthma increases T cell susceptibility to corticosteroid inhibition. Clin Exp Allergy 2003; 33(8):1090-6.
26. Gemou-Engesaeth V, Fagerhol MK, Toda M, Hamid Q, Halvorsen S, Groegaard JB, Corrigan CJ. Expression of activation markers and cytokine mRNA by peripheral blood CD4 and CD8 T cells in atopic and nonatopic childhood asthma: effect of inhaled glucocorticoid therapy. Pediatrics 2002; 109(2):E24.
27. Lourenço O, Mafalda Fonseca A, Taborda-Barata L. T cells in sputum of asthmatic patients are activated independently of disease severity or control Allergol Immunopathol (Madr) 2009; 37(6):285-92.
28. Kosaka S, Tamauchi H, Terashima M, Maruyama H, Habu S, Kitasato H. IL-10 controls Th2-type cytokine production and eosinophil infiltration in a mouse model of allergic airway inflammation. Immunobiology 2011; 216:811-20.
29. Matsumoto K, Inoue H, Tsuda M, Honda Y, Kibe A, Machida K, Yoshiura Y, Nakanishi Y. Different roles of interleukin-10 in onset and resolution of asthmatic responses in allergen-challenged mice. Respirology 2005; 10:18-26.
30. Mack DG, Lanham AM, Falta MT, Palmer BE, Maier LA, Fontenot AP. Deficient and dysfunctional regulatory T cells in the lungs of chronic beryllium disease subjects. Am J Respir Crit Care Med 2010; 181:1241-9.

# SERUM VISFATIN IS ELEVATED IN CHINESE WOMEN WITH POLYCYSTIC OVARY SYNDROME, BUT MIGHT NOT BE A RELIABLE PREDICTOR OF THEIR GLUCOSE INTOLERANCE

Y. HONG, XM. ZHAO, L.L. HUANG, L. LI, X.L. CHEN and D.Z. YANG

*Department of Obstetrics and Gynecology, Memorial Hospital of Sun Yat-Sen University, Guangzhou, China*

*Received November 16, 2011 – Accepted February 24, 2012*

**Both visfatin and polycystic ovary syndrome (PCOS) were previously reported to be in relation to abnormal glucose metabolism (AGM). The hypothesis was investigated in this paper that plasma visfatin level are elevated in Chinese women with PCOS, and could substitute oral glucose tolerance test (OGTT) as a simple predictor for their glucose intolerance. This cross-sectional study enrolled 119 women (91 newly diagnosed PCOS patients and 28 eumenorrheic age- and BMI- matched controls); anthropometric, hormonal, and metabolic parameters including serum visfatin were simultaneously measured in all participants. Plasma visfatin levels were compared between controls and PCOS subjects with various glucose metabolism status diagnosed by OGTT using 75 g of glucose. Pearson correlation coefficients were calculated to determine the correlations between various parameters. Receiver Operating Characteristic (ROC) analysis was performed to examine the diagnostic test performance of visfatin. Plasma visfatin levels were found to be significantly higher in our PCOS population compared to healthy controls ($P<0.05$). An increase in fasting visfatin concentrations with a worsening degree of glucose intolerance among PCOS patients was described. However, the difference did not reach statistical significance. In addition, visfatin was unexpectedly found to correlate with neither age, anthropometric, hormonal nor metabolic parameters. As a predictor for glucose intolerance to distinguish PCOS individuals with normal or abnormal glucose metabolism, visfatin was found to possess low potentially predictive ability according to ROC curve analysis. In conclusion, serum visfatin is significantly elevated in Chinese women with PCOS, but might not be a reliable predictor of their glucose intolerance.**

Polycystic ovary syndrome (PCOS), one of the most frequent gynecologic endocrine disorders affecting approximately 7% of reproductive women (1), is currently defined by presenting at least two of three following features: ovarian dysfunction (oligo- and/or anovulation), clinical and/or biochemical signs of hyperandrogenism and polycystic ovarian morphology. It is closely linked to insulin resistance (IR), and type 2 diabetes mellitus (T2DM). IR is recognized to be an integral feature of PCOS. Both lean and obese women with PCOS appear to harbor a greater degree of insulin resistance, compared with their healthy counterparts (2, 3). Several studies have shown that women with PCOS are at increased risk of developing abnormal glucose metabolism (AGM), i.e. impaired glucose tolerance (IGT)

*Key words: visfatin, polycystic ovary syndrome, predictor, insulin resistance, abnormal glucose metabolism, glucose intolerance*

*Mailing address:* Prof. Dongzi Yang,
Department of Obstetrics and Gynecology,
Memorial Hospital of Sun Yat-Sen University,
Yanjiang West Road #107,
Guangzhou, 510120, China
Tel: +86 20 81332131 Fax: +86 20 81332011
e-mail: yangdz57@gmail.com



0393-974X (2012)

and T2DM (4, 5) .Furthermore, PCOS has been regarded as a significant non-modifiable risk factor for T2DM. Accordingly, patients with PCOS are at a substantially increased risk for cardiovascular disease (6).

Visfatin, a novel adipokine predominantly secreted by visceral adipose tissue, was first reported in 2005 by Fukuhara (7) to mimic the glucose-lowering action of insulin through a distinct binding site on the insulin receptor. According to some investigators, plasma concentrations of visfatin are elevated in patients with obesity, IGT and T2DM (8, 9), states characterized by insulin resistance. And elevated visfatin levels are typically also observed in gestational diabetes mellitus (GDM) (10). Visfatin has thus been considered to play a potential role in insulin resistance and glucose metabolism. Recently, the relationships between visfatin and metabolic parameters, such as insulin resistance and dyslipidemia in PCOS women, have been examined. Two studies from Asia found that plasma visfatin was markedly elevated in PCOS (11, 12).

With the aforementioned in mind, we hypothesize that there will be a difference in plasma visfatin concentrations among Chinese PCOS subjects with different glucose tolerance. Given the potential effects of drugs and obesity on insulin sensitivity, plasma visfatin concentrations can possibly be altered in such patients when the treatment is initiated. Therefore, in the present study, circulating visfatin levels were investigated in patients with newly diagnosed and previously untreated PCOS who had no confounding factors for insulin sensitivity. Also, the purpose of this study is to assess the association between visfatin and marker of insulin resistance such as homeostasis model assessment (HOMA) among women with PCOS in different disordered glucose metabolism. Finally, whether plasma visfatin level could substitute oral glucose tolerance test (OGTT) as a good predictive factor for glucose intolerance in Chinese women with PCOS was also evaluated.

## MATERIALS AND METHODS

*Study group*

A total of 932 adult PCOS patients were diagnosed consecutively at Gynecological Endocrinology Outpatient Department at the Sun Yat-sen Memorial Hospital of Sun Yat-sen University from January, 2004 to March, 2010. Among them, 91 patients who were newly diagnosed and previously untreated were included in this study. During the same period, 28 healthy, normally menstruating women with no sign of hyperandrogenism who were on routine check-up, had complete clinical records and had signed the consent forms were served as control subjects. All women were of Han Chinese origin and non-smokers. The diagnosis of PCOS was established according to the Rotterdam criteria (13), by the presence of at least two out of the following three criteria: i) oligo- and/or anovulation (i.e. ≤8 menstrual periods in a year or menstrual cycles more than 35 days in length), ii) clinical hyperandrogenism [i.e. acne or modified Ferriman–Gallwey scores ≥8 (3)] or biochemical hyperandrogenism (i.e. serum total testosterone (TT)≥2.6 nmol/l, free testosterone (FT)≥6.0 pg/ml, testosterone and FT normal values were determined by the clinical laboratory of the gynecology department at the Memorial Hospital of Sun Yat-Sen University), and iii) ultrasonographic findings of ovarian polycystic morphology (i.e. presence of ≥12 follicles in each ovary measuring 2–9 mm in diameter) and exclusion of related disorders such as hypothyroidism, hyperprolactinemia, and adrenal hyperplasia by physical examination and lab testing of TSH, prolactin (PRL), and serum 17a-hydroxyprogesterone (17a-OHP). All controls were euthyroid according to clinical evaluation and thyroid-stimulating hormone (TSH) measurement. Furthermore, no women were on any medication within the previous 3 months, including oral contraceptives, glucocorticoids, ovulation induction agents, antidiabetic and antiobesity drugs, or estrogenic, antiandrogenic, or antihypertensive medication, or drugs known to affect carbohydrate and lipid metabolism.

None of the women studied had known cardiovascular disease, thyroid disease, neoplasms, hypertension, renal impairment or any other systemic disease that could possibly affect their reproductive physiology. Furthermore, no women were on any medication within the previous 3 months, including oral contraceptives, glucocorticoids, ovulation induction agents, antidiabetic and antiobesity drugs, or estrogenic, antiandrogenic, or antihypertensive medication, or drugs known to affect carbohydrate and lipid metabolism.

Informed consent was obtained from all women and the study was approved by the institutional review board of the hospital.

*Anthropometry*

All subjects underwent anthropometric measurements, i.e. weight, height, and waist to hip circumference ratio (WHR). The BMI was calculated as body weight

in kilograms divided by height in meters squared (kg/m2). Waist circumference was obtained as the smallest circumference at the level of the umbilicus. Hip circumference was obtained as the widest circumference at the level of the buttocks.

*Biochemical and hormonal analysis*

After an overnight fast, blood samples were collected between 08:00 and 10:00 a.m. on the 3rd-5th day after a spontaneous menses or independent of cycle phase in the presence of amenorrhea. Samples were stored at −70°C and measured within 6 months.

Plasma free-testosterone (FT), sex hormone binding globulin (SHBG), dehydroepiandrosterone sulfate (DHEAS), and 17-hydroxyprogesterone (17-OHP) were measured by enzyme-linked immunosorbent assay (ELISA). Testosterone, LH, FSH, PRL, TSH and insulin were measured by chemiluminescence (ACS180 · SE, Bayer, Germany). Free androgen index (FAI) was calculated as serum testosterone (nmol/L) ×100/SHBG (nmol/L) ratio (3). In women who matched the criteria for PCOS, PRL, TSH, and 17-hydroxyprogesterone (17-OHP) were also measured to exclude hyperprolactinemia, hypothyroidism, and non-classic 21-hydroxylase deficiency, respectively.

Fasting venous blood samples were also used to measure the levels of glucose, insulin, TC, TG, and HDL-C. Plasma glucose was measured by the glucose oxidase method (Hitachi 7600) and plasma insulin was measured using a chemiluminescence immunometric assay and commercial kit (Immulite 2000 Analyzer; CPC). TC, HDL-C, and TG were measured using an enzymatic calorimetric method with the 7600 autoanalyzer (Hitachi 7600). The LDL cholesterol level was calculated using the Friedewald equation. HOMA was applied to estimate the degree of IR. The equation used to obtain this value is as follows: HOMA-IR=[fasting plasma glucose (mmol/L)*insulin (μU/mL)]/22.5 (3).

For controls, fasting blood samples were collected and the same methodologies described above were used to measure TSH, fasting plasma glucose (FPG), fasting insulin (FIns), TG, TC, HDL-C, LDL-C. HOMA-IR was also calculated.

*Oral glucose tolerance test*

An OGTT was used to evaluate glucose metabolism in PCOS group. A standardized 75-g oral glucose load was ingested after a 10- to 12-h overnight fast. Blood samples were collected from an antecubital vein at baseline and at 1 and 2 h after glucose ingestion. All women had normal fasting glucose levels (<6.1mmol/l). A 2-h glucose value of >7.8 mmol/l was considered as IGT and of >11.1 mmol/l as T2DM according to the WHO definition (14).

*Statistical analysis*

Statistical analysis was carried out with SPSS 11.0 (SPSS, Chicago, IL, USA). The normal distribution of all studied parameters was checked with histograms and the Kolmogorov- Smirnoff test. After testing, all serum values except visfatin showed normal distribution. Log transformation was performed on visfatin before further analysis. Comparisons between groups were made with Student's *t*-test. Pearson correlation coefficients were calculated to determine the correlations between various parameters. Visfatin was used as diagnostic parameter. ROC analysis was performed to examine its diagnostic test performance, i.e. the ability to distinguish PCOS women with and without abnormal glucose metabolism. Sensitivity against (1- specificity) was plotted at each level, and the area under the curve (AUC) which reflects the probability of correctly identifying PCOS women with normal or abnormal glucose metabolism. The Youden index (sensitivity + specificity -1) was calculated to determine the best compromise between sensitivity and specificity; the closer the value is to 1, the greater the diagnostic power. Two-tailed $P<0.05$ was considered statistically significant.

## RESULTS

A total of 91 women with PCOS and 28 controls were studied in our research. Clinical and endocrine features of the two groups are summarized in Table I. Serum visfatin level and fasting plasma glucose concentration were found to be significantly higher in PCOS group compared to the control group. However, there were no statistically significant differences in terms of age, BMI, WC, WHR, SBP, DBP, FIN and HOMA-IR.

Further investigation in the PCOS group showed that twenty-four subjects (26.4%) were categorized as having IGT and five (5.5%) as having T2DM. Visfatin level seemed to be the highest in T2DM subgroup, while the lowest in PCOS women with normal glucose tolerance (NGT). However, in contrast with our expectation, there was no significant difference between each subgroup (Fig. 1). Given the quite small amount of PCOS subjects with T2DM (n=5), we combined IGT and T2DM subgroups to form abnormal glucose tolerance (AGT) group with relatively large sample size. Even after this manipulation, the difference of visfatin between PCOS women with NGT and AGT still did not reach the statistical significance as Table II showed.

**Table I.** *Clinical and endocrine features of the study groups.*

| | PCOS group (n=91) | Control group (n=28) | ***P*** value [a] |
|---|---|---|---|
| Age (y) | 27.28±4.35 | 28.62±5.36 | NS |
| BMI (kg/m$^2$) | 22.48±3.43 | 21.93±3.63 | NS |
| WC(cm) | 75.85±8.64 | 76.67±8.74 | NS |
| WHR | 0.83±0.07 | 0.82±0.05 | NS |
| SBP(mmHg) | 110.69±12.75 | 108.34±11.93 | NS |
| DBP(mmHg) | 72.37±8.52 | 72.12±8.33 | NS |
| FPG(mmol/l) | 5.03±0.35 | 4.52±0.28 | <0.05 |
| FIN(mIU/l) | 8.04±3.01 | 6.10±2.12 | NS |
| HOMA-IR | 1.82±0.88 | 1.75±0.81 | NS |
| Log Visfatin (ng/ml) | 1.23±0.60 | 0.76±0.36 | <0.05 |

*Data are presented as mean ± SD. BMI: body mass index; WC: waist circumference; WHR: waist circumference to hip circumference ratio; SBP: systolic blood pressure; DBP: diastolic blood pressure; FPG: fasting plasma glucose; FIN: fasting insulin; HOMA-IR: homeostasis model assessment of insulin resistance; NS: not significant.*
[a] PCOS versus control. A Mann-Whitney test was used.

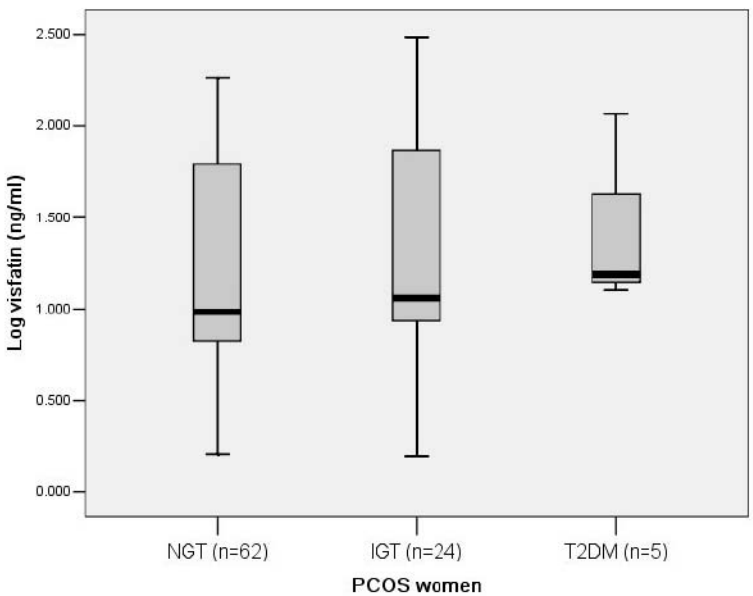


**Fig. 1.** *Box and whisker plots depicting the serum visfatin levels in PCOS patients with different glucose metabolism status. Solid lines inside boxes depict the median visfatin level, whereas the upper and lower limits of the boxes and whiskers indicate 75th, 25th and 95th, and 5th percentiles.*

Moreover, there were no differences between two groups with regard to hormonal, anthropometric, lipid metabolic parameters except FPG.

Unexpectedly, in all the subjects as a whole, visfatin was found to correlate with neither age, anthropometric, hormonal nor metabolic parameters. In addition, we performed the correlation analysis in the PCOS and control group. The results remained

**Table II.** *Clinical and endocrine features of NGT-PCOS group and AGM-PCOS group.*

| | NGT-PCOS group (n=62) | AGM-PCOS group (n=29) | ***P*** value |
|---|---|---|---|
| Age (y) | 27.02±4.68 | 28.06±3.19 | NS |
| BMI(kg/m$^2$) | 22.32±3.32 | 22.94±3.82 | NS |
| WC (cm) | 75.15±8.32 | 77.68±9.43 | NS |
| WHR | 0.82±0.06 | 0.84±0.05 | NS |
| SBP (mmHg) | 108.29±12.4 | 117.47±11.5 | NS |
| DBP (mmHg) | 71.65±8.5 | 74.41±8.4 | NS |
| FPG (mmol/l) | 4.90±0.45 | 5.20±0.67 | <0.05 |
| FIN (mIU/l) | 7.76±3.02 | 9.17±3.46 | NS |
| HOMA-IR | 1.72±0.83 | 2.06±0.92 | NS |
| FSH(IU/L) | 8.61±2.30 | 6.84±2.29 | NS |
| LH(IU/L) | 11.19±6.03 | 10.74±6.63 | NS |
| T(nmol/L) | 2.40±1.06 | 2.44±1.54 | NS |
| FT(pg/mL) | 4.54±2.10 | 3.40±1.87 | NS |
| SHBG(nmol/L) | 67.42±9.60 | 55.66±9.58 | NS |
| FAI | 6.74±2.35 | 6.11±3.18 | NS |
| TG(mmol/L) | 1.30±0.68 | 1.41±0.71 | NS |
| TC(mmol/L) | 5.02±0.77 | 5.07±0.87 | NS |
| HDL-C(mmol/L) | 1.55±0.30 | 1.40±0.40 | NS |
| LDL-C(mmol/L) | 2.97±0.60 | 3.01±0.93 | NS |
| Log Visfatin | 1.20±0.59 | 1.33±0.65 | NS |

*Data are presented as mean ± SD. FSH: follicle-stimulating hormone; LH: luteinizing hormone; T: total testosterone; FT: free testosterone; SHBG: sex hormone-binding globulin; FAI: free androgen index; TG: triglycerides; TC:, total cholesterol; HDL-C: high-density lipoprotein cholesterol; LDL-C: low-density lipoprotein cholesterol; PRL: prolactin; NS: not significant.*

the same as above, and are shown in Table III.

The diagnostic value of the visfatin assay was tested by the ROC curve. As displayed in Fig. 2, AUC for visfatin reached a value of 0.554 (0.371–0.725, 95% confidence interval). The best cut-off value that discriminates PCOS women with abnormal glucose metabolism from other PCOS women is 190ng/mL, with a sensitivity of 16.1% and a specificity of 100%.

## DISCUSSION

This study was designed to investigate the plasma visfatin levels in Chinese women with newly diagnosed PCOS who were free of any medication including over the counter drugs. Plasma visfatin levels were found to be significantly higher in our PCOS population compared to healthy controls in this paper that supported previous ones (11, 12, 15-17). We also described herein an increase in fasting visfatin concentrations with a worsening degree of glucose intolerance among PCOS patients. However, the difference did not reach statistical significance. In addition, visfatin was unexpectedly found to correlate with neither age, anthropometric, hormonal nor metabolic parameters. Furthermore, to our knowledge, this is the first study to investigate the possibility of substituting visfatin for OGTT as a simple predictor for glucose intolerance to distinguish PCOS individuals with normal or abnormal glucose metabolism, though the result seems unfavorable.

Adipose tissue, previously considered to be just an energy storage site, has emerged as a highly active endocrine organ secreting a wide range of soluble bioactive compounds and, most likely, playing a

**Table III.** *Relationships of serum visfatin with anthropometric, biochemical and hormonal parameters in PCOS and Control group respectively.*

| Parameter | PCOS group | | Control group | | Parameter | PCOS group | | Control group | |
|---|---|---|---|---|---|---|---|---|---|
| | *R* | *P* | *R* | *P* | | *R* | *P* | *R* | *P* |
| Age | -0.153 | 0.179 | -0.068 | 0.842 | FSH | -0.049 | 0.672 | -0.684 | 0.096 |
| BMI | -0.091 | 0.403 | -0.691 | 0.058 | LH | 0.202 | 0.076 | -0.525 | 0.175 |
| WC | -0.087 | 0.452 | 0.071 | 0.758 | T | 0.162 | 0.159 | -0.384 | 0.348 |
| WHR | -0.042 | 0.721 | 0.034 | 0.774 | FT | 0.217 | 0.063 | 0.094 | 0.832 |
| SBP | 0.163 | 0.158 | 0.112 | 0.374 | SHBG | -0.079 | 0.503 | 0.266 | 0.564 |
| DBP | 0.042 | 0.719 | 0.053 | 0.874 | FAI | -0.156 | 0.175 | -0.463 | 0.345 |
| 0-h glucose | 0.109 | 0.317 | -0.110 | 0.377 | TG | -0.064 | 0.584 | 0.027 | 0.966 |
| 2-h glucose | 0.132 | 0.240 | -0.066 | 0.887 | CHOL | -0.076 | 0.524 | 0.752 | 0.093 |
| 0-h insulin | 0.002 | 0.982 | -0.263 | 0.528 | HDL | -0.007 | 0.955 | -0.232 | 0.708 |
| HOMA-IR | -0.061 | 0.585 | -0.254 | 0.543 | LDL | -0.036 | 0.766 | 0.500 | 0.391 |

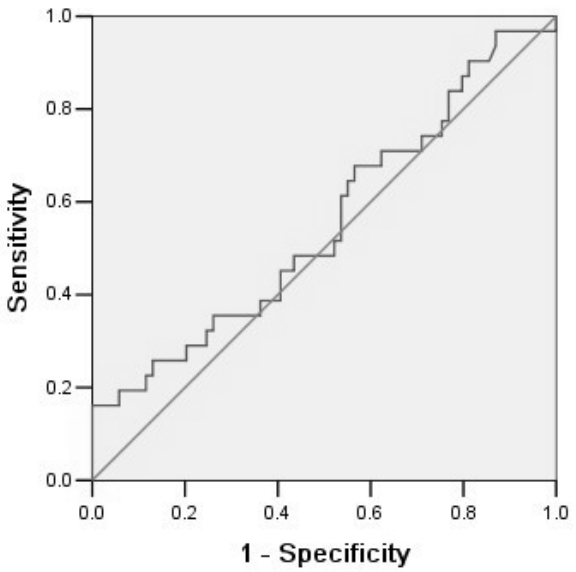


**Fig. 2.** *Receiver operating characteristic curve for visfatin giving the diagnostic value of serum visfatin in Chinese PCOS patients with abnormal glucose metabolism.*

profound role in significant aspects of metabolism (18). This can partly explain the link between obesity, insulin resistance, beta-cell dysfunction, endothelial dysfunction, and atherosclerosis (19). Predominantly produced in and secreted from visceral adipose tissue, visfatin expression is increased in animal models of obesity, and its plasma concentrations are increased in humans with abdominal obesity (20), type 2 diabetes mellitus (8, 9, 21) or gestational diabetes (10). PCOS is a challenging entity that is involved in several metabolic abnormalities such as obesity, glucose intolerance and dyslipidemia. According to proven evidence (12) but through unclear mechanisms, PCOS patients tend to be more obese, especially in an android fat distribution pattern, and more insulin-resistant than the healthy population. Therefore, as expected, visfatin expression and/or circulating visfatin levels have been reported to be significantly higher in PCOS sufferers compared to healthy controls of similar BMI and age (11, 12, 15-17), with which our finding is in agreement. At the same time, no difference has been reported in a few studies concerning lean, or obese women with PCOS (20, 22, 23). In literature (24), rather than being secreted, visfatin has been shown to be released from fat cells during lipolysis which might be stimulated by the development of obesity, upper body fat distribution, or both. The lipolytic effect in PCOS subjects is augmented because of a selective increase in the function of protein kinase A–hormone-sensitive lipase complex in visceral fat cells (25), leading to the final elevation of visfatin levels. On the other hand, the increased visfatin in PCOS women was speculated to possibly be a compensatory response to insulin resistance in specific tissues or a marker of tissue-specific inflammatory cytokine action, which may account, in particular, for the higher omental visfatin expression. Nonetheless, most studies in this field were focused on one adipokine, thus overlooking the potentially significant metabolic effects of the interplay between various adipokines in this specific

population. The meanings of hypervisfatinemia in PCOS women currently are still unclear.

More recently, visfatin has been described as a regulator of insulin secretion via improving β-cell function (21, 26). Circulating visfatin concentrations were shown to be correlated with the volume of visceral fat and increase in parallel with hyperglycemia, but this effect is suppressed by exogenous hyperinsulinemia or somatostatin infusion (8, 27). These findings suggest that visfatin may play a pathophysiological role in glucose homeostasis. However, the relevant data is quite limited and conflicting. Chen et al. found a positive association between visfatin and the presence of T2DM, even after adjustment for BMI, age, sex, smoking status, blood pressure, and lipid profile (8). Dogru et al., studying visfatin levels in 40 subjects with newly diagnosed diabetes or glucose intolerance, found that visfatin levels were higher in the diabetic patients when compared to controls, but not when compared to glucose intolerant patients (pre-diabetes), suggesting that visfatin might be involved in the pathogenesis of T2DM but not at the early stages (9). In this study, in order to exclude the interference of medication, we enrolled only PCOS patients who were newly diagnosed, possibly had IGT or DM, but were previously untreated. Moreover, the present study addressed the natural behavior of visfatin levels in IGT and T2DM at the time of diagnosis and excluded the effects of hypoglycemic medication. In support with Dogru, we found, in PCOS subjects, a similar tendency of visfatin increasing with the development of glucose metabolism dysregulation (Fig. 1), which did not reach statistical significance probably due to the relatively small amount of PCOS subjects in T2DM subgroup. Accordingly, we combined the PCOS individuals with either IGT or T2DM into AGM group in a large enough sample size. Even after this manipulation, the difference of visfatin between PCOS women with NGT and AGM still did not reach the statistical significance. In keeping with the current study, Takebayashi found no correlation between diabetes and visfatin (28), while another study, demonstrated decreased visfatin in patients with T1DM and inverse relationship between A1C and visfatin levels (29). Therefore, despite numerous publications during the following 6 years after the first paper of visfatin, its role in abnormal metabolism, besides glucose intolerance, remains to be elucidated.

As common metabolic traits in PCOS, insulin resistance and abdominal obesity have been extensively studied concerning their relationship with visfatin, while conflicting results were obtained. Chan et al. (11) found a significant positive correlation between visfatin levels and BMI in subjects with PCOS but not in normal healthy women. Likewise, some insulin resistance surrogates such as FIN and HOMA were found to be closely correlated with visfatin levels (15, 16, 22). However, more current reports have described no associations with BMI, fat distribution, insulin resistance or markers of insulin sensitivity (17, 20, 30). The present study also failed to detect any relationship of serum visfatin to insulin levels, HOMA-IR, BMI or WHR not only in PCOS group but also in healthy controls. Moreover, hyperandrogenemia parameters in our study were not found to be correlated with visfatin. This observation was in contrast with almost all previous articles except Chan's report. Several studies have shown that approximately 10–40% of PCOS women, including both lean and obese patients, suffer from abnormal glucose metabolism, i.e. IGT or T2DM (8, 9). Moreover, both the annual progression rates from normal glucose tolerance to IGT, and from IGT to T2DM are high (31). Accordingly, PCOS is regarded as a risk factor for the development of T2DM and general screening of PCOS patients for IGT and/or T2DM has been recommended annually or at least every 2 years (13). Though suggested as a screening parameter for abnormal glucose metabolism, fasting glucose concentrations were demonstrated to be within normal range in a substantial proportion of PCOS women with IGT or even T2DM (5), indicating its insensitiveness as a satisfactory predictor. In comparison, OGTT, as a dynamic method, may provide a relatively more precise estimate of insulin resistance (32). However, this procedure is correspondingly time-consuming, which may limit its use as a general screening instrument in PCOS women, especially adolescent ones. Therefore, we investigated the ability of plasma visfatin level as a rapid and simple method which could be desirable to direct the need to perform an OGTT for those PCOS individuals who are most likely to be suffering from abnormal glucose metabolism. To define the

best discriminating parameter between normal and abnormal metabolism, ROC curves, a method often used to investigate such an issue, were calculated and analyzed in our study. But unexpectedly, the present study fails to demonstrate in a Chinese PCOS population that serum visfatin is a reliable predictor of glucose intolerance, as diagnosed using OGTT. The threshold for visfatin at 190ng/ml (sensitivity 16.1%, specificity 100%) obtained the best compromise between sensitivity and specificity, based on the optimal Youden index in a poor level at 0.161. This discrepancy from our anticipation might be partly explained by the finding that visfatin showed no correlation with insulin resistance in our PCOS group and other ethnic reports (17, 23), possibly as a result within the complex context of this specific category of disorder.

In conclusion, serum visfatin is significantly elevated in Chinese women with PCOS, but might not be a reliable predictor of their glucose intolerance. Due to the relatively small sample size and cross-sectional nature of the current study, we did not prove the cause-effect relationship between visfatin and either PCOS or abnormal glucose metabolism in PCOS. However, it is worthy to note that PCOS patients present hypervisfatinemia accompanying with higher fasting glucose level. Further studies with larger populations are worthwhile to evaluate the role of visfatin in the pathogenesis of both PCOS and glucose intolerance.

## ACKNOWLEDGEMENTS

This study was financially supported by the Science Technology Research Project of Guangdong Province (2010B031600058), the Science Technology Research Project of Guangzhou city (2010Y1-C431), 2010 Key Project of Research of the National Ministry of Health, and the National Science Technology Research Project (81070466) in China.

## REFERENCES

1. Azziz R, Woods KS, Reyna R, Key TJ, Knochenhauer ES, Yildiz BO. The prevalence and features of the polycystic ovary syndrome in an unselected population. J Clin Endocrinol Metab 2004; 89:2745-9.
2. Dunaif A. Insulin resistance and the polycystic ovary syndrome: mechanism and implications for pathogenesis. Endocr Rev 1997;18:774-800.
3. Hong Y, Yang DZ, Liu W, Zhao XM, Chen XL, Li L. Dyslipidemia in relation to body mass index and insulin resistance in Chinese women with polycystic ovary syndrome. J Biol Reg Homeos Ag 2011; 25:365-74.
4. Gambineri A, Pelusi C, Manicardi E, Vicennati V, Cacciari M, Morselli-Labate AM, Pagotto U, Pasquali R. Glucose intolerance in a large cohort of Mediterranean women with polycystic ovary syndrome: phenotype and associated factors. Diabetes 2004; 53:2353-8.
5. Legro RS, Kunselman AR, Dodson WC, Dunaif A. Prevalence and predictors of risk for type 2 diabetes mellitus and impaired glucose tolerance in polycystic ovary syndrome: a prospective, controlled study in 254 affected women. J Clin Endocrinol Metab 1999; 84:165-9.
6. Engin-Ustun Y, Ustun Y, Meydanli MM, Kafkasli A, Yetkin G. Are polycystic ovaries associated with cardiovascular disease risk as polycystic ovary syndrome? Gynecol Endocrinol 2006; 22:324-8.
7. Fukuhara A, Matsuda M, Nishizawa M, et al. Visfatin: a protein secreted by visceral fat that mimics the effects of insulin. Science 2005; 307:426-30.
8. Chen MP, Chung FM, Chang DM, Tsai JC, Huang HF, Shin SJ, Lee YJ. Elevated plasma level of visfatin/pre-b cell colony-enhancing factor in patients with type 2 diabetes mellitus. J Clin Endocrinol Metab 2006; 91:295-9.
9. Dogru T, Sonmez A, Tasci I, et al. Plasma visfatin levels in patients with newly diagnosed and untreated type 2 diabetes mellitus and impaired glucose tolerance. Diab Res Clin Pract 2007; 76:24-29.
10. Lewandowski KC, Stojanovic N, Press M, et al. Elevated serum levels of visfatin in gestational diabetes: a comparative study across various degrees of glucose tolerance. Diabetologia 2007; 50:1033-7.
11. Chan TF, Chen YL, Chen HH, Lee CH, Jong SB, Tsai EM. Increased plasma visfatin concentrations in women with polycystic ovary syndrome. Fertil Steril 2007; 88:401-5.
12. Jongwutiwes T, Lertvikool S, Leelaphiwat S, Rattanasiri S, Jultanmas R, Weerakiet S. Serum visfatin in Asian women with polycystic ovary

syndrome. Gynecol Endocrinol 2009; 25: 536-42.
13. Rotterdam ESHRE/ASRM-Sponsored PCOS Consensus Workshop Group. Revised 2003 consensus on diagnostic criteria and long-term health risks related to polycystic ovary syndrome. Fertil Steril 2004; 81:19-25.
14. Genuth S, Alberti KG, Bennett P, et al. Follow-up report on the diagnosis of diabetes mellitus. Diabetes Care 2003; 26:3160-7.
15. Tan BK, Chen J, Digby JE, Keay SD, Kennedy CR, Randeva HS. Increased visfatin messenger ribonucleic acid and protein levels in adipose tissue and adipocytes in women with polycystic ovary syndrome：parallel increase in plasma visfatin. J Clin Endocrinol Metab 2006; 91:5022-8.
16. Ozkaya M, Cakal E, Ustun Y, Engin-Ustun Y. Effect of metformin on serum visfatin levels in patients with polycystic ovary syndrome. Fertil Steril 2010; 93:880-4.
17. Gen R, Akbay E, Muslu N, Sezer K, Cayan F. Plasma visfatin level in lean women with PCOS: relation to proinflammatory markers and insulin resistance. Gynecol Endocrinol 2009; 25:241-5.
18. Koerner A, Kratzsch J, Kiess W. Adipocytokines: leptin—the classical, resistin—the controversical, adiponectin—the promising, and more to come. Best Pract Res Clin Endocrinol Metab 2005; 19:525-46.
19. Bulcao C, Ferreira SR, Giuffrida FM, Ribeiro-Filho FF. The new adipose tissue and adipocytokines. Curr Diabetes Rev 2006; 2:19-28.
20. Berndt J, Kloting N, Kralisch S, Kovacs P, Fasshauer M, Schon MR, Stumvoll M, Bluher M. Plasma visfatin concentrations and fat depot-specific mRNA expression in humans. Diabetes 2005; 54:2911-16.
21. Lopez-Bermejo A, Chico-Julia B, Fernandez-Balsells M, Recasens M, Esteve E, Casamitjana R, Ricart W, Fernandez-Real JM. Serum visfatin increases with progressive beta-cell deterioration. Diabetes 2006; 55:2871-5.
22. Kowalska I, Straczkowski M, Nikolajuk A, et al. Serum visfatin in relation to insulin resistance and markers of hyperandrogenism in lean and obese women with polycystic ovary syndrome. Hum Reprod 2007; 22:1824-9.
23. Pagano C, Pilon C, Olivieri M, et al. Reduced plasma visfatin/pre-B cell colony-enhancing factor in obesity is not related to insulin resistance in humans. J Clin Endocrinol Metab 2006; 91:3165-3170.
24. Rongvaux A, Shea RJ, Mulks MH, Gigot D, Urbain J, Leo O, Andris F. Pre- B-cell colony-enhancing factor, whose expression is up-regulated in activated lymphocytes, is a nicotinamide phosphoribosyltransferase, a cytosolic enzyme involved in NAD biosynthesis. Eur J Immunol 2002; 32:3225-34.
25. Ek I, Arner P, Ryden M, Holm C, Thorne A, Hoffstedt J, Wahrenberg H. A unique defect in the regulation of visceral fat cell lipolysis in the polycystic ovary syndrome as an early link to insulin resistance. Diabetes 2002; 51:484-92.
26. Revollo, JR, Korner A, Mills KF, et al. Nampt/PBEF/Visfatin regulates insulin secretion in beta cells as a systemic NAD biosynthetic enzyme. Cell Metabolism 2007; 6:363-75.
27. Haider DG., Schindler K, Schaller G, Prager G, Wolzt M, Ludvik B. Increased plasma visfatin concentrations in morbidly obese subjects are reduced after gastric banding. J Clin Endocrinol Metab 2006; 91:1578-81.
28. Takebayashi K, Suetsugu M, Wakabayashi S, Aso Y, Inukai T. Association between plasma visfatin and vascular endothelial function in patients with type 2 diabetes mellitus. Metabolism 2007; 56 451-8.
29. Toruner F, Altinova AE, Bukan N, Arslan E, Akbay E, Ersoy R, Arslan M. Plasma visfatin concentrations in subjects with type 1 diabetes mellitus. Horm Res 2009; 72:33-37.
30. Pepene CE. Evidence for serum visfatin but not adiponectin or resistin as an independent predictor of endothelial dysfunction in polycystic ovary syndrome. Clin Endocrinol (Oxf) 2012; 76:119-25.
31. Salley KE, Wickham EP, Cheang KI, Essah PA, Karjane NW, Nestler JE. Glucose intolerance in polycystic ovary syndrome – a position statement of the Androgen Excess Society. J Clin Endocrinol Metab 2007; 92:4546-56.
32. de Paula Martins W, Santana LF, Nastri CO, Ferriani RA, de Sa MF, Dos Reis RM. Agreement among insulin sensitivity indexes on the diagnosis of insulin resistance in polycystic ovary syndrome and ovulatory women Eur J Obstet Gynecol Reprod Biol 2007; 133:203-7.

# EFFECT OF TANNIN EXTRACT AGAINST *PSEUDOMONAS AERUGINOSA* PRODUCING METALLO BETA-LACTAMASE

S. GHAFOURIAN[1,2], R. MOHEBI[1], Z. SEKAWI[2], M. RAFTARI[3], V. NEELA[2], E. GHAFOURIAN[1], E. ABOUALIGALEHDARI[1], M. RAHBAR[4] and N. SADEGHIFARD[1]

*[1]Clinical Microbiology Research Center, Ilam University of Medical Sciences, Ilam, Iran; [2]Department of Medical Microbiology and Parasitology, Faculty of Medicine and Health Sciences, University Putra Malaysia, Selangor, Malaysia; [3]Faculty of Food Science and Technology, University Putra Malaysia, Selangor, Malaysia; [4]Department of Microbiology, Iranian Reference Health Laboratories, Tehran, Iran*

*Received February 22, 2012 – Accepted March 27, 2012*

**Carbapenems are the most potent beta-lactam agents with a broad-spectrum activity against Gram-negative and Gram-positive bacteria. They are stable in the presence of penicillinases and cephalosporinases. This study was focused on frequency of metallo beta- lactamase (MBL) among *Pesudomonas aeruginosa* strains isolated in patients with urinary tract infection, effect of tannin against PA positive strains which produced bla*VIM* or bla*IMP* and both of these genes (Species). Detection of MBL was performed by phonotypic and genotypic methods. Tannin extract was tested against *P. aeruginosa* producing MBL. During the study period, 240 *P. aeruginosa* isolates were identified. Among them 64 (26.6%) isolates were imipenem non-susceptible and confirmed by imipenem/EDTA. Our results revealed that the growth of bla*VIM* positive *P. aeruginosa* inhibited at 15µg/ml concentration. The experiment repeated for bla*IMP*-positive *P. aeruginosa* and *P. aeruginosa* which harbored bla*IMP* and bla*VIM*, the results showed 35µg/ml was the best concentration for inhibition of *P. aeruginosa*-positive bla*IMP* and also *P. aeruginosa* bla*IMP* and bla*VIM*. In conclusion, tannin was effective against *P. aeruginosa* producing bla*VIM* and bla*IMP* and both of them so it can be substituted with common antibiotics. The result showed significantly *P. aeruginosa*-harbored blaIMP was more responsible for imipenem resistance than *P. aeruginosa*-positive bla*VIM*. Interestingly, tannin was more effective against MBL – *P. aeruginosa* in comparison with current antibiotics.**

One of the factors responsible for the development of ever-increasing resistance to antimicrobial agents has been their widespread overuse and misuse. Consequently, the rational use of antimicrobial agents is imperative in establishing a successful strategy to control and prevent the development of further resistance. The careful selection of the appropriate antimicrobial agent including dose, duration of treatment, and route of administration, coupled with antimicrobial resistance surveillance, are all important to the success of this strategy (1). Carbapenems are the most potent beta-lactam agents with a broad-spectrum activity against Gram-negative and Gram-positive bacteria. They are stable in the

*Key words: Pseudomonas aeruginosa, tannin, urinary tract infection*

*Mailing address:* Dr. Nourkhoda Sadeghifard,
Clinical Microbiology Research Center,
Ilam University of Medical Sciences,
6931994585, Ilam, Iran
Tel: +989187465523
Fax: +988412227136
e-mail: sadeghifard@gmail.com



0393-974X (2012)

presence of penicillinases and cephalosporinases. However, some classes A, B, and D beta-lactamase as defined by Ambler et al. (2) can hydrolyze carbapenems. In particular, class B β-lactamases, termed MBLs, are an increasingly serious clinical problem because they have a very broad substrate profile which includes penicillins, expanded-spectrum cephalosporins and carbapenems, and exclude only azteronam as a monobactam. During the past decade, various kinds of MBLs, including IMP and VIM types, have increased in prevalence in PA around the world (3).

With resistance seriously reducing the number of efficient antimicrobial agents, there is an increasing need for current comprehensive and accurate susceptibility surveillance data to allow informed therapeutic choices. For example, in selecting an empiric treatment for a nosocomial infection, prevalent resistance patterns should be considered, and the antimicrobial agents chosen should be effective and not further promote the development of resistance. Thus, antimicrobial surveillance programs which provide extensive information on the pattern and development of bacterial resistance in different geographical regions are vital in the fight against bacterial resistance. Evaluation of such data allows changes to be made in antibiotic prescribing practices and infection control procedures, with the ultimate aim of minimizing the development and spread of antimicrobial resistance (4).

bla*IMP* and bla*VIM* MBLs (class B) are increasingly scattered in PA and are slowly but steadily increasing in prevalence (5). Bla *IMP* and bla*VIM* enzymes can be plasmid-mediated and are transferable, although chromosomal gene integration is common. Major clinical problems that have arisen with MBL-producing PA have involved the clonal spread of producer strains, often of serotype O12; gene transfer seems rare. In Thessaloniki, a strain with bla*VIM-2* enzyme persisted for over three years and >200 isolates were obtained (6); in Cali (Colombia), another persisted for four years, infecting patients and surviving in sink traps and fittings (7). Although such outbreaks are disturbing, this concern should not be overplayed; even in the Far East where they seem most prevalent, producers account for <2% of *P. aeruginosa* isolates and are greatly outnumbered by isolates that owe multi-resistance to combinations of AmpC expression (8). This study was focused on frequency of metallo beta- lactamase (MBL) among *P. aeruginosa* strains isolated in urinary tract infection, effect of tannin against *P. aeruginosa* positive strains which produced VIM or IMP and both of these genes.

## MATERIALS AND METHODS

*Bacterial strains*

Two hundred and forty clinical isolates of *P. aeruginosa* were obtained during a one-year period from January 2008 in Ilam Hospitals in Ilam city in the west of Iran. Isolates were collected from patients with urinary tract infections. Identification of organisms was carried out by the standard laboratory technique.

*Bacterial growth condition*

The isolates were grown to mid-exponential phase in nutrient broth at room temperature in a rotary incubator (150 rpm) after which the cells were harvested by centrifugation at 600 rpm for 10 minutes and washed thrice with phosphate buffer. The washed cells were re-suspended in the buffer and the turbidity was adjusted to an optical density of 0.85 at 600 nm. An aliquot (0.2 ml) of the cell suspension was inoculated into Mueller-Hinton agar and incubated at 37°C for 24 h. The plate count was determined after the incubation period.

*Disc diffusion*

Muller Hinton (MH) agar plates seeded with 1 ml of standard culture using spread plate technique was used. Plates were allowed to stand for 15 mins before the different concentrations of tannin discs were applied. Sterile absorbent discs were placed into tannin concentrations for 10 mins before being applied directly onto inoculated agar plates. Control sterile discs were also applied. Plates were incubated at 37°C for 24 h and zones of inhibition were measured.

For antibiotic susceptibility testing, the antimicrobial disks were applied to the plates. Placing the disks individually, they were gently pressed down into the agar. The disks were commonly placed at least 20 mm apart from each other on MH agar plate. This prevented overlapping of the inhibition zones as well as any possible errors in measurements. After placing the disks on the plate, the plate was inverted and incubated at 37°C for 24 h. After the incubation, the diameter of the zones of complete inhibition (including the diameter of the disk) was measured and recorded in millimeters. It was possible to make the measurements with a ruler on the undersurface of the plate without opening the lid.

*Spectrophotometric assay*

An aliquot of a fresh culture of PA was transferred to a flask containing 100 mL of tryptone soy broth and incubated at 32.5±2.5ºC for no longer than 24 h. The suspension obtained from this growth, containing $10^7$-$10^8$ CFU / ml, was used as the inoculum. Solutions of reference standard were prepared containing various concentrations (5, 10, 15, 20, 25, 30, 35, 40, 45, 50, 60, 70, 80, 90 and 100 ug/mL) of tannin, employing tryptone-soy broth as the diluent. Aliquots of 100 µL of each tannin extract were transferred to a microplate. Also, aliquots of 100 µl of tryptone-soy broth were inoculated with PA at 0.5 McFarland concentration.

A microplate spectrophotometer (Biotek Elx808, WI, USA) was used for incubation and reading of microplates. Incubation was performed at a temperature of 37±1ºC for a period of 24 h. Absorbances were measured at 630 nm.

*Detection of MBL performed by phonotypical and genotypic methods*

*Antibiotic drug susceptibility determination.* The isolates were tested for aztreonam, ceftazidime, piperacillin, tazobactam, imipenem, ciprofloxacin and amikacin (9).

*Phonotypical detection.* An MBL phenotypic detection method was designed using a single agar plate and comprised three components. In the combined-disk test, two imipenem disks (10 µg), one containing 10 µl of 0.1 M (292 µg) anhydrous Ethylene diamine tetra acetic acid (EDTA), were placed 25 mm apart (center to center). An increase in zone diameter of 4 mm around the imipenem -EDTA disk compared to that of the imipenem disk alone was considered positive for an MBL(10).

Polymerase chain reaction (PCR) was used for detection of bla*VIM* and bla*IMP* genes.

The bla*VIM* and bla*IMP* genes were searched for by PCR amplification with the following sets of primers: for bla*VIM*, bla*VIM*-forward (5CAGATTGCCGATGGTGTTTGG-3) and bla*VIM*-Reverse (5 AGGTGGGCCATTCAGCCAGA-3); also for bla*IMP*, bla*IMP*-forward (5 GGAATAGAGTGGCTTAATTCTC-3) and bla*IMP*-reverse (5 GTGATGCGTCYCCAAYTTCACT-3) (11).

*Plant material collection.* Tannin obtained from surface of acorn.

The cell line used was Normal African Green Monkey Kidney Epithelial Cells (Vero Line). For the cell culture, Vero cells were routinely maintained in RPMI-1640 medium supplemented with 10% heat inactivated fetal bovine serum, 100 IU/mL penicillin, and 100 µg/mL streptomycin, pH 7.4 in an incubator (Sanyo, Japan) with a humidified atmosphere of 5% CO2 + 95% air at 37°C. The extracts were prepared by boiling surface of acorn (15 g) twice, each time for 1 h with 150 mL of 95% ethanol. After the solution had cooled, the extract was carefully decanted away from the residual solids, centrifuged for 15 min at 3000 rpm and sterile filtered through a 0.45 µm filter. Dissolved constituents were completely dried into powders under vacuum at 100°C in a drying closet for 3 h and in desiccators for 1 day. Dried powders were finally dissolved in distilled water or 95% ethanol, filtered, and stored at 4°C (12).

.

*Toxicity assay*

The cells were plated in 96-well flat bottom plates at 5000–1000 cells/well and were coated overnight. Then the cells were treated with different concentrations of the tannin ethanol herbal extracts (0–100 µg/mL) with a maximal final ethanol concentration of 1%. After 24 h, 3-(4,5-Dimethylthiazol-2-yl)-2,5-Diphenyltetrazolium Bromide (MTT) assay as a described below was used to monitor cell growth (13).

*MTT assay for cell proliferation*

MTT stock was prepared (MTT stock solution: 5mg/ml MTT (Promega) in RPMI-1640 without phenol red). This solution is filtered through a 0.2 mm filter and stored at 2-8°C. MTT working solution was prepared as follows: 1:10 dilution of the 5mg/ml stock (MTT in RPMI without phenol red). For the MTT assay, cultured cells were washed with warm RPMI-1640 without phenol red. Then, 1 ml MTT working solution was added into wells being assayed. The plate was incubated at 37°C for 30 mins to 3 h. At the end of the incubation period, the medium was moved if working with attached cells. The converted dye was solubilized with 1ml acidic isopropanol (0.04 M HCl in absolute isopropanol) and pipetted up and down several times to make sure the converted dye dissolved completely. The dye solutions were transferred into a 1.5 ml Eppendorf tube and centrifuged at 13,000 rpm for 2 mins. The supernatant was transferred into a new Eppendorf tube. Absorbance of the converted dye was measured at a wavelength of 570 nm with background subtraction at 650 nm.

## RESULTS

During the study period 240 PA isolates were identified. Among them 64 (26.6%) isolates were imipenem non-susceptible and confirmed by imipenem/EDTA. The findings showed that 65% (n=156), 75% (n=180), 40.4% (97), 46.25% (n=111), 51.25% (n=123), 79.1% (n=190) and 74.1% (n=178) were resistant to aztreonam, ceftazidime, piperacillin, tazobactam, ciprofloxacin and amikacin,

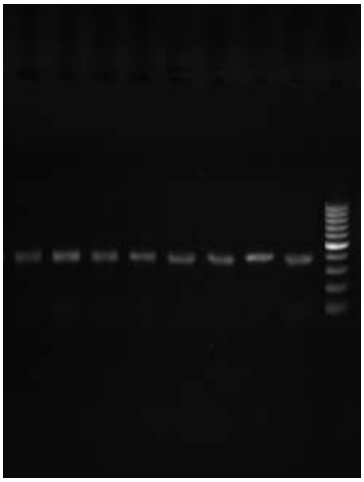

**Fig. 1.** *PCR amplification of blaVIM gene, right to left: Marker=100bp, 1-8 blaVIM=400bp. 100bp.*

**Fig. 2.** *PCR amplification of blaIMP , marker=100bp, blaIMP=250bp.*

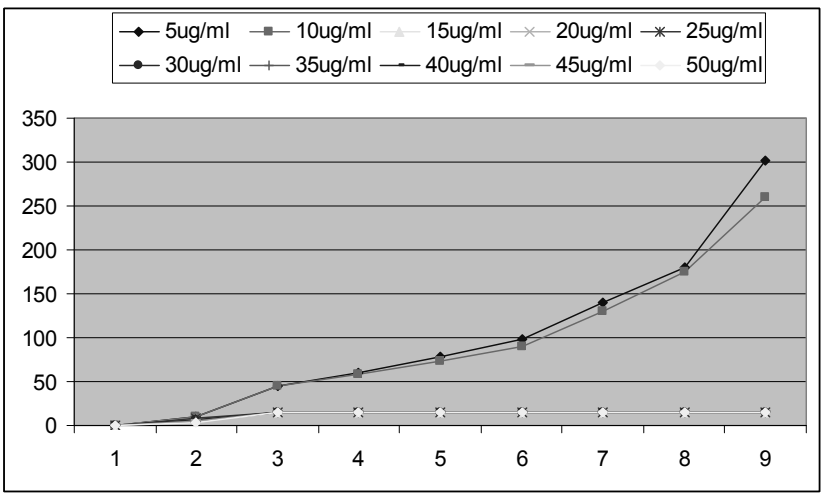


**Fig. 3.** *Different concentration of tannin against P. aeruginosa-harbored blaVIM during 24 hours.*

respectively.

MBL production was identified in 20 isolates (8.3%) by PCR. The bla*VIM* was the most common MBL type (90%, 18 of 20 PA) (Fig. 1), two bla*IMP* were identified (Fig. 2). Among 20 MBL positive strains, one *P. aeruginosa* harbored both bla*VIM* and bla*IMP*.

The turbidimetric assay for evaluation of tannin was based on the interaction between the tannin and *P. aeruginosa* and on the meaning of the turbidity. The interaction between the tannin and *P. aeruginosa* occurs such that the antibiotic inhibits microbial growth. In this way, turbidity provided by microbial growth was inversely proportional to the antibiotic concentration. *P. aeruginosa* should be sensitive to the tannin tested and should grow in liquid culture medium indifferently depending on the concentration of tannin.

The experimental conditions chosen were those that yielded best dose-response curve. Solutions

with concentrations in the range 1 to 100 µg / ml of tannin were evaluated, employing tryptone-soy broth inoculated with *P. aeruginosa.*

The microbial growth curves of solutions at various concentrations (5, 10, 15, 20, 25, 30 , 35, 40, 45and 50 µg / ml) of tannin in tryptone-soy broth inoculated with *P. aeruginosa* positive for bla*VIM* incubated for 24 h (absorbance measured at 630 nm) are shown in Fig. 3. The microbial growth observed was faster for low concentrations of tannin than for high concentrations.

The findings revealed that the growth of bla*VIM*-positive *P. aeruginosa* inhibited at 15µg/ ml concentration. The experiment was repeated for bla*IMP* positive *P. aeruginosa* and also *P. aeruginosa* which harbored blaIMP and bla*VIM*: the results showed 35ug/ml was the best concentration for inhibition of PA-positive bla*IMP* and also *P. aeruginosa*-positive bla*IMP* and bla*VIM*.

Percentage cell viability of cell lines were carried out by using trypan blue dye. It showed the percentage viability Vero cell line live 70-72% which are most suitable to perform cytoxicity studies.

The cytotoxicity study was carried out for plant extract of surface of acorn (tannin). This extract was screened for its cytotoxicity against Vero cell line at different concentrations to determine the IC50 (50% growth inhibition) by MTT assay.

*Determination of Cytotoxicity by MTT assay*

The cytotoxicity activity of tannin on Vero cells was determined by using the MTT reduction assay. The growth inhibitory effects of tannin on Vero cell lines after 24 h exposures were examined. It was found that the percentage growth inhibition increased with increasing concentration steadily up to 55 µg ml, and IC50 value of this assay was 0.245. The ethanolic extract of tannin leaves showed significantly ($IC_{50}$ 55mg/ml).

## DISCUSSION

Among the beta-lactamases, the genetically mobile MBL is present among the most feared, because of its ability to hydrolyze virtually all beta-lactams, except monobactams, and to spread horizontally. Because of their geographic spread, these enzymes are among the greatest concerns to the medical communities. The rates of occurrence and number of enzyme types of MBL have escalated since 2000 in Asia, Europe, and Latin America.

The results of this analysis demonstrate the continued effectiveness of carbapenems against *P. aeruginosa*-producing MBLs. MBLs of the bal*IMP* and bla*VIM* families are a greater concern in non-fermenters bacteria.

During the past decade, various kinds of MBLs, including IMP and VIM types, have increased in prevalence in *P. aeruginosa* around the world (3). The genes encoding MBLs are transferable and have been reported in *P. aeruginosa* worldwide since their first identification in Japan in 1988 (5). Five types of acquired MBLs in *P. aeruginosa* have been described globally: IMP, VIM, SPM, GIM, and SIM, which are carried on integrons (5, 8), among which VIM-type MBL genes were reported to be predominant in *P. aeruginosa* isolates from Europe and Taiwan (5). Among the infections caused by CRPA, MBL-producing *P. aeruginosa* isolates are associated with higher mortality (14). In addition, MBL-producing *P. aeruginosa* isolates are usually co resistant to other current commercially available drugs resulting in limited treatment choice (5).

Of 126 isolates of *P. aeruginosa,* seventy isolates were resistance to imipenem and only eight bla*VIM* gene obtained (15) but in our study in Ilam distribution of bla*VIM* was more than Tehran and our findings reported first detection of bla*IMP* in Iran.

In conclusion, tannin was effective against *P. aeruginosa* producing bla*VIM* and bla*IMP* and both of them those can be substituted with common antibiotics. The result showed significantly PA harbored blaIMP was more responsible for imipenem resistance than *P. aeruginosa*-positive bla*VIM*. Interestingly, tannin was more effective against MBL – *P. aeruginosa* in compression of current antibiotics.

## ACKNOWLEDGEMENTS

Ilam University of Medical Sciences provided partial support for the laboratory studies and interpretation.

## REFERENCES

1. Niederman MS. Appropriate use of antimicrobial

agents: Challenges and strategies for improvement. Crit Care Med 2003; 31:608-16.
2. Ambler RP. The structure of β-lactamases. Phil.Trans R Soc Lond B Biol Sci 1989; 289:321-31.
3. Nordmann P, Poirel L. Emerging carbapenemases in Gram-negative aerobes. Clin Microbiol Infect 2002; 8:321-31.
4. Finch R. Antibiotic resistance from pathogen to disease surveillance. Clin Microbiol Infect 2002; 8:317-20.
5. Walsh TR, Toleman MA, Poirel L, Nordmann P. Metallo-beta-lactamases: the quiet before the storm? Clin Microbiol Rev 2005; 18:306-25.
6. Pournaras S, Woodford N, Palepou MFI, Babini GS, Douboyas, Livermore DM. Outbreak of infections caused by Pseudomonas aeruginosa producing VIM-1 carbapenemase in Greece. J Clin Microbiol 2000; 38:1290-92.
7. Crespo MP, Woodford N, Sinclair A, et al. Outbreak of carbapenem-resistant Pseudomonas aeruginosa producing VIM-8, a novel metallo-beta-lactamase, in a tertiary care centre in Cali, Colombia. J.Clin Microbiol 2004; 42:5094-101.
8. Lee K, Kim YA, Park YJ, et al. Increasing prevalence of imipenem-resistant Pseudomonas aeruginosa and molecular typing of metallo-beta-lactamase producers in a Korean hospital. Microb Drug Resist 2005; 11:355-9.
9. Babay HAH. Antimicrobial Resistance among Clinical Isolates of Pseudomonas aeroginosa from patient in teaching hospital, Riadeh, Saudi Arabia, 2001- 2005. Jpn J Infect Dis 2007; 60:123-6.
10. Yong D, Lee K, Yum JH, Shin HB, Rossolini GM, Chong Y. Imipenem-EDTA disk method for differentiation of metallo-beta-lactamase producing clinical isolates of Pseudomonas spp. and Acinetobacter spp. J Clin Microbiol 2002; 40:3798-801.
11. Docquier JD, Riccio ML, Mugnaioli C, et al. IMP-12, a new pRlasmid-encoded metallo-beta-lactamase from a Pseudomonas putida clinical isolate. Antimicrob Agents Chemother 2003; 47:1522e1528.
12. Shoemaker M, Hamilton B, Dairkee SH, Cohen I, Campbell MJ. In vitro anticancer activity of twelve Chinese medicinal herbs. Phytother Res 2005; 19:49-651.
13. Philip D, Kaleena PK, Valivittan K. In vitro cytotoxicity and anticancer activity of Sanseviera roxburghiana. Int J Curr Pharmac Res 2011; 3(3):71-73.
14. Laupland KB, Parkins MD, Church DL, et al. Population-based epidemiological study of infections caused by carbapenem-resistant Pseudomonas aeruginosa in the Calgary Health Region: importance ofnmetallo-beta-lactamase (MBL)–producing strains. J Infect Dis 2005; 192:1606-12.
15. Yazdi HR, Nejad JB, Peerayeh SN, Mostafaee M. Prevalence and detection of metallo--lactamase (MBL)-producing Pseudomonas aeruginosa strains from clinical isolates in Iran. Ann Microbiol 2007; 57(2):293-95.

# PALATABILITY, DIGESTIBILITY AND EMOTIONAL PATTERN IN 60 HEALTHY VOLUNTEERS AFTER INGESTION OF AN ICED DESSERT PRESENTED IN FOUR DIFFERENT FLAVOURS: A SUBJECTIVE EVALUATION

M. GARZARO, L. RAIMONDO, G. PECORARI, G. RIVA, M. SENSINI, N. NAQE and C. GIORDANO

*I^st ENT Division, Clinical Physiopathology Department, University of Turin, Italy*

*Received February 6, 2011 - Accepted February 28, 2012*

**Several variables lead to changes in human and animal eating behavior and food choices. A pivotal role is played by food palatability, represented by food, smell, taste, texture, appearance and temperature. The aim of our study is to assess the potential differences in palatability and digestibility of four different flavoured iced desserts, consumed at the end of a standardized meal, and their impact on the emotional status of 60 healthy volunteers. Sixty healthy volunteers, after ENT and psychological assessment, were asked to fill out a Psycho-Emotional Questionnaire (PEQ) to assess their basal emotional pattern before the consumption of an iced dessert at the end of a standard meal, after which they completed an Organoleptic-Sensory Questionnaire (OSQ), a Dynamic Digestibility Questionnaire (DDQ) and again the PEQ. Four different flavors (lemon, tangerine, pineapple and chocolate) were tested on 4 consecutive days on the same subjects. Most of the 60 subjects, by means of OSQ, found taste, aspect, texture and smell of the 4 flavours pleasant, lemon and tangerine were the freshest and lightest. The DDQ identified pineapple and chocolate dessert as those less digestible. By means of PEQ we recorded an improvement in joy, mood and activation, associated with good data of digestibility and palatability after the consumption of all flavors. Our data showed that all flavors improve joy, mood and activation, after their consumption, without statistically significant differences. However, among the tested flavours, lemon and tangerine appear to be the most pleasant and those which facilitate the digestive process.**

It is largely accepted that in humans and animals several variables, often not related to physiological needs, lead to changes in eating behaviour and food choices; in particular, emotional status plays a pivotal role in influencing quantity, quality and frequency of food intake (1).

A greater tendency to consume healthy foods during positive emotions and a greater tendency to consume junk food during negative emotions have been demonstrated by Lyman et coll. (2). Moreover, higher food consumption was registered during depression or fatigue, whereas a lower intake was associated with fear, pain and tension: these data reported by Mehrabian demonstrate a direct relationship between emotions and food intake amount. The same authors observed that high emotional arousal tends to inhibit the desire to eat (3).

Other factors that can influence dietary habits are represented by food appearance, smell, temperature

*Key words: emotion, digestion, iced dessert, digestive herbs*

*Mailing address:* Luca Raimondo, MD
1st ENT Division,
Department of Clinical Physiopathology,
San Giovanni Battista Hospital, Via Genova, 3
10126 Turin, Italy
Tel: +39 011 6336688 Fax: +39 011 6336650
e-mail: l.raimondo@hotmail.it



0393-974X (2012)

or taste: the sum of these items represents food "palatability". Its definition is still discussed: some authors identify palatability as an objective property of food, while others think it is the immediate effect of a particular food on ingestion (4).

The palatability of foods plays a pivotal role on a subject's food intake and emotional status and, on the other hand, emotional arousals influence the appetite and palatability. Moreover, hunger and heaviness after food ingestion deeply influence eating behaviour, because of variations in timing and quality of the digestive process (5).

In a previous preliminary report on a sample of ten volunteers, we demonstrated, by means of objective and subjective measures, that an iced dessert containing medicinal plant extracts could improve the digestibility of a standardized meal (5). Moreover, in another two papers it was demonstrated that an improvement of joy, activation and mood was associated with good data of digestibility and palatability showing a positive correlation between pleasure in eating the tested iced dessert and emotional status (6, 7).

The aim of our study is to assess the potential differences in palatability and digestibility of four different flavored iced desserts, consumed at the end of a standardized meal, and their impact on the emotional status of 60 healthy volunteers.

## MATERIALS AND METHODS

This study was a monocentric and prospective investigation performed from January to March 2010, at 1st ENT Division of the University of Turin. Inclusion criteria were: non-smokers or drinkers, absence of general, ENT, neurological, ophthalmological, gastrointestinal pathologies, and absence of pathological eating behaviors. Sixty healthy volunteers (median age 36.7 yrs - range 20-68) underwent the following research protocol.

*Pre-test evaluation day*

Each subject underwent accurate medical anamnesis, ENT evaluation with flexible fiber optic endoscopy, evaluation of taste and smell using "Sniffing Sticks" and taste stripes, and psychological assessment using the following questionnaires: Eating Disorder Inventory - 2nd edition (EDI-2), Rosenberg Self-Esteem Scale, Eysenck test and Hospital Anxiety and Depression Scale (HADS).

*Test days*

Each subject was asked to fill out a Psycho-Emotional Questionnaire (PEQ) to assess his basal emotional pattern before the consumption of the iced dessert after a standard meal. This meal was composed of ham-mozzarella sandwich, fruit salad, 50 cl of mineral still water and one flavored iced dessert. After the meal each subject completed an Organoleptic-Sensory questionnaire (OSQ), aDynamic Digeribility Questionnaire (DDQ) and again the PEQ. Each flavor was tested on four consecutive days.

*Product test composition*

Lemon flavor iced dessert: water, sugar, yogurt, lemon juice (8%), vegetable fat, modified starch, flavor enhancer (sorbitol syrup), milk protein, alcohol (1%), thickening agents (pectin), emulsifier (sucrose ester of fatty acid), natural flavors, infusion of digestive herbs.

Tangerine flavor iced dessert: water, sugar, yogurt, tangerine juice (9%), vegetable fat, modified starch, alcohol (1.1%), milk proteins, flavor enhancer (sorbitol syrup), citric acid, flavoring agents, thickening agents (pectin), plant extracts, emulsifier (sucrose ester of fatty acid), infusion of digestive herbs.

Chocolate flavor iced dessert: whole milk, sugar, water, chocolate 7% [sugar, cocoa mass, cocoa butter, emulsifier: lecithin (soy), flavoring agents] vegetable fat, cocoa, skimmed milk powder, flavoring agents, alcohol (0.8%), liquid coffee extract, modified starch, infusion of digestive herbs, thickening agents (sodium alginate, gellan gum), artichoke extract.

Pineapple flavor iced dessert: water, sugar, yogurt, pineapple puree (11%), vegetable fat, pineapple juice (3%), modified starch, alcohol (1.2%), milk proteins, flavor enhancer (sorbitol syrup), citric acid, thickening agents (pectin), emulsifier (sucrose ester of fatty acid), flavoring agents, concentrated lemon juice, infusion of digestive herbs.

*Digestive plants*

Lemon scented verbena (*Lippia citriodora* H.B. et K. = Verbena tryphylla L'Her = *Aloysia tryphylla* (L'Her) Britton = *Aloysia citriodora* (Cav.) Ort., fam. *Verbenaceae*). Processed materials and finished products: enriched extract of dried and chopped leaves from cultivated flowering plants, obtained by ultrasonic methods (ratio1/9 drug/extract) in EtOH 95°C; Analytical profile: TLC and SIM/GC/MS analysis gave the expected chromatographic behavior, in particular with absence of thujones and presence of 2-5 mg/L of eucalyptol and 0.25-1.5 g/Kg for citral and limonene < 0.1 g/Kg in the essential oil. Lemon balm (*Melissa officinalis* L., fam. *Lamiaceae*). Processed materials and finished products: enriched hydroalcoholic extract, obtained by concentration and pasteurization procedures of infusing twice the fresh flowering tops using the ratio 1:3 solvent/

raw material; analytical profile: the SIM/GC/MS analyses gave, in particular, ethyleugenol <0.5 mg/Kg (inferior to detectable limit), thujones 2-5 mg/Kg, eucalyptol and methyleugenol < 0.1 mg/g and pulegone 10 ppm, as well as rosmarinic acid 11.97 mg/g. Artichoke (*Cynara scolymus L*. Sp. Pl. = *Cynara scolymus* L. = *C. cardunculus* subsp. scolymus (L.) Hegi= *C. hortensis* Mill, fam. *Compositae Tubuliflorae*). Processed materials and finished products: enriched extract obtained by hydroalcoholic extraction for 1 week (3 days at 40°C and 4 days at room temp. using the ratio 4:1 solvent/raw material) and percolation of first-year dried leaves. Analytical profile: content of cynarin in the used extract, as obtained by HPLC analysis, was determined in 5 mg/Kg (±1 mg).

*Psycho-Emotional Questionnaire (PEQ)*

This is a tool composed of 12 items, already used in literature by Macht et al. (7), to describe the psychological state of the tested subject: hunger, desire to eat, tension, activation, guilt, anger, fear, sadness, joy, boredom, loneliness and mood. Mood was rated on a bipolar scale from 0 (extremely bad) to 10 (extremely good), the other items on an unipolar 7-point scale from 0 (not at all) to 6 (very strongly). Table II shows the percentage of subjects who reported a score > 0 for each item, except for mood that is expressed as a mean value.

*Organoleptic-Sensorial Questionnaire (OSQ)*

The aim of this 6-item questionnaire is to evaluate organoleptic characteristics of the tested product such as smell, aspect, texture, freshness, pleasantness, sweetness and lightness. For each question tested subjects could choose an answer from different pre-determined choices or give a score from 0 (not good at all) to 10 (extremely good).

*Dynamic Digestibility Questionnaire (DDQ)*

This questionnaire investigates the onset, the permanence and the disappearance of subjective feeling of gastric heaviness after 5, 60 and 180 minutes from the ingestion of meal. Each subject was asked to quantify gastric heaviness on a Visual Analogue Scale (VAS) that is represented by a 10 cm line anchored with two verbal descriptor to the extremities indicating “no heaviness” 0 cm and “worst imaginable heaviness” 10 cm.

*Statistical analysis*

All statistical analyses were carried out using Statistical Package for Social Sciences (SPSS), version 16.0. Percentages were compared by means of inference percentages test, while the *t*-test and the Analysis Of VAriance (ANOVA) were used to assess differences between groups in the mean of continuous variables. Furthermore, multiple comparison analysis was always performed by adopting the Bonferroni method in order to have a stricter criterion on whether to accept an effect as significant. A *p* value less than 0.05 was considered statistically significant.

## RESULTS

From March to May 2011, 60 healthy volunteers (30 males and 30 females) were enrolled in our study following all inclusion criteria. All subjects were non- or light smokers or drinkers, and not affected by general, ENT, neurological, ophthalmological, gastrointestinal or psychiatric pathologies; moreover, the results of the Eating Disorders Inventory (EDI) showed that their eating behavior was not pathological.

*Psycho-Emotional Questionnaire (PEQ)*

The results obtained from the analysis of data recorded with this questionnaire reveal that for negative emotions, the emotional patterns of male and female subjects before and after the ingestion of the iced desserts tested are almost superimposable with the exception of sense of guilt that is significantly higher in the female population after the consumption of chocolate dessert ($p<0.05$). A statistically significant difference between the percentages of subjects experiencing activation and joy, before and after product consumption, was observed for all flavors ($p<0.05$). A statistically significant improvement of mood mean value was recorded after the ingestion of the four tested flavors ($p<0.05$). The desire to eat was significantly higher only after the consumption of the Lemon dessert ($p<0.05$). Data are summarized in Table I.

*Organoleptic-Sensorial Questionnaire (OSQ)*

Analyzing data collected by this questionnaire (Table II), we observed that the mean value of global appreciation of tested products was 7.49, lemon and tangerine reported values of global appreciation statistically significantly higher (8.41 and 8.25, respectively) than pineapple and chocolate (6.50 and 4.72, respectively) ($p<0.05$). Data regarding the aspect and texture are superimposable in the four tested products, whereas, for smell, chocolate is the less fragrant ($p<0.05$) (Table II). During dessert tasting the enrolled subjects judged lemon

**Table I.** *Psycho-Emotional Questionnaire (PEQ): results.*

| | LEMON | | TANGERINE | | PINEAPPLE | | CHOCOLATE | |
|---|---|---|---|---|---|---|---|---|
| | Pre | Post | Pre | Post | Pre | Post | Pre | Post |
| *Hunger* | 21% | 23% | 20% | 22% | 24% | 23% | 31% | 29% |
| *Desire to eat* | 46%* | 71%* | 43% | 36% | 43% | 43% | 40% | 50% |
| *Tension* | 3% | 4% | 7% | 8% | 2% | 5% | 2% | 6% |
| *Activation* | 56%* | 78%* | 53%* | 81%* | 60%* | 85%* | 60%* | 63%* |
| *Guilt* | 4% | 6% | 1% | 1% | 0% | 2% | 5% | 15% |
| *Anger* | 12% | 11% | 10% | 12% | 14% | 14% | 2% | 6% |
| *Fear* | 1% | 1% | 0% | 0% | 0% | 0% | 2% | 0% |
| *Sadness* | 27% | 25% | 20% | 17% | 14% | 11% | 7% | 3% |
| *Joy* | 71%* | 93%* | 68%* | 88%* | 75%* | 93%* | 65%* | 88%* |
| *Boredom* | 11% | 10% | 10% | 10% | 0% | 0% | 6% | 4% |
| *Loneliness* | 24% | 24% | 2% | 0% | 0% | 0% | 11% | 7% |
| *Mood* (mean) | 7.5* | 9.3* | 7.1* | 8.8* | 7.1* | 9* | 7,8* | 9.6* |

** statistically significant differences ($p<0.05$)*

and tangerine as the freshest and lightest flavors ($p<0.05$) and pineapple as the sweetest one ($p<0.05$). After the consumption of the tested products, a good subjective digestive experience was reported by 92% (lemon), 89% (tangerine), 62% (pineapple) and 58% (chocolate) of the sample; a statistically significant difference between the first two flavors and the last two was observed ($p<0.05$). No statistically significant differences were observed between male and female population.

*Dynamic Digestibility Questionnaire (DDQ)*

The percentages of subjects experiencing gastric heaviness at 5, 60 and 180 minutes after the ingestion of the standardized enhanced meal were statistically significant higher for chocolate and pineapple. Data are reported in Table III. No statistically significant differences were observed between male and female population.

## DISCUSSION

Human emotions strongly influence eating behaviour. Many studies investigated the effects of anger, fear, joy and other emotions on food intake: for example during anger subjects reported an increase of impulsive, irregular and fast eating; during joy, however, an increase of hedonic eating is reported (8).

**Table II.** *Organoleptic-Sensorial Questionnaire (OSQ): data regarding smell, texture, aspect and taste.*

| | SMELL | | TEXTURE | | ASPECT | |
|---|---|---|---|---|---|---|
| ***LEMON*** | *No smell* | 0% | *Not Homogeneous* | 27% | *Not attractive at all* | 3% |
| | *Indifferent smell* | 13% | *Quite Creamy* | 43% | *Indifferent* | 27% |
| | *Not good at all* | 0% | *Very Creamy* | 7% | *Not attractive* | 27% |
| | *Not good* | 10% | *Quite Granulose/iced* | 13% | *Quite attractive* | 33% |
| | *Quite good* | 10% | *Very Granulose/iced* | 7% | *Very attractive* | 10% |
| | *Very good* | 67% | *Doughy* | 3% | | |
| ***TANGERINE*** | *No smell* | 11% | *Not Homogeneous* | 25% | *Not attractive at all* | 1% |
| | *Indifferent smell* | 10% | *Quite Creamy* | 45% | *Indifferent* | 29% |
| | *Not good at all* | 0% | *Very Creamy* | 7% | *Not attractive* | 27% |
| | *Not good* | 8% | *Quite Granulose/iced* | 16% | *Quite attractive* | 30% |
| | *Quite good* | 11% | *Very Granulose/iced* | 7% | *Very attractive* | 13% |
| | *Very good* | 60% | *Doughy* | 0% | | |
| ***PINEAPPLE*** | *No smell* | 10% | *Not Homogeneous* | 21% | *Not attractive at all* | 5% |
| | *Indifferent smell* | 24% | *Quite Creamy* | 43% | *Indifferent* | 25% |
| | *Not good at all* | 0% | *Very Creamy* | 7% | *Not attractive* | 30% |
| | *Not good* | 6% | *Quite Granulose/iced* | 11% | *Quite attractive* | 30% |
| | *Quite good* | 15% | *Very Granulose/iced* | 13% | *Very attractive* | 10% |
| | *Very good* | 45% | *Doughy* | 5% | | |
| ***CHOCOLATE*** | *No smell* | 35% | *Not Homogeneous* | 20% | *Not attractive at all* | 10% |
| | *Indifferent smell* | 30% | *Quite Creamy* | 43% | *Indifferent* | 20% |
| | *Not good at all* | 0% | *Very Creamy* | 14% | *Not attractive* | 37% |
| | *Not good* | 10% | *Quite Granulose/iced* | 10% | *Quite attractive* | 33% |
| | *Quite good* | 5% | *Very Granulose/iced* | 10% | *Very attractive* | 0% |
| | *Very good* | 20% | *Doughy* | 3% | | |

**MEAN VALUES OF TASTE FEELINGS**

| | | | | |
|---|---|---|---|---|
| *LEMON* | *Freshness* | 8.59* | *Sweetness* | 6.44* |
| | *Pleasantness* | 7.78 | *Lightness* | 8.61* |
| *TANGERINE* | *Freshness* | 8.25* | *Sweetness* | 6.38* |
| | *Pleasantness* | 7.06 | *Lightness* | 8.24* |
| *PINEAPPLE* | *Freshness* | 5.47* | *Sweetness* | 8.38* |
| | *Pleasantness* | 7.19 | *Lightness* | 5.27* |
| *CHOCOLATE* | *Freshness* | 5.69* | *Sweetness* | 6.34* |
| | *Pleasantness* | 7.91 | *Lightness* | 4.72* |

** statistically significant differences ($p<0.05$)*

**Table III.** *Dynamic Digestibility Questionnaire (DDQ): data regarding gastric heaviness.*

| | LEMON | TANGERINE | PINEAPPLE | CHOCOLATE |
|---|---|---|---|---|
| **No gastric heaviness** | 85% | 88% | 68% | 50% |
| **Gastric heaviness at 5 min** | 15% | 13% | 30% | 50% |
| **Gastric heaviness at 60 min** | 3% | 3% | 18% | 38% |
| **Gastric heaviness at 180 min** | 3% | 3% | 18% | 35% |

*Statistically significant differences were observed between lemon-tangerine and chocolate-pineapple.*

Stress is associated with unhealthy changes in food choice; an almost equal number of respondents reported overeating and undereating during stress situations, whereas recent specific stressors elicited more reports of under- than overeating (9).

Mood can be deeply influenced by food intake; a recent theory demonstrated that meals high in carbohydrates increase the rate of tryptophan entering the brain, leading to an increase in level of neurotransmitter serotonin, which positively modulates mood. Moreover, endorphin release in the brain, stimulated by all palatable foods, is responsible for mood elevation (10).

In our previous study on 100 healthy volunteers, after ingestion of an iced coffee flavour dessert, we observed a statistically significant improvement of mood, by means of PEQ (11).

In this paper we would like to evaluate the potential differences in terms of palatability and digestibility of four different flavored iced desserts and their impact on the psycho-emotional status of the enrolled subjects. Most of the 60 subjects found the iced desserts tested pleasant, in terms of taste, aspect, texture and smell; as predictable, of the four tested flavours, lemon and tangerine showed the highest values of freshness and lightness ($p<0.05$), while pineapple was judged as the sweetest one ($p<0.05$).

In order to evaluate the digestibility of these products we administered a specific questionnaire (DDQ) that investigates the onset, the permanence and the disappearance of subjective feeling of gastric heaviness; chocolate and pineapple seem to be the less appreciated in terms of digestibility of the four flavours tested ($p<0.01$). These findings are remarkable since a good digestive experience plays a main role in determining whether a food will be avoided in the future, due to the associations with emotional status and mood.

Emotions differ in antecedent conditions, physiological correlates, frequency of occurrence and duration and therefore there is a different associability with eating (12). Associations between an emotion and eating behaviour should be stronger if this emotion occurs more frequently in eating contexts than other emotions and leads to physiological and behavioural changes that are related to eating.

In our study we investigated the emotional status just before and after the ingestion of an iced dessert in 60 subjects. By means of PEQ we recorded an improvement of joy, mood and activation, associated with good data of digestibility and palatability after the consumption of all flavours ($p<0.01$). The results seem to show a positive correlation between pleasure in eating such a product and emotional status. Moreover, an increased desire to eat has been demonstrated after the consumption of the lemon flavour iced dessert ($p<0.05$) and an increased sense of guilt, in the female cohort, after the ingestion of the chocolate dessert; this last finding strongly agrees with literature data regarding chocolate consumption, which, in the form of craving, may induce negative affects such as guilt, anxiety and depression (13-15).

Our data show that all flavours improve joy, mood and activation after their consumption, without statistically significant differences. However, of the flavours tested, lemon and tangerine appear to be

the most pleasant and to be those which facilitate the digestive process.

## REFERENCES


1. Booth DA. Psychology of nutrition. Taylor & Francis: London, 1994.
2. Lyman B. A psychology of food, more than a matter of taste. Van Nostrand Reinhold: New York, 1982.
3. Mehrabian A. Basic dimensions for a general psychological theory. Oelgeschlager, Gunn & Hain: Cambridge, 1980.
4. Gasbarrini G, Piano S, Nesci A, et al. Palatabilità dei cibi, influenza sull'introito alimentare, lo stato emotivo e i processi digestivi. Minerva Gastroenterol Dietol 2009; 55(S):1-7.
5. Garzaro M, Pecorari G, Nadalin J, Raimondo L, Palmo A, Baccega M, Giordano C. Objective and subjective assessment of digestion after ingestion of an iced dessert in healthy volunteers. J Biol Regul Homeost Agents 2010; 24(2):215-20.
6. Garzaro M, Raimondo L, Pecorari G, Sensini M, Riva G, Palmo A, Giordano C. Digestibility, palatability and emotional status after ingestion of an iced dessert: analysis of subjective responses in 100 healthy volunteers. J Biol Regul Homeost Agents 2011; 25(1):101-7.
7. Garzaro M, Raimondo L, Nadalin J, Pecorari G, Giordano C. Subjective assessment of palatability, digestibility and emotions in healthy volunteers after ingestion of an iced dessert: preliminary report. J Biol Regul Homeost Agents 2010; 24(4):391-5.
8. Macht M. Characteristics of eating in anger, fear, sadness and joy. Appetite 1999;33:129-39
9. Desmet PMA, Schifferstein HNJ. Sources of positive and negative emotions in food experience. Appetite 2008; 50:290-301.
10. Benton D, Donohoe R. The effects of nutrients on mood. Public Health Nutrition 1999; 2(3):403-9.
11. Wallis DJ, Hetherington MM. Emotions and eating. Self reported and experimentally induced changes in food intake under stress. Appetite 2009; 52:355-62.
12. Scherer KR, Tannenbaum P. Emotional experiences in everyday life: a survey approach. Motiv Emot 1986; 10:295-314.
13. Fletcher BC, Pine KJ, Woodbridge Z, Nash A. How visual images of chocolate affect the craving and guilt of female dieters. Appetite 2007; 48(2):211-7.
14. Petrarca C, Lazzarin F, Pannellini T, Iezzi M, Braga M, Mistrello G, Falagiani P, Di Giampaolo L, Di Gioacchino M. Monomeric allergoid intragastric administration induces local and systemic tolerogenic response involving IL-10-producing CD4(+)CD25(+) T regulatory cells in mice. Int J Immunopathol Pharmacol 2010; 23(4):1021-31.
15. Chiesa C, Pacifico L, Anania C, Poggiogalle E, Chiarelli F, Osborn JF. *Helicobacter pylori* therapy in children: overview and challenges. Int J Immunopathol Pharmacol 2010; 23(2):405-16.

# pPKCα-MEDIATED EFFECT ON *IN VITRO* Aβ PRODUCTION IN RESPONSE TO γ SECRETASE INHIBITOR LY411575 IN RAT CTXTNA2 ASTROCYTES

P. SOZIO[1], M. RAPINO[2], V. DI VALERIO[3], S. LASERRA[1], S. PACELLA[3], A. DI STEFANO[1] and A. CATALDI[3,4]

*[1]Dipartimento di Scienze del Farmaco, Università G. d'Annunzio, Chieti, Italy; [2]Istituto di Genetica Molecolare del CNR, Unità di Chieti, Università G. d'Annunzio, Chieti, Italy; [3]Dipartimento di Medicina e Scienze dell'Invecchiamento, Università G. d'Annunzio, Chieti, Italy; [4]Cattedra di Anatomia Umana, Facoltà di Farmacia, Università G. d'Annunzio, Chieti, Italy*

*Received June 17, 2011 – Accepted March 30, 2012*

**Alzheimer's Disease implies memory and cognitive impairment due to β amyloid accumulation, presence of reactive microglia and astrocytes, loss of synapses, neural network dysfunctions and modifications of neuronal signalling. A key role in such events is played by astrocytes, which actively secrete high levels of β amyloid protein originating from sequential cleavage of APP by α,β and γ secretases. Since inhibition of such process could represent an important strategy against the occurrence of Alzheimer's Disease, in this paper the role played by pPKC α in the *in vitro* β amyloid production in response to γ secretase inhibitor in rat cortical astrocytes is reported. pPKC α increased expression seems to be related to decreased β amyloid production in parallel to increased astrocytes viability and decreased iNOS expression in the presence of 10 μM LY411575. Thus γ secretase inhibitor, activating pPKC α intracellular pathway could be suggested to prevent or reduce downstream toxic events, representing a useful strategy to counteract Alzheimer's disease.**

Alzheimer's disease (AD), the most common neurodegenerative disorder that affects the elderly, is characterized by memory and cognitive impairment paralleled by β amyloid (Aβ) peptide accumulation, by presence of reactive microglia and astrocytes and degeneration of neuronal processes, such as loss of synapses, neural network dysfunction (1) and modifications of neuronal signalling (2). Even though neuronal cells are largely involved in the occurrence of such disease, microglia and astrocytes triggering the onset and progress of disease is largely recognized (2). In particular, recent research suggests that astrocytes are not simply passive support for neurons but are active participants in neural information processing in the brain. Concerning Alzheimer's Disease, astrocytes are reported to secrete high levels of Aβ (3), significantly contributing to the formation of Aβ plaques (4). Aβ, in turn, can disrupt astrocytic calcium signalling and glio-transmitter release processes, vital for astrocytes neuro-communication (2). Aβ peptide formation, moreover, originates from sequential cleavage of the membrane spanning amyloid precursor protein (APP) by a secretase, β-site APP cleaving enzyme (BACE I) (β secretase)and a multiprotein complex termed γ secretase. The amyloid cascade hypothesis implies the activity of β and γ secretases which mediate the cleavage of APP and the formation of amyloidogenic Aβ fragment (1-42), which compacts into amyloid

*Key words: pPKC a, iNOS, β amyloid plaques, Alzheimer's disease, LY411575*

*Mailing address:* Prof. A. Cataldi,
Dipartimento di Medicina,
e Scienze dell'Invecchiamento,
Via dei Vestini, 31,
66100 Chieti, Italy
Tel: +39 0871 3554508 Fax: +39 0871 3554507
e-mail: a.cataldi@unich.it



0393-974X (2012)

**DISCLOSURE: ALL AUTHORS REPORT NO CONFLICTS OF INTEREST RELEVANT TO THIS ARTICLE.**

plaques. On the contrary, the cleavage of APP within the Aβ segment (non-amyloidogenic processing) by α secretase forms sAPP and prevents the formation of Aβ (5-7). The occurrence of AD implies oxidative stress which could determine additional damage in the brain by activating nitric oxide (NO) signalling pathway (8-9), whose key role in the response of the central nervous system has been recently recognized (8). NO signalling pathway is driven by three isoforms of NOS (1,2,3): NOS 1, or nNOS, neuronal, mainly observed in neuron (10), NOS 3,or eNOS, endothelial, present in vascular endothelium, involved in the control of blood pressure, vascular remodelling and angiogenesis (11) and NOS 2,or iNOS, inducible, known to be expressed and activated both in astrocytes and in neurons (12-13). In addition Protein Kinases C (PKC) have been shown to activate α secretase which, leading to the secretion of the soluble fragment of APP (sAPP), prevents the formation of Aβ, created by β and γ secretases and is involved in the regulation of NO signalling pathway (9, 14-16).

Since recently amyloid lowering strategies seem to support the hypothesis of slowing or completely healing AD progression (17-18), our attention has been focused on the *in vitro* PKCa-mediated molecular events which drive γ secretase inhibitor LY411575 effects on CTXNA2 astrocytes, deriving from brain frontal cortex of 1-day-old Sprague Dawley rat.

As is well-known, clinical trials of LY411575 and LY450139 have been halted by Eli Lilly because of results from two long-term phase III studies. The results showed a decline in cognition when compared to placebo. In addition, these compounds were shown to be associated with an increased risk in skin cancer, attributed to Notch processing (19). Although still unclear, the negative trial results may be attributed to the stimulation of γ secretase due to a rebound effect, thus resulting in overall stimulation of Aβ production, or the inhibition of γ secretase resulting in the inhibition of processing of not only APP but also of other substrates relevant for cognition (20, 21). The increase of Aβ levels, when the concentrations of the drug decrease, could be caused by activation of two different active sites on the γ secretase complex. However, this does not answer all the observations, and it is clear that a full understanding of the pharmacodynamics of γ secretase still remains unclear (22).

For the above reasons we carried out the evaluation of pPKCα-mediated effects on Aβ production. This study could help us to better understand the biological activity of γ secretase inhibitor LY411575, probably responsible for the side effects associated with the use of selective γ secretase inhibitors rather than γ secretase modulators.

## MATERIALS AND METHODS

*Cell culture and LY411575, γ secretase inhibitor, treatment*

CTXTNA2 cell line, established from primary cultures of type 1 astrocytes from brain frontal cortex tissue of 1-day-old Sprague Dawley rats, was obtained by ECACC(Salisbury, UK). Cells were maintained in DMEM, 10% FBS at 37°C, 5%$CO_2$ until sub-confluence and incubated for 24 h with concentrations ranging from 0.01 μM to 10 μM LY411575, γ secretase inhibitor (Eli Lilly Corporate Center Indianapolis, Indiana USA),dissolved in DMSO. For detection of cell viability, Trypan blue dye exclusion test was performed

*Western blotting*

Cell lysates (20 μg) were electrophoresed and transferred to nitrocellulose membrane. Nitrocellulose membranes, blocked in 5% non-fat milk, 10 mmol/L Tris pH 7.5, 100 mmol/L NaCl, 0.1% Tween-20, were probed with mouse APP (Millipore, Billerica, MA, USA) and β amyloid (Alpha Diagnostic Intl., San Antonio, Texas, USA), Bax, rabbit iNOS, nNOS monoclonal antibodies (Santa Cruz, Santa Cruz Biotechnology, CA, USA), rabbit PKCα monoclonal antibody (Abcam, Cambridge, MA, USA), goat pPKCα polyclonal antibody (Santa Cruz, Santa Cruz Biotechnology, CA, USA), then incubated in the presence of specific enzyme conjugated IgG horseradish peroxidase. Immunoreactive bands were detected by ECL detection system (Amersham Intl., Buckinghamshire, UK) and analysed by densitometry. Densitometric values, expressed as Integrated Optical Intensity (I.O.I.), were estimated in a CHEMIDOC XRS system by the QuantiOne 1-D analysis software (BIORAD, Richmond, CA, USA). Obtained values were normalized basing on densitometric values of internal β tubulin. Statistical analysis was performed using the analysis of variance (ANOVA). Results are expressed as mean ± SD. Values of $p<0.05$ were considered statistically significant.

## RESULTS

To evaluate the *in vitro* inhibitory activity of

A

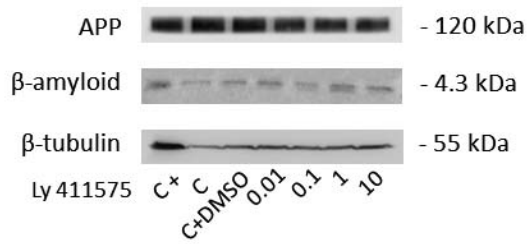


B

| | APP | β-amyloid |
|---|---|---|
| C | 1.99 ± 0.18 | 0.26 ± 0.02 |
| C+DMSO | 2.30 ± 0.19 | 0.19 ± 0.01 |
| 0.01 µM | 2.60 ± 0.21 | 0.19 ± 0.01 |
| 0.1 µM | 2.50 ± 0.22 | 0.18 ± 0.01 |
| 1 µM | 2.01 ± 0.19 | 0.23 ± 0.01 |
| 10 µM | 1.88 ± 0.17 | 0.17 ± 0.01 |

**Fig. 1.** *Expression of APP (amyloid precursor protein) and β amyloid in CTXNA2 astrocytes not exposed (C) and exposed to different concentrations of LY 411575 for 24 h.* ***A)*** *Western blotting is the most representative out of three different consistent experiments. As shown, samples were normalised by incubating membranes in the presence of β tubulin monoclonal antibody. Alzheimer's rat cerebral cortex lysate was used as positive control (C+).* ***B)*** *Densitometric analysis performed on three different consistent experiments is expressed as Integrated Optical Intensity (I.O.I.) (± SD) *10 µM LY411575 vs *C: $p<0.05$*

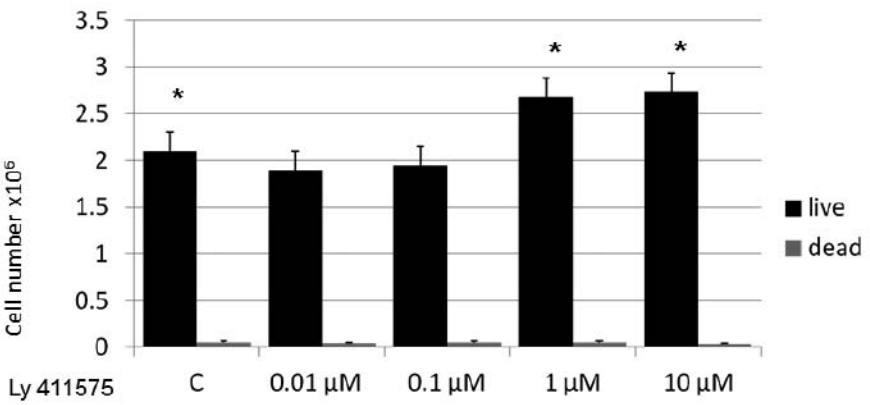


**Fig. 2.** *Cell viability and death analysis assessed by Trypan blue dye exclusion test in CTXNA2 astrocytes not exposed (C) and exposed to different concentrations of LY411575 for 24 h. Data represented are the mean (± S.D.) of three independent consistent experiments.*

LY411575 on γ secretase, CTXTNA2 rat astrocytes were treated for 24 h with inhibitor concentrations ranging from 0.01 µM to 10 µM. Increased inhibitor concentrations reduces Aβ production, due to γ secretase activity on APP (Fig.1), and increases cell viability, determined after 24 h of treatment by Trypan

A

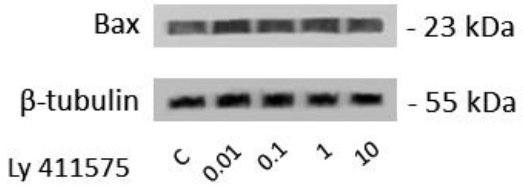


B

Bax

| | |
|---|---|
| C | 0.21 ± 0.02 * |
| 0.01 µM | 0.56 ± 0.04 |
| 0.1 µM | 0.38 ± 0.03 |
| 1 µM | 0.35 ± 0.03 |
| 10 µM | 0.22 ± 0.02 * |

**Fig. 3.** *Expression of Bax in CTXNA2 astrocytes not exposed (C) and exposed to different concentrations of LY411575 for 24 h.* ***A****) Western blotting is the most representative out of three different consistent experiments. As shown, samples were normalised by incubating membranes in the presence of β tubulin monoclonal antibody.* ***B****) Densitometric analysis performed on three different consistent experiments is expressed as Integrated Optical Intensity (I.O.I.) (± SD). *10 µM LY411575 vs *C: p<0.05*

A

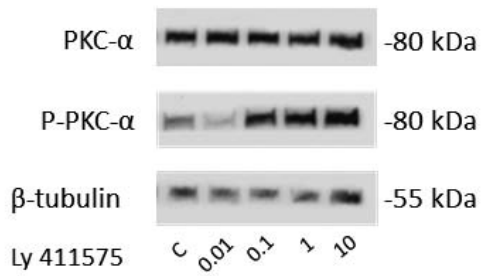


B

| | PKC-α | p-PKC-α | p-PKC-α/PKC-α |
|---|---|---|---|
| C | 1.34 ± 0.11 | 0.37 ± 0.02 | 0.28 ± 0.02 * |
| 0.01 µM | 1.72 ± 0.13 | 0.30 ± 0.02 | 0.17 ± 0.01 |
| 0.1 µM | 1.77 ± 0.15 | 1.03 ± 0.09 | 0.58 ± 0.03 |
| 1 µM | 1.48 ± 0.12 | 1.32 ± 0.11 | 0.89 ± 0.06 |
| 10 µM | 0.93 ± 0.07 | 1.43 ± 0.12 | 1.54 ± 0.12 * |

**Fig. 4.** *Expression of PKCa and pPKCa in CTXNA2 astrocytes not exposed (****C****) and exposed to different concentrations of LY 411575 for 24 h.* ***A****) Western blotting is the most representative out of three different consistent experiments. As shown, samples were normalised by incubating membranes in the presence of β tubulin monoclonal antibody.* ***B****) Densitometric analysis performed on three different consistent experiments is expressed as Integrated Optical Intensity (I.O.I.) (± SD). *10 µM LY411575 pPKCa vs *C pPKCa: p<0.05*

A

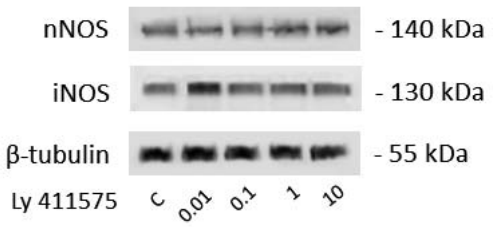


B

| | nNOS | iNOS |
|---|---|---|
| C | 0.42 ± 0.04 | 0.57 ± 0.06 * |
| 0.01 µM | 0.52 ± 0.05 | 0.97 ± 0.08 |
| 0.1 µM | 0.42 ± 0.03 | 0.52 ± 0.04 |
| 1 µM | 0.45 ± 0.04 | 0.67 ± 0.05 |
| 10 µM | 0.44 ± 0.04 | 0.42 ± 0.03 * |

**Fig. 5.** *Expression of nNOS and iNOS in CTXNA2 astrocytes not exposed (C) and exposed to different concentrations of LY411575 for 24 h.* ***A)*** *Western blotting is the most representative out of three different consistent experiments. As shown, samples have been normalised by incubating membranes in the presence of β tubulin monoclonal antibody.* ***B)*** *Densitometric analysis performed on three different consistent experiments is expressed as Integrated Optical Intensity (I.O.I.) (± SD). *10 µM LY411575 iNOS vs *C iNOS: $p<0.05$.*

Blue dye exclusion test (Fig.2). This effect is further supported by pro-apoptotic Bax molecule expression reduction to control levels after 10 µM inhibitor concentration treatment (Fig.3). Both such responses are triggered by intracellular molecular signals which include PKC (23, 24). Among PKC isoforms (α,δ,ε,ζ) assayed (not shown), basing on results concerning PKC ε activation in the brain of an AD rat model (25), only pPKCα level significantly increases in parallel to increased inhibitor concentration (Fig.4). Since NO signalling pathway plays a key role in the central nervous system (8, 9), both nNOS and iNOS enzyme levels were then checked by Western blotting analysis. While the expression of iNOS, related to inflammatory events (13), decreases upon exposure to different concentrations of inhibitor, expression of nNOS, constitutively expressed by nerve cells, does not modify (Fig. 5).

## DISCUSSION

The study of the biochemical mechanisms involved in the occurrence of AD can allow to identify specific therapeutical targets. Among such targets, either a, β and γ secretases involved in the β amyloid peptide formation originated from sequential cleavage of the membrane spamming APP, or intracellular signalling proteins as PKCs are included (14, 15, 25). To this aim we treated CTXTNA2 primary astrocytes with LY411575,a well-known γ secretase inhibitor (26). As here reported, *in vitro* LY411575 increased concentrations lead to reduction in Aβ production in parallel to increased cell viability and decreased pro-apoptotic Bax molecule expression. Since, as recently reported by our group (9), NO signalling pathway is involved in the occurrence of morphological and biochemical modifications in Aβ 1-40 infused rat brain, we checked the *in vitro* behaviour of such pathway evidencing no modification concerning nNOS level, but decreased level of iNOS, a well-known enzyme involved in the inflammatory response in AD (10), in parallel to increased LY411575 concentration, further suggesting a reduced oxidative and inflammatory response. In addition, in alignment with other authors who have reported that PKC can not only influence

and regulate *in vivo* synaptic remodelling, induction of protein synthesis, learning and memory processes (27, 28), but also the altered signal transduction system in AD (14-15, 25, 29), here we report an increased pPKCα level in 10 μM LY411575-treated astrocytes. Basing on such evidence, the increased PKC phosphorylation upon γ secretase inhibitor treatment, in parallel to decreased Aβ production could be due both to α secretase activation via PKC, allowing the formation of soluble Aβ, which does not form plaques, and to inhibition of γ secretase, which normally leads to fibrillar Aβ formation.

Thus, all these results suggest the possibility of Aβ lowering strategies, based on inhibition of γ secretase, in parallel to the activation of α secretase by pPKCα metabolic pathway in the attempt to counteract or slow AD damage. In order to validate this hypothesis, works are in progress, silencing or inhibiting such PKCα target.

## ACKNOWLEDGEMENTS

The authors wish to thank Prof A. Antonucci for his help in the interpretation of morphological and biochemical results. This work was supported by Prof. A. Di Stefano and Prof. A. Cataldi MIUR 2011 60% Grants.

## REFERENCES

1. Agostinho P, Cunha RA, Oliveira C. Neuro-inflammation, oxidative stress and the pathogenesis of Alzheimer's disease. Curr Pharm Des 2010; 16:2766-78.
2. Vincent AJ, Gasperini R, Foa L. Astrocytes in Alzheimer's disease: emerging roles in calcium dysregulation and synaptic plasticity. J Alzheimers Dis 2010; 223:699-714.
3. Busciglio J, Gabuzda BH, Matsudaira P. Generation of β-amyloid in the secretory pathway in neuronal and non-neuronal cells, Proc Natl Acad Sci USA 1993; 90:2092-6.
4. Siman R, Card J, Nelson R. Expression of β amyloid precursor protein in reactive astrocytes following neuronal damage. Neuron 1989; 3:275-85.
5. Selkoe DJ. The cell biology of β amyloid precursor protein and pre-senilin in Alzheimer's disease. Trends Cell Biol 1998; 8:447-53.
6. Vassar R, Bennett BD, Babu-Khan S. β secretase cleavage of Alzheimer's amyloid precursor protein by the trans membrane aspartic protease BACE. Science 1999; 286: 735-41.
7. Elvang AB, Volbracht C, Pedersen LO. Differential effects of γ secretase and BACE1 inhibition on brain Aβ levels in vitro and in vivo. J Neurochem 2009; 110:1377-87.
8. Pepicelli O, Raiteri M, Fedele E. The NOS/sGC pathway in the rat central nervous system: a microdialysis overview. Neurochem Int 2004; 45:787-97.
9. Zara S, Di Stefano A, Nasuti C, Rapino M, Patruno A, Pesce M, Sozio P, Cerasa LS, Cataldi A. Morphological and molecular modifications in rats infused with Aβ (1-40),as a model of Alzheimer's disease, in response to a new lipophilic molecular combination codrug-1. Exp Gerontol 2010; 464:273-81.
10. Simic G, Lucassen PJ, Krsnik Z. nNOS expression in reactive astrocytes correlates with increased cell death related DNA damage in the hippocampus and entorhinal cortex in Alzheimer's disease. Exp Neurol 2010; 16:512-26.
11. Shaul PW. Regulation of endothelial nitric oxide synthase: location, location, location. Annu Rev Physiol 2002; 64:749-74.
12. Buskila Y, Amitai Y. Astrocytic iNOS-dependent enhancement of synaptic release in mouse neocortex. J Neurophysiol 2010; 103:1322-8.
13. Lüth HJ, Holzer M, Gärtner U, Staufenbiel M, Arendt T. Expression of endothelial and inducible NOS-isoforms is increased in Alzheimer's disease, in APP23 transgenic mice and after experimental brain lesion in rat: evidence for an induction by amyloid pathology. Brain Res 2001; 14:57-67.
14. Alkon DL, Sun MK, Nelson TJ. PKC signalling deficits: a mechanistic hypothesis for the origins of Alzheimer's disease, Trends Pharmacol Sci 2007; 28:51-60.
15. de Barry J, Liegeois CM, Janoshazi A. Protein Kinase C as a peripheral biomarker for Alzheimer's disease. Exp Gerontol 2010; 45:64-69.
16. Rashid G, Bernheim J, Green J. Parathyroid hormone stimulates the endothelial nitric oxide synthase through protein kinase A and C pathways. Nephrol

Dial Transplant 2007; 22:2831-7.
17. Haass C, Selkoe DJ. Soluble protein oligomers in neurodegeneration: lessons form the Alzheimer's amyloid beta peptide. Nat Rev Mol Cell Biol 2007; 8:101-12.
18. Sheng B, Gong K, Miu YN. Inhibition of γ secretase activity reduces Aβ production, reduces oxidative stress, increases mitochondrial activity and leads to reduced vulnerability to apoptosis: implications for the treatment of Alzheimer's disease. Free Rad Biol Med 2009; 46:1362-75.
19. Panelos J, Massi D. Emerging role of Notch signaling in epidermal differentiation and skin cancer. Cancer Biol Ther 2009; 8:1986-93.
20. Michener MS, Holahan MA, Gilberto DB, et al. Nonhuman primate model for prediction of human Aβ effects. Targeting γ-secretase; effects of enzyme inhibition vs. modulation of cleavage specificity on CSF and plasma Aβ in conscious rhesus monkeys. Alzheimer's Dementia 2006; 2:S252.
21. Costa RM, Drew C, Silva AJ. Notch to remember. Trends Neurosci 2005; 28:429-35.
22. Oehlrich D, Berthelot DJ, Gijsen HJ. γ-Secretase Modulators as potential disease modifying anti-Alzheimer's drugs. J Med Chem 2011; 54:669-98.
23. Skovronsky DM, Moore DB, Milla ME. Protein kinase C-dependent alpha-secretase competes with beta-secretase for cleavage of amyloid-beta precursor protein in the trans-golgi network. J Biol Chem 2000; 275:2568-75.
24. Díaz-Rodríguez E, Montero JC, Esparís-Ogando A. Extracellular signal-regulated kinase phosphorylates tumor necrosis factor alpha-converting enzyme at threonine 735: a potential role in regulated shedding. Mol Biol Cell 2002; 6:2031-44.
25. Zara S, Rapino M, Sozio P, Di Stefano A, Nasuti C, Cataldi A. Ibuprofen and lipoic acid codrug 1 control Alzheimer's disease progression by down-regulating Protein Kinase C ε – mediated Metalloproteinase 2 and 9 levels in β-amyloid infused Alzheimer's disease rat model. Brain Research 2011; 1412:79-87.
26. Wu WL, Zhang L. γ secretase inhibitors for the treatment of Alzheimer's disease. Drug Dev Res 2009; 7:94-100.
27. Nelson TJ, Sun MK, Hongpaisan J. Insulin, PKC signaling pathways and synaptic remodelling during memory storage and neuronal repair. Europ J Pharmacol 2008; 58:76-87
28. Sun MK, Alkon DL Protein kinase C activators as synaptogenic and memory therapeutics. Arch Pharm 2009; 342:689-98.
29. Pascale A, Amadio M, Govoni S. The aging brain, a key target for the future : the protein kinase C involvement. Pharmacol Res 2007; 55:560-9.

# CYANIDIN REDUCES PREADIPOCYTE DIFFERENTIATION AND RELATIVE ChREBP EXPRESSION

A. POMPEI[1], E. TONIATO[2], P. INNOCENTI[3], I. D'ALIMONTE[3], C. CELLINI[3], D. MATTOSCIO[3,4], R. COTELLESE[3], D. BOSCO[1], R. CICCARELLI[3], V. DADORANTE[5], N. D'ORAZIO[3], S. MARTINOTTI[3,5] and I. ROBUFFO[1]

*[1]Institute of Molecular Genetics, National Research Council, Section of Chieti, Chieti, Italy; [2]Department of Oral Science Nano and Biotechnology, University of Chieti-Pescara, Italy; [3]Department of Biomedical Sciences, University of Chieti-Pescara, Italy; [4]Aging Research Center (CeSI), Gabriele D'Annunzio University Foundation, Chieti, Italy; [5]Department of Clinical Pathology, St. Annunziata Hospital, Chieti, Italy*

*Received December 27, 2011 – Accepted March 14, 2012*

The first two authors contributed equally to the paper

**Adipogenesis is a continuous process even in adult adipose tissue for the presence of preadipocytes that, when subjected to appropriate stimuli can proliferate and differentiate. ChREBP, the essential transcription factor for lipogenesis, is expressed in all tissues, but mainly in lipogenic organs. In this study, we focused on ChREBP expression during preadipocytes differentiation. Since it was found that cyanidin-3 reduces body weight in mice even in the presence of a high-fat diet, by decreasing levels of blood glucose and by improving insulin sensitivity, we studied the effect of this substance on adipogenic differentiation. For this purpose we used preadipocytes obtained from subcutaneous and visceral human adipose explant tissue, characterized and stimulated to differentiate in selective media. On cytofluorimetric analysis these cells showed mesenchymal markers (CD29, CD90, CD44), whereas they were negative for hematopoietic markers (CD45, CD10, CD117,CD31). ChREBP expression levels were quantified by immunoelectron-microscopy and western blotting analysis. In this report we show that ChREBP is expressed in preadipocytes (both nuclear and cytoplasmic compartments); the cytoplasmic level of ChREBP increased by 50% on day seven of differentiation into mature adipocytes. Cyanidin reduced differentiation by 20% (as evaluated by red oil O staining) and the expression of ChREBP. In addition, cyanidin-treated cells showed abnormal morphology, a square shape with irregular size, probably due to the fact that cyanidin may interfere with the extracellular matrix. These findings suggest that dietary cyanidin, may have inhibitory effects on adipogenesis.**

Adipose tissue has been ignored for a long time because considered only as a place of energy reserve, it is now defined, with regard to its dynamic role in metabolism, an endocrine glandular tissue (1). In the last twenty years there has been a greater interest, due to the increase in the incidence of obesity and

*Key words: adipogenesis, preadipocytes differentiation, ChREBP, cyanidin 3-glucoside, C3G, immunoelectron-microscopy*

*Mailing address*: Dr Iole Robuffo,
Institute of Molecular Genetics,
National Research Council,
Section of Chieti, via dei Vestini, 29,
NPD pal. C, II liv, 66100 Chieti, Italy
Tel.: +39 08713554035
e-mail: robuffo@unich.it



0393-974X (2012)

complications associated with it (2). Adipose tissue is involved in numerous biological processes (3). Proteins secreted by adipose tissue are involved in energy homeostasis and in the regulation of neuro-endocrine, immune and cardiovascular functions (4, 5).

Adipogenesis is a continuous process even in adults when exposed to growth factors, hormones and increased fatty acids in the blood. In fact, preadipocytes contained in adipose tissue, if subjected to appropriate stimuli can proliferate and differentiate (6). Adipogenesis, as all organogenic processes, begins in the prenatal period, but as osteogenesis, the process never ends.

Several steps are involved during preadipocyte differentiation into mature adipocytes. These stages are regulated by the activation of a transcriptional cascade involving the nuclear receptor PPARγ (peroxisome proliferator activated receptors) (7, 8) and some family members C/EBP (CAAT/enhancer binding protein) (9). Ishii et al. (10) discovered a new transcription factor, ChREBP (carbohydrate response element binding protein) responsible for lipogenesis in the liver and adipose tissue. ChREBP is a major modulator of adipocyte biology and its expression in adipose tissue is regulated by the combination of glucose and insulin (11, 12).

ChREBP is a transcription factor able to regulate metabolic gene expression in response to high glucose, converting excess glucose into triglycerides (de novo lipogenesis) (13). It binds specifically to the lipogenic genes Chre (carbohydrate response element) DNA sequence motifs near Acetyl CoA carboxylase, Fatty acid synthase, and Pyruvate kinase (LPK) (14). It is up-regulated by insulin, glucose, antidiabetic agents, while it is deleted from fatty acids. ChREBP is activated in response to high concentrations of glucose (11) and can move continuously between the cytoplasm and nucleus independent of glucose concentrations (15). The metabolite Glucose-6-phosphate is necessary to mediate ChREBP activation (16).

Since ChREBP is expressed in all tissues, but mainly in lipogenic organs such as the liver, adipose tissue, and pancreas (17) the aim of the present study was to investigate ChREBP expression also in preadipocytes and in mature adipocytes. Recent studies show that cyanidin 3-glucoside, a water-soluble anthocyanin belonging to the flavonoids family, may regulate obesity and insulin sensitivity (18), increase adipocytokines (leptin, adiponectin) secretion (19) and activate adipocyte specific genes (20). Cyanidin 3-glucoside improves insulin sensitivity by regulating the glucose transporter 4 in adipose tissue and striated muscles (21).

For the multiple biological activities of cyanidin, we also wanted to evaluate the effect of this antioxidant on preadipocytes proliferation, differentiation and ChREBP expression. For this purpose we used preadipocytes derived from subcutaneous or visceral adipose tissue explants. These cells were characterized under undifferentiating conditions, were induced to differentiate with 3-isobutyl-1-methylxanthine (IBMX), dexamethasone and insulin until full differentiation (as assessed by Oil red O staining) in the presence or absence of cyanidin.

## MATERIALS AND METHODS

*Adipose tissue explant culture*

After informed consent, human preadipocytes were isolated from adipose tissue obtained from 10 patients undergoing surgery. Of these patients those with cancer were excluded, and only those with hiatal hernia and cholecystectomy were included in the study.

After removal, the subcutaneous or visceral adipose tissue was immediately placed in phosphate buffer before use. After repeated washings in PBS, samples were sliced in small pieces and treated with 0.05% collagenase in D-MEM at 37°C for 30 min. Neutralized with the same volume with 10% FBS, placed in Falcon 50 ml and centrifuged at 1200 for 10 min. After removing the supernatant, the cellular fraction was resuspended in D-MEM with 10% FBS and centrifuged again. Cells were plated in a humidified incubator at 37°C in an atmosphere of 5% CO2 (v/v).

*Cell differentiation*

Preadipocyte cells were grown to 70-80% confluence in Dulbecco's modified Eagle's medium (DMEM) supplemented with 10% FBS, 0.584g/L glutamine, 5 mM glucose, 5 mM sodium acetate, 10μg/ml penicillin, 10μg/ml streptomycin. The medium was changed every 48 h and viability was checked with trypan blue. At about 80% confluence cells were induced to differentiation in a adipogenesis-inducing medium (high glucose D-MEM supplemented with 10% FCS, 1.7 μmol /L insulin , 0.5 mM 3-isobutyl-1-methylxanthine (IBMX), 1μM dexamethasone, 10μg/mlpenicillin, 10μg/ml streptomycin) for at least seven days, until full

differentiation.

*The effect of cyanidin on lipid accumulation*

To evaluate the effect of cyanidin, the cells received the cyanidin premixed with differentiative culture medium as described below. Cyanidin (cyanidin 3-glucoside or C3G) (Sigma) was dissolved in dimethyl sulfoxide (Sigma-Aldrich) to produce a 4 mM stock solution. Aliquots of stock solutions were stored at -70°C and used as soon as possible after preparation. Preadipocytes were treated with 100 µM C3G ( 0.1% dimethyl sulfoxide) at 37°C in a humidified atmosphere (5% $CO_2$/95% air)

*Differentiation assay (neutral lipid accumulation)*

Lipid accumulation in adipocytes was determined by oil red-O staining in confluent cells, and in cells differentiated with or without cyanidin 3-glucoside. To determine adipocytes count, cells were grown on slides, fixed in 4% formaldehyde in PBS for 10 min, washed with 60% isopropanol and stained with 0.2% Oil red O in 60% isopropanol for 10 minutes. To remove unincorporated dye, they were then washed several times with water and destained in 60% isopropanol for 15 minutes.

Four adjacent 1-mm squares were counted, blind to group, using a inverted microscope and using criterion described for quantification of adipocyte differentiation. Cells were then observed at optical Zeiss microscope an photographed. The percentage of cells that underwent adipogenic differentiation was expressed as number of red oil O positive cells/total number of cells x 100%.

*Statistical analysis*

Where appropriate, statistical analyses were performed using Student's *t* test. Differences of adipocyte numbers among cell cultures with *P*-values <0.05 were considered statistically significant.

*Flow cytometry*

Preadipocytes at 80% confluence were examined for surface and intracellular expression using flow citometry. The following monoclonal antibodies conjugated to fluorochrome were used: fluorescein isothiocyanate-conjugated anti CD-90 (CD90-FITC), FITC-conjugated anti-CD44 (CD44-FITC), FITC-conjugated anti-CD31 (CD31-FITC), phycoerytrin (PE)-conjugated anti-CD45 (CD45-PE), PE- conjugated anti-CD29 (CD29-PE), PE-conjugated anti-CD117 (CD117-PE) and phycoerytrin (PE)-cyanin (cy7)- conjugated anti-CD10 (CD10-PE-cy7) were obtained from Becton Dickinson (BD, San Jose, CA).

Adherent cells were treated with EDTA at 37°C for 10 min. Cells were washed with 2 ml Phosphate Buffered Saline (PBS, 0.1% sodium azide and 0.4% bovine serum albumin) and centrifuged at 400g for 8 min each time at 4°C. Staining of surface antigens: Samples resuspended in 100 µl washing buffer containing appropriate surface antibody, were incubated for 30 min at 4°C in the dark. Cells were then washed, centrifuged and resuspended in 0.5% paraformaldehyde. Staining of intracellular antigens: Cells were resuspended in 1 ml of FACS lysing solution, vortexed and incubated for 10 min at room temperature in the dark. Samples were centrifuged and incubated at room temperature for 10 min in the dark in 1ml of Perm2 (BD). After washing cells were resuspended in 100 µl washing buffer containing appropriate intracellular antibody and incubated for 30 min at 4°C in the dark. Cells were then washed, centrifuged and resuspended in 0.5% paraformaldehyde for 5 min at room temperature. Finally cells were analysed on BD FACSCanto flow cytometer. Data acquisition and analysis were then performed using DIVA software. Twenty thousands non-debris events in the morphological gate were recorded for each sample. Quality control included staining with combinations of relevant and irrelevant antibodies to asses non specific fluorescence.

*Transmission electron microscopy*

For transmission electron microscopy, cells were fixed with 2.5% glutaraldehyde in 0.1 M cacodylate buffer, pH 7.4, postfixed with 1% OsO4, dehydrated in graded ethanol and embedded in Epon 812. Thin sections were then cut and stained with uranyl acetate and lead citrate for ultrastructural observation. Sections were photographed using a Philips 268 D electron microscope (FEI).

*Immunoelectronmicroscopy*

For immunolocalization of ChREBP protein, cells were fixed with a mixture of 4% paraformaldehyde / 1% glutaraldehyde in 0.1 M cacodylate buffer, pH 7.4, for 1 h and washed twice with the same buffer. Cells were dehydrated sequentially in 50, 75 and 90% dimethylformamide and embedded in Bioacryl resin (British Biocell, Cardiff, United Kingdom), followed by UV polymerization. Ultrathin sections were cut and mounted on 200-mesh nickel grids. To block nonspecific binding sites, grids were treated for 10 min at room temperature with a blocking buffer TBS (0.05 M Tris-Hcl, 1% sodium azide and 0.1% bovine serum albumin), pH 7.6. The grids were treated with 5% skim milk powder for 30 min and incubated overnight at 4°C with 1:30 dilution of anti-ChREBP (Santa Cruz biotechnology, inc).

After several washes with TBS, grids were incubated for 1 h with 20 nm gold particles, conjugated with rabbit anti-goat IgG (Biocell, GB) diluted 1: 10 in TBS, pH 8.2. Grids were then washed three times in TBS and once in distilled water, and stained with uranyl acetate. Controls

were represented by untreated cells and by cells treated with secondary antibody alone.

All sections were finally examined and photographed using a Philips 268 D electron microscope (FEI). For each sample at least 100 cells were examined counting the total number of gold particles separately in cytoplasm and nuclei and assessing their presence per unit areas (100 $cm^2$ at x11000) in both compartments.

*Western Blotting*

For ChREBP detection, protein lysates were separated with 12% sodium dodecyl sulfate (SDS) polyacrilyamide gel electrophoresis (PAGE) under reducing conditions and transferred onto nitrocellulose membrane. Trans-blots were incubated overnight at 4°C with a goat antibody anti-ChREBP (Santa Cruz biotechnology, inc), diluted 1:100 in TBS-T with 5% skim milk powder.

Membranes were washed with TBS-T and incubated for 1 h at room temperature with the horseradish peroxidase-conjugated secondary antibody anti-goat diluted 1:1000 (R & D system) in TBS-T with 5% skim milk. Bands were visualized by chemiluminescent reaction using ECL Western Blotting Detection System kit (GE Healthcare, Buckinghamshire, UK) and BIOMAX-MR film (Eastman Kodak). The nitrocellulose filter was stripped and incubated with primary mouse monoclonal anti-ß Actin antibody (Sigma) 1:500 with, washed in TBS-T and incubated with secondary antibody antimouse (Calbiochem) 1:4000.

## RESULTS

*Characterization of cells deriving of human adipose tissue*

Cells isolated from human adipose tissue and grown under undifferentiating condition showed a fibroblast-like morphology (Fig. 1A). When these cells were cultured using appropriate differentiating media, as described in the Methods section, they underwent to adipogenic differentiation. Flow cytometric analysis showed that undifferentiated cells expressed typical mesenchimal markers (Fig. 2) on the membrane surface CD29, CD90, CD44, whereas they resulted negative for hematopoietic stem cells markers CD10, CD117, blood derived cells marker CD45 and, endothelial progenitor cells marker CD31.

*Differentiation*

The primary cultures of human adipose derived preadipocytes were differentiated into adipocytes in the differentiation medium until full differentiation (7 days). The adipocyte differentiation (lipid accumulation) was observed by Red oil O staining in smears from confluent cells. Mature adipocytes and preadipocyte colonies were counted manually using an inverted microscope. Lipids appear as bright red perinuclear vesicles, often as grape-like clusters of small vesicles (Fig. 1 B). Unilocular (single, very large lipid vacuole) adipocytes rarely form in attached, *in vitro*-differentiated adipocytes. Mature adipocytes (Fig. 3) showed large lipid vacuoles that occupy most of the cytoplasm, pushing the nucleus to the periphery. Preadipocytes, fibroblast-like showed intracytoplasmic inclusion vacuoles that are much smaller ad not red coloured (Fig. 1A).

*The effect of cyanidin on lipid accumulation and on the morphology*

To determine whether cyanidin reduced the preadipocyte differentiation, we cultured human adipose derived preadipocytes for 7 days in Adipogenic Differentiation Medium in the presence and absence of cyanidin, then measured cell

**Table I.** *Immunogold quantitative evaluation of ChREBP protein in cytoplasmic and nuclear compartments of undifferentiated preadipocytes, differentiated and cyanidin-differentiated cells.*

100 $cm^2$ (10x10) at 11000 of magnification

| | Undifferentiated | Differentiated | Differentiated +Cyanidin |
|---|---|---|---|
| Nucleus | 39.6 ± 3.2 | 43 ± 5.4 | 41 ± 2.8 |
| Cytoplasm | 68.44 ± 6.1 | 102.5 ± 9.1 | 75.8 ± 6.7 * |

Number of particles per 100 $cm^2$ at x 11000

*Data are the mean of at least five observations. ± SEM. * $p<0.05$ vs differentiated cells*

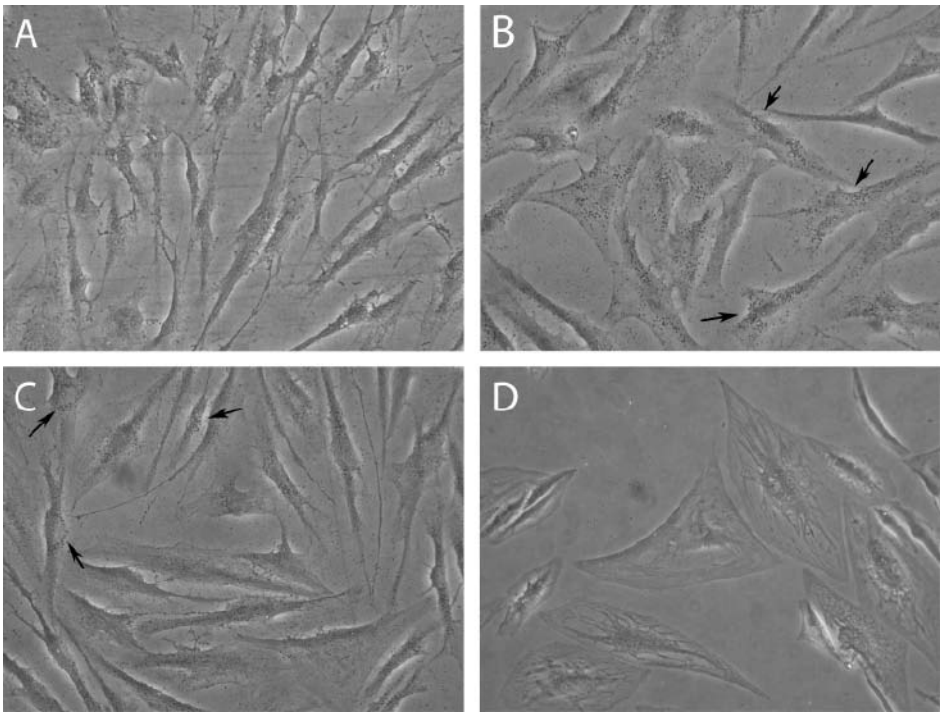


**Fig. 1.** *In vitro differentiation of preadipocytes.* ***A)*** *Undifferentiated cells showing typical fibroblast-like morphology.* ***B)*** *Adipogenic differentiation of preadipocytes cultured for 7 days in a specific differentiating medium, mesasured by Red Oil O staining showing lipids accumulation (arrows).* ***C)*** *Adipogenic differentiation in the presence of 100 μM cyanidin (arrows: lipid accumulation). The number of stained cells in the cyanidin-treated was reduced. Note the abnormal morphology, square shape with irregular size (**D**).*
*Original magnification: A, C, D, x 200.*

differentiation at several doses of substances. Cells that had been cultured with 100 μg/ml cyanidin for 7 days reduced significantly cell differentiation.

Large numbers of Oil Red O-positive lipid droplets were observed in the cytoplasm of the cells differentiated without cyanidin (Fig. 1B). In contrast, the number of stained cells in the cyanidin-treated group was reduced about 20% (Fig. 1C; Fig. 4). Treatment of adipocytes with 100 μM of C3G produced no cytotoxic effect (cell viability more than 95%, apoptosis and or necrosis). In addition, cyanidin-treated cells showed abnormal morphology: a square shape with irregular size, as shown in Fig. 1 C, D.

*ChREBP espression in human adipose derived preadipocyte and in differentiated adipocytes in presence of cyanidin*

The ultrastructural immunolocalization of ChREBP was achieved by the postembedding immunogold technique which allows for the quantitative/qualitative evaluation of the reaction.

Bioacryl resin was chosen to ensure a high preservation of protein antigenicity, even though some morphological details might be lost. For each sample at least 100 cells were examined counting the total number of gold particles separately in cytoplasm and nuclear compartments and assessing their presence per unit areas (100 $cm^2$ at 11000 of magnification) in both compartments (Table I).

As shown in Fig. 5, the immunolabeling was clearly detectable both in nuclear (A) and cytoplasmic (B) compartment of undifferentiated cells, with some cluster in proximity of nuclear membrane.

Interestingly, within 7 days of differentiation, the cytoplasmic labeling of mature adipocytes was increased by 50% compared with preadipocytes (Table I, Fig. 6), while it did not seem to affect the nucleus. ChREBP was less expressed in cells differentiated in the presence of cyanidin (Fig.7).

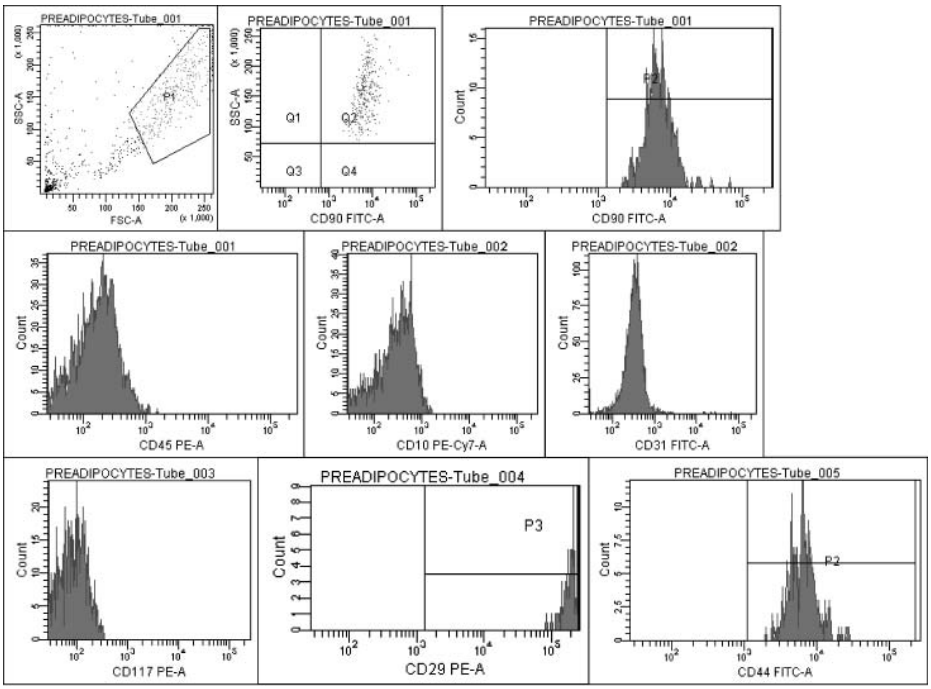


**Fig. 2.** *Characterization of the immunophenotypic profile of preadipocytes, isolated from human adipose tissue, grown under undifferentiating conditions, by flow citometric analysis. Cells resulted negative for CD45$^-$ (blood derived cells), CD31$^-$ (endothelial progenitor cells), CD10$^-$, CD117$^-$ (hematopoietic stem cells) markers and positive for mesenchymal markers CD29$^+$, CD90$^+$, CD44$^+$.*

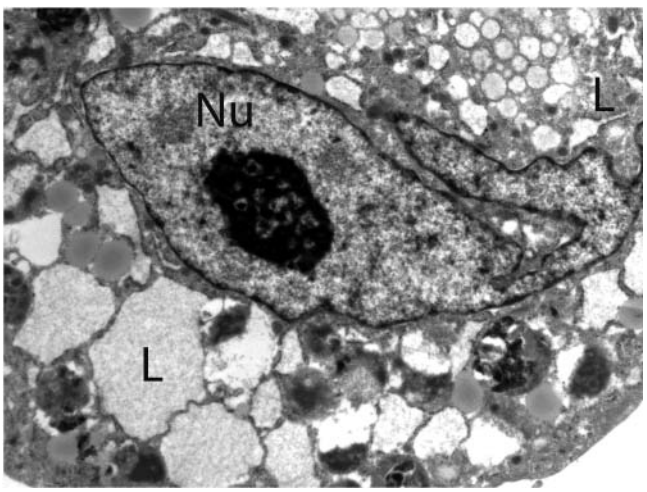


**Fig. 3.** *Transmission electron microscopy features of mature adipocyte. Human adipose derived preadipocytes cultured for 7 days in adipogenic differentiative medium. During differentiation process, mature adipocytes tend to have large lipid vacuoles that occupy most of the cytoplasm, pushing the nucleus to the periphery. Unilocular (single, very large lipid vacuole) adipocytes rarely form in attached, in vitro-differentiated adipocytes.*
*Nu: nucleus; L: lipids. Original magnification: x 5600*

Under the electronic microscope we observed the different distribution of gold granules in mature adipocytes during the process of differentiation (Fig. 6): cluster near the pore complex (a,b), granules mostly distributed inside the rough endoplasmic reticulum (b) and mitochondria (d).

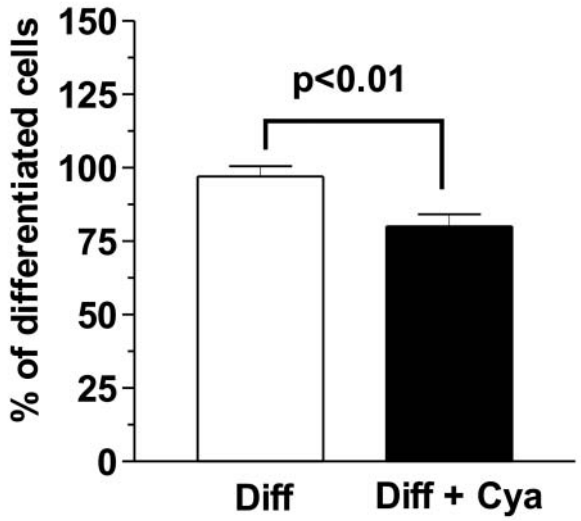


**Fig. 4.** *Human adipose derived preadipocytes cultured for 7 days in adipogenic differentiative medium with or without cyanidin. The number of cells containing visible lipid droplets by oil red O staining is shown as a percentage of the total cells counted (mean ± SEM). n= 6 P < 0.01.*

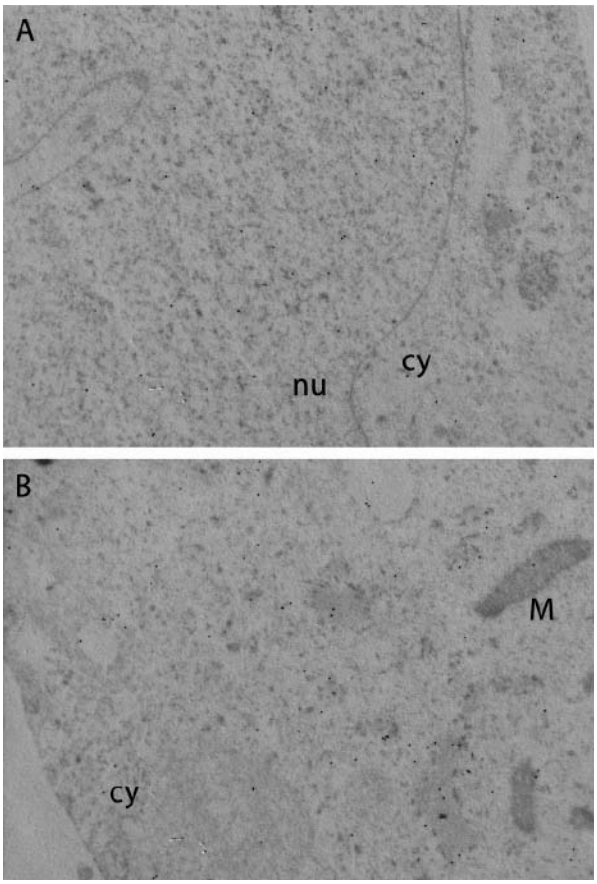


**Fig. 5.** *Immunogold detection of ChREBP protein. Electron micrographs of uncounterstained sections of Human adipose derived preadipocytes. Squares (100 cm2 at x 11000) were randomly chosen to count the number of 20-nm gold particles in the various cell compartments.* ***A****) nucleus (nu) and cytoplasm (cy);* ***B****) cytoplasm (cy), M: mitochondrion (M). Original magnification A, B: x 11000.*

To investigate the protein levels, proteins were extracted from the cells and Western blots performed. A band of 95 kDa was detected. As shown in Fig. 8 the levels of ChREBP showed a dramatic increase on day 7 of differentiation when compared to undifferentiated state. When the differentiation of the cells was performed in the presence of cyanidin, a decrease of ChREBP was seen.

## DISCUSSION

Adipose tissue plays a crucial role in the development of diseases (23). Recent studies are increasingly conducted to better understand the relationship between lipid intake and chronic degenerative diseases (atherosclerosis, cardiovascular disease, cancer, colorectal cancer and breast cancer). The white adipose tissue is actively involved in regulatory function and can affect other tissues: hypothalamus, pancreas, liver, skeletal muscle, kidney and immune system. Hormones and other adipose tissue products such as leptin, angiotensin, inflammatory cytokines, coagulation factors and steroids are involved in neuroendocrine, immune and cardiovascular functions and in the regulation of energy homeostasis (5, 24)

Adipogenesis is a continuous process even in adults and the balance of accumulation and mobilization of triglycerides in adipose tissue is controlled by several hormones (3), cytokines and other factors involved in metabolism. The primary role of the adipocyte is to store triacilglycerol during the period of caloric excess and to mobilize this reserve when missing. The mature adipocytes are almost exclusively organized for such purposes. They possess enzymes involved in lipolysis and

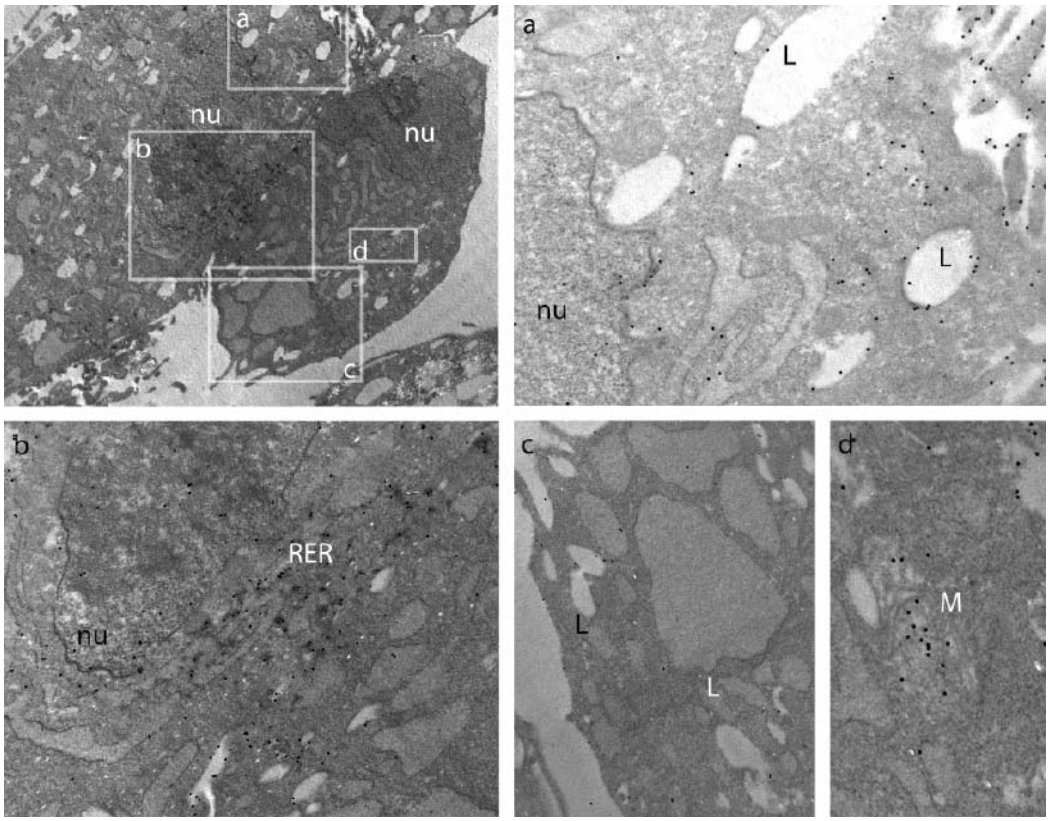


**Fig. 6.** *Subcellular localization of ChREBP in differentiated adipocytes cultured for 7 days in adipogenic differentiative medium by immunogold labeling and electron microscopy. The labeling of 20-nm gold particles appears localized close to the nuclear envelope (**a**, **b**) inside the rough endoplasmic reticulum (RER) (b) and in the mitochondria (M) (**d**); whereas the granules are sparsely present where the cytoplasm is whole occupied by lipid vacuoles (L) (**c**).*
*a,b,c,d, d higher magnifications of mature adipocytes (x 4400) at the top of the panel.*
*Original magnification a: x22000; b: x14000; c: x18000; d: x22000.*

lipogenesis. Adipocyte function is acquired during embryonic development in preparation for the post-natal period, when stored energy is needed.

It has been shown that ChREBP (carbohydrate response element binding protein) is responsible of lipogenesis in the liver and adipose tissue (10). It is a transcription factor able to regulate metabolic gene expression in response to high glucose, converting excess glucose into triglycerides (de novo lipogenesis) (12). Since ChREBP is expressed in all tissues, but mainly in lipogenic organs such as liver, adipose tissue, pancreas (17) we wanted to see if it was also expressed in preadipocytes e mature adipocytes. For this purpose we isolated predipocytes from subcutaneous or visceral human adipose tissue explant. Patients with cancer were excluded to avoid problems related to tumorigenicity. These fibroblast-like cells, (Fig. 1A) compared by other authors to mesenchymal stem cells (25-27), for the ability to differentiate under adipogenic culture conditions into adipocytes, showed mesenchymal markers CD29, CD90, CD44 on cytofluorimetric analysis, whereas they were negative for CD45 (blood derived cells), CD31 (endothelial progenitor cells), CD10, CD117 (hematopoietic stem cells) markers (Fig. 2). When these cells were cultured by using appropriate differentiating media, they underwent to adipogenic differentiation. During this process, mature adipocytes showed large lipid vacuoles that occupy most of the cytoplasm, pushing the nucleus to the periphery (Fig. 3).

Using red oil O lipids appeared as bright red

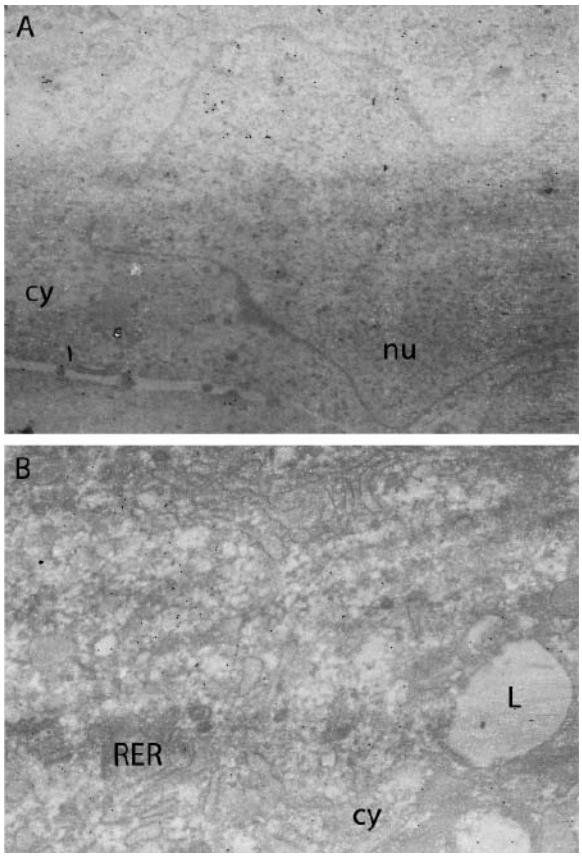


**Fig. 7.** *Immunogold detection in human adipose derived preadipocytes cultured for 7 days in adipogenic differentiative medium in presence of 100 μM cyanidin. Cells are lower differentiated, 20-nmgold granules are distributed in nuclear (**A**) and cytoplasmic (**B**) compartments, inside the rough endoplasmic reticulum (RER). Nu:nucleus, cy:cytoplasm, L: lipid vacuoles. Original magnification A, B: x 11000.*

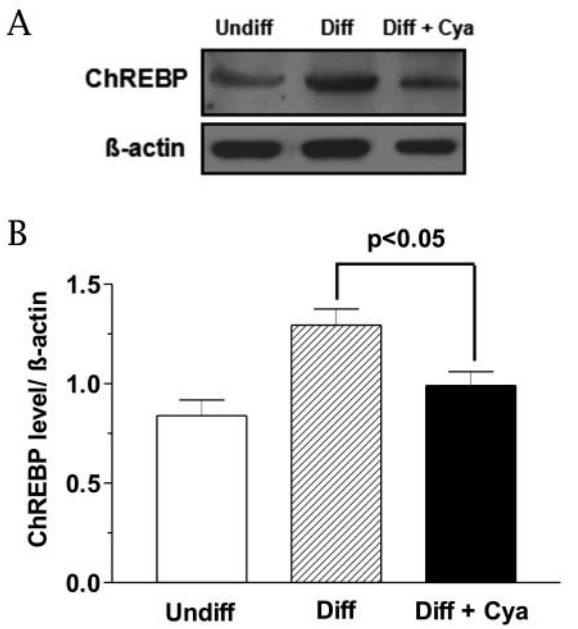


**Fig. 8.** *ChREBP expression in isolated preadipocytes and differentiated adipocytes in the presence or absence of cyanidin. A representative Western blotting as compared to β-actin (**A**). The molecular weight of protein is 95 KDa. **B**) densitometric analysis of ChREBP expression. Quantification of ChREBP level compared to β-actin expressed as mean ± SEM, n=3, *p < 0.05.*

perinuclear vesicles, often as grape-like clusters of small vesicles. Unilocular ( single, very large lipid vacuole) adipocytes rarely formed in, *in vitro*-differentiated attached adipocytes (Fig. 1B).

In this paper we report the evidence of ChREBP in human adipose derived preadipocyte and in mature adipocytes, as assayed by western blotting and *in situ* immunocytochemical analysis (Figs. 8, 5, and 6). In preadipocytes immunoelectron microscopy has shown a considerable presence of this enzyme in the cytoplasmic and nuclear compartments with some clusters close to the nuclear pore complexes, allowing us to speculate on a possible translocation from cytoplasm to the nucleus (Fig. 5 A, B). While in differentiated adipocytes for 7 days in Adipogenic Differentiation Medium, the cytoplasm immunolabeling was increased by 50% compared with preadipocytes (Table I, Fig. 6). ChREBP was also identified inside the rough endoplasmic reticulum because of the increased demand of differentiation by mature adipocytes, in mitochondria, near nuclear pore complex and in the cytosol with large clusters. The aim of our study was also to assess the modulation of proliferation, differentiation and expression of ChREBP in the presence of the antioxidant cyanidin. We used the cyanidin for its multiple biological activities: antibacterial, anti-carcinogenic, vaso-protective, anti-inflammatory, anti-obesity, anti-diabetics, antioxidant (20).

Anthocyanins have also demonstrated their positive effects on the biosynthesis and maintenance of collagen and elastin and to

suppress cancer cells growth of *in vitro* (28). These pigments also play an effective action to protect walls of blood vessels (promoting good circulation), and perform other important physiological roles, including that of modulators of resistance and capillary permeability, platelet inhibitors and vasodilators.

Cyanidin-3 improves insulin sensitivity through the regulation of glucose transporter 4 (GLUT- 4) in adipose tissue and striated muscle. Given the antiproliferative effects of other flavonoids on preadipocyte cultures (29), we hypothized that also cyanidin would reduce preadipocyte proliferation. Despite flavonoids (genistein and norigenin) (30, 31), inhibited preconfluent preadipocyte proliferation, time and dose dependent, surprisingly we found that cyanidin had no antiproliferative effect (Data not shown). Cyanidin instead reduced by 20% preadipocyte differentiation (Fig. 1C, Fig. 4).

In addition, when cells were differentiated in the presence of cyanidin, they showed abnormal morphology (Fig. 1 D), probably due to the fact that the cyanidin could interfere with the extracellular matrix. In fact the extracellular matrix plays an important role in the process of adipogenesis (22). It helps cells to bind together and regulates many cellular functions, such as adhesion, migration, proliferation, and differentiation.

Since it was found that cyanidin-3 reduces body weight in mice even in the presence of a high-fat diet (32), decreasing levels of blood glucose and improving insulin sensitivity regulating the glucose transporter-4, we studied the effect of this substance during the differentiation.

Evidence of modulation of ChREBP expression has been assessed during cyanidin treatment. The amount of gold particles does not appear to undergo evident changes upon cyanidin treatment in the nucleus, though a considerable decrease in the reaction at cytoplasm level can be observed, as shown by immunoelectron-microscopy (Fig. 5, Fig. 7). At western blotting analysis we observed a decreased expression of ChREBP (Fig. 8) in cyanidin-treated cells respect to differentiate in absence of the substance. Table 1 further shows the occurrence of modulation of ChREBP after cyanidin treatment. This minor expression of ChREBP is due, probably to the fact that there is a reduction in the number of differentiated cells (20%) or because cyanidin inhibits glucose uptake by acting on GLUT-4.

These findings in cultured adipose cells suggest that dietary cyanidin, may have inhibitory effects on adipogenesis, so foods rich in anthocyanins could be recommended not only for their anti-inflammatory properties, but also to regulate obesity with its decreased secretion of proteins involved in many pathological processes.

## ACKNOWLEDGEMENTS

We thank Andrea A. Spadaccini for technical assistance.

This work was supported by grants from the National Research Council Italy; Grant Number: RSTL 2007- id: 813-CDS040

## REFERENCES

1. Scherer PE. Adipose tissue: from lipid storage compartment to endocrine organ. Diabetes 2006; 55:1537-45.
2. Chudek J, Wiecek A. Adipose tissue, inflammation and endothelial dysfunction. Pharmacol Reports 2006; 58:81-8.
3. Fruhbeck G, Gomez-Ambrosi J, Muruzabal FJ, Burrell MA. The adipocyte: a model for integration of endocrine and metabolic signaling in energy metabolism regulation. Am J Physiol Endocrinol Metab 2001; 280:827-47.
4. Guzik TJ, Mangalat D, Korbut R. Adipocytokines ñ novel link between inflammation and vascular function? Journal of physiology and pharmacology 2006; 57:505-28.
5. Ferder l, Inserra F, Martinez-Maldonado M. Inflammation and the metabolic syndrome: role of angiotensin II and oxidative stress. Curr Hypertens Rep 2006; 8:191-8.
6. Bennett CN, Ross SE, Longo KA, Bajnok L, Hemati N, Johnson KW, Harrison SD, MacDougald OA. Regulation of Wnt signaling during adipogenesis. J Biol Chem 2002; 277:30998-1004.
7. Hamza MS, Pott S, Vega VB, et al**.** De-novo identification of PPARgamma/RXR binding sites and direct targets during adipogenesis. PLoS One

2009; 4(3):4907-12.
8. Tontonoz P, Hu E, Spiegelman BM**.** Stimulation of adipogenesis in fibroblasts by PPAR gamma 2, a lipid-activated transcription factor Cell 1994; 79:1147-56.
9. Hishida T, Nishizuka M, Osada S, Imagawa M. The role of C/EBPdelta in the early stages of adipogenesis. Biochimie 2009; 91(5):654-7.
10. Ishii S, IIzuka K, Miller BC, and Uyeda K. Carbohydrate response element binding protein directly promotes lipogenic enzyme gene transcription. PNAS 2004; 101:15597-602.
11. Iizuka K. ChREBP: a glucose-activated Transcription Factor involved in the development of Metabolic Syndrome. Endocrine Journal 2008; 55:617-24.
12. Postic C, Dentin R, Denechaud PD, Girard J. ChREBP, a transcriptional regulator of glucose and lipid metabolism. Annu Rev Nutr 2007; 27:179-92.
13. Strable MS, Ntambi JM. Genetic control of de novo lipogenesis: role in diet-induced obesity. Crit Rev Biochem Mol Biol 2010; 45:199-214.
14. Tsatsos NG, Davies MN, O'Callaghan BL, Towle HC. Identification and function of phosphorylation in the glucose-regulated transcription factor ChREBP. Biochem J 2008; 411:261-70.
15. Davies MN, O'Callaghan BL, Towle HC. Glucose activates ChREBP by increasing its rate of nuclear entry and relieving repression of its transcriptional activity. J Biol Chem 2008; 283:24029-38.
16. Li MV, Chen W, Harmancey RN, Nuotio-Antar AM, Imamura M, Saha P, Taegtmeyer H, Chan L. Glucose-6-phosphate mediates activation of the carbohydrate responsive binding protein (ChREBP). Biochem Biophys Res Commun 2010; 395:395-400.
17. Fukasawa M, Ge Q, Wynn RM, Ishii S, Uyeda K. Coordinate regulation/localization of the carbohydrate responsive binding protein (ChREBP) by two nuclear export signal sites: discovery of a new leucine-rich nuclear export signal site. Biochem Biophys Res Commun 2010; 391:1166-9.
18. Guo H, Xia M, Zou T, Ling W, Zhong R, Zhang W. Cyanidin 3-glucoside attenuates obesity-associated insulin resistance and hepatic steatosis in high-fat diet-fed and db/db mice via the transcription factor FoxO1. J Nutr Biochem 2011; 23(4):349-60.
19. Tsuda T, Ueno Y, Aoki H, Koda T, Horio F, Takahashi N, Kawada T, Osawa T. Anthocyanin enhances adipocytokine secretion and adipocyte-specific gene expression in isolated rat adipocytes.Biochem Biophys Res Commun 2004; 316:149-57.
20. Tsuda T, Ueno Y, Kojo H, Yoshikawa T, Osawa T. Gene expression profile of isolated rat adipocytes treated with anthocyanins Biochim Biophys Acta 2005; 1733:137-47.
21. Sasaki R, Nishimura N, Hoshino H, et al. Cyanidin 3-glucoside ameliorates hyperglycemia and insulin sensitivity due to downregulation of retinol binding protein 4 expression in diabetic mice. Biochem Pharmacol 2007; 74:1619-27.
22. Mariman EC, Wang P. Adipocyte extracellular matrix composition, dynamics and role in obesity. Cell Mol Life Sci 2010; 67:1277-92.
23. Kershaw EE, Flier JS. Adipose tissue as an endocrine organ. J Clin Endocrinol Metab 2004; 89:2548-56.
24. Trayhurn P, Wood IS. Adipokines: inflammation and the pleiotropic role of white adipose tissue. Br J Nutr 2004; 92:347-55.
25. D' Alimonte I, Nargi E, Mastrangelo F, et al. Vascular endothelial growth factor enhances in vitro proliferation and osteogenic differentiation of human dental pulp stem cells. J Biol Regul Homeost Agents 2011; 25:57-69.
26. Sengenès C, Lolmède K, Zakaroff-Girard A, Busse R, Bouloumié A. Preadipocytes in the human subcutaneous adipose tissue display distinct features from the adult mesenchymal and hematopoietic stem cells. J Cell Physiol 2002; 205:114-22.
27. Yoshimura K, Shigeura T, Matsumoto D, et al. Characterization of freshly isolated and cultured cells derived from the fatty and fluid portions of liposuction aspirates. J Cell Physiol 2006; 208:64-76.
28. LaVecchia C, Tavani A. Fruit and vegetables, and human cancer. EurJ Cancer Prev 1998; 7:3-8.
29. Fimognari C, Berti F, Nusse M, Cantelli Forti G, Hrelia P. In vitro antitumor activity of cyanidin-3-O-beta-glucopyranoside. Chemotherapy 2005; 51:332-5.
30. Harmon AW, Harp JB. Differential effects of flavonoids on 3T3-L1 adipogenesis and lipolysis. Am J Physiol Cell Physiol 2001; 280:807-13.
31. Harmon AW, Patel YM and Harp JB. Genistein

inhibits CCAAT/enhancer-binding protein b (C/EBPb) activity and 3T3-L1 adipogenesis by increasing C/EBP homologous protein expression. Biochem J 2002; 367:203-8.

32. Tsuda T, Horio F, Uchida K, Aoki H, Osawa T. Dietary cyanidin 3-O-beta-D-glucoside-rich purple corn color prevents obesity and ameliorates hyperglycemia in mice. J Nutr 2003; 133:2125-30.

# *REV-ERBα* AND THE CLOCK GENE MACHINERY IN MOUSE PERIPHERAL TISSUES: A POSSIBLE ROLE AS A SYNCHRONIZING HINGE

G. MAZZOCCOLI[1], Y. CAI[2], S. LIU[2], M. FRANCAVILLA[3], F. GIULIANI[3], A. PIEPOLI[4], V. PAZIENZA[4], M. VINCIGUERRA[5], T. YAMAMOTO[6] and T. TAKUMI[7]

*[1]Department of Medical Sciences, Division of Internal Medicine and Chronobiology Unit, Scientific Institute and Regional General Hospital "Casa Sollievo della Sofferenza", S.Giovanni Rotondo (FG), Italy; [2]Department of Neurology and Neurobiology, Xuanwu Hospital of Capital Medical University, Key Laboratory for Neurodegenerative Diseases of Ministry of Education, Beijing, P.R. China; [3]Computing Unit, Scientific Institute and Regional General Hospital "Casa Sollievo della Sofferenza", S.Giovanni Rotondo (FG), Italy; [4]Research Laboratory and Division of Gastroenterology, IRCCS Scientific Institute and Regional General Hospital "Casa Sollievo della Sofferenza", San Giovanni Rotondo, Italy; [5]Institute of Hepatology, Birkbeck University of London, London, United Kingdom; [6]Life Science Laboratory, Advanced Material Laboratories, Sony Corporation, Shinagawa, Tokyo, Japan; [7]Laboratory of Integrative Bioscience, Graduate School of Biomedical Sciences, Hiroshima University, Hiroshima, Japan*

*Received September 2, 2011 – Accepted March 13, 2012*

**Rhythmic oscillations of cellular biological processes are driven by translational-transcriptional feedback loops that realize molecular clocks ticking in every single cell, driven by neural and humoral outputs from the suprachiasmatic nuclei of the hypothalamus that are entrained by environmental photon inputs. The nuclear receptor *REV-ERBα* has the capability to reset the molecular oscillators of peripheral tissues. The aim of our study was to evaluate the clock gene machinery function in light/dark cycles (LD) and in constant darkness (DD) exploiting in particular the *REV-ERBα* pattern of expression by using data from two independent experimental settings to reduce procedure related influences. In the LD study C57BL/6 male mice housed on a 12L:12D cycle were sacrificed at 4 h intervals. Liver, kidney, spleen, thymus and testis were harvested and blood was collected. Expression levels of *PER1, PER2*, *CRY1, CRY2*, *BMAL1, REV-ERBα, CLOCK* were evaluated by qRT-PCR. In the DD study Balb/c male mice in the third DD cycle as a continuation of the dark phase of the last LD cycle were sacrificed at 4 h intervals. Lung, heart, liver, stomach, kidney, spleen, and testis were harvested and mRNA expression of *PER1, PER2*, *CRY1, CRY2*, *BMAL1, REV-ERBα, CLOCK,* was evaluated by qRT-PCR. A statistically significant difference was found for the size of the semi-interquartile range of acrophases of clock gene expression in different organs evaluated in LD and DD conditions (4:38±1:12h versus 1:16±0:10h, p=0.026). A statistically significant difference was found for the acrophases of clock gene expression in different organs evaluated in LD (p=0.01) and in DD (p<0.0001). In LD study only *REV-ERB* α showed concomitant expression in the different peripheral tissues with the phase peaking around 07:03±0.8h. In**

*Key words: clock genes, REV-ERBα, light-dark cycle*

*Mailing address:* Dr Gianluigi Mazzoccoli,
Department of Medical Sciences,
Division of Internal Medicine and Chronobiology Unit,
Scientific Institute and Regional General Hospital,
"Casa Sollievo della Sofferenza",
San Giovanni Rotondo (FG), Italy
Tel: +39 0882 835228 Fax: +39 0882 410563
e-mail: g.mazzoccoli@operapadrepio.it



0393-974X (2012)

**the DD study all the core clock genes showed concomitant phases in different peripheral mouse tissues and *REV-ERB* α expression peaked around 07:09±0.9h. In conclusion, *REV-ERB α* is the only clock gene that maintains its timing of oscillation in the LD study and in the DD study and its phase of expression remains concomitant in the different mouse peripheral tissues in the presence of LD alternance, or in constant darkness. Oscillation in REV-ERB α ligands (heme, carbon monoxide) may affect not only the phase and amplitude of circadian rhythms, but also physiological outputs of the circadian system and REV-ERB α may participate in the entrainment of central and peripheral clocks, functioning as a synchronizing hinge of the clock gene machinery.**

Terrestrial biological systems operate on a 24-hour temporal scale corresponding to the period of rotation of our planet on its axis and to the rhythmic exposition of its surface to the sun, leading to day–night cycles. Living organisms and humans possess circadian (about 24-hour) life rhythms, generated by an internal timing system, that allows them to adapt to changing enviromental conditions and to optimize their bodily functions and activity when most needed (1). The circadian timing system comprises central and peripheral components structured in an input pathway, including detectors in the retinal ganglion cells, that receive photic informations and transmit them via the retino-hypothalamic tract to the central master oscillator, represented by the suprachiasmatic nuclei (SCN) of hypothalamus, that drive the rhythmic oscillations of metabolic, physiological and behavioural processes by neural or humoral output pathways (2). The central clock located in the SCN can function autonomously, without any external input, but it can be reset by environmental cues such as light. In all body tissue peripheral clocks maintain circadian rhythms, modulate transcription factors in a paracrine fashion to regulate tissue-specific gene expression and are thought to be synchronized by the master clock to ensure temporally coordinated physiology. The synchronization mechanisms implicate various humoral signals, including circulating entraining factors such as glucocorticoids and melatonin (3). Central and peripheral oscillators are timed by an intracellular mechanism composed of a set of interlocking transcription-translation feedback loops completing one cycle each day. The positive limb of the loop is represented by the basic helix– loop–helix PAS transcription factors CLOCK (or its paralog NPAS2) and BMAL1, which heterodimerize and bind to E-box enhancer elements in the promoters of the *Period* genes (*PER*1-3) and *Cryptochrome* genes (*CRY*1 and *CRY*2), which are at the center of the core negative feedback loop. The *PER* and *CRY* mRNAs then give rise to PER and CRY proteins that, along with Casein KinaseI δ/ε (CKI δ/ε), interact to form a repression complex that translocates back into the nucleus, interact directly with CLOCK and BMAL1, and result in loss of their activation activity. *TIM* is a core circadian clock gene in Drosophila melanogaster and is retained in mammals, but its role in mammalian circadian clock function is yet unclear. TIM and its partner TIPIN interact with components of the DNA replication system to regulate DNA replication processes under both normal and stress conditions. The molecular clock regulates clock-controlled genes (CCGs), as *DBP*, that follow tissue-specific expression patterns, also defined output genes, i.e., genes involved in the functional output of an organ, as only those including key cell cycle regulators and tumor suppressors are expressed in all tissues studied (4-7).

The phase of clock gene expression in peripheral tissues may be entrained by restricted feeding, so that the nutritional and hormonal signals elicited by feeding serve to synchronize peripheral clocks to the underlying metabolic oscillators (8). On the other hand, CLOCK-BMAL1 heterodimer activates an auxiliary loop promoting the expression of the nuclear receptors REV-ERB *α* (encoded by *NR1D1*) and REV-ERB β (encoded by *NR1D2*), that in turn, negatively control the rhythmic transcription of *BMAL1*, as the REV-ERB *α/β* protein binds to ROR elements of the *BMAL1* promoter and represses *BMAL1* transcription. This stabilizing negative loop is important for precise control of the circadian pacemaker. REV-ERBs regulate a number of physiological functions including the circadian rhythm, lipid metabolism, and cellular differentiation (9-12).

Heme is associated with the ligand-binding domains of the REV-ERB *α/β* with a 1:1

stoichiometry, it enhances the thermal stability of the proteins, and causes the recruitment of the co-repressor NCoR1, leading to repression of *BMAL1* gene. Heme regulation of REV-ERBs may link the control of metabolism and the mammalian clock and these nuclear receptors may link clock genes and metabolic gene expression, integrating energy flux with time-of-day dependent gene transcription within metabolic tissues, optimizing the co-occurrence between nyctohemeral alternance of anabolic and catabolic states and the behavioural cycles of sleep-wake, rest-activity and fasting-feeding. REV-ERBs are highly dynamic receptors that are responsive not only to heme, but also to redox and gases, as carbon monoxide, suggesting new mechanisms for the systemic coordination of molecular clocks and metabolism (13-15).

The information regarding the sequence of activation of the core clock genes with different environmental lighting cues and in different tissues are yet unclear, therefore we decided to address this issue using a subset of data published elsewhere (16, 17) to evaluate the pattern of clock gene machinery functioning in mouse peripheral tissues under different light-dark cycle conditions and under two different experimental settings.

## MATERIALS AND METHODS

*LD STUDY*

*Animals*

Eight-week-old C57BL/6 male mice were housed individually on a 12L:12D light-dark cycle (lights-on at 08:00 h; lights-off at 20:00 h), with food and water available *ad libitum*, for two weeks after arrival at the animal facility. Care of the mice was in accordance with the Institutional Animal Care and Use Committee guidelines at the Capital Medical University and in agreement with the ethical standards.

*RNA Preparation For SYBR Green I-based analysis*

Three to four mice at each of the six time points were sacrificed at 4-h intervals beginning at 09:00 h local time (=01 HALO =Hours After Light Onset). Liver, kidney, spleen, thymus and testis were harvested and stored in RNAlater (Qiagen, Alameda, California, USA), and blood was collected into the PAX gene Blood RNA tubes (Qiagen, Alameda, California, USA). Total RNA was extracted from peripheral blood and lymphoid organs using either a PAXgene blood RNA kit or RNAeasy kit (Qiagen, Alameda, California, USA) according to the user's manual. To eliminate genomic DNA, total RNA was treated with RQ1 RNase free DNase I (Promega, San Luis Obispo, California, USA) according to the user's manual.

*Quantitative Reverse Transcription PCR*

To generate single-strand cDNAs, total RNA (1μg) was reverse transcribed using Superscript II (Invitrogen, Carlsbad, California, USA) and random hexamers. For SYBR Green I-based analysis, the cDNA equivalent of 50 ng of total RNA from each sample was amplified in an Opticon II system (MJ Research, Waltham, Massachusetts, USA) using a SYBRGreen I real-time PCR kit (Takara, Otsu Shiga, Japan). Each sample was analyzed in duplicate to ensure the accuracy of the data. *18S*, a housekeeping gene, was used to normalize the differences in sample RNA content.

*Primer Sequences Used in Real-Time Quantitative RT-PCR*

SYBR Green

*PER1* Forward CATGACTGCACTTCGGGAGC, Reverse CTTGACACAGGCCAGAGCGTA;

*PER2* Forward GGCTTCACCATGCCTGTTGT, ReverseGGAGTTATTTCGGAGGCAAGTGT;

*CRY1* Forward TTGCCTGTTTCCTGACTCGT, Reverse GACAGCCACATCCAACTTCC;

*CRY2* Forward TCGGCTCAACATTGAACGAA, Reverse GGGCCACTGGATAGTGCTCT;

*BMAL1* Forward ACATAGGACACCTCGCAGAA, Reverse AACCATCGACTTCGTAGCGT;

*REV-ERBα*ForwardCGTTCGCATCAATCGCAACC, Reverse ATGTGGAGTAGGTGAGGTC;

*CLOCK* Forward CCTATCCTACCTTCGCCACACA Reverse TCCCGTGGAGCAACCTAGAT;

*18S* Forward TTCGGAACTGAGGCCATGAT, Reverse TTTCGCTCTGGTCCGTCTTG;

*DD STUDY*

*Animals*

Male Balb/c mice purchased 5 weeks post-partum from Japan SLC (Hamamatsu, Japan), were exposed to 2 weeks of light-dark (LD) cycles and then kept in complete darkness as a continuation of the dark phase of the last LD cycle. mRNA expression was examined in the third dark-dark (DD) cycle. All protocols of experiments using animals in this study were approved by the OBI (Osaka Bioscience Institute) Animal Research Committee.

*RNA Preparation For SYBR Green I-based analysis*

Three to four mice at each of the six time points were sacrificed at 4 h intervals beginning at 09:00 h local time

(=01 HALO =Hours After Light Onset) in the third dark-dark (DD) cycle. Lung, heart, liver, stomach, kidney, spleen, and testis were harvested and stored in RNAlater (Qiagen, Alameda, California, USA). Total RNA was extracted from peripheral organs using either a RNAeasy kit (Qiagen, Alameda, California, USA) according to the user's manual. To eliminate genomic DNA, total RNA was treated with RQ1 RNase free DNase I (Promega, San Luis Obispos, California, USA) according to the user's manual.

*Quantitative Reverse Transcription PCR*

Real-time quantitative RT-PCR was performed by using an ABI PRISM 7000 (Applied Biosystems). The PCR primers were designed with Primer Express software (Applied Biosystems), and the sequences of the forward and reverse primers were as follows:

*PER1* Forward CAGGCTAACCAGGAATATTACCAGC, Reverse CACAGCCACAGAGAAGGTGTCCTGG;
*PER2* Forward GGCTTCACCATGCCTGTTGT, Reverse GGAGTTATTTCGGAGGCAAGTGT;
*CRY1* Forward CCCAGGCTTTTCAAGGAATGGAACA, Reverse TCTCATCATGGTCATCAGACAGAGG;
*CRY2* Forward GGGACTCTGTCTATTGGCATCTG, Reverse GTCACTCTAGCCCGCTTGGT;
*BMAL1* Forward GCAGTGCCACTGACTACCAAGA, Reverse TCCTGGACATTGCATTGCAT;
*REV-ERBα* Forward CGTTCGCATCAATCGCAACC, Reverse GATGTGGAGTAGGTGAGGTC;
*CLOCK* Forward CCTATCCTACCTTGGCCACACA, Reverse TCCCGTGGAGCAACCTAGAT;
*GAPDH* Forward ACGGGAAGCTCACTGGCATGGCCTT, Reverse CATGAGGTCCACCACCCTGTTGCTG

Specificity of gene amplification was confirmed by measuring the size and purity of the PCR product by gel electrophoresis, and by analyzing the dissociation curve with ABI PRISM 7000 SDS software (Applied Biosystems). For a 25-µl PCR reaction, 50 ng cDNA template was mixed with the forward and reverse primers to a final concentration of 300 nM each and 12.5 µl of 2x SYBR Green PCR Master Mix (Applied Biosystems). The reaction was first incubated at 50°C for 2 min, then at 95°C for 10 min, followed by 40 cycles of 95°C for 15 sec and 60°C for 1 min. Each gene-specific PCR was performed in triplicate. *GAPDH* primers were used as the control.

*Statistical analysis*

Original values of gene expression level for each CGs were normalized to percent of mean to reduce inter-subject variability in levels prior to analyses for time-effects on grouped data. Using grouped data, overall gene expression levels were then analyzed for time-effect across the six time points by one-way analysis of variance (ANOVA) or Kruskal-Wallis one-way ANOVA on Ranks followed by all pair-wise multiple comparison procedures (Student-Newman-Keuls method or Dunn's method) as indicated. Each time-series of expression levels was analyzed for circadian rhythm characteristics by the single cosinor procedure involving the fit of a 24h cosine curve to the data by least-squares linear regression using the Chronolab statistical package (18), in order to accurately describe waveforms and rhythm characteristics (e.g., amplitude, phase). An $R^2$ value and a p value for the rejection of the zero-amplitude assumption were determined for each component in the cosine model separately and overall, with rhythm detection considered statistically significant if $p \leq 0.05$ for any period tested. Circadian (24h) characteristics were summarized from the 24h cosine model. Rhythm characteristics determined from the best-fitting cosine model include the mesor (the middle of the cosine representing an adjusted average if unequal sampling), the amplitude, A (half the distance from the peak and trough of the best fitting curve, with 2A indicating a predictable range of change), and the phase (Ø) of the cosine model (referenced to an external event, such as local midnight or time of light onset), with the peak of a single component cosine called the acrophase, aØ (acro = peak). Acrophases (hh:mm) and residuals calculated on acrophases were then analyzed by one-way analysis of variance (ANOVA) or Kruskal-Wallis one-way ANOVA on Ranks followed by all pair-wise multiple comparison procedures (Student-Newman-Keuls method or Dunn's method) as indicated. The semi-interquartile range was evaluated as a measure of spread or dispersion of acrophase values. It was computed as one half the difference between the 75th percentile (Q3) and the 25th percentile (Q1) in accordance to the formula for semi-interquartile range calculation: (Q3-Q1)/2. $P \leq 0.05$ was considered statistically significant.

## RESULTS

Results are expressed as mean±standard error (SE). A statistically significant difference was found for the size of the semi-interquartile range of acrophases of clock gene expression in the different mouse peripheral tissues considered evaluated in LD and DD conditions (4:38±1:12h versus 1:16±0:10h p=0.026).

*LD STUDY*

Residuals calculated on acrophases (hh:mm)

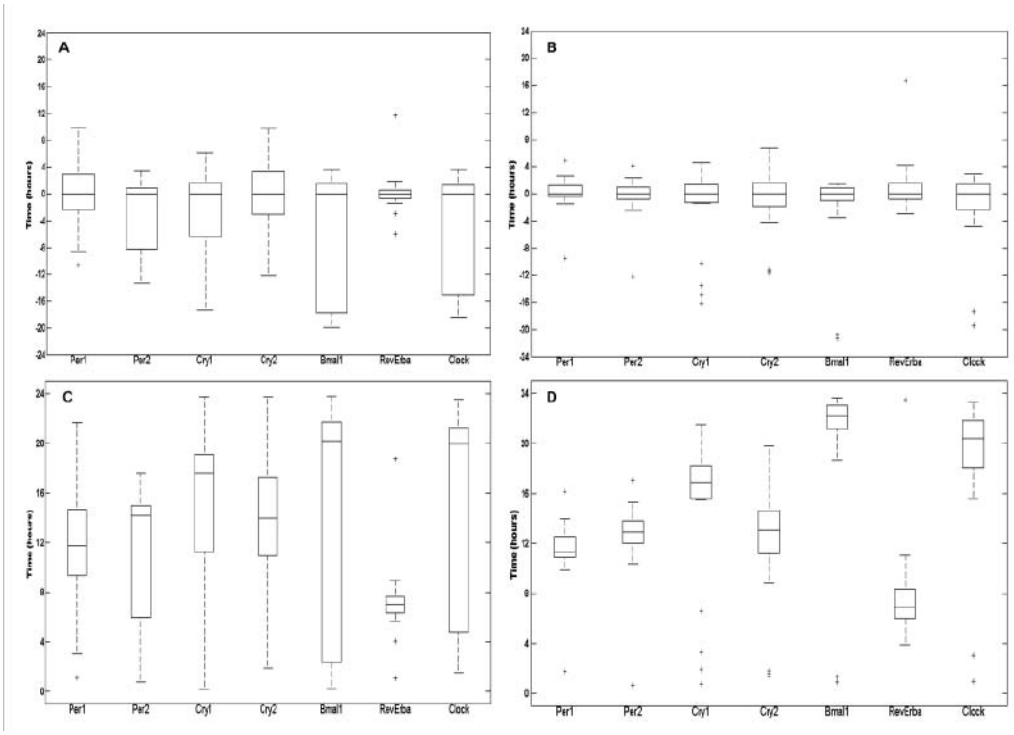


**Fig. 1.** ***A)*** *Residual plot showing the residuals of clock gene expression values on the vertical axis and the peripheral tissues on the horizontal axis in mice housed individually on a 12L:12D light-dark cycle (lights-on at 08:00 h; lights-off at 20:00 h).* ***B)*** *Residual plot showing the residuals of clock gene expression values on the vertical axis and the peripheral tissues on the horizontal axis in mice housed individually on a 12D:12D light-dark cycle (constant darkness).* ***C)*** *x-y plot showing the acrophases of clock gene expression values on the vertical axis and the peripheral tissues on the horizontal axis in mice housed individually on a 12L:12D light-dark cycle (lights-on at 08:00 h; lights-off at 20:00 h).* ***D)*** *x-y plot showing the acrophases of clock gene expression values on the vertical axis and the peripheral tissues on the horizontal axis in mice housed individually on a 12D:12D light-dark cycle (constant darkness). Boxes represent the interquartile range (IQR) and the horizontal bar the median relative expression. Expression values that do not fall within 1.5 x IQR are outliers and are indicated by circles where appropriate.*

from single 24-h cosinor analyses for circadian time-effects for each CG in each tissue when sampled every 4 h in mice housed individually on a 12L:12D light-dark cycle (lights-on at 08:00 h; lights off at 20:00 h) are listed in Table IA and shown in Fig. 1. A. A significant 24-h rhythmic component was found for PER1 in liver, kidney, spleen, thymus, testis and blood, for PER2 in liver, kidney, spleen, thymus, and blood, for CRY1 in liver, kidney, spleen and testis, for CRY2 in liver, kidney, spleen and blood, for BMAL1 in liver, kidney, spleen and testis, for REV-ERB α in liver, kidney, spleen, thymus, and blood, for CLOCK in liver, kidney, thymus and blood. *REV-ERB* α showed concomitant expression in the different peripheral tissues with the phase peaking around 07:03±0.8h. Kruskal-Wallis One Way ANOVA on Ranks run on mean acrophase hours in the different tissues showed a statistically significant difference (P=0.01) (Fig. 1.C and Table IB)

*DD STUDY*

Residuals calculated on acrophases (hh:mm) from single 24-h cosinor analyses for circadian time-effects for each CG in each tissue when sampled every 4 h in mice housed individually on a 12D:12D light-dark cycle (costant darkness) are listed in Table IIA and shown in Fig. 1.B. A significant 24-h rhythmic component was found for PER1 in lung, heart, liver, stomach, spleen and kidney, for PER2 in lung, heart, liver, stomach, spleen and kidney, for CRY1 in lung, heart, liver, spleen and kidney, for CRY2 in heart, spleen and kidney, for BMAL1 in lung, heart, liver,

**Table IA.** *Residuals calculated on acrophases (h:m) from single 24 h cosinor analyses for circadian time-effects for each clock gene in each tissue when sampled in triplicate every 4 h in mice housed individually on a 12L:12D light-dark cycle (lights-on at 08:00 h; lights off at 20:00 h).*

| | *Per1* | *Per2* | *Cry1* | *Cry2* | *Bmal1* | *RevErbα* | *Clock* |
|---|---|---|---|---|---|---|---|
| liver | 1:22 | 1:34 | 2:06 | 0:01 | 1:53 | 0:00 | 1:17 |
| | 2:57 | 0:10 | 0:13 | 1:12 | 1:15 | -1:04 | 0:03 |
| | 1:31 | 0:07 | -1:38 | -2:01 | 3:35 | 1:51 | -2:32 |
| kidney | 7:31 | -10:33 | 1:34 | 5:04 | 0:43 | -6:00 | -18:26 |
| | 9:53 | -1:45 | 4:47 | 5:28 | 1:37 | 0:16 | 1:10 |
| | -8:44 | -13:25 | -16:08 | -12:07 | -19:52 | -3:00 | -16:04 |
| spleen | 0:03 | 0:39 | 1:31 | 0:01 | 1:49 | 0:25 | 3:35 |
| | 0:48 | 0:53 | 0:04 | 0:04 | 1:30 | 0:03 | 0:20 |
| | 0:08 | 0:07 | 2:57 | 9:04 | -19:58 | 1:24 | 1:18 |
| testis | 6:05 | 1:57 | -4:54 | 3:16 | 0:36 | 11:40 | 0:33 |
| | -6:04 | 3:22 | -17:13 | 9:46 | -19:37 | -1:26 | 2:55 |
| | -5:03 | -8:14 | -4:50 | -7:17 | -8:20 | 0:19 | -14:10 |
| thymus | 0:03 | 0:49 | 1:18 | 0:24 | 1:12 | 0:36 | 1:22 |
| | 0:35 | 0:18 | 0:04 | 0:37 | 0:36 | 0:44 | 0:03 |
| | -2:22 | -1:42 | 6:11 | -7:01 | -19:03 | 0:36 | -15:07 |
| blood | 9:56 | -12:35 | -6:28 | -3:02 | -7:44 | 1:46 | -17:22 |
| | 0:46 | 1:11 | -6:19 | -2:51 | -17:40 | 0:00 | 2:58 |
| | -10:39 | -10:49 | -17:25 | -10:48 | -17:49 | 0:05 | -16:29 |

stomach, spleen, kidney and testis, for REV-ERBα in lung, heart, liver, stomach, spleen and kidney, for CLOCK in lung, heart, liver and kidney. *REV-ERB* α showed concomitant expression in the different peripheral tissues with the phase peaking around 07:09±0.9h. Kruskal-Wallis One Way ANOVA on Ranks run on mean acrophase hours in the different tissues showed a statistically significant difference ($P<0.0001$) (Fig.1.D and Table IIB).

## DISCUSSION

Multiple rhythms in mammalian peripheral tissues are regulated by circadian clocks driven by the rhythmic expression of the core clock genes, that in turn control the oscillations in expression patterns of clock controlled cell-specific genes regulating specific tissue-organ functions. Light exposure entrains the phase of the SCN and influences the functional activity of peripheral organs, inducing rapid changes in the expression of clock genes and output genes by variations in hormone levels, and in particular of melatonin and cortisol/corticosterone secretion, and by using SCN neural outputs, represented by the autonomic innervations (19, 20).

In the L:D study C57BL/6J mice were entrained to a 12-hour light, 12-hour dark cycle (LD12:12) under constant temperature for two weeks and then

**Table IB.** *Acrophases (hh:mm) from single 24 h cosinor analyses for circadian time-effects for each clock gene in each tissue when sampled in triplicate every 4 h in mice housed individually on a 12L:12D light-dark cycle (lights-on at 08:00 h; lights off at 20:00 h).*

| | *Per1* | *Per2* | *Cry1* | *Cry2* | *Bmal1* | *RevErbα* | *Clock* |
|---|---|---|---|---|---|---|---|
| liver | 13:07 | 15:46 | 19:41 | 14:01 | 22:06 | 7:02 | 21:14 |
| | 14:41 | 14:21 | 17:48 | 15:11 | 21:27 | 5:58 | 20:00 |
| | 13:16 | 14:18 | 15:56 | 11:58 | 23:48 | 8:54 | 17:25 |
| kidney | 19:16 | 3:37 | 19:09 | 19:03 | 20:56 | 1:03 | 1:30 |
| | 21:38 | 12:26 | 22:22 | 19:27 | 21:49 | 7:19 | 21:08 |
| | 3:00 | 0:46 | 1:26 | 1:52 | 0:20 | 4:02 | 3:52 |
| spleen | 11:41 | 14:50 | 19:06 | 13:57 | 22:02 | 6:37 | 23:32 |
| | 10:56 | 13:18 | 17:30 | 13:54 | 21:43 | 6:59 | 20:18 |
| | 11:53 | 14:03 | 20:33 | 23:03 | 0:14 | 8:27 | 21:15 |
| testis | 17:51 | 16:07 | 12:41 | 17:15 | 19:36 | 18:43 | 19:23 |
| | 5:40 | 17:33 | 0:22 | 23:45 | 0:34 | 5:37 | 22:52 |
| | 6:41 | 5:57 | 12:44 | 6:42 | 11:51 | 7:22 | 5:46 |
| thymus | 11:48 | 15:00 | 18:53 | 14:24 | 21:25 | 6:27 | 21:19 |
| | 11:09 | 14:29 | 17:39 | 14:37 | 20:48 | 6:18 | 19:53 |
| | 9:21 | 12:29 | 23:46 | 6:57 | 1:08 | 7:39 | 4:49 |
| blood | 21:41 | 1:34 | 11:05 | 10:56 | 12:27 | 8:49 | 2:35 |
| | 10:58 | 15:22 | 11:15 | 11:07 | 2:32 | 7:04 | 22:55 |
| | 1:05 | 3:21 | 0:10 | 3:11 | 2:22 | 7:08 | 3:27 |

sacrificed, whereas in the D:D study Balb/c mice were entrained to a 12-hour light, 12-hour dark cycle (LD12:12) under constant temperature for two weeks, and then were transferred to constant darkness (DD12:12) before they were sacrificed. This strategy excludes light-regulated genes that are not under endogenous circadian control eliminating the masking effect of light/dark cycle on gene expression.

Data from the two experimental conditions show that the clock genes have different patterns of expression among mouse peripheral tissues when evaluated in a 12-hour light, 12-hour dark cycle or in constant darkness. In LD12:12 only *REV-ERB* α shows concomitant expression in the different peripheral tissues with the phase peaking around 07:00h in all the considered tissues. On the other hand, when mice were kept in a DD12:12 condition all the core clock genes showed concomitant phases in different mouse tissues, with *REV-ERB* α anyway peaking around 07:00h. This evidence is corroborated by the finding of a statistically significant difference in the size of the semi-interquartile range of acrophases of clock gene expression in the different organs evaluated in LD and DD conditions (4:38±1:12h *vs* 1:16±0:10h p=0.026).

This close meta-analysis of the phase relationship between the profiles of clock gene expression in

**Table IIA.** *Residuals calculated on acrophases (h:m) from single 24 h cosinor analyses for circadian time-effects for each clock gene in each tissue when sampled in triplicate every 4 h in mice housed individually on a 12D:12D light-dark cycle (constant darkness).*

| | *Per1* | *Per2* | *Cry1* | *Cry2* | *Bmal1* | *RevErbα* | *Clock* |
|---|---|---|---|---|---|---|---|
| lung | 0:25 | -2:32 | 1:18 | -11:40 | 0:46 | 0:48 | 2:54 |
| | 0:12 | 0:13 | 1:26 | 1:19 | 1:03 | 4:10 | -19:29 |
| | 1:07 | 1:15 | 2:20 | -2:30 | 0:51 | 0:00 | 1:18 |
| heart | 2:38 | 4:09 | 3:27 | -11:26 | 0:58 | 0:45 | 2:47 |
| | 2:31 | 1:11 | 0:00 | 0:27 | 0:19 | -1:07 | -1:14 |
| | 1:08 | 2:21 | 1:43 | 2:16 | 0:16 | 1:13 | 1:46 |
| liver | 4:49 | 2:22 | -10:18 | 6:45 | -3:33 | 1:57 | 0:33 |
| | 0:25 | 0:13 | -1:23 | 0:18 | 0:17 | 0:30 | 0:32 |
| | -1:26 | 0:25 | 0:06 | -1:41 | 0:24 | 0:14 | 0:30 |
| stomach | 0:00 | 0:02 | 0:25 | -4:15 | 0:38 | -1:10 | 0:20 |
| | 0:29 | 0:44 | 0:24 | 0:43 | 0:33 | 1:19 | -2:15 |
| | 2:13 | 0:25 | -1:20 | 0:19 | -1:14 | 3:03 | -4:50 |
| spleen | 0:06 | 0:13 | 0:19 | 0:00 | 0:59 | -1:05 | 0:07 |
| | 0:24 | -1:38 | 4:36 | -11:16 | -2:38 | -2:58 | 2:39 |
| | 0:34 | -1:14 | 0:03 | 0:14 | 1:25 | 0:24 | -2:21 |
| kidney | 0:24 | 0:51 | 0:57 | 0:18 | 1:22 | 0:33 | 2:42 |
| | 0:01 | 0:56 | 0:12 | 2:23 | 0:00 | 0:26 | -2:25 |
| | -1:11 | 0:00 | -16:10 | 0:28 | 1:26 | 0:47 | 0:00 |
| testis | 1:33 | 0:45 | 0:22 | 2:25 | -20:53 | 2:25 | -2:22 |
| | 0:36 | 0:52 | -13:35 | 0:08 | 0:29 | -1:17 | 0:49 |
| | -9:33 | -12:13 | -15:00 | 3:43 | -21:17 | 16:38 | -17:23 |

different peripheral tissues of mice kept under different environmental lighting condition suggests a key role for *REV-ERB* α in the coordination of the multiple peripheral endogenous clocks and the prevailing of different mechanisms of peripheral clock entrainment in the absence of photon cues. Evidence for this is reinforced by the fact that data are obtained under two different experimental settings, eliminating the possibility of procedure related influences on the clock gene expression pattern.

Light rapidly induces *PER1* expression in the adrenal gland *via* the SCN-sympathetic nervous system, whereas the effect of light cue on the re-entrainment of the food dominated peripheral clocks is yet unclear. The light-induced changes in the expression patterns of clock genes are organ and time-of-day specific, nocturnal light exposure has immediate effects on the peripheral tissues by means of rapid changes in the expression level of several clock genes in different organs and the Autonomic

**Table IIB.** *Acrophases (h:m) from single 24 h cosinor analyses for circadian time-effects for each clock gene in each tissue when sampled in triplicate every 4 h in mice housed individually on a 12D:12D light-dark cycle (constant darkness).*

| | *Per1* | *Per2* | *Cry1* | *Cry2* | *Bmal1* | *RevErbα* | *Clock* |
|---|---|---|---|---|---|---|---|
| lung | 10:54 | 10:21 | 18:11 | 1:23 | 22:58 | 7:40 | 23:19 |
| | 11:07 | 12:40 | 18:19 | 14:24 | 23:15 | 11:03 | 0:55 |
| | 12:26 | 14:09 | 19:13 | 10:33 | 21:20 | 6:52 | 21:43 |
| heart | 13:58 | 17:03 | 20:21 | 1:37 | 23:11 | 6:07 | 23:11 |
| | 13:51 | 14:04 | 16:53 | 13:30 | 22:31 | 5:45 | 19:10 |
| | 12:28 | 15:15 | 18:36 | 15:19 | 22:28 | 8:05 | 22:11 |
| liver | 16:08 | 15:16 | 6:35 | 19:49 | 18:38 | 8:49 | 20:57 |
| | 11:45 | 13:07 | 15:30 | 12:45 | 21:55 | 7:22 | 20:56 |
| | 9:52 | 12:28 | 16:47 | 11:22 | 21:48 | 6:38 | 20:54 |
| stomach | 11:19 | 12:56 | 16:28 | 8:48 | 21:34 | 5:42 | 20:04 |
| | 11:49 | 13:38 | 17:18 | 12:20 | 22:45 | 8:11 | 18:08 |
| | 13:33 | 13:19 | 15:33 | 13:23 | 20:57 | 9:56 | 15:34 |
| spleen | 11:13 | 12:40 | 17:13 | 13:03 | 21:13 | 5:46 | 20:17 |
| | 10:55 | 11:14 | 21:30 | 1:48 | 19:33 | 3:53 | 23:04 |
| | 10:45 | 11:39 | 16:50 | 12:49 | 23:37 | 6:28 | 18:04 |
| kidney | 10:55 | 13:45 | 17:51 | 13:21 | 23:34 | 6:19 | 23:07 |
| | 11:20 | 11:57 | 16:41 | 15:28 | 22:12 | 6:26 | 17:59 |
| | 10:07 | 12:54 | 0:43 | 12:35 | 23:38 | 7:39 | 20:24 |
| testis | 12:52 | 12:08 | 17:16 | 15:29 | 1:18 | 9:18 | 18:02 |
| | 10:43 | 12:01 | 3:17 | 13:12 | 22:41 | 5:34 | 21:14 |
| | 1:46 | 0:40 | 1:53 | 16:47 | 0:54 | 23:31 | 3:00 |

Nervous System (ANS) plays a role in the light effect on peripheral organs, not only for the pineal and adrenal but also for the liver. The changes in liver core clock gene and CCG expression observed after nocturnal light exposure are dependent on an intact input from the ANS and do not depend on changes in the secretion of hormones such as melatonin and cortisol/corticosterone, suggesting that the autonomic innervation of the liver is essential for the transmission of the light information, most likely via the SCN, in order to adjust the liver metabolism immediately according to the light changes in the environment (21).

An abrupt 12-h phase shift of feeding schedule and LD cycle entrains the peripheral clocks with gene- and tissue specific circadian resetting properties and the food cue is a principal timing cue for peripheral clocks, while the light-dark cycle can only indirectly entrain the circadian rhythm of the molecular oscillators in peripheral tissues (22-25).

When the most powerful environmental cue, light/dark alternance, is not present, as in constant darkness, other synchronizers prevail, possibly operating via the nuclear receptors. REV-ERB α links clock gene machinery and metabolic state in every single cell of central and peripheral tissues and is capable of resetting the clock machinery at a cellular and tissue level in a time-dependent fashion (26, 27). Gene expression of many nuclear receptors exhibits robust daily cycles in a wide range of tissues, including the liver, skeletal muscle, and brown and white fats, suggesting the crucial role of these transcriptional regulators in orchestrating metabolic cycles, as well as core clock functions. Nutrient intake provides an important timing cue for the metabolic activity and clock phase in peripheral tissues. Meal timing in rodents, as well as in humans, resets the phase of hepatic lipogenesis and plasma leptin concentrations and exerts profound effects on peripheral clocks. The cellular redox status, represented by the nicotinamide adenine dinucleotide cofactors NAD(H) and NADP(H), regulate the transcriptional activity of CLOCK/BMAL1 and NPAS2/BMAL1 heterodimers. The reduced forms of these cofactors increase DNA binding, whereas the oxidized forms decrease binding, thus coupling activity of these core clock components with the metabolic state of the cell (28).

In vertebrates, a hierarchy of signals within SCN pacemaker neurons in the brain and downstream extra-SCN neurons generates entraining cues to maintain phase alignment between oscillators in multiple peripheral tissues. The synchronization of individual cellular clocks in peripheral organs is probably accomplished by immediate-early genes that interpret the cyclic systemic signals and convey this phase information to core clock components (29, 30). Oscillation in REV-ERB α ligands (heme, carbon monoxide) may affect not only the phase and amplitude of circadian rhythms, but also physiological outputs of the circadian system and REV-ERB α may participate in the entrainment of central and peripheral clocks. The circadian clock and heme biosynthesis are reciprocally regulated as the clock machinery controls heme biosynthesis through regulation of the rate-limiting enzyme aminolevulinate synthase 1 (*ALAS*1), and NPAS2 has a heme-binding motif. Heme controls activity of the BMAL1-NPAS2 transcription complex in vitro by inhibiting DNA binding in response to carbon monoxide and differentially modulates expression of *PER1* and *PER2* in vivo by a mechanism involving NPAS2 and PER2 (31-34).

In conclusion, the results of the two studies conducted in mice kept under different light/dark cycles highlight a possible role of *REV-ERB*α as a synchronizing hinge in the clock gene machinery and among different tissues under different environmental lighting conditions. The nuclear receptor REV-ERB α is part of the clock circuitry and plays an important role in keeping proper timing of the clock, linking the clock gene machinery to the metabolic pathways and might drive the circadian oscillators when the light cues are not operating.

## ACKNOWLEDGEMENTS

This work was supported by “Italian Ministry of Health” grant RC1203ME46 through Department of Medical Sciences, Division of Internal Medicine and Chronobiology Unit, IRCCS Scientific Institute and Regional General Hospital “Casa Sollievo della Sofferenza”, Opera di Padre Pio da Pietrelcina, San Giovanni Rotondo (FG), Italy.

## REFERENCES

1. Edery I. Circadian Rhythms In A Nutshell. Physiol Genomics 2000; 3:59-74.
2. Hastings MH, Reddy AB, Maywood ES. A clockwork web: circadian timing in brain and periphery, in health and disease. Nat Rev Neurosci 2003; 4:649-61.
3. Schibler U, Sassone-Corsi P. A web of circadian pacemakers. Cell 2002; 111:919–22.
4. Nagoshi E, Saini C, Bauer C, Laroche T, Naef F, Schibler U. Circadian gene expression in individual fibroblasts: cell-autonomous and self-sustained oscillators pass time to daughter cells. Cell 2004; 119 :693-705.
5. Filipski E, King VM, Etienne MC, Li XM, Claustrat B, Granda TG. Persistent twenty-four hour changes in liver and bone marrow despite suprachiasmatic nuclei ablation in mice. Am. J Physiol Regul Integr Comp Physiol 2004; 287:R844-51.
6. Eide EJ, Vielhaber EL, Hinz WA, Virshup DM.The

Circadian Regulatory Proteins BMAL1 and Cryptochromes Are Substrates of Casein Kinase Iε. J Biol Chem 2002; 277:17248-54.
7. Sahar S, Zocchi L, Kinoshita C, Borrelli E, Sassone-Corsi P. Regulation of BMAL1 protein stability and circadian function by GSK3beta-mediated phosphorylation. PLoS One 2010; 5(1):e8561.
8. Stokkan KA, Yamazaki S, Tei H, Sakaki Y, Menaker M. Entrainment of the circadian clock in the liver by feeding. Science 2001; 291:490-93.
9. Preitner N, Damiola F, Lopez-Molina L, Zakany J, Duboule D, Albrecht U, The orphan nuclear receptor REV-ERBalpha controls circadian transcription within the positive limb of the mammalian circadian oscillator. Cell 2002; 110:251-60.
10. Duez H, Staels B. Rev-erbα gives a time cue to metabolism. FEBS Letters 2008; 582:19-25.
11. Duez H, Staels B. Nuclear receptors linking circadian rhythms and cardiometabolic control. Arterioscler Thromb Vasc Biol 2010; 30(8):1529-34.
12. Burris TP. Nuclear hormone receptors for heme: REV-ERBalpha and REV-ERBbeta are ligand-regulated components of the mammalian clock. Mol Endocrinol 2008; 22(7):1509-20.
13. Raghuram S, Stayrook KR, Huang P, Rogers PM, Nosie AK, McClure DB, Burris LL, Khorasanizadeh S, Burris TP, Rastinejad F. Identification of heme as the ligand for the orphan nuclear receptors REV-ERBalpha and REV-ERBbeta. Nat Struct Mol Biol 2007; 14(12):1207-13.
14. Fontaine C, Staels B. The orphan nuclear receptor Rev-erbalpha: a transcriptional link between circadian rhythmicity and cardiometabolic disease. Curr Opin Lipidol 2007; 18(2):141-6.
15. Pardee KI, Xu X, Reinking J, Schuetz A, Dong A, Liu S, Zhang R, Tiefenbach J, Lajoie G, Plotnikov AN, Botchkarev A, Krause HM, Edwards A. The structural basis of gas-responsive transcription by the human nuclear hormone receptor REV-ERBbeta. PLoS Biol 2009; 7(2):e43.
16. Liu S, Cai Y, Sothern RB, Guan Y, Chan P. Chronobiological analysis of circadian patterns in transcription of seven key clock genes in six peripheral tissues in mice. Chronobiol Int 2007; 24(5):793-820.
17. Sothern RB, Yamamoto T, Cornélissen G, Takumi T, Halberg F. Central and peripheral circadian clock genes, their statistical analysis for rhythms, and relationship to health and disease Scripta Medica 2009; 82 (3):133-63.
18. Mojón A, Fernández JR, Hermida R. Chronolab: an interactive software package for chronobiologic time series analysis written for the Macintosh computer. Chronobiol Int 1992; 9(6):403-12.
19. Li S, Lin JD. Molecular control of circadian metabolic rhythms. J Appl Physiol 2009; 107(6):1959-64.
20. Panda S, Antoch MP, Miller BH, Su AI, Schook AB, Straume M, Schultz PG, Kay SA, Takahashi JS, Hogenesch JB. Coordinated transcription of key pathways in the mouse by the circadian clock. Cell 2002; 109(3):307-20.
21. Cailotto C, Lei J, van der Vliet J, van Heijningen C, van Eden CG, Kalsbeek A, Pévet P, Buijs RM. Effects of nocturnal light on (clock) gene expression in peripheral organs: a role for the autonomic innervation of the liver. PLoS One 2009; 4(5):e5650.
22. Albrecht U, Sun ZS, Eichele G, Lee CC. A differential response of two putative mammalian circadian regulators, mper1 and mper2, to light. Cell 1997; 91:1055-64.
23. Damiola F, Le Min HN, Preitner N, Kornmann B, Fleury-Olela F, Schibler U. Restricted feeding ncouples circadian oscillators in peripheral tissues from the central pacemaker in the suprachiasmatic nucleus. Genes Dev 2000; 14:2950-61.
24. Ishida A, Mutoh T, Ueyama T, Bando H, Masubuchi S, Nakahara D, Tsujimoto G, Okamura H: Light activates the adrenal gland: timing of gene expression and glucocorticoid release. Cell Metab 2005; 2:297-307.
25. Wu T, Jin Y, Ni Y, Zhang D, Kato H, Fu Z. Effects of light cues on re-entrainment of the food-dominated peripheral clocks in mammals. Gene 2008; 419:27-34.
26. Meng QJ, McMaster A, Beesley S, et al. Ligand modulation of REV-ERBalpha function resets the peripheral circadian clock in a phasic manner. J Cell Sci 2008; 121:3629-35.
27. Zhang J, Kaasik K, Blackburn MR, Lee CC. Constant darkness is a circadian metabolic signal in mammals. Nature 2006; 439(7074):340-3.
28. Maury E, Ramsey KM, Bass J. Circadian rhythms

and metabolic syndrome: from experimental genetics to human disease. Circ Res 2010; 106(3):447-62.
29. Kornmann B, Schaad O, Reinke H, Saini C, Schibler U. Regulation of circadian gene expression in liver by systemic signals and hepatocyte oscillators. Cold Spring Harb Symp Quant Biol 2007; 72:319-30.
30. Kaasik K, Lee CC. Reciprocal regulation of heme biosynthesis and the circadian clock in mammals. Nature 2004; 430(6998):467-71.
31. Duez H, Staels B. The nuclear receptors Rev-erbs and RORs integrate circadian rhythms and metabolism. Diab Vasc Dis Res 2008; 5(2):82-8.
32. Yin L, Wu N, Lazar MA. Nuclear receptor Rev-erb alpha: a heme receptor that coordinates circadian rhythm and metabolism. Nucl Recept Signal 2010; 8:e001.
33. Duez H, Staels B. Rev-erb-alpha: an integrator of circadian rhythms and metabolism. J Appl Physiol 2009; 107(6):1972-80.
34. Teboul M, Gréchez-Cassiau A, Guillaumond F, Delaunay F. How nuclear receptors tell time. J Appl Physiol 2009; 107(6):1965-71.

# ANALYSIS OF GENE EXPRESSION IN PENICILLIN G INDUCED PERSISTENCE OF *CHLAMYDIA PNEUMONIAE*

M. DI PIETRO[1], A. TRAMONTI[2], F. DE SANTIS[1], D. DE BIASE[3], G. SCHIAVONI[1], S. FILARDO[1], C. ZAGAGLIA[1] and R. SESSA[1]

*[1]Department of Public Health and Infectious Diseases, "Sapienza" University, Rome, Italy; [2]Institute of Molecular Biology and Pathology, CNR, c/o Department of Biochemical Sciences "A. Rossi Fanelli", "Sapienza" University, Rome, Italy; [3]Department of Medico-Surgical Sciences and Biotechnologies, "Sapienza" University, Latina, Italy*

*Received October 12, 2011 – Accepted December 15, 2011*

***Chlamydia pneumoniae* is responsible for respiratory tract infections and has been associated to chronic diseases such as atherosclerosis. The involvement of *C. pneumoniae* in chronic diseases may be correlated to its ability to induce persistent forms in which *Chlamydiae* remain viable but are not cultivable. The aim of our study is to investigate *C. pneumoniae* specific gene activities associated with the development of Chlamydial persistence in a cell culture system in the presence of penicillin G. Chlamydia-infected HEp-2 cells were incubated with or without penicillin G for up to 72 hours. The relative mRNA expression levels of early and late genes in treated and untreated cell cultures were determined by Real-time RT-PCR. Our results revealed a consistent down-regulation of Chlamydial *hctA* and *hctB* genes (p=0.012 and p=0.003 respectively) in association with up-regulation of *htrA* gene (p=0.002) during penicillin G-induced persistence suggesting these gene sets as leading candidate for *in vivo* investigation of the development of persistent Chlamydial infection. In conclusion, the Chlamydial expression pattern of *hctA*, *hctB,* and *htrA* genes may be helpful to identify target molecules to diagnose and treat Chlamydia-associated chronic diseases.**

*Chlamydia pneumoniae* is responsible for upper and lower respiratory tract infections such as pharyngitis and pneumonia (1). Over the last decade, several reports in the literature have suggested that *C. pneumoniae* infection may contribute to the pathogenesis of chronic diseases such as atherosclerosis, Alzheimer's disease and multiple sclerosis (2-5). *C. pneumoniae* is an obligate intracellular pathogen with a unique biphasic developmental cycle. During the developmental cycle, *Chlamydiae* alternate between infectious, elementary bodies (EB) that have been considered metabolically inactive, and noninfectious, metabolically active reticulate bodies (RB).

The involvement of *C. pneumoniae* in chronic diseases may be correlated to characteristic features of this pathogen including the ability to induce persistent forms, in which *Chlamydiae* remain viable but are not cultivable (6, 7) and are remarkably characterized by an enlarged aberrant shape (6,7). *C. pneumoniae* persistent forms are inherently more suited to evade the host immune response and are difficult to eradicate with antibiotics (8).

The persistent forms can rise under stressful

*Key words: C. pneumoniae, persistent infection, penicillin, Real-time PCR*

*Mailing address:* Prof.ssa Rosa Sessa,
Department of Public Health and Infectious Diseases,
"Sapienza" University, P.le Aldo Moro 5,
00185 Rome, Italy
Tel.: +39 0649914102
Fax: +39 0649914634
e-mail: rosa.sessa@uniroma1.it



0393-974X (2012)

growth conditions, imposed by immunological responses, antibiotics or nutrient deprivation (6). In particular, exposure to IFN-γ or antibiotics as well as iron-depletion are conditions that occur frequently *in vivo*. For example, low levels of IFN-γ may evoke the persistence of *C. pneumoniae* since it is well known that anti-chlamydial immune response strongly depends on the production of IFN-γ (9). Likewise, limitation of iron, an essential element for replication of *C. pneumoniae* in host cells, may convert them into so-called persistent forms (10). Lastly, antibiotic-induced persistence is particularly important since persistent *C. pneumoniae* infection could occur as result of widespread use of antimicrobial agents. Inadequate doses or duration of therapy may result in incomplete clearance of the microrganism, with inhibition of chlamydial growth, allowing for subsequent relapse; hence, an unsuitable antimicrobial therapy may allow *Chlamydiae* to persist *in vivo* leading to development of chronic diseases (11, 12).

Considering the significant implication of the persistent infection in the pathogenesis of chronic diseases, several *in vitro* models of persistence have been developed to better investigate the cellular and molecular mechanisms that occur in the development cycle of *C. pneumoniae*.

Characteristic features of persistence models are the reduction of infectious chlamydial progeny due to a lack of conversion of RB to EB and the distinct transcriptional profile of *C. pneumoniae* (6, 7).

To date IFN-γ-induction and iron depletion models of *C. pneumoniae* persistence (13-21) have been well characterized than antibiotic-induced persistence (20,22). Therefore, the aim of our study was to investigate *C. pneumoniae* specific gene activities associated with the development of persistence in a cell culture system in presence of antibiotic; the investigation was carried out into the state of persistence of *C. pneumoniae* AR-39, established in HEp-2 cells in the presence of penicillin G.

## MATERIALS AND METHODS

*Cell culture and growth of C. pneumoniae*

*C. pneumoniae* AR-39 (ATCC 53592) was propagated in HEp-2 cells (ATCC CCL 23) grown in Dulbecco's Modified Eagle's Medium (DMEM) with 4.5 g/l glucose supplemented with 10% heat-inactivated fetal calf serum (FCS). *C. pneumoniae*-infected HEp-2 cells were centrifuged at 900 x g for 60 min at 37°C. The supernatant was removed and replaced with DMEM containing 4.5 g/l glucose and supplemented with 10% FCS, 1 mM HEPES and 2 µg cycloheximide/ml. Infected cultures were incubated for 72 h at 37°C in a 5% $CO_2$ atmosphere. *C. pneumoniae* elementary bodies were harvested by scraping off cultured cells with a cell scraper and then by vortexing the mixture with sterile glass beads for 2 min. Host cell nuclei and debris were separated from EBs by centrifugation at 500 x g for 10 min at 4°C. Harvested EBs were stored in aliquots in sucrose-phosphate-glutamate buffer (SPG; 0.2 M sucrose, 3.8 mM $KH_2PO_4$, 6.7 mM $Na_2HPO_4$, 5.5 mM glutamic acid at pH 7.4) at -70 C until use.

*Induction of persistence*

Confluent HEp-2 monolayers ($10^6$ cells) grown in 24-well culture plates were infected with *C. pneumoniae* at a multiplicity of infection (MOI) of 30 and centrifuged at 900 x g at 37 °C for 1 h. The inoculum was then aspired and fresh supplemented DMEM with or without penicillin G at a final concentration of 500 U/ml was added to each well. Infected and treated HEp-2 monolayers were incubated at 37 °C in a 5% $CO_2$ atmosphere and were maintained for up to 72 h.

*Assay for infectivity*

To analyze the production of infectious chlamydial progeny in cell cultures, cell preparations harvested at given time points, were sonicated and passaged onto fresh HEp-2 cells grown on glass coverslip in 24-well plates. The plates were centrifuged at 900 g for 1 h at 37°C, the inoculum was removed and the cells were fed with fresh DMEM medium supplemented with 2% FCS and 2 µg cycloheximide/ml. The plates were incubated for 72 h at 37°C in a 5% $CO_2$ atmosphere. After incubation, the cells were fixed with methanol for 10 min and stained with FITC-conjugated monoclonal antibody against chlamydial LPS (Pathfinder Chlamydia Culture Confirmation System, Bio-Rad). The total number of Inclusion Forming Unit (IFU) was enumerated by counting twenty microscope fields using a fluorescence microscope (100X magnification).

*Assay for measurement of chlamydial genomic DNA*

Total genomic DNA was isolated from *C. pneumoniae*-infected HEp-2 cells, in presence and in absence of penicillin G, using a QIAamp DNeasy Tissue kit according to the manufacturer's instructions. DNA was eluted in a final volume of 100 µl and stored at -20°C. Quantification of *C. pneumoniae* DNA was performed by real-time PCR

assay, as previously described (23). Briefly, real-time PCR assay was based on FRET hybridization probes and LightCycler instrument (Roche). PCR primers and probes target an internal 128 bp region of *C. pneumoniae PstI* species-specific fragment.

*Expression levels analysis by real-time PCR*

Total RNA was extracted from *C. pneumoniae*-infected HEp-2 cells, in presence and in absence of penicillin G, using the High Pure RNA Isolation Kit (Roche) including DNase I treatment, according to the manufacturer's instructions. The absence of bacterial DNA was confirmed by real-time PCR specific for *C. pneumoniae PstI* species-specific fragment.

The quantity and quality of total RNA were determined using gel agarose electrophoresis and UV spectrophotometry ($O.D._{260}$ and the 260 nm / 280 nm ratio). Aliquots of 10 µg of total RNA were denatured at 65°C for 15 min in presence of 2 M formaldehyde and 50% formamide and electrophoresed for 2.5 h at 4 V/cm on a 1.2% agarose gel containing 2 M formaldehyde in BES buffer (25 mM BES at pH 7.0, 15 mM sodium acetate, 0.5 mM EDTA).

Measurement of mRNA expression levels using quantitative reversion transcription PCR (RT-qPCR) was performed in two steps. First, 0.5 µg of total RNA were reverse transcribed into cDNA using random hexamer primers and the iScript Select cDNA Synthesis Kit (Bio-Rad) following the manufacturer's instructions. Two different reverse transcription reactions were carried out for each RNA. Then, RT-qPCR reactions were performed on the Chromo4 instrument (Bio-Rad) using the FastStart SYBR Green Master kit (Roche). Cycling parameters for all reactions were as follows: denaturation at 95°C for 10 min; 40 cycles of denaturation at 95°C for 15 sec, annealing and extension at 60°C for 20 sec. The quality of amplicons was evaluated with the melting curve analysis from 65°C to 95° C. The relative gene expression ratio of a target gene was calculated as described by Pfaffl (24) using the rRNA 16S gene as normalizer.

PCR primers (Table I) were designed from the complete genome sequence of *C. pneumoniae* AR-39 (http://www.ncbi.nlm.nih.gov Refseq NC_002179 GeneBank AE002161) and checked for homology to the human genome using BLAST algorithm to achieve a high probability for *C. pneumoniae*-specific products. All RT-qPCR assays were performed in triplicate for each target gene.

*Statistical analysis*

Results were expressed as mean ± standard deviation (SD) of three independent experiments performed in triplicate. Statistical significance of differences was analyzed by Student's *t* test. Values of $p \leq 005$ were considered statistically significant.

## RESULTS

In order to establish the time period of exposure to penicillin G that resulted in a state of persistence of *C. pneumoniae*, we initially determined the temporal kinetics of *C. pneumoniae* persistence. Chlamydia-infected HEp-2 cells were incubated with or without penicillin G for 24, 48 and 72 hours. The assay for infectivity and the measurement of Chlamydial genomic DNA were carried out for each time point.

The number of infectious Chlamydial EB and the relative levels of accumulation of *C. pneumoniae* chromosomal DNA in penicillin G treated and untreated HEp-2 cells are shown in Fig.1.

At 24 h and 48 h post-infection the number of infectious chlamydial EB as well as the number of chlamydial genomic copies remained unaltered in penicillin G- treated cell cultures when compared to untreated cells. In contrast, at 72 h post infection, penicillin G significantly reduced both the number

**Table I.** *Sequences of primers used in RT-qPCR.*

| Gene | Forward (5'-3') | Reverse (5'-3') | Amplicon (bp) |
|---|---|---|---|
| *ompA* | GGGAGCTGAATTCCAATATGCACAGTCC | TAGGTAGTTTTGGCTGAGCAATGCGG | 305 |
| *groEL* | CTTGCAGAAGCAATCTATAGCGAAGGTC | GAGGTATCCACGGTTGAAGTTCATTCC | 318 |
| *hctA* | ACTTAGCTAAAGCAGAGAAAGGAAACAAGGC | TTATTTTCTAAATCCGCGTGCTTTGGAAGG | 314 |
| *hctB* | GTAAGACGGCTGCTAAAAAGACAGTAGC | GAGCCATGCTTTCTCGTAGCTGTTGAAG | 316 |
| *htrA* | CCTATAGATGCGGAACTCGCTGCTTG | GAGCCATGCTTTCTCGTAGCTGTTGAAG | 316 |
| *rRNA 16S* | GCCGTAAACGATGCATACTTGATGTGG | CCTAAGTGCTGGCAACTAACGATAAGGG | 331 |

**Table II.** *Expression levels at 72 hours post-infection.*

| Gene | Penicillin G | Untreated | P-value |
|---|---|---|---|
| *ompA* | 1.00±0.00 | 1.80±0.41 | 0.029 |
| *groEL* | 1.31±0.32 | 1.11±0.21 | 0.469 |
| *hctA* | 1.01±0.02 | 1.91±0.56 | 0.012 |
| *hctB* | 1.00±0.00 | 3.52±1.59 | 0.003 |
| *htrA* | 1.90±0.29 | 1.00±0.00 | 0.002 |

of infectious chlamydial EB and the number of chlamydial genomic copies ($p = 0.04$ and $p = 0.015$ respectively).

The reduced number of infectious chlamydial EB observed at 72 h demonstrated the development of *C. pneumoniae* persistence induced by penicillin G. Consequently, the 72 h penicillin G treatment period was chosen to study the effect of the antibiotic on the expression of specific chlamydial genes during persistent infection. The relative mRNA expression levels of *ompA*, *groEL*, *hctA*, *hctB*, and *htrA* genes in penicillin G treated and in untreated cell cultures are shown in Table II.

Real-time PCR results revealed that penicillin G treatment had no effect on chlamydial *groEL* expression when compared to untreated cell cultures while induced a modest down-regulation of the *ompA* gene ($p=0.029$). Similarly, chlamydial *hctA* expression was down-regulated during penicillin G-induced persistence ($p=0.012$). A more significant decrease in the expression was observed for the *hctB* gene relative to the control ($p = 0.003$). Conversely *htrA* gene was found to be up-regulated ($p= 0.002$) (Fig. 2).

## DISCUSSION

Persistence is the hallmark of chlamydial infection and is particularly important since it offers a link between *C. pneumoniae* and chronic diseases including atherosclerosis (5, 6). Indeed, the persistence has been suggested as a mechanism that leads to the inflammatory response, contributing to pathological changes such as atherosclerotic plaque observed in patients with cardiovascular diseases (5).

Genome-wide analyses as well as studies targeting transcriptional activity of selected genes of *C. pneumoniae* have increased our knowledge of molecular changes that occur in the development cycle of this bacterium during persistent infection (6, 13, 15-21). However, the mechanisms that evoke and maintain the persistence of *C. pneumoniae in vivo* remain elusive and understanding of these different mechanisms will open up new therapeutic avenues that could be employed against chronic diseases associated with this pathogen.

In the present study, the state of *C. pneumoniae* persistence in HEp-2 cells induced by penicillin G (500U/ml) was characterized by a decrease in both infectious chlamydial progeny and the number of chlamydial genomic copies. This latter observation strongly suggests that high concentrations of penicillin G inhibit chlamydial genome replication. On the contrary, it was observed that low concentrations of penicillin G unaffected chlamydial genome replication (25). The same trend was observed when *C. pneumoniae* was exposed to low and high doses of IFN- γ (13, 16).

We used an RT-qPCR approach to analyze the transcription of two early genes (*ompA*, *groEL*) and three late genes (*hctA*, *hctB, htrA*) of *C. pneumoniae*. *OmpA* and *groEL* genes are well known to encode for chlamydial major outer membrane protein (MOMP) and heat shock protein 60 (HSP60) respectively. *HctA* and *hctB* genes encode for proteins (Hc-1 and Hc-2 DNA-binding proteins) involved in DNA condensation required for RB to EB differentiation. Lastly, *htrA* gene encodes for a predicted serine protease which is responsible for the proteolysis of damaged or misfolded proteins often in response to external stimuli (6, 26).

Regarding the chlamydial *ompA* and *groEL* genes, we observed a down-regulation of *ompA* gene and stable expression of *groEL* gene in response to penicillin G. The expression of *ompA* and *groEL* genes has been extensively studied in various models of persistent chlamydial infection without a uniform outcome. Indeed both up-regulation and down-regulation as well as a stable expression of chlamydial *ompA* and *groEL* genes have been reported in persistent infection models (6, 18-21, 27-29).

Our study is the first investigating the expression of *hctA* gene of *C. pneumoniae* and to demonstrate

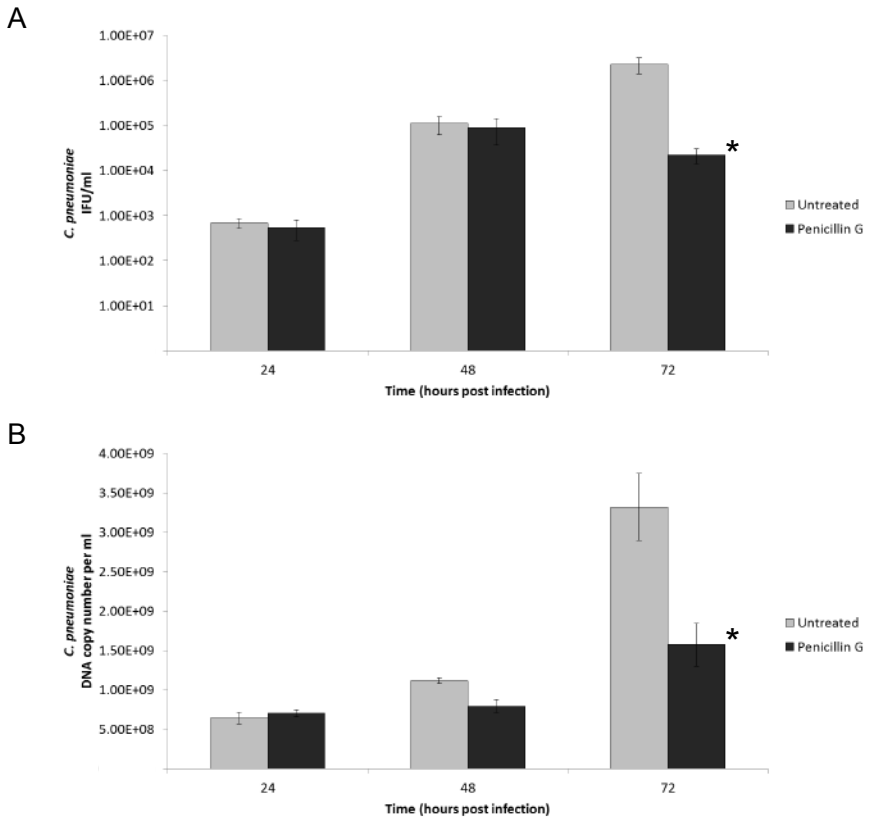


**Fig. 1.** *Effect of penicillin G on the production of infectious chlamydial EB (**A**) and accumulation of chlamydial DNA (**B**) in HEp-2 infected with C. pneumoniae. HEp-2 cells were infected with C. pneumoniae (MOI= 30) and treated with penicillin G (500 U/ ml) for 24, 48 and 72 h. Treated and untreated infected cells were harvested at indicated time intervals and the number of infectious EB as well as C. pneumoniae DNA were assessed as described in Material and Methods. Experiments were performed in triplicate. Data are expressed as means ± standard deviation. *p<0.05 vs untreated HEp-2 cultures*

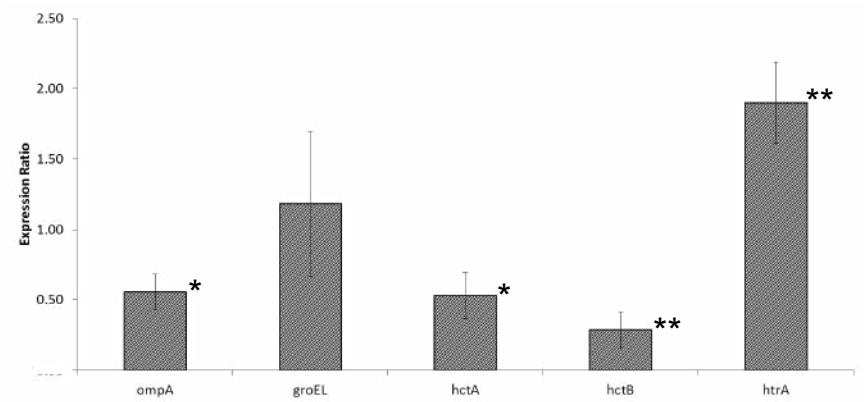


**Fig. 2.** *mRNA expression levels of selected genes of C. pneumoniae determined by RT-qPCR, at 72 hours post infection, in cell monolayers treated with penicillin G compared to untreated cells. The relative expression ratios were normalized with the rRNA 16S gene and the results are shown as treated / untreated ratio. * p < 0.05 vs untreated cell monolayers; ** p < 0.01 vs untreated cell monolayers.*

its down-regulation in a persistence model. A similar finding has also been observed in *C. trachomatis* during IFN-γ-induced persistence (30, 31) and in *C. psittaci* in penicillin G, IFN-γ and iron limitation models (32).

Regarding the chlamydial *hctB* and *htrA* genes, there are no studies on *C. pneumoniae* persistence induced by penicillin G. The observed low mRNA expression level of *hctB* gene is in agreement with findings on *C. pneumoniae* in IFN-γ and iron depletion models (19, 21) and on *C. trachomatis* when exposed to penicillin G and IFN-γ (28, 30). The up-regulation of *htrA* transcription, observed in our study, has also been reported in *C. pneumoniae* during IFN-γ–induced and iron depletion persistence (17-19,21) as well as in *C. trachomatis* when exposed to penicillin G and IFN-γ (26).

Importantly, our results suggest that leading candidate gene sets for *in vivo* investigation of the development of persistent chlamydial infection may be *hctA* and *hctB*, which are down-regulated in association with up-regulation of *htrA* gene.

In conclusion, the Chlamydial expression pattern of *hctA*, *htrA*, and *hctB* genes may be helpful to identify target molecules to diagnose and treat Chlamydia-associated chronic diseases.

## ACKNOWLEDGEMENTS

Part of this study was supported by grants from Center for Social Disease Research, "Sapienza" University" Rome, to R. Sessa.

## REFERENCES

1. Saikku P. The epidemiology and significance of *Chlamydia pneumoniae*. J Infect 1992; 25(S): 27-34.
2. Di Pietro M, Schiavoni G, del Piano M, et al. *Chlamydia pneumoniae* and atherosclerosis: the role of mast cells. J Biol Regul Homeost Agents 2009; 23(2):65-9.
3. Sessa R, Nicoletti M, Di Pietro M, Schiavoni G, Santino I, Zagaglia C, del Piano M, Cipriani P. *Chlamydia pneumoniae* and atherosclerosis: current state and future prospective. Int J Immunopathol Pharmacol 2009; 22(1):9-14.
4. Hammond CJ, Hallock LR, Howanski RJ, Appelt DM, Little CS, Balin BJ. Immunohistological detection of *Chlamydia pneumoniae* in the Alzheimer's disease brain. BMC Neurosci 2010; 11:121.
5. Fainardi E, Castellazzi M, Tamborino C, Seraceni S, Tola MR, Granieri E, Contini C. *Chlamydia pneumoniae*-specific intrathecal oligoclonal antibody response is predominantly detected in a subset of multiple sclerosis patients with progressive forms. J Neurovirol 2009; 15(5-6):425-33.
6. Hogan RJ, Mathews SA, Mukhopadhyay S, Summersgill JT, Timms P. Chlamydial persistence: beyond the Biphasic Paradigm. Infect Immun 2004; 72(4):1843-55.
7. Schoborg RV. Chlamydia persistence -- a tool to dissect chlamydia--host interactions. Microbes Infect 2011; 13(7):649-62.
8. Gieffers J, Füllgraf H, Jahn J, Klinger M, Dalhoff K, Katus HA, Solbach W, Maass M. *Chlamydia pneumoniae* infection in circulating human monocytes is refractory to antibiotic treatment. Circulation 2001; 103(3):351-6.
9. Brunham RC, Rey-Ladino J. Immunology of Chlamydia infection: implications for a *Chlamydia trachomatis* vaccine. Nat Rev Immunol 2005; 5:149-61.
10. Raulston JE. Response of *Chlamydia trachomatis* serovar E to iron restriction in vitro and evidence for iron-regulated chlamydial proteins. Infect Immun 1997; 65:4539-47.
11. Beatty WL, Morrison RP, Byrne GI. Persistent *Chlamydiae:* from cell culture to a paradigm for chlamydial pathogenesis. Microbiol Rev 1994; 58(4):686-99.
12. Kutlin A, Roblin PM, Hammerschlag MR. Effect of prolonged treatment with azithromycin, clarithromycin, or levofloxacin on *Chlamydia pneumoniae* in a continuous-infection model. Antimicrob Agents Chemother 2002; 46:409-12.
13. Byrne GI, Ouellette SP, Wang Z, Rao JP, Lu L, Beatty WL, Hudson AP. *Chlamydia pneumoniae* expresses genes required for DNA replication but not cytokinesis during persistent infection of HEp-2 cells. Infect Immun 2001; 69(9):5423-9
14. Pantoja LG, Miller RD, Ramirez JA, Molestina RE, Summersgill JT. Characterization of *Chlamydia pneumoniae* persistence in HEp-2 cells treated with gamma interferon. Infect Immun 2001; 69(12):7927-

32.
15. Molestina RE, Klein JB, Miller RD, Pierce WH, Ramirez JA, Summersgill JT. Proteomic analysis of differentially expressed *Chlamydia pneumoniae* genes during persistent infection of HEp-2 cells. Infect Immun 2002; 70(6):2976-81.
16. Mannonen L, Kamping E, Penttilä T, Puolakkainen M. IFN-gamma induced persistent *Chlamydia pneumoniae* infection in HL and Mono Mac 6 cells: characterization by real-time quantitative PCR and culture. Microb Pathog 2004; 36(1):41-50.
17. Mukhopadhyay S, Miller RD, Sullivan ED, Theodoropoulos C, Mathews SA, Timms P, Summersgill JT. Protein expression profiles of *Chlamydia pneumoniae* in models of persistence versus those of heat shock stress response. Infect Immun 2006; 74(7):3853-63.
18. Polkinghorne A, Hogan RJ, Vaughan L, Summersgill JT, Timms P. Differential expression of chlamydial signal transduction genes in normal interferon gamma-induced persistent *Chlamydophila pneumoniae* infections. Microbes Infect 2006; 8(1):61-72.
19. Mäurer AP, Mehlitz A, Mollenkopf HJ, Meyer TF. Gene Expression Profiles of *Chlamydophila pneumoniae* during the Developmental cycle and Iron Depletion-Mediated Persistence. PLoS Pathog 2007; 3(6):e83.
20. Klos A, Thalmann J, Peters J, Gérard HC, Hudson AP. The transcript profile of persistent *Chlamydophila (Chlamydia) pneumoniae* in vitro depends on the means by which persistence is induced. FEMS Microbiol Lett 2009; 291(1):120-26.
21. Timms P, Good D, Wan C, Theodoropoulos C, Mukhopadhyay S, Summersgill J, Mathews S. Differential transcriptional responses between the interferon-gamma-induction and iron-limitation models of persistence for *Chlamydia pneumoniae*. J Microbiol Immunol Infect 2009; 42(1):27-37.
22. Gieffers J, Rupp J, Gebert A, Solbach W, Klinger M. First-Choice antibiotics at subinhibitory concentrations induce persistence of *Chlamydia pneumoniae*. Antimicrob Agents Chemother 2004; 48(4):1402-5.
23. Schiavoni G, Di Pietro M, Ronco C, et al. *Chlamydia pneumoniae* infection as a risk factor for accelerated atherosclerosis in hemodialysis patients. J Biol Regul Homeost Agents 2010; 24(3):367-75.
24. Pfaffl MW. A new mathematical model for relative quantification in real-time RT-PCR. Nucleic Acids Res 2001; 29:2002-7.
25. Lamden PR, Pickett MA, Clarke IN. The effect of penicillin on *Chlamydia trachomatis* DNA replication. Microbiology 2006; 152:2573-8.
26. Huston WM, Theodoropoulos C, Mathews SA, Timms P. *Chlamydia trachomatis* responds to heat shock, penicillin induced persistence, and IFN-gamma persistence by altering levels of the extracytoplasmic stress response protease HtrA. BMC Microbiol 2008; 8:190.
27. Mathews S, George C, Flegg C, Stenzel D, Timms P. Differential expression of ompA, ompB, pyk, nlpD and Cpn0585 genes between normal and interferon–γ treated cultures of *Chlamydia pneumoniae*. Microb Pathog 2001; 30:337-45.
28. Nicholson T, Stephens RS. Chlamydial genomic transcriptional profile for penicillin-induced persistence, p. 611-614. In: Chlamydial infections. J. Schachter, G. Christiansen, I. N. Clarke, M. R. Hammerschlag, B. Kaltenboeck, C.-C. Kuo, R. G. Rank, G. L. Ridgway, P. Saikku, W. E. Stamm, R. S. Stephens, J. T. Summersgill, P. Timms, and P. B. Wyrick (ed.), Proceedings of the Tenth International Symposium on Human Chlamydial Infections. International Chlamydia Symposium, San Francisco, Calif., USA, 2002.
29. Oullette SP, Hatch TP, AbdelRahman YM, Rose LA, Belland R, Byrne G. Global transcriptional upregulation in the absence of increased translation in Chlamydia during IFN- γ-mediated host cell tryptophan strarvation. Mol Microbiol 2006; 62:1387-401.
30. Jones LM, Gaston JSH, Pearce JH. Induction of abnormal *Chlamydia trachomatis* by exposure to interferon–γ or amino acid deprivation and comparative antigenic analysis. Microb Pathog 2001; 30:299-309.
31. Belland RJ, Nelson DE, Virok D, Crane DD, Hogan D, Sturdevant D, Beatty WL, Caldwell HD. Transcriptome analysis of chlamydial growth during IFN-gamma-mediated persistence and reactivation. Proc Natl Acad Sci USA 2003; 100(26):15971-6.
32. Goellner S, Schubert E, Liebler-Tenorio E, Hotzel

H, Saluz HP, Sachse K. Transcriptional Response Patterns of *Chlamydophila psittaci* in different in vitro models of persistent infection. Infect Immun 2006; 74(8):4801-8.

# IS THERE A POTENTIAL APPLICATION OF A FERMENTED NUTRACEUTICAL IN ACUTE RESPIRATORY ILLNESSES? AN *IN-VIVO* PLACEBO-CONTROLLED, CROSS-OVER CLINICAL STUDY IN DIFFERENT AGE GROUPS OF HEALTHY SUBJECTS

F. MAROTTA[1], Y. NAITO[2], S. JAIN[3], A. LORENZETTI[1], V. SORESI[1], A. KUMARI[4], P. CARRERA BASTOS[5], C. TOMELLA[1] and H. YADAV[3]

*[1]ReGenera Research Group for Aging Intervention, Milan, Italy; [2]Immunology Research Institute and Clinic, Nagoya, Japan; [3]NIDDK, National Institute of Health, Bethesda, USA; [4]Université du Québec, Institut National de la Recherche Scientifique, Centre Eau, Terre and Environnement, Québec, Canada; [5]Center for Primary Health Care Research, Faculty of Medicine at Lund University Malmö, Sweden*

*Received January 23, 2011 – Accepted February 28, 2012*

**The role of oxidants in viral diseases is fairly complex because it includes metabolic regulation both of host metabolism and viral replication. However, a role for reactive oxygen species (ROS) and reactive nitrogen species (RNS) as mediators of virus-induced lung damage is supported by studies and antioxidants can thus be expected to act at many different levels. The aim of the present pilot study was to test an antioxidant nutraceutical approach on some relevant immunological parameters known to be affected in common seasonal respiratory tract infection. The study population consisted of 90 sedentary healthy patients, previously selected as being GSTM1-positive, divided into three groups: A) 20-40 years; B) 41-65 years; B) over 65 years. Each patients was administered a life style and dietary questionnaire. Subjects were supplemented for 6 weeks with either 9g/day (4.5g twice a day sublingually) of a fermented papaya preparation (Osato Research Institute, Gifu, Japan) or placebo. After a further month period of wash out, subjects were treated again in a crossover manner. Parameters checked were as follows: routine blood tests with WBC formula, saliva flow rate and secretary IgA and lysozyme production and redox gene expression of Phase II enzyme and SOD from upper airways cells (from nasal lavage). Salivary secretion rate showed an age-related decline and was significantly increased by FPP supplementation only in the youngest age-group ($p<0.05$). Subjects treated with FPP showed a significantly higher lever of IgA and lisozyme production., irrespective of age group while their baseline production was significantly lower in the oldest age-group as compared to the youngest one (C vs A, $p<0.05$). FPP treatment brought about a significant upregulation of all phase II enzyme and SOD gene expression tested in nasal lavage cells. In conclusion, FPP supplementation during 1 month resulted in higher salivary IgA and increase in phase II and SOD enzyme expression, i.e the most important antioxidant in the respiratory tract. The biological significance of these effects i.e., whether it will help reducing the whole respiratory oxidative stress in the human airway and, hopefully, the incidence and/or severity of URTI remains to be demonstrated in longer clinical trials.**

Influenza and flu-like syndromes represent a ubiquitous worldwide health issue causing

*Key words: fermented papaya preparation, epigenomic modification, nasal lavage*

*Mailing address:*
Prof. F. Marotta, MD, PhD
Piazza Firenze, 12
20154 Milano, Italy
Fax +390233004713
e-mail: fmarchimede@libero.it



0393-974X (2012)

remarkable morbidity and, in some cases, mortality, particularly when affecting infants, elderly people, and frail persons with respiratory and chronic cardiovascular diseases (1). Vaccines can provide only partial benefit in the control of influenza epidemics due also to the constant and abrupt change of the antigenic surface proteins of the virus (2) and thus the available options for the prevention and treatment of this condition have still considerable limitations. On the other hand, some antiviral molecules are not active against influenza B viruses, while their clinical utility is limited by significant adverse side effects and the rapid emergence of resistant strains in the clinical setting (3). Moreover, the usefulness of vaccines in the long-term facilities has been reported to be modest (4). To date, there are only scanty reports in the literature on the efficacy of different therapeutic approaches such as antioxidants during influenza virus infection. Oda et al. (5) documented that administration of pyran polymer conjugated superoxide dismutase protected mice against potentially lethal doses of influenza virus. Indeed, while the role of a proper antioxidant-rich dietary recommendation remains undisputed (6). old home remedies have been found to have a therapeutic rationale *in vitro* (7). Indeed, the role that extracellular ROS and RNS play in the pathogenesis of influenza-induced acute lung injury is not fully unfolded as yet. As a matter of fact, lungs have several potential cellular sources of ROS (8) and an upregulation of xanthine oxidase may contribute to enhanced oxidative stress after viral disease. Indeed, elevated levels of xanthine oxidase, together with increased GSSG and malonildealdehyde have been demonstrated in mouse lung homogenates and BALF after influenza infection (9). One of the crucial defences against oxidative stress is represented by the redox cycling of glutathione. Hennet et al. (10) have shown that murine influenza infection brings about a decrease in total glutathione and in vitamins C and E. This is likely to be due to the development of GSH adducts and S-nitrosylation, as shown by the elevated NO-reactive molecules and nitrotyrosine formation during infection.

The recognized importance of ROS in respiratory inflammation has generated recent interest in therapeutic measures to prevent or reduce ROS-related phenomena. As current standard treatment may not specifically address this issue, additional therapies protecting against ROS may represent a significant step in reducing the morbidity of respiratory disease. These findings have been paralleled by a number of studies tackling the issue of natural approaches to treat acute respiratory seasonal syndromes (11-13). Although the matter is still debated due to the sample limitation, safety issues and great dispersion of data (14), there is a general call to approach the issue under a wider therapeutic perspective (15). A number of studies have demonstrated that a fermented papaya preparations is able to exert a significant protective antioxidant properties despite being devoid of any antioxidant vitamin as such (16, 17). The aim of the present pilot study was to test this compound on some key point immunological parameters known to be affected in common seasonal respiratory tract infection so to provide a scientific rationale for a longer observational study in clinics. In particular, our current investigation intended to explore a strategy to enhance a relevant endogenous cytoprotective response planned to prevent cellular damage from ROS.

## MATERIALS AND METHODS

*GSTM-1 genotype analysis*

PCR analysis was performed in 25 μL reaction buffer containing 0.5mmol/L of dNTPs, 2.0mmol/L of $MgCl_2$, 12.5 pmol of each primer, about 150 ngDNA, and 1.25U of thermostable Taq DNA polymerase, using a programmable thermocycler. The primers used for GSTM1 were 5'-GAACTCCCTGAAAAGCTAAGC and 5'-GTTGGGGCTCAAATATACGGT GG. The PCR protocol included an initial melting temperature set at 94°C for a 5-min period followed by 35 cycles of amplification (with the apparatus set as follows: 2 min at 94°C, 1 min at 59°C, and extension for 1 min at 72°C). A final 10-min extension step processed at 72°C terminated the process. The final PCR product from co-amplification of GSTM1 (215 bp) was visualized on an ethidium bromide-stained 2.0% agarose gel. GSTM-1 genotype frequency was consistent with the expectations for the Hardy–Weinberg equilibrium (data not shown). The genotype of DNA samples was identified blindly and controls were equipped and set up in association with every single PCR operation as blank control (without DNA template), positive control, and negative control. Subjects who were found to be homozygous for *GSTM1 null* were excluded from analysis of GSTM1 expression.

*Study group*

The study population consisted of 90 sedentary, non-smoker patients without infectious or viral disease, steroid or immunosuppressive therapy, major debilitating diseases and prior or ongoing cancer. Common illnesses such as hypertension, compensated uncomplicated diabetes, dislipidemia did not constitute exclusion from recruitment. The use of inhaled, topical, or systemic corticosteroids or any other immune modulating medications was forbidden during the study period. Patients were divided into three groups, of 30 subjects each, based on different age: A) 20-40 years; B) 41-65 years; B) over 65 years. Each patients was administered a detailed life style questionnaire together with the web-based version of the National Institutes of Health Diet History Questionnaire (food frequency questionnaire consisting of 124 food items that includes both portion sizes and dietary supplement questions) to assess diet history over the past month and along the study period. Data indicate that this instrument provides reasonable nutrient estimates and sufficient reliability and validity (18). Patients were advised not to use any multivitamin supplement or fortified food while maintaining their usual diet.

Subjects were supplemented for 1 month with either 9g/day (4.5g twice a day sublingually) of a certified fermented papaya preparation (Osato Research Institute, Gifu, Japan) made under ISO 9001 (production quality), ISO 14001 (environmental protection) and ISO 22000 (food safety) from a patented biofermentation process of non-GMO charged papaya or placebo (same amount of flavoured sugar finely ground). After a further 6-weeks period of wash out, subjects were treated again in a cross-over manner.

*Parameters*

Routine blood tests with WBC formula**,** saliva flow rate and secretory IgA and lysozyme production and redox gene expression from upper airways cells (from nasal lavage).

*Saliva collection and analysis*

Subjects were instructed not to eat, use gum, candy, breath mints, tobacco or drink anything except water for one hour before collection appointments and to remove any lipstick or lip-aid. After an initial swallow to empty the mouth, unstimulated whole saliva was collected by expectoration into a pre-weighed vial (7 ml capacity plastic tubes with screw top) for 2 min with eyes open, head tilted slightly forward and making minimal orofacial movement. All saliva samples were stored frozen in capped test tubes at -20°C for later analysis. Detection of IgA in saliva was performed by sandwich ELISA. In these assays, polystyrene Maxisorb F96 microtitre plates (NUNC, Roskilde, Denmark) were coated overnight at 4ºC with 0.2µg/well of affinity purified rabbit anti-IgA antibodies with alpha chain-specificity in 0.05 M $NaHCO_3$, pH: 9.5. Blocking was performed by use of phosphate buffer containing 0.5% bovine serum albumin (BSA) at room temperature for 90 min. One hundred microliters of saliva samples (in duplicate) and standard samples (in duplicate) were pipetted into the microtitre wells. The plates were incubated for 90 min at 37ºC. The wells were washed 5 times with washing solution. Then, 100 µl of goat anti-human IgA conjugated with hours radish peroxidase were pipetted into each well, and the plates were incubated for 30 min at 37ºC. The wells were washed 5 times with washing solution and tapped dry. A fresh substrate solution, tetramethylbenzidine (100 µl), was added, and the plates were incubated for 15 min at room temperature. The enzyme reaction was stopped with 100 µl of 1 N HCl. Salivary IgA levels were detected by use of a standard curve. The percent coefficient of variation (%CV) for this ELISA was 3.6%. This technique identifies the peak rate of formation of antigen-antibody complexes by measuring their precipitation in the presence of a known concentration of sIgA antigen and expressed as mg/dL. Saliva flow rate (ml $-min^{-1}$) was determined by weighing and its density was assumed to be 1.0 $g \cdot ml^{-1}$. Samples were defrosted and microcentrifuged for 10 minutes before testing to remove any foreign matter, and 200 gL of clear supernatant was aspirated and assayed. Salivary lysozyme concentration was measured by an Elisa method. Briefly, a 96-well microtitre Elisa plate was coated overnight at 4°C with 200µl of rabbit antihuman lysozyme at a concentration of 7.0mg/l in sodium bicarbonate buffer (pH9.6). Then the well was washed with phosphate buffered solution (PBS) containing 0.05% (v/v) Tween 20 (PBS/Tween) and blot dried. The plate was stored at -20°C until assay. A 200µl aliquot of 2% w/v bovine serum albumin in PBS/Tween was added and left at room temperature for 2h. The plate was washed with PBS/Tween 20, 100 µl of sample diluted (1/50) in PBS and 100 µl biotinylated lysozime (1/1000) was added to each well. The plate was incubated at 37°C for 60 minutes. The well was then washed with PBS/Tween 20, 200 µl avidine alkaline phosphatise diluted in 1/3000 in PBS was added and incubated at 37°C for 60 minutes. After washing, 200 µl of enzyme substrate p-nitrophenyl phosphate sodium (0.1% w/v) in dietheanolamine buffer (pH 9.8) was added and incubated in the dark for 30 minutes at room temperature. The reaction was stopped with 50 µl of M NaOH. The absorbance was read with Bio-Rad microplate reader set at 405 nm. Each test included five two-fold dilutions of purified human urine lysozyme from which a standard curve was generated. The lysozyme secretion was

calculated by multiplying the absolute concentration with the absolute saliva flow rate.

*Epigenomic in vivo modification of upper airway cells*

*Nasal lavage.* Nasal lavage was carried out using the method described by Noah and Becker (19) by repetitive spraying of sterile normal saline irrigation solution (4 ml total) into the nostril with the subject's head tilted back at an angle of ~70° from vertical, followed by voluntary expelling of the fluid by the subject into a specimen collection cup. Both nostrils were washed in this way, and the resulting nasal lavage fluid (NLF) from both sides was combined. Nasal wash samples were immediately placed on ice and clarified by centrifugation at 14,000 × *g* in an Eppendorf centrifuge. Cytocentrifuge slides were prepared, fixed, and stained using modified Wright stain for differential cell counts by microscopic evaluation of 200 consecutive cells at high magnification. The remainder of the NLF was centrifuged at 500g × 7 min to remove cells and debris, and the cell pellets were isolated from nasal lavage samples, resuspended in 350µl lyses buffer, and stored at −80 °C until RT-PCR analysis.

*Semi-quantification assessment of Phase II enzyme gene expression.* Gene expression was measured by real-time quantitative reverse transcriptase polymerase chain reaction. Total RNA was extracted by Trizol, following the maker's instruction (Invitrogen, Paisley, UK) and treated with DNAse I (Sigma, USA). 0.3–1.0 µg RNA was routinely extracted from a nasal lavage sampling. RNA quality and quantity was confirmed by UV spectrophotometry and agarose gel electrophoresis. One µg of total RNA was reverse-transcribed with random hexamers and Moloney murine leukaemia virus–reverse transcriptase at a final volume of 20 µl. Specific cDNA amplification of human GSTM1, GSTP1 and HO1 was carried out with 2 µl of cDNA in a Light Cycler by using FastStart DNA Master SYBR Green I (Roche). The specific primers used were 5′GGGACGCTCCTGATTATGAC3′ and 5′GCAAACCATGGCCGCTTCCC3′ for GSTM1; 5′TCCGCTGCAAATACATCTCC3′ and 5′TGTTTCCCGTTGCCATTGAT3′ for GSTP1; 5'-CAGGCAGAGAATGCTGAG-3' and 5'-GCTTCACATAGCGCTGCA-3' for HO-1; (5 '-3'): CATCATCAATTTCGAGCAGA and GCCACACCATCTTTGTCAGCAG for SOD and ACAGTCAGCCGCATC-3' and 5'-AGGTGCGGCTCCCTA- 3' for GAPDH. The quantification was performed by crossing-point extrapolation into a standard curve with known cDNA concentrations by using Light Cycler system software. Relative units represent the ratio of concentration between the specific mRNA and the housekeeping mRNA. Quality of cDNA was confirmed by PCR amplification of fragment from the control gene ubiquitin C. Expression of genes was assessed by a 7500 Real Time PCR System (Applied Biosystems, USA) as total quantification, by using TaqMan Gene Expression Assays of the same maker. Bacterial plasmids containing coding sequences of GAPDH served as standard for total quantification of gene expression. PCR measurements was performed in triplicate. The expression was normalized to the expression of GAPDH, a housekeeping gene, and quantified using a PC based densitometric semiquantitative analysis using NIH image software by expressing arbitrary units. For each individual, gene expression at baseline (pre-challenge) was considered the calibrator and was given an arbitrary figure of 1.0 and relative increase in gene expression following FPP treatment was calculated in reference to this value.

## RESULTS

All subjects completed the study reporting no side effects. Routine biochemical values were within normal limits at the entry and were unaffected by FPP supplementation (data not shown)

*Saliva analysis*

Saliva flow rate showed a significant age-related decline ($p<0.05$, Fig. 1). FPP treatment brought about a significant increase of the salivary secretion rate only in the A group ($p<0.05$) while it did not affect the other age groups studied. Salivary IgA but not lysozyme production was significantly lower in the oldest age-group as compared to the youngest one (C *vs* A, $p<0.05$, Fig. 2). FPP treatment brought about a significant increase of these parameters in all age-groups ($p<0.05$) and the final values were comparable among the groups. Lysozyme concentration was unaffected by aging process. There was no significant correlation between salivary flow rate and either sIgA or lysozyme secretion, irrespective of the treatment or age group.

*Epigenomic in vivo modification of Phase II enzyme gene expression (GSTM1, GSTP1 and HO1) of upper airway cells*

Expression of phase II enzymes and SOD significantly increased in NLF samples of subjects given FPP as compared to baseline values and placebo control. Fig. 4 shows the NLF data for each age group. In contrast, no significant change in phase

II enzyme or SOD expression was observed for subjects completing the protocol with placebo. No significant difference was observed for each enzyme among the different age-group, either at baseline or after treatment.

## DISCUSSION

It is known that the presence of local antibody at mucosal surfaces in the form of secretory IgA (s-IgA) correlates with protection against bacterial and viral pathogens in humans and experimental animals (20). Unlike IgG, s-IgA consists of protease-resistant immunoglobulin dimers adapted to function in the external environment of the mucosa in the absence of other immune accessory mechanisms. s-IgA functions to intercept pathogens before they enter the body. These antibodies protect mucosal epithelium by cross-linking and agglutinating microorganisms, thus enhancing their entrapment and clearance in mucus and in some cases by blocking and sterically hindering the microbial surface molecules that mediate epithelial cell attachment (21). It has been reported that the salivary secretion rate may inversely influence the IgA concentration in saliva and salivary IgA levels seem to be higher in elderly subjects as compared to younger controls (22) although this data is debated (23). In our study the concentration of sIgA was unexpectedly lower in the eldest age-group. At the moment ,we do not have a clear explanation but past smoking habit, environmental exposure and possibly a higher perceived stress might have been confounding factors in this group. As a matter of fact FPP supplementation enabled a significant and comparable increase of sIgA in all subjects while also significantly enhancing the salivary flow rate, but only in the youngest group. No significant correlation was found between salivary flow rate and either sIgA or lysozyme concentration. It has been suggested that lysozyme may mitigate the inflammatory response and pathogenesis of chronic bronchitis by providing an accessory antibacterial defense mechanism and indirectly lowering the neutrophil chemotaxis and activation of alveolar macrophages (24). Interestingly, in our study we showed that lysozyme secretion was enhanced by FPP administration. Although at the moment we cannot provide a specific mechanism of action for such findings, based on prior in vitro and very recent animal studies (25, 26) we can envisage and indirect action through the demonstrated monocyte-activating action which may have triggered a higher lysozyme secretion. Interestingly, a recent study shows that low secretion rate of either IgA and lysozyme in elite athletes was associated with an increased risk of of upper respiratory infection (27). A number of experimental evidences suggests that the lethal effect of influenza virus infection is

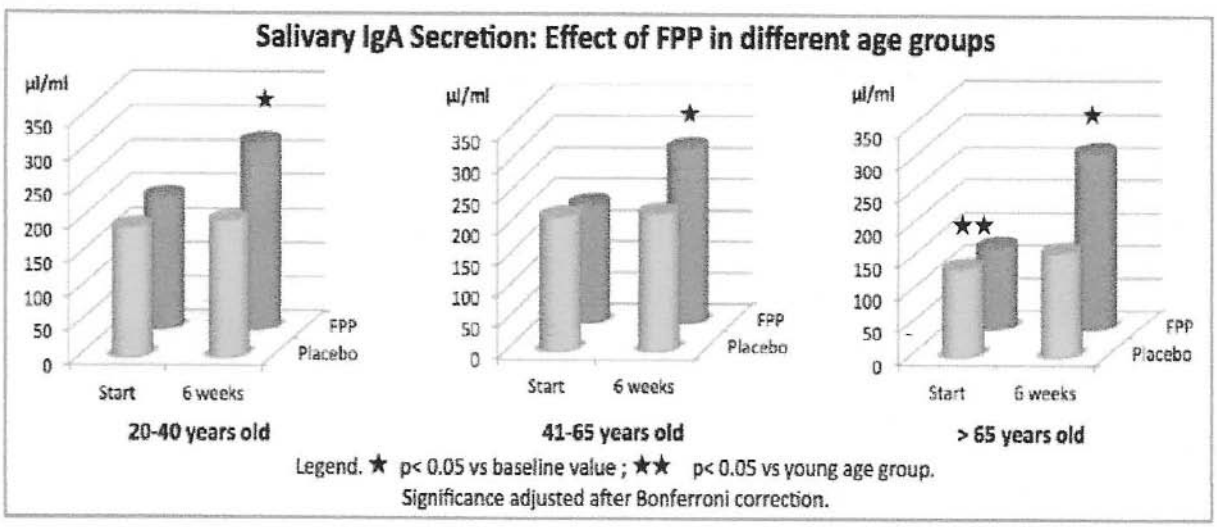


**Fig. 1.** ** p< 0.05 vs baseline value;. Significance adjusted after Bonferroni correction. Triangled dots: FPP, squared dots: placebo. A significant inverse correlation between age and salivary flow rate occurred (r: 0.71, p<0.05).*

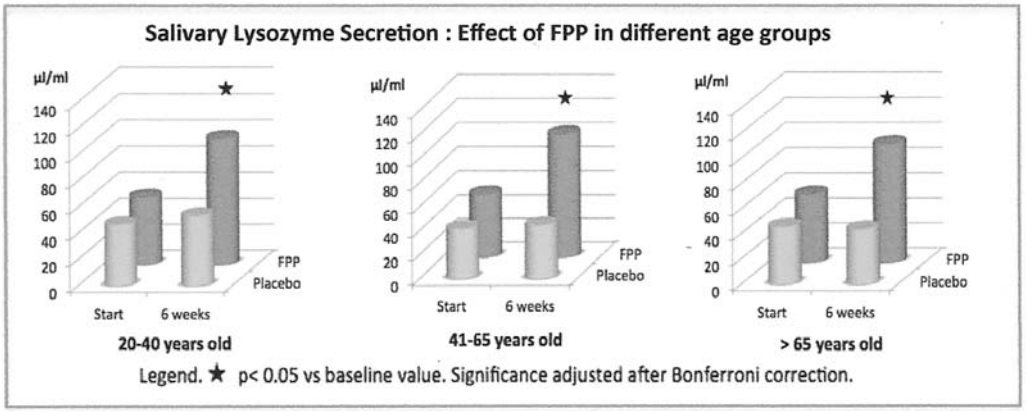


**Fig. 2.** ** p< 0.05 vs baseline value; ** p<0.05 vs young age group. Significance adjusted after Bonferroni correction. Triangled dots: FPP, squared dots: placebo.*

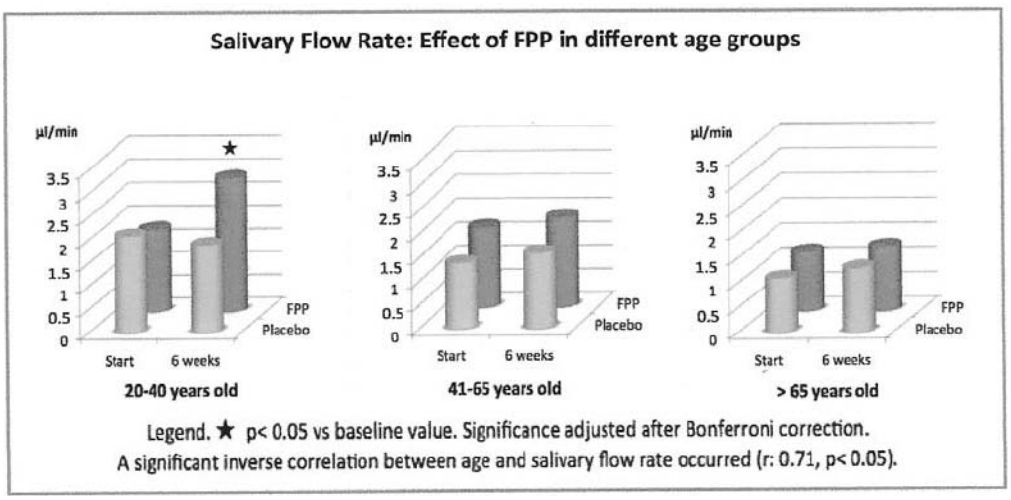


**Fig. 3.** ** p< 0.05 vs baseline value; Significance adjusted after Bonferroni correction. Triangled dots: FPP, squared dots: placebo.*

determined by immunopathological consequences of the host rather than by the direct cytopathic effect of viral replication (28). In such a setting, a role for reactive oxygen species (ROS) and reactive nitrogen species (RNS) as mediators of virus-induced lung damage has been suggested by several studies (8, 29, 30) in which exogenous antioxidant treatment has clearly shown to decrease lung damage and mortality in influenza-infected mice. Further, it is likely that ROS may also contribute to an increased viral titer after influenza infection. It has been shown that superoxide may be produced both by influenza-activated leukocytes or by xanthine oxidase, the activity of which is increased in influenza-infected lungs (8) as well as by other local sources such as airway epithelial cells (31). Normal cellular defence mechanisms that protect against free radicals start with the antioxidant enzymes cascade where SODs are a major extracellular antioxidant in the lung especially by the alveolar type II pneumocytes (32). Previous studies (8, 33) on the effects of using exogenous SODs in influenza- induced lung injury have shown protective responses possibly through its inhibitory action against virus-induced inflammatory and oxidant responses in the lung.

Confirming our very recent study analyzing systemic leukocytes (34), we showed that FPP treatment enabled a significant upregulation of SOD also in nasal lavage cells. These data hold some potential relevance when considering that Suliman

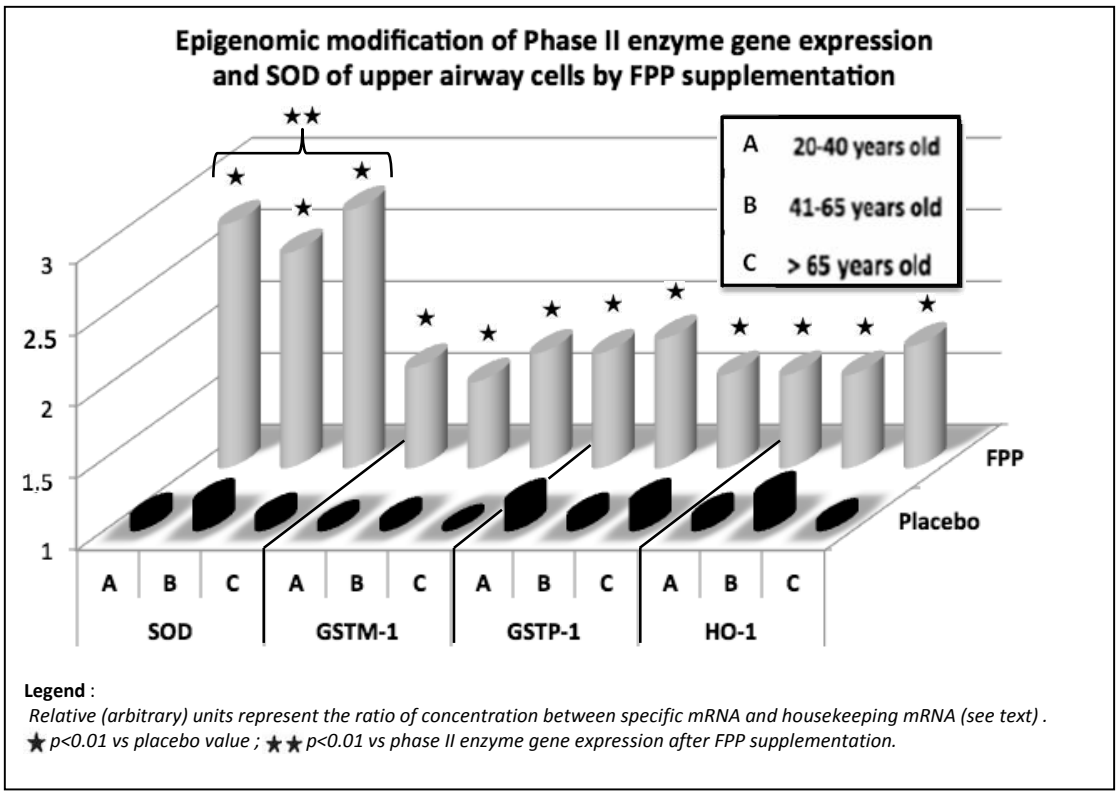


**Fig. 4.** *Relative (arbitrary) units represent the ratio of concentration between the specific mRNA and the housekeeping mRNA (see text). * p<0.01 vs placebo value (black bars); ** p<0.01 vs phase II enzyme gene expression after FPP supplementation.*

et al. (35) have envisaged that pharmacological supplementation of airway extra-cellular SOD compounds may provide an opportunity to therapeutically attenuate pathological events that follow influenza virus infection. On the other hand, the effect of cold exposure on the antioxidant defence system is a complex issue and it appear to be both tissue specific and dependent on the duration of the cold exposure experience (36). Indeed, while in some cases compensatory changes may take place in the antioxidant defence system of trained individuals (37), a significant decrease of blood glutathione is a rather constant feature (38). One more relevant finding in our study was the significant gene upregulation of phase II enzyme tested at the nasal lavage cell level. These inducible Phase II enzymes represent an early and sensitive reaction to ROS and act by scavenging them and metabolizing xenobiotics such as air pollutants (39). Although the concomitant measurement of SOD would have added a further value to this data, from our prior study we had shown that FPP could significantly improve SOD plasma status (40). The comparable response of all of the measured PII enzymes, might suggest a common pathway of induction by FFP, i.e. Nrf-2 activation, although we lack specific measurement of it. Indeed, most of the genes for proteins involved in the cellular antioxidant defense and in phase II detoxification share a common regulation via the redox- and electrophile-sensitive transcription factor NF-E2-related factor (41), which binds to the *cis*-acting antioxidant or electrophilic response element (ARE/EpRE) (42) and future studies will be directed to clarify the possible multimodal action of FPP in biological systems.

In conclusion, FPP supplementation during one

month resulted in higher concentration of salivary IgA and lysozyme together with a significant increase in phase II enzyme and SOD expression in the human airway. The biological significance of this effect i.e., whether it will help to reduce respiratory oxidative stress in the human airway and, consequently, the incidence of URTI remains to be demonstrated in longer clinical trials preferably targeted to specific cohorts of patients as well as examining possible genetic polymorphisms affecting Phase II enzymes as a further relevant variable.

## REFERENCES


1. Lui, K J, Kendal AP. Impact of influenza epidemics on mortality in the United States from October 1972 to May 1985. Am J Public Health 1987; 77**:**712-16.
2. Couch, RB, Keitel W, Cate TR, Quarles JA, Taber LA, Glezen WP. Prevention of influenza virus infections by current inactivated influenza virus vaccines,. *In* Brown LE, Hampson AW and Webster RG(ed.), Options for the control of influenza III. Elsevier, Amsterdam, The Netherlands, 1996; p. 97-106.
3. Hayden FG, Hay HJ. Emergence and transmission of influenza A viruses resistant to amantadine and rimantidine. Curr Top Microbiol Immunol 1992; 176**:**119-30.
4. Jefferson T, Rivetti D, Rivetti A, Rudin M, Di Pietrantonj C, Demicheli V. Efficacy and effectiveness of influenza vaccines in elderly people: a systematic review. Lancet 2005; 366:1165-74.
5. Oda T, Akaike T, Hamamoto T, Suzuki F, Hirano T, Maeda H. Oxygen radicals in influenza-induced pathogenesis and treatment with pyran polymer-conjugated SOD. Science 1989; 244:974-6.
6. Han SN, Meydani M, Wu D, Bender BS, Smith DE, Vina J, Cao G, Prior RL, Meydani SN. Effect of long-term dietary antioxidant supplementation on influenza virus infection. J Gerontol A Biol Sci Med Sci 2000; 55:496-503.
7. Rennard BO, Ertl RF, Gossman GL, Robbins RA, Rennard SL. Chicken soup inhibits neutrophils chemotaxis in vitro. Chest 2000; 118:1150-7.
8. Folz RJ and Crapo JD. Pulmonary oxygen toxicity. In: Current Pulmonology (15th ed.), edited by Tierney DF. Chicago, IL: Mosby Year Book, 1994, p. 113-36.
9. Akaike T, Ando M, Oda T, Doi T, Ijiri S, Araki S, Maeda H. Dependence on O2 generation by xanthine oxidase of pathogenesis of influenza virus infection in mice. J Clin Invest 1990; 85:739-74.
10. Hennet T, Peterhans E, Stocker R. Alterations in antioxidant defences in lung and liver of mice infected with influenza A virus. J Gen Virol 1992; 73:39-46.
11. Lau JT, Leung PC, Wong EL, et al. The use of an herbal formula by hospital care workers during the severe acute respiratory syndrome epidemic in Hong Kong to prevent severe acute respiratory syndrome transmission, relieve influenza-related symptoms, and improve quality of life: a prospective cohort study. J Altern Complement Med 2005; 11:49-55.
12. Ruffa MJ, Wagner ML, Suriano M, Vicente C, Nadinic J, Pampuro S, Salomon H, Campos RH, Cavallaro L. Inhibitory effect of medicinal herbs against RNA and DNA viruses Antivir Chem Chemother 2004; 15:153-9.
13. Park KJ. Evaluation of in vitro antiviral activity in methanol extracts against influenza virus type A from Korean medicinal plants. Phytother Res 2003; 17:1059-63.
14. Chen XY, Wu TX, Liu GJ, Wang Q, Zheng J, Wei J, Ni J, Zhou LK, Duan X, Qiao JQ. Chinese medicinal herbs for influenza. Cochrane Database Syst Rev 2005; 25:CD004559.
15. Sengupta S, Strauss RP, Corbie-Smith G, Thrasher A. What can the elderly do to protect themselves from the flu in addition to getting a flu vaccination? Am J Public Health 2004; 94:905-11.
16. Marotta F, Yoshida C, Barreto R, Naito Y, Packer L. Oxidative-inflammatory damage in cirrhosis: effect of vitamin E and a fermented papaya preparation. J Gastroenterol Hepatol 2007; 22:697-703.
17. Aruoma OI, Colognato R, Fontana I, et al. Molecular effects of fermented papaya preparation on oxidative damage, MAP Kinase activation and modulation of the benzo[a]pyrene mediated genotoxicity. Biofactor 2006; 26:147-59.
18. Subar AF, Thompson FE, Kipnis V, Midthune D, Hurwitz P, McNutt S, McIntosh A, Rosenfeld S. Comparative validation of the Block, Willett, and National Cancer Institute food frequency

questionnaires : the Eating at America's Table Study. Am J Epidemiol 2001; 154:1089-99.
19. Noah TL, Becker S. Chemokines in nasal secretions of normal adults experimentally infected with respiratory syncytial virus. Clinical Immunol 2000; 97:43-49.
20. Mestecky J, Kutteh WH, Jackson S, et al. Mucosal immunity in the female genital tract: relevance to vaccination efforts against the human immunodeficiency virus. AIDS Res Hum Retroviruses 1994;10:S11-9.
21. Kilian M, Mestecky J, Russell MW. Defense mechanisms involving Fc-dependent functions of immunoglobulin A and their subversion by bacterial immunoglobulin A proteases. Microbiol Rev 1988; 52:296-303.
22. Eliasson L, Birkhed D, Osterberg T, Carlén A. Minor salivary gland secretion rates and immunoglobulin A in adults and the elderly. Eur J Oral Sci 2006; 114:494-9.
23. Mungia R, Cano SM, Johnson DA, Dang H, Brown JP. Interaction of age and specific saliva component output on caries. Aging Clin Exp Res 2008; 20:503-8.
24. Taylor DC, Cripps AW, Clancy RL. A possible role for lysozyme in determining acute exacerbation in chronic bronchitis. Clin Exp Immunol 1995; 102:406-16.
25. Rimbach G, Park YC, Guo Q, et al. Nitric oxide synthesis and TNF-alpha secretion in RAW 264.7 macrophages: mode of action of a fermented papaya preparation. Life Sci 2000; 67:679-94.
26. Collard E, Roy S. Improved function of diabetic wound-site macrophages and accelerated wound closure in response to oral supplementation of a fermented papaya preparation. Antioxid Redox Signal 2010; 13:599-606.
27. Cunniffe B, Griffiths H, Proctor W, Davies B, Baker JS, Jones KP. Mucosal immunity and illness incidence in elite rugby union players across A Season. Med Sci Sports Exerc 2011; 43:388-97.
28. Shimomura E, Suzuki F, Ishida N. Characterization of cells infiltrating the lungs of x-irradiated and nude mice after influenza virus infection. Microbiol Immunol 1982; 26:129-38.
29. Akaike T, Noguchi Y, Ijiri S, Setoguchi K, Suga M, Zheng YM, Dietzschold B, Maeda H. Pathogenesis of influenza virus-induced pneumonia: involvement of both nitric oxide and oxygen radicals. Proc Natl Acad Sci USA 1996; 93:2448-53.
30. Rott R, Klenk HD, Nagai Y, Tashiro M. Influenza viruses M, cell enzymes, and pathogenicity. Am J Respir Cell Mol Biol 1995; 152: S16-S19.
31. Kobzik L, Bredt DS, Lowenstein CJ, Drazen J, Gaston B, Sugarbaker D, Stamler JS. Nitric oxide synthase in human and rat lung: immunocytochemical and histochemical localization. Am J Respir Cell Mol Biol 1993; 9:371-7.
32. Su WY, Folz R, Chen JS, Crapo JD, Chang LY. Extracellular superoxide dismutase mRNA expressions in the human lung by in situ hybridization. Am J Respir Cell Mol Biol 1997; 16:162-70.
33. Akaike T, Noguchi Y, Ijiri S, Setoguchi K, Suga M, Zheng YM, Dietzschold B, Maeda H. Pathogenesis of influenza virus-induced pneumonia: involvement of both nitric oxide and oxygen radicals. Proc Natl Acad Sci USA 1996; 93:2448-53.
34. Marotta F, Koike K, Lorenzetti A, Jain S, Signorelli P, Metugriachuk Y, Mantello P, Locorotondo N. Regulating redox balance gene expression in healthy individuals by nutraceuticals: a pilot study. Rejuvenation Res 2010; 13:175-8.
35. Suliman HB, Ryan LK, Bishop L, Folz RJ. Prevention of influenza-induced lung injury in mice overexpressing extracellular superoxide dismutase. Am J Physiol Lung Cell Mol Physiol 2001; 280:L69-L78.
36. Venditti P, De Rosa R, Portero-Otin M, Pamplona R, Di Meo S. Cold-induced hyperthyroidism produces oxidative damage in rat tissues and increases susceptibility to oxidants. Int J Biochem Cell Biol 2004; 36:1319-31.
37. Siems WG, Brenke R, Sommerburg O, Grune T. Improved antioxidant protection in winter swimmers. QJM 1999; 92:193-8.
38. Ohno H, Kondo T, Fujiwara Y, Tagami S, Kuroshima A, Kawakami Y. Effects of cold stress on glutathione and related enzymes in rat erythrocytes. Int J Biometeorol 1991; 35:111-13.
39. Xu C, Li CY, Kong AN. Induction of phase I, II and III drug metabolism/transport by xenobiotics. Arch Pharm Res 2005; 28:249-68.
40. Marotta F, Reizakovic I, Tajiri H, Safran P, Ideo G.

Abstinence-induced oxidative stress in moderate drinkers is improved by fermentd papaya preparation. Hepatogastroenterology 1997; 44:1360-6.
41. Hayes JD, McMahon M. NRF2 and KEAP1 mutations: permanent activation of an adaptive response in cancer. Trends Biochem Sci 2009; 34:176-88.
42. Venugopal R, Jaiswal AK. Nrf1 and Nrf2 positively and c-Fos and Fra1 negatively regulate the human antioxidant response element-mediated expression of NAD(P)H:quinone oxidoreductase1 gene. Proc Natl Acad Sci USA 1996; 93:14960-5.

# EFFECTS OF VISFATIN/PBEF/NAMPT ON FEEDING BEHAVIOR AND HYPOTHALAMIC NEUROMODULATORS IN THE RAT

L. BRUNETTI, L. RECINELLA, C. DI NISIO, A. CHIAVAROLI, S. LEONE, C. FERRANTE, G. ORLANDO and M. VACCA

*Department of Drug Sciences, G. d'Annunzio University, Chieti, Italy*

*Received December 22, 2011 – Accepted May 21, 2012*

**Visfatin, also known as pre-B cell colony enhancing factor (PBEF) or nicotinamide phosphoribosyltransferase (NAMPT), is a cytokine that is produced by adipose tissue, skeletal muscle, liver and immune cells. We studied the effects of visfatin/PBEF/NAMPT on feeding behavior, hypothalamic steady state concentrations of aminergic neurotransmitters and hypothalamic mRNA levels of anorexigenic peptides, such as cocaine- and amphetamine-regulated transcript (CART) peptide, corticotropin-releasing hormone (CRH), proopiomelanocortin (POMC), and orexigenic peptides, such as agouti-related peptide (AgRP) and neuropeptide Y (NPY). Forty-eight rats were injected in the arcuate nucleus (ARC) of the hypothalamus with either saline or visfatin/PBEF/NAMPT (3 μg). Food intake was recorded 1, 2 and 24 h following injection, and either dopamine (DA), norepinephrine (NE), serotonin (5-hydroxytryptamine, 5-HT) or peptide gene expression were evaluated 2 and 24 h after visfatin/PBEF/NAMPT administration. Compared to vehicle, visfatin/PBEF/NAMPT significantly increased food intake, as evaluated 1, 2 and 24 h post-injection. Visfatin/PBEF/NAMPT treatment led to a significant decrease of DA steady state concentration, CART and CRH mRNA levels. Consequently, visfatin/PBEF/NAMPT could play an orexigenic role in the ARC, and the effect could be mediated by modulation of DA, CART and CRH activity in the hypothalamus.**

Feeding behavior is finely modulated by a complex interplay of neurotransmitters, neuropeptides, cytokines and hormones in the central nervous system, where the arcuate nucleus (ARC) of the hypothalamus is known to play a pivotal role in this cross-talk signalling (1). The ARC includes two populations of first-order neurons expressing either neuropeptide Y (NPY)/ agouti-related peptide (AgRP), which enhance food intake, or proopiomelanocortin (POMC)/ cocaine- and amphetamine-regulated transcript (CART) peptide, which have an inhibitory effect on food intake. Both NPY/AgRP and POMC/CART peptide neurons project to second-order neurons, located partially in the paraventricular nucleus (PVN), producing anorexigenic peptides such as corticotropin-releasing hormone (CRH) (2). The ARC neurons, lying above the median eminence, where the blood-brain barrier is not complete, can be modulated by hormones involved in both short- and long-term regulation of energy homeostasis (3). Moreover, the hypothalamic control of feeding by gastrointestinal or adipose tissue-derived hormones (adipokines) has also been shown to be modulated by aminergic neurotransmitters, such as dopamine (DA), norepinephrine (NE) and serotonin (5-hydroxytryptamine, 5-HT), which play a pivotal role in the transduction of peripheral afferents into

*Key words: feeding, hypothalamus, NAMPT, PBEF, visfatin*

*Mailing address*: Prof. Michele Vacca,
Department of Drug Sciences,
G. d'Annunzio University,
School of Pharmacy,
via dei Vestini, 31 66013 Chieti, Italy
Tel.: +39 0871 355 4467 Fax: +39 0871 355 4762
e-mail: mvacca@unich.it



0393-974X (2012)

**DISCLOSURE: ALL AUTHORS REPORT NO CONFLICTS OF INTEREST RELEVANT TO THIS ARTICLE.**

satiety and feeding signals (4). Adipose tissue, besides its energy-storage role, is now regarded as a dynamic endocrine organ secreting a variety of adipokines, which are able to affect energy homeostasis, both peripherally and at hypothalamic level (5). In particular, adipokines might provide a plausible link between obesity, insulin resistance, endothelial dysfunction, and atherosclerosis (6).

Visfatin has been described as a 52 kDa peptide hormone secreted by adipose tissue, in particular visceral adipose tissue (7), even if other studies found no differences between visceral and subcutaneous fat depots (8, 9). The same peptide was previously identified as pre-B cell colony enhancing factor (PBEF), a cytokine stimulating the maturation of B cell precursors, that is produced in several tissues, including liver, bone marrow and skeletal muscle (10). It was also identified as nicotinamide phosphoribosyltransferase (NAMPT), the rate-limiting enzyme in nicotinamide adenine dinucleotide (NAD) biosynthesis from nicotinamide in mammals (11). Visfatin/PBEF/NAMPT was initially shown to exert insulin-mimetic effects by binding to and activating insulin receptors (7), although its physiological relevance remains controversial. Revollo et al. (12) failed to confirm the insulin-mimetic effects of visfatin/PBEF/NAMPT, but a significant physiological role in the regulation of pancreatic islet B-cell function through the NAD biosynthetic activity was reported, suggesting a connection between this peptide and glucose metabolism. Although elevated circulating visfatin/PBEF/NAMPT concentrations were reported to be associated with type 2 diabetes (13), other clinical studies did not find the same association (14-15). Moreover, even more conflicting results with regard to correlation of visfatin/PBEF/NAMPT with obesity have been reported. Higher plasma visfatin/PBEF/NAMPT levels were found in obese subjects (8). Conversely, other studies indicated opposite results (16) or no association (14).

Regarding the feeding behavior, intracerebroventricular (ICV) injection of visfatin/PBEF/NAMPT has been shown to increase food intake in chicks, where it seems to be more potent than other central orexigenic factors, such as NPY (17). On the other hand, ICV administration of visfatin/PBEF/NAMPT has been found to exert anorexigenic effects in rats (18).

In the present study, we aimed to investigate the feeding modulatory effect of visfatin/PBEF/NAMPT acutely injected into the ARC of the rat, and the hypothalamic DA, NE and 5-HT activity, by measuring their steady state concentrations. In addition, we evaluated the effects of visfatin/PBEF/NAMPT on gene expression of hypothalamic neuropeptides which play key roles in feeding regulation, such as CART peptide, CRH, POMC, AgRP, and NPY.

## MATERIALS AND METHODS

*Animals and drugs*

Male adult Wistar rats (200-250 g) were housed in plexiglas cages (40 cm × 25 cm × 15 cm), one rat per cage, in acclimatized colony rooms (22±1°C; 60% humidity), on a 12/12 h light/dark cycle (light phase: 07:00-19:00 h), with free access to tap water and food, 24 h/day throughout the study, with no fasting periods. Rats were fed a standard laboratory diet (3.5% fat, 63% carbohydrate, 14% protein, 19.5% other components without caloric value; 3.20 kcal/g). Housing conditions and experimentation procedures were strictly in accordance with the European Community ethical regulations on the care of animals for scientific research.

Rat recombinant visfatin/PBEF/NAMPT was purchased from Enzo Life Sciences AG, Lausen, Switzerland.

*In vivo intrahypothalamic treatment*

Forty-eight rats were anesthetized by intraperitoneal injection of chloral hydrate (400mg/kg) (Farmalabor, Milano, Italy), treated with ketoprofen (1.4mg/kg) (Dompé farmaceutici, Milano, Italy) to sustain analgesia and placed in a stereotaxic instrument (David Kopf Instruments, Tujunga, CA, USA). After a midline incision, the skull was scraped clean, washed with a sterile saline solution, and disinfected with iodopovidone 10% solution. A drop of lidocaine 2% solution (Farmalabor, Milano, Italy) was applied into the incision. Coordinates for placement of a cannula into the ARC of the hypothalamus were as follows: anteroposterior (AP), -3 mm, (or +3 mm posterior to the bregma); mediolateral (ML), 0 mm; dorsoventral (DV), -7 mm (19). The site for the cannula was marked. Small holes were drilled into the skull and stainless-steel screws were placed. A hole was drilled through the skull, in the marked site, for the placement of the 21-gauge stainless-steel cannula (1.7 cm long), which was stereotaxically implanted into the ARC. The

lateral coordinate was 0 mm, but the hole drilled through the skull for the placement of the cannula was larger than a point due to drill-bit. Hence, we carefully and slowly implanted the cannula into the hole, sideways rather than in the midpoint. We paid attention to avoid the sagittal sinus: not a drop of blood was spilled during cannula placement in the rats enrolled in our study.

Once in place, the cannula was attached to the skull using dental cement (Formatray, Salerno, Italy). Sterile obturators were inserted into the cannulas to prevent them from clogging and to reduce the potential for brain infection.

Immediately after surgery, rats were injected subcutaneously with 1 ml of sterile saline solution and 1 ml of 5% glucose solution (Galenica Senese, Siena, Italy) and intraperitoneally with amoxicillin (20mg/kg) (Farmalabor, Milano, Italy).

Seventy-two hours after surgery, rats (24 animals for each group) were injected, in the ARC, at 09:00 h, with 10 µl of either vehicle (saline) or visfatin/PBEF/NAMPT (3 µg). The rats were gently hand-held while the obturators were removed.

Food intake was recorded 1, 2 and 24 h after treatment. Twenty-four animals (12 for each group) were sacrificed by decapitation, 2 and 24 h after administration, for neurotransmitter activity assessment and gene expression analysis, respectively. Immediately after sacrifice, we carefully examined the skull, brain and blood vessels of each rat, and found no damage; we observed only the small hole produced by the cannula on the upper surface of the ARC. The lower surface was intact.

*Hypothalamic neurotransmitter extraction and high performance liquid chromatography (HPLC) determination*

After sacrifice, brains (n=24) were rapidly removed and individual hypothalami dissected. Hypothalamic tissues were homogenized in ice bath for 2 min with Potter-Elvehjem homogenizer in 1 ml of 0.05 N perchloric acid containing 0.004% sodium EDTA and 0.010% sodium bisulfite. The homogenate was 5-fold diluted in chromatographic mobile phase and centrifuged at 4,500 x *g* for 10 min. The supernatant was filtered on 0.45 µm PTFE sterile filters (Whatman) and directly injected for HPLC. Neurotransmitter recovery was satisfactory (≥90%) and reproducible, with percentage relative standard deviation ≤10%.

The HPLC apparatus consisting of a Jasco (Tokyo, Japan) PU-2080 chromatographic pump and an ESA (Chelmsford, MA, USA) Coulochem III coulometric detector, equipped with micro dialysis cell (ESA-5014b) porous graphite working electrode and solid state palladium reference electrode. The analytical cell was set at −0.150 V, for detector 1 and at +0.300 V, for detector 2, with a range of 100 nA. The chromatograms were monitored at the analytical detector 2. Integration was performed by Jasco Borwin Chromatography software, version 1.5. The chromatographic separation was performed by isocratic elution on Phenomenex Kinetex reverse phase column (C18, 150 mm×4.6 mm i.d., 2.6 µm). The mobile phase was (10:90, v/v) acetonitrile and 75 mM pH 3.00 phosphate buffer containing octanesulfonic acid 1.8 mM, EDTA 30 µM and triethylamine 0.015% v/v. Flow rate was 0.6 ml/min and the samples were manually injected through a 20 µl loop. Neurotransmitter peaks were identified by comparison with pure standard retention time. Neurotransmitter concentrations in the samples were calculated by linear regression curve (y = bx + m) obtained with standard. Neither internal nor external standard were necessary for neurotransmitter quantification, in the hypothalamus homogenate, and all tests performed for method validation yielded results in accordance to limits indicated in official guidelines for applicability in laboratory trials. The standard stock solutions of DA, NE and 5-HT at 2 mg/ml were prepared in bidistilled water containing 0.004% EDTA and 0.010% sodium bisulfite. The stock solutions were stored at 4°C. Work solutions (1.25-20.00 ng/ml) were daily obtained progressively diluting stock solutions in mobile phase.

*RNA extraction*

After sacrifice, brains (n=24) were rapidly removed and individual hypothalami immediately dissected and stored in RNA*later* solution (Ambion, Austin, TX, USA), for gene expression analysis, at -20°C until further processed.

Total hypothalamic RNA was extracted using TRI Reagent (Sigma-Aldrich, St. Louis, MO) according to the manufacturer's protocol. In brief, each rat hypothalamus was homogenized in 1 ml of TRI Reagent. The homogenized samples were centrifuged at 12,000 x *g* for 10 min at 4°C to remove the insoluble material. The supernatant was added to 0.2 ml of chloroform and the samples were centrifuged at 12,000 x *g* for 15 min at 4°C. The aqueous phase was removed and mixed with 0.5 ml of isopropyl alcohol. After centrifugation at 12,000 x *g* for 10 min at 4°C, the gel-like RNA pellet was washed with 1 ml of 75% ethanol and dissolved in RNase-free water. Contaminating DNA was removed using 2 units of RNase-free DNase 1 (DNA-free kit, Ambion, Austin, TX), according to the manufacturer's instructions. The RNA solution was quantified at 260 nm by spectrophotometer reading (BioPhotometer, Eppendorf, Hamburg, Germany) and its purity was assessed by the ratio at 260 and 280 nm readings. The quality of the extracted RNA samples was also determined by electrophoresis through agarose gels

and staining with ethidium bromide, under UV light.

*Reverse transcription and real-time reverse transcription polymerase chain reaction (real-time RT PCR)*

One µg of total RNA extracted from each sample in a 20 µl reaction volume was reverse transcribed using High Capacity cDNA Reverse Transcription Kit (Applied Biosystems, Foster City, CA, USA) according to the manufacturer's manual. Reactions were incubated in a 2720 Thermal Cycler (Applied Biosystems, Foster City, CA) initially at 25°C for 10 min, then at 37°C for 120 min and finally at 85°C for 5 s.

Gene expression was determined by quantitative real-time PCR using TaqMan probe-based chemistry (Applied Biosystems, Foster City, CA, USA). Reactions were performed in MicroAmp Fast Optic 96-well Reaction Plates (Applied Biosystems, Foster City, CA, USA) on an ABI PRISM 7900 HT Fast Real-Time PCR System (Applied Biosystems, Foster City, CA, USA). PCR primers and TaqMan probes were obtained from Applied Biosystems (Assays-on-Demand Gene Expression Products, Rn00567382_m1 for CART gene, Rn01462137_m1 for CRH gene, Rn00595020_m1 for POMC gene, Rn01431703_g1 for AgRP gene, Rn00561681_m1 for NPY gene). B-actin (Applied Biosystems, Foster City, CA, USA, Part No. 4352340E) was used as the housekeeping gene. In accordance with the manufacturer's instructions, each amplification reaction was performed with 10 µl of TaqMan Fast Universal PCR Master Mix (2X), No AmpErase UNG (Applied Biosystems, Foster City, CA, USA), 1 µl of primer probe mixture, 1 µl of cDNA, 8 µl of nuclease-free water. The thermal cycling conditions (fast operational mode) were: 95°C for 20 s, followed by 40 cycles of amplification at 95°C for 1 s and 60°C for 20 s. The real-time PCR was carried out in triplicate for each cDNA sample in relation to each of the investigated genes. In addition to samples, individual runs included no-template controls (one for each Assay-on-Demand Gene Expression Product) and a reverse transcriptase minus control (for AgRP gene Assay-on-Demand Gene Expression Product). Data were elaborated with the Sequence Detection System (SDS) software version 2.3 (Applied Biosystems, Foster City, CA, USA). The comparative $2^{\triangle\triangle}$ method was used to quantify the relative abundance of mRNA and then determine the relative changes in individual gene expression (relative quantification) (20). This method uses a calibrator sample to enable a comparison of gene expression levels in different samples. The values obtained indicate the changes in gene expression in the sample of interest by comparison with the calibrator sample, after normalization to the housekeeping gene.

*Statistical analysis*

Statistical analysis was performed using GraphPad Prism version 5.01 for Windows (GraphPad Software, San Diego, CA). Food intake, gene expression data, deriving from relative quantification, and hypothalamic steady state concentrations of DA, NE, 5-HT were collected from each of the 48 animals used in the experimental procedure and means ± S.E.M. were determined for each experimental group and analyzed by unpaired *t* test. As for gene expression analysis, 1.00 (calibrator sample) was considered the theoretical mean for the comparison. Differences were considered to be significant when *P* was less than 0.05.

## RESULTS

Compared to vehicle, intrahypothalamic injection of visfatin/PBEF/NAMPT (3 µg) induced a significant increase in food intake, as evaluated 1, 2, and 24 h after treatment (Fig. 1).

When we evaluated hypothalamic aminergic neurotransmitter levels, we found a significant reduction of hypothalamic DA steady state concentration after visfatin/PBEF/NAMPT treatment, without any effect on NE and 5-HT (Table I).

Furthermore, we found a significant reduction of CART and CRH gene expression in visfatin/PBEF/NAMPT treated rats, while POMC, AgRP and NPY gene expression was not modified in respect to vehicle (Fig. 2).

## DISCUSSION

The regulation of food intake and energy expenditures is integrated in the hypothalamus, where peripheral hormone and neurotransmitter signallings convey timely updated information about energy needs and metabolic substrate availability (1). To date, clinical studies have provided conflicting results concerning the possible associations between circulating visfatin/PBEF/NAMPT levels and anthropometric and biochemical parameters in obesity and type 2 diabetes (8, 13-16).

Recently, visfatin/PBEF/NAMPT was shown to be present in human cerebrospinal fluid at 10% plasma concentrations and it has been suggested that this peptide could get through the blood-brain barrier, possibly via an active transport mechanism (21). However, visfatin/PBEF/NAMPT also seems to be expressed in the brain (22).

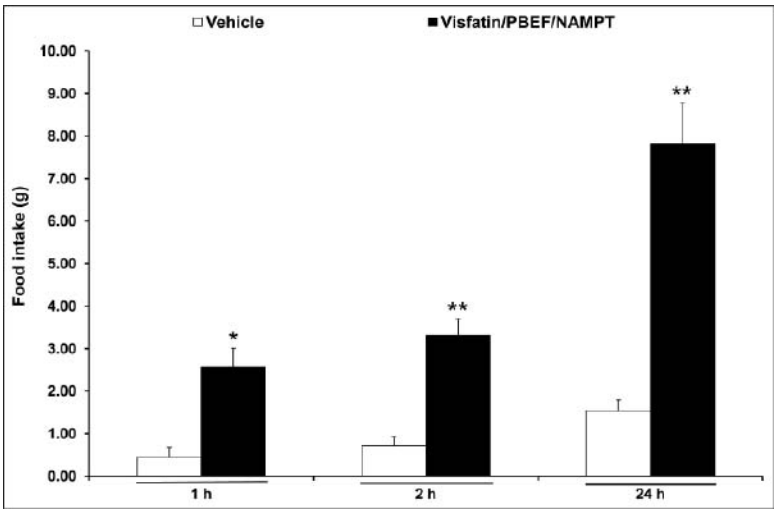


**Fig. 1.** *Food intake (in grams) in rats fed a standard laboratory diet and treated with either vehicle or visfatin/PBEF/NAMPT (3 μg). Vehicle or visfatin/PBEF/NAMPT was administered by intrahypothalamic injections, during the light phase, at 09:00 h. Food intake was recorded 1, 2 and 24 h after treatment in each group of rats. Values represent the means ± S.E.M. Compared to vehicle, visfatin/PBEF/NAMPT significantly increased food intake, as evaluated 1, 2, and 24 h post-injection. *P<0.001 vs vehicle; **P<0.0001 vs vehicle.*

**Table I.** *Hypothalamic amine steady state concentrations (ng/mg wet tissue).*

| | Vehicle | Visfatin/PBEF/NAMPT |
|---|---|---|
| Dopamine | 0.39 ± 0.05 | 0.12 ± 0.04* |
| Norepinephrine | 1.59 ± 0.09 | 1.51 ± 0.15 |
| Serotonin | 0.80 ± 0.08 | 0.79 ± 0.07 |

*Hypothalamic dopamine (DA), norepinephrine (NE) and serotonin (5-hydroxytryptamine) steady state concentrations (ng/mg wet tissue) 2 h after treatment with visfatin/PBEF/NAMPT (3 μg), as determined by HPLC. Values represent the means ± S.E.M. Compared to vehicle, visfatin/PBEF/NAMPT significantly decreased DA steady state concentration. *P<0.05 vs vehicle.*

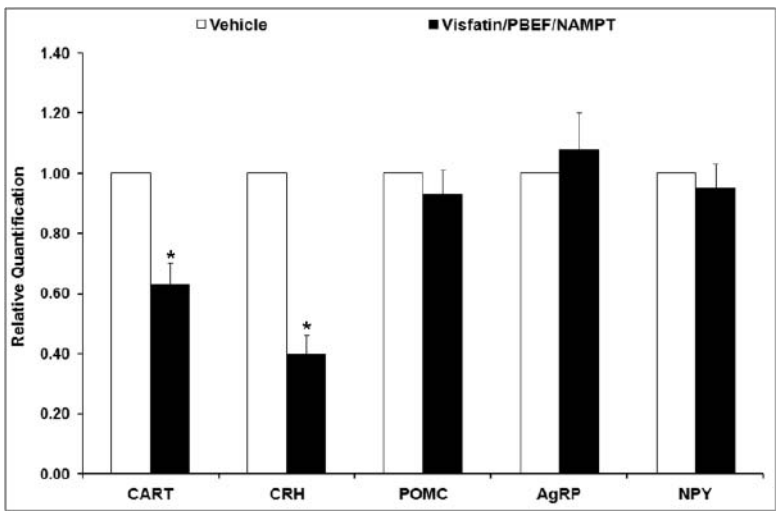


**Fig. 2.** *Relative gene expression of hypothalamic anorexigenic and orexigenic neuropeptides 24 h after treatment with visfatin/PBEF/NAMPT (3 μg), as determined by real-time RT PCR. Data were calculated using the $2^{\triangle\triangle}$ method; they were normalized to B-actin mRNA levels and then expressed as relative to vehicle (calibrator sample, defined as 1.00). Values represent the means ± S.E.M. Compared to vehicle, visfatin/PBEF/NAMPT significantly decreased cocaine- and amphetamine-regulated transcript (CART) and corticotropin-releasing hormone (CRH) gene expression. *P<0.0001 vs vehicle.*

Previous data on the role of visfatin/PBEF/NAMPT in feeding modulation have been inconsistent. In chicks, ICV injection of visfatin/PBEF/NAMPT stimulated feeding (17), while in rats ICV administration of visfatin/PBEF/NAMPT decreased food intake and body weight (18).

Visfatin/PBEF/NAMPT levels seem to follow the pattern of feeding stimulatory hormone. In the liver, both the mRNA and peptide levels increase upon fasting (23), which is typical of feeding stimulating hormones such as ghrelin, which displays increased mRNA in gastric cells and plasma peptide levels during fasting (24). Conversely, the concentrations of fasting serum visfatin/PBEF/NAMPT decrease after 7 days of overfeeding (25), mimicking the decrease of plasma ghrelin levels observed following 2 weeks of overfeeding in healthy men (26).

Our current findings showing that the acute administration of visfatin/PBEF/NAMPT into the ARC significantly increases food intake in rats (Fig. 1) support a feeding stimulatory role of this peptide in the rat, in agreement with previous data on chicks (17). The conflicting results of ours in respect to Park et al. (18), which showed an anorectic effect of visfatin/PBEF/NAMPT in the rat, could be partially explained by the different routes of administration (we injected rats directly in the ARC, while Park et al. injected intracerebroventricularly) and by the different time of administration (2 h into the light phase in our model *vs* 2 h before the dark phase in Park et al. experiments). Regarding the site of injection, the administration of visfatin/PBEF/NAMPT directly into the ARC, as effected in our experiments, could better target the hypothalamic nuclei controlling feeding behavior. Catecholamines and serotonin can be regarded as central transducers of peripheral signalling at the hypothalamic level. In particular, the role of DA in feeding control is still unsettled, with both inhibitory and stimulatory effects. On one side, DA administration into the perifornical hypothalamus inhibits food intake (4), and increased DA transmission is associated with the anorectic effects of amphetamines (27). On the other hand, DA is able to stimulate feeding, after its injection into the lateral hypothalamus and higher DA levels are found in the brain of obese rats (4). In our experiment we have found a significant reduction in hypothalamic DA steady state concentrations after visfatin/PBEF/NAMPT treatment (Table I), which could be related to the feeding stimulatory role of visfatin/PBEF/NAMPT observed *in vivo*. Actually, the reduction of DA levels induced by visfatin/PBEF/NAMPT could be related to NAMPT activity to induce NAD biosynthesis (11), and NAD has been found to increase dopamine release in rat striatal slices, with consequent decrease in DA steady state levels (28). POMC/CART peptide producing neurons are mainly located in the ARC, and they project to the PVN where they stimulate CRH producing neurons. The roles of CART peptide and CRH as central mediators of anorectic pathways is well established. Central administration of CART peptide decreases both normal and starvation-induced feeding in rats (29). In addition, chronic administration of CART peptide reduces food intake and causes weight loss (30), and neutralizing antibodies to the endogenous peptide cause an increase in feeding (31). Possible mediators of the anorectic effects of CART peptide in the hypothalamus include the stimulated secretion of CRH and thyrotropin-releasing hormone by second order neurons in the PVN (32). Leptin activates POMC/CART peptide expressing neurons (33). Interestingly, both fasted rats and rodent models of obesity, such as leptin receptor-deficient Zucker *fa/fa* rats and leptin-deficient *ob/ob* mice, have reduced CART mRNA levels in the ARC. Administration of leptin to *ob/ob* mice normalized CART mRNA content in the ARC, inhibiting food intake (29). Moreover, CRH has been reported to play a key role in modulating the anorexigenic effect of leptin (34) and central leptin injections increased CRH gene expression in the PVN of fasted rats (35).

Consequently, the significant reduction of the gene expression of the anorectic mediators CART peptide and CRH shown in our experiments (Fig. 2), is consistent with the observed increase in food intake following visfatin/PBEF/NAMPT administration (Fig. 1).

In conclusion, the modulation of DA, CART and CRH activity induced by intrahypothalamic injection of visfatin/PBEF/NAMPT could account for the feeding stimulatory effect of this peptide. On the other hand, NE, 5-HT, POMC, AgRP and NPY seem not to be involved in the modulation of feeding

induced by visfatin/PBEF/NAMPT.

## ACKNOWLEDGEMENTS

This work was supported by an Italian Ministry of Education grant.

## REFERENCES

1. Kalra SP, Dube MG, Pu S, Xu B, Horvath TL, Kalra PS. Interacting appetite-regulating pathways in the hypothalamic regulation of body weight. Endocr Rev 1999; 20:68-100.
2. Schwartz MW, Woods SC, Porte D Jr, Seeley RJ, Baskin DG. Central nervous system control of food intake. Nature 2000; 404:661-71.
3. Cone RD, Cowley MA, Butler AA, Fan W, Marks DL, Low MJ. The arcuate nucleus as a conduit for diverse signals relevant to energy homeostasis. Int J Obes Relat Metab Disord 2001; 25(S)5:S63-7.
4. Brunetti L, Di Nisio C, Orlando G, Ferrante C, Vacca M. The regulation of feeding: a cross talk between peripheral and central signalling. Int J Immunopathol Pharmacol 2005; 18:201-12.
5. Galic S, Oakhill JS, Steinberg GR. Adipose tissue as an endocrine organ. Mol Cell Endocrinol 2010; 316:129-39.
6. Bulcão C, Ferreira SR, Giuffrida FM, Ribeiro-Filho FF. The new adipose tissue and adipocytokines. Curr Diabetes Rev 2006; 2:19-28.
7. Fukuhara A, Matsuda M, Nishizawa M, et al. Visfatin: a protein secreted by visceral fat that mimics the effects of insulin. Science 2005; 307:426-30. Retraction in: Fukuhara A, Matsuda M, Nishizawa M et al. Science 2007; 318:565.
8. Berndt J, Klöting N, Kralisch S, Kovacs P, Fasshauer M, Schön MR, Stumvoll M, Blüher M. Plasma visfatin concentrations and fat depot-specific mRNA expression in humans. Diabetes 2005; 54:2911-6.
9. Varma V, Yao-Borengasser A, Rasouli N, et al. Human visfatin expression: relationship to insulin sensitivity, intramyocellular lipids, and inflammation. J Clin Endocrinol Metab 2007; 92:666-72.
10. Samal B, Sun Y, Stearns G, Xie C, Suggs S, McNiece I. Cloning and characterization of the cDNA encoding a novel human pre-B-cell colony-enhancing factor. Mol Cell Biol 1994; 14:1431-7.
11. Rongvaux A, Shea RJ, Mulks MH, Gigot D, Urbain J, Leo O, Andris F. Pre-B-cell colony-enhancing factor, whose expression is up-regulated in activated lymphocytes, is a nicotinamide phosphoribosyltransferase, a cytosolic enzyme involved in NAD biosynthesis. Eur J Immunol 2002; 32:3225-34.
12. Revollo JR, Körner A, Mills KF, et al. Nampt/PBEF/Visfatin regulates insulin secretion in beta cells as a systemic NAD biosynthetic enzyme. Cell Metab 2007; 6:363-75.
13. Chen MP, Chung FM, Chang DM, Tsai JC, Huang HF, Shin SJ, Lee YJ. Elevated plasma level of visfatin/pre-B cell colony-enhancing factor in patients with type 2 diabetes mellitus. J Clin Endocrinol Metab 2006; 91:295-9.
14. Ingelsson E, Larson MG, Fox CS, et al. Clinical correlates of circulating visfatin levels in a community-based sample. Diabetes Care 2007; 30:1278-80.
15. Takebayashi K, Suetsugu M, Wakabayashi S, Aso Y, Inukai T. Association between plasma visfatin and vascular endothelial function in patients with type 2 diabetes mellitus. Metabolism 2007; 56:451-8.
16. Pagano C, Pilon C, Olivieri M, et al. Reduced plasma visfatin/pre-B cell colony-enhancing factor in obesity is not related to insulin resistance in humans. J Clin Endocrinol Metab 2006; 91:3165-70.
17. Cline MA, Nandar W, Prall BC, Bowden CN, Denbow DM. Central visfatin causes orexigenic effects in chicks. Behav Brain Res 2008; 186:293-7.
18. Park BS, Jin SH, Park JJ, Park JW, Namgoong IS, Kim YI, Lee BJ, Kim JG. Visfatin induces sickness responses in the brain. PLoS One 2011; 6:e15981.
19. Paxinos G, Watson C. The rat brain in stereotaxic coordinates. Ed. Academic Press. New York, 2007.
20. Livak KJ, Schmittgen TD. Analysis of relative gene expression data using real-time quantitative PCR and the 2(-Delta Delta C(T)) Method. Methods 2001; 25:402-8.
21. Hallschmid M, Randeva H, Tan BK, Kern W, Lehnert H. Relationship between cerebrospinal fluid visfatin (PBEF/Nampt) levels and adiposity in humans. Diabetes 2009; 58:637-40.

22. McGlothlin JR, Gao L, Lavoie T, Simon BA, Easley RB, Ma SF, Rumala BB, Garcia JG, Ye SQ. Molecular cloning and characterization of canine pre-B-cell colony-enhancing factor. Biochem Genet 2005; 43:127-41.
23. Yang H, Yang T, Baur JA, et al. Nutrient-sensitive mitochondrial NAD+ levels dictate cell survival. Cell 2007; 130:1095-107.
24. Lee HM, Wang G, Englander EW, Kojima M, Greeley GH Jr. Ghrelin, a new gastrointestinal endocrine peptide that stimulates insulin secretion: enteric distribution, ontogeny, influence of endocrine, and dietary manipulations. Endocrinology 2002; 143:185-90.
25. Sun G, Bishop J, Khalili S, et al. Serum visfatin concentrations are positively correlated with serum triacylglycerols and down-regulated by overfeeding in healthy young men. Am J Clin Nutr 2007; 85:399-404.
26. Robertson MD, Henderson RA, Vist GE, Rumsey RD. Plasma ghrelin response following a period of acute overfeeding in normal weight men. Int J Obes Relat Metab Disord 2004; 28:727-33.
27. Samanin R, Garattini S. Neurochemical mechanism of action of anorectic drugs. Pharmacol Toxicol 1993; 73:63-8.
28. Pearl SM, Antion MD, Stanwood GD, Jaumotte JD, Kapatos G, Zigmond MJ. Effects of NADH on dopamine release in rat striatum. Synapse 2000; 36:95-101.
29. Kristensen P, Judge ME, Thim L, et al. Hypothalamic CART is a new anorectic peptide regulated by leptin. Nature 1998; 393:72-6.
30. Larsen PJ, Vrang N, Petersen PC, Kristensen P. Chronic intracerebroventricular administration of recombinant CART(42-89) peptide inhibits and causes weight loss in lean and obese Zucker (fa/fa) rats. Obes Res 2000; 8:590-6.
31. Lambert PD, Couceyro PR, McGirr KM, Dall Vechia SE, Smith Y, Kuhar MJ. CART peptides in the central control of feeding and interactions with neuropeptide Y. Synapse 1998; 29:293-8.
32. Stanley SA, Small CJ, Murphy KG, et al. Actions of cocaine- and amphetamine-regulated transcript (CART) peptide on regulation of appetite and hypothalamo-pituitary axes in vitro and in vivo in male rats. Brain Res 2001; 893:186-94.
33. Elias CF, Aschkenasi C, Lee C, Kelly J, Ahima RS, Bjorbaek C, Flier JS, Saper CB, Elmquist JK. Leptin differentially regulates NPY and POMC neurons projecting to the lateral hypothalamic area. Neuron 1999; 23:775-86.
34. Uehara Y, Shimizu H, Ohtani K, Sato N, Mori M. Hypothalamic corticotropin-releasing hormone is a mediator of the anorexigenic effect of leptin. Diabetes 1998; 47:890-3.
35. Schwartz MW, Seeley RJ, Campfield LA, Burn P, Baskin DG. Identification of targets of leptin action in rat hypothalamus. J Clin Invest 1996; 98:1101-6.

# CLOCK GENE EXPRESSION IN MOUSE KIDNEY AND TESTIS: ANALYSIS OF PERIODICAL AND DYNAMICAL PATTERNS

G. MAZZOCCOLI[1], M. FRANCAVILLA[2], F. GIULIANI[2], F. AUCELLA[3], M. VINCIGUERRA[4], V. PAZIENZA[5], A. PIEPOLI[5], G. BENEGIAMO[5], S. LIU[6] and Y. CAI[6]

*[1]Department of Medical Sciences, Division of Internal Medicine and Chronobiology Unit, IRCCS Scientific Institute and Regional General Hospital "Casa Sollievo della Sofferenza", San Giovanni Rotondo, Italy; [2]Computing Unit, IRCCS Scientific Institute and Regional General Hospital "Casa Sollievo della Sofferenza", San Giovanni Rotondo, Italy; [3]Department of Nephrology, IRCCS Scientific Institute and Regional General Hospital "Casa Sollievo della Sofferenza", San Giovanni Rotondo, Italy; [4]Institute of Hepatology, Birkbeck College, London, United Kingdom; [5]Research Laboratory and Gastroenterology Unit, IRCCS Scientific Institute and Regional General Hospital "Casa Sollievo della Sofferenza", San Giovanni Rotondo, Italy; [6]Department of Neurology and Neurobiology, Xuanwu Hospital of Capital Medical University, Key Laboratory for Neurodegenerative Diseases of Ministry of Education, Beijing, P.R. China*

*Received October 20, 2011 – Accepted May 14, 2012*

**Molecular clocks drive circadian rhythmicity of cellular functions in peripheral tissues and organs, kidney included, whereas in the testis this clockwork seems constitutively active. We have evaluated the periodicity and the dynamics of expression of the clock genes *BMAL1, CLOCK, PER1, PER2, CRY1, CRY2* and *REV ERBα* over 24 h in the kidney and testis using a mouse model. The periodicity was explored by single cosinor, and dynamics were explored by calculation of fractional variations of gene expression related to time intervals. Kidney and testis were harvested at 4-h intervals over a 24-h period from eight-week-old C57BL/6 male mice housed individually on a 12 h light (L)-dark (D) cycle (lights on at 08:00 h; lights off at 20:00 h) and mRNA was extracted and analyzed by Quantitative Real-time Reverse Transcription PCR. A statistically significant difference was evidenced between kidney and testis for the original values of expression level of *BMAL1*, *PER1, PER2 CRY1*, *CRY2* and *REV ERBα*. A statistically significant difference was evidenced between kidney and testis for the fractional variation of *BMAL1*, *PER2*, *CRY1*, *CRY2* and *REV ERBα*. A significant 24-h rhythmic component was found for *BMAL1, CLOCK, PER1, PER2, CRY1, CRY2* and *REV ERBα* in the kidney, whereas no core clock gene showed circadian rhythmicity in the testis. Fractional variations provided significant circadian rhythms for *BMAL1, PER2, CRY, CRY2* and *REV ERBα* in the kidney, whereas in the testis the fractional variation calculations showed no circadian rhythmicity, but quantitative comparison showed statistically significant differences in only 16.7% of the time points studied. In conclusion, in the kidney the clock gene machinery shows circadian oscillation of mRNA levels and time-related variations in the rate of change of clock gene expression. In the testis the clock genes do not show circadian rhythmicity of expression and the dynamics of variation are not characterized by a periodical pattern, but are quantitatively similar to those observed in the kidney. These data suggest that in the testis the clock gene machinery shows a tissue-specific pattern of function and clock genes may play a different role in the**

*Key words: clock gene, circadian rhythm, kidney, testis, fractional variation*

*Mailing address:* Dr Gianluigi Mazzoccoli,
Department of Medical Sciences,
Division of Internal Medicine and Chronobiology Unit,
Scientific Institute and Regional General Hospital
"Casa Sollievo della Sofferenza", San Giovanni Rotondo (FG), Italy
Tel: +39 0882 835228 Fax: +39-0882 410563
e-mail: g.mazzoccoli@tin.it



0393-974X (2012)

**testis with regard to other peripheral tissues, maybe in relation to the presence of developmental and differentiation phenomena.**

Living organisms are characterized by time related variations of biological processes and functions and the rhythmic changes of many physiological parameters show a periodicity that corresponds to the 24-h terrestrial day (1, 2). Circadian rhythmicity in mammals is driven by a circadian timing system, timed by pacemaker neurons of the suprachiasmatic nuclei of the hypothalamus (SCN), that are entrained by the environmental light/dark cycle and in turn synchronize peripheral clocks present in nearly all tissue cells (3, 4). These molecular circadian clocks are encoded by a set of core clock genes (*BMAL1*, *CLOCK* or its paralog *NPAS2*, *PERIOD*, *CRYPTOCHROME*, *TIMELESS*, *REVERB α/β*), coding for transcriptional activators and repressors realizing an autoregulatory transcription-translation feedback loop that completes one cycle in approximately 24 hours (5-7). The *PERIOD* genes (*PER1-3*) and *CRYPTOCHROME* genes (*CRY1-2*) constitute the negative limb of the loop and are transcriptionally activated by the basic helix–loop–helix PAS transcription factors *CLOCK* and *BMAL1*, which heterodimerize and bind to E-box enhancer elements in the promoters of these genes, functioning as the positive limb of the feedback loop (8, 9). The *PER* and *CRY* mRNAs translated into their respective proteins, along with Casein Kinase I δ/ε (CKI δ/ε), interact to form a repression complex that translocates back into the nucleus, interacts directly with *CLOCK* and *BMAL1*, and result in loss of their activation activity (10-12). An auxiliary loop is represented by the nuclear receptors REV-ERB α/β, as CLOCK and BMAL1 also activate the expression of *REV-ERB α/β*, that in turn negatively controls the rhythmic transcription of *BMAL1* (13, 14). The core clock genes drive also the rhythmic expression of the clock-controlled genes which are responsible for various metabolic or proliferative functions and link the physiological processes to the circadian environment, controlling tissue/organ key functions and making these functions available at specific times during each day when they are most needed (15).

In the kidney, diurnal changes of renal blood flow and renal cellular functions regulate Na+ concentration and renal Na+ excretion and a number of genes display a significant diurnal variation in animal models (16), whereas in the testis the expression of clock genes seems non-rhythmic (17).

The aim of our study is to evaluate in a mouse model the periodical and dynamical patterns of clock gene expression in the genito-urinary system, focusing on the kidney and testis and using a data subset (18). Periodicity relates to the oscillatory pattern of clock gene expression, whereas the dynamics and rate of change in clock gene expression may influence the molecular cascade from the clock gene oscillators to cellular function. The periodicity was explored by the least squares fit of a 24-hour cosine curve to the data, and dynamics were explored by calculation of fractional variations of gene expression related to time intervals.

## MATERIALS AND METHODS

*Animals*

Eight-week-old C57BL/6 male mice were housed individually on a 12-h light (L)-dark (D) cycle (lights on at 08:00 h; lights off at 20:00 h), with food and water available *ad libitum*, for two weeks after arrival at the animal facility. Care of the mice was in accordance with the Institutional Animal Care and Use Committee guidelines at the Capital Medical University and in agreement with the ethical standards. For SYBR Green I-based analysis, three to four mice at each of the six time points were sacrificed at 4-h intervals over a 24-h period beginning at 09:00 h (= 01 HALO = Hours After Light Onset). Kidney and testis were harvested and stored in RNAlater (Qiagen, Alameda, California, USA). Total RNA was extracted from organs using RNAeasy kit (Qiagen, Alameda, California, USA) according to the manufacturer's instructions. To eliminate genomic DNA, total RNA was treated with RQ1 RNase free DNase I (Promega, San Luis Obispo, California, USA) according to the manufacturer's instructions.

*Real-time Quantitative Reverse Transcription PCR*

To generate single-strand cDNAs, total RNA (~1μg) was reverse transcribed using Superscript II (Invitrogen, Carlsbad, California, USA) and random hexamers. For SYBR Green I-based analysis, the cDNA equivalent of 50 ng of total RNA from each sample was amplified in an

Opticon II system (MJ Research, Waltham, Massachusetts, USA) using a SYBRGreen I real-time PCR kit (Takara, Otsu Shiga, Japan). Each sample was analyzed in duplicate to ensure the accuracy of the data. 18S, a housekeeping gene, was used to normalize the differences in sample RNA content.

*Primer Sequences Used in Real-Time Quantitative Reverse Transcription PCR (SYBR Green I)*

*BMAL1* Forward ACATAGGACACCTCGCAGAA Reverse AACCATCGACTTCGTAGCGT

*CLOCK* Forward CCTATCCTACCTTCGCCACACA Reverse TCCCGTGGAGCAACCTAGAT

*PER1* Forward CATGACTGCACTTCGGGAGC Reverse CTTGACACAGGCCAGAGCGTA

*PER2* Forward GGCTTCACCATGCCTGTTGT Reverse GGAGTTATTTCGGAGGCAAGTGT

*CRY1* Forward TTGCCTGTTTCCTGACTCGT Reverse GACAGCCACATCCAACTTCC

*CRY2* Forward TCGGCTCAACATTGAACGAA Reverse GGGCCACTGGATAGTGCTCT

*REV-ERB*α Forward CGTTCGCATCAATCGCAACC Reverse GATGTGGAGTAGGTGAGGTC

18S Forward TTCGGAACTGAGGCCATGAT Reverse TTTCGCTCTGGTCCGTCTTG

*Statistics*

The fractional variation (in percent) between single timepoint gene expression values was calculated to evaluate the dynamics (% change) of the rise and fall in gene expression between 4h time points (19). The fractional variation between single time point values was calculated according to the formula:

$$FV = \left| \frac{y(t_{n+1}) - y(t_n)}{y(t_n)} \right| \%$$

where *y* is the original gene expression level, *t* is the sampling time and *n* ranges from 1 (first sample) to 6 (the last sample).

Rates of change were calculated between time points (e.g., $PER1_{(tn+1)}$ relative abundance level minus $PER1_{(tn)}$ relative abundance level, divided by $PER1_{(tn)}$ relative abundance level x 100 = % change). For statistical analyses, direction of this change (+ or –) was ignored in order to focus on the quantity of change, since the computations in reverse (i.e., time 1 minus time 2/time 1 x 100) would give the same quantity change, but with the opposite + or – sign).

Original values of gene expression levels and fractional variation calculations for each clock gene were normalized to percent of mean to reduce inter-subject variability in levels prior to analyses for time-effects on grouped data. This is widely carried out in grouped analyses for biological rhythms in order to detect and describe the 24-h pattern unaffected by differences in average levels between subjects.

Gene expression data were assigned to actual collection time and fractional rates were assigned to the mid-point of each 4-h calculation span (e.g., 11:00h for 09:00-13:00h, etc.).

Using grouped data, overall gene expression levels and fractional rates were then analyzed for time-effect across the six time points by one-way analysis of variance (ANOVA) and Kruskal-Wallis one-way ANOVA on Ranks followed by all pairwise multiple comparison procedures (Student-Newman-Keuls method or Dunn's method) as indicated.

Gene expression original values and fractional variations were then analyzed for differences between kidney and testis by Student's *t*-test or Mann Whitney Rank Sum test as indicated.

Each time-series of expression levels and fractional variations was analyzed for circadian rhythm characteristics by the single cosinor procedure involving the fit of a 24-h cosine curve to the data by least-squares linear regression using the Chronolab statistical package, in order to accurately describe waveforms and rhythm characteristics (e.g., amplitude, phase). An $R^2$ value and a p value for the rejection of the zero-amplitude assumption were determined for each component in the cosine model separately and overall, with rhythm detection considered statistically significant if $p \leq 0.05$ for any period tested. Circadian (24h) characteristics were summarized from the 24-h cosine Rhythm characteristics determined from the best-fitting cosine model include the mesor (the middle of the cosine representing an adjusted average if unequal sampling), the amplitude, A (half the distance from the peak and trough of the best fitting curve, with 2A indicating a predictable range of change), and the phase (Ø) of the cosine model (referenced to an external event, such as local midnight or time of light onset), with the peak of a single component cosine called the acrophase, aØ (acro = peak).

## RESULTS

### *Original Values of clock gene expression levels in kidney and testis*

As shown in Fig. 1, a statistically significant difference was evidenced between kidney and testis for the expression of *BMAL1* at 01:00h (p=0.009), 05:00h (p=0.002), 09:00h (p=0.001) and 13:00h (p=0.006), *CLOCK* at 05:00h (p=0.019), *PER1* at

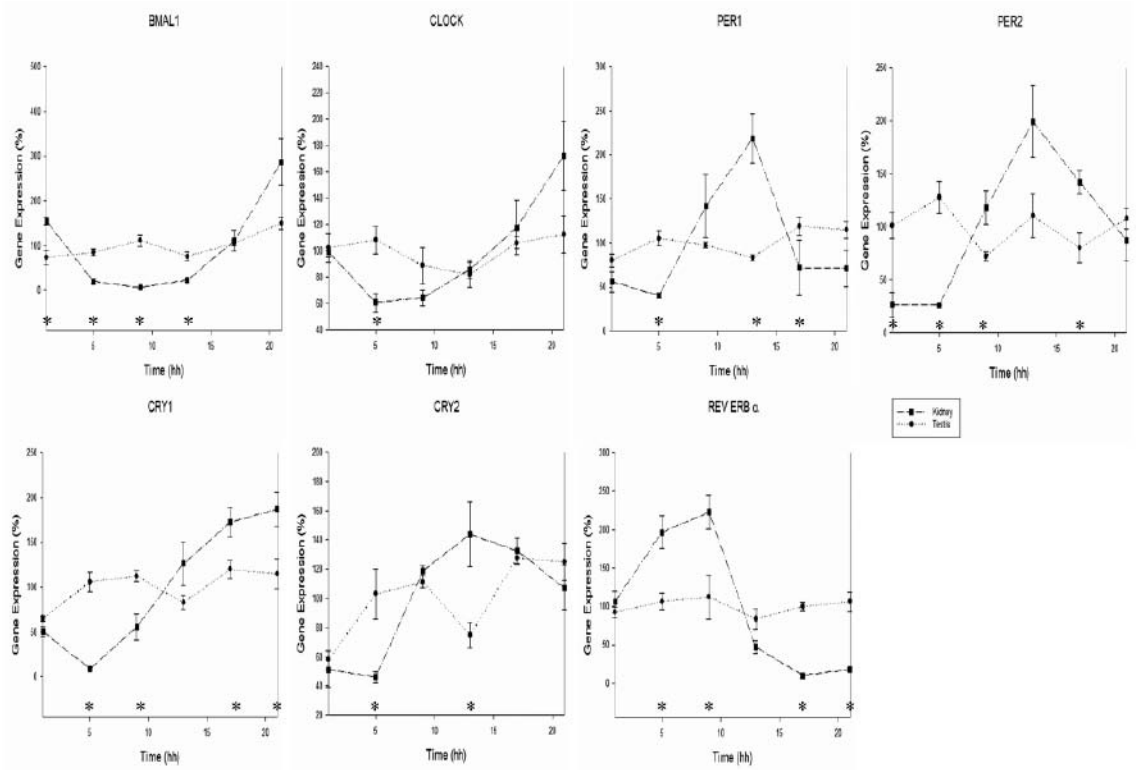


**Fig. 1.** *x-y plots showing the 24-h profiles of expression level changes in mouse clock genes in kidney and testis. Gene expression data assigned to actual collection time. * p< 0.05*

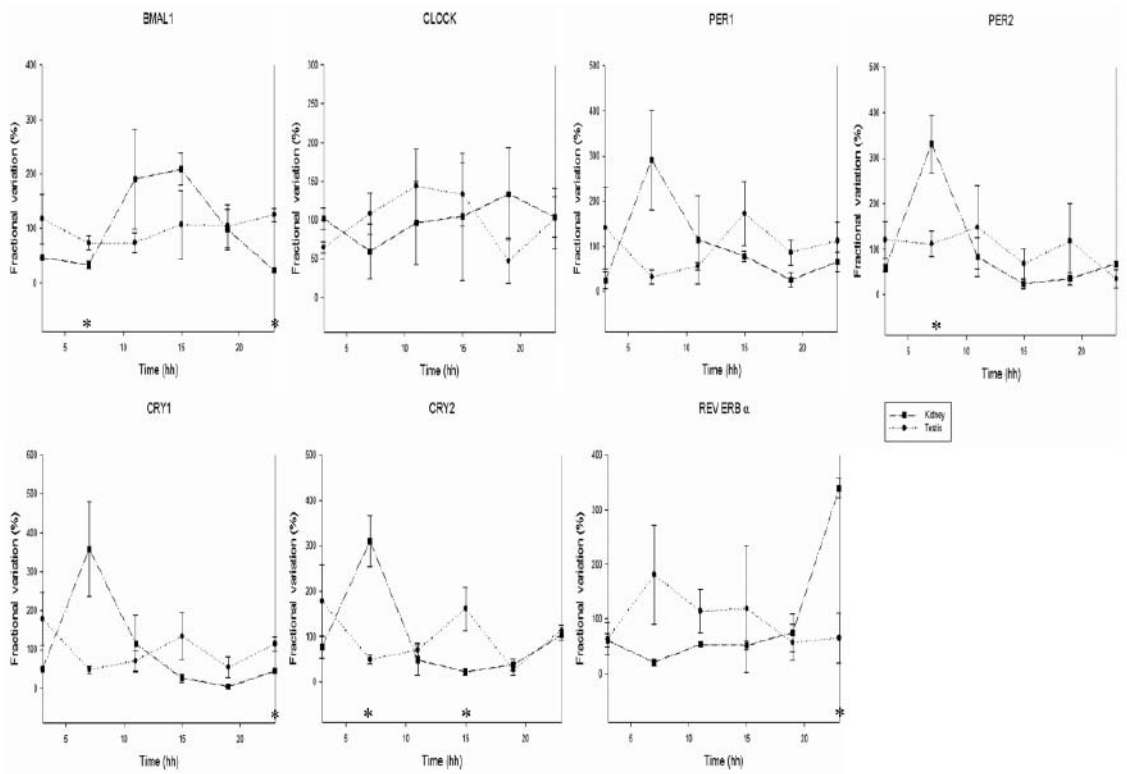


**Fig. 2.** *x-y plots showing the 24-h profiles of fractional variations calculated among single timepoint clock genes expression levels in kidney and testis. Fractional variations assigned to the mid-point of each 4-h calculation span. * p< 0.05*

**Table I.** *Rhythm parameters for mRNA expression calculated on original values normalized to % of mean.*

| | ANOVA | | | Single Cosinor | | | |
|---|---|---|---|---|---|---|---|
| Gene symbol | F | p | p | MESOR | Amplitude | Acrophase | (95% Confidence Limits) |
| | | | | ***Kidney*** | | | |
| *BMAL1* | 21.1 | <0.001 | <0.001 | 100.00±12.60 | 131.24±17.83 | 320.1±7.8 | (303, 337) |
| *CLOCK* | 8.2 | 0.001 | <0.001 | 100.00±6.45 | 49.18±9.13 | 300.1±10.6 | (277, 323) |
| *PER1* | 7.6 | 0.002 | 0.004 | 100.00±12.72 | 72.17±17.99 | 186.0±14.3 | (154, 218) |
| *PER2* | 13.6 | <0.001 | <0.001 | 100.00±7.46 | 85.51±10.55 | 211.7±7.1 | (196, 2279 |
| *CRY1* | 22.0 | <0.001 | <0.001 | 100.00±7.09 | 90.72±10.03 | 265.2±6.3 | (252, 279) |
| *CRY2* | 10.6 | <0.001 | <0.001 | 100.00±5.31 | 51.95±7.51 | 219.6±8.3 | (202, 238) |
| *REV ERBα* | 41.6 | <0.001 | <0.001 | 100.00±7.74 | 114.28±10.95 | 96.6±5.5 | (85, 108) |
| | | | | ***Testis*** | | | |
| *BMAL1* | 6.4 | 0.004 | 0.278 | 100.00±7.33 | 17.34±10.37 | 292.2±34.3 | (0, 0) |
| *CLOCK* | 1.2 | 0.370 | 0.151 | 100.00±4.31 | 12.65±6.10 | 345.8±27.6 | (0, 0) |
| *PER1* | 4.4 | 0.016 | 0.380 | 100.00±4.38 | 8.90±6.19 | 282.6±39.8 | (0, 0) |
| *PER2* | 7.2 | 0.003 | 0.496 | 100.00±6.60 | 11.32±9.33 | 32.5±47.3 | (0, 0) |
| *CRY1* | 4.7 | 0.013 | 0.579 | 100.00±6.03 | 9.09±8.53 | 226.8±53.8 | (0, 0) |
| *CRY2* | 7.8 | 0.002 | 0.439 | 100.00±7.15 | 13.34±10.10 | 251.1±43.4 | (0, 0) |
| *REV ERBα* | 0.5 | 0.783 | 0.858 | 100.00±6.01 | 4.74±8.51 | 65.4±102.8 | (0, 0) |

*Using grouped data, overall gene expression levels were analyzed for time-effect across the six time points by one-way analysis of variance (ANOVA) and Kruskal-Wallis one-way ANOVA on Ranks followed by all pairwise multiple comparison procedures (Student-Newman-Keuls method or Dunn's method) as indicated. Single Cosinor: fit of 24 h cosine to all data by least squares linear regression. Acrophase, the crest time of rhythm, is expressed in degrees.*

**Table II.** *Rhythm parameters for fractional variations calculated on mRNA level values normalized to % of mean.*

| | ANOVA | | | Single Cosinor | | | |
|---|---|---|---|---|---|---|---|
| Gene symbol | F | p | p | MESOR | Amplitude | Acrophase | (95% Confidence Limits) |
| | | | | ***Kidney*** | | | |
| *BMAL1* | 3.8 | 0.028 | 0.004 | 100.0±17.07 | 97.51±24.14 | 207.3±14.2 | (175, 239) |
| *CLOCK* | 0.2 | 0.947 | 0.616 | 100.00±18.69 | 26.42±26.43 | 288.0±57.3 | (0, 0) |
| *PER1* | 2.6 | 0.082 | 0.096 | 100.00±27.88 | 92.58±39.43 | 123.7±24.4 | (0, 0) |
| *PER2* | 12.8 | <0.001 | 0.013 | 100.00±22.18 | 107.14±31.37 | 101.8±16.8 | (63, 140) |
| *CRY1* | 5.2 | 0.009 | 0.016 | 100.00±28.59 | 134.33±40.43 | 110.7±17.2 | (71, 151) |
| *CRY2* | 13.0 | <0.001 | 0.019 | 100.00±21.07 | 96.31±29.80 | 85.7±17.7 | (44, 127) |
| *REV ERBα* | 46.7 | <0.001 | 0.010 | 100.0±21.00 | 106.36±29.69 | 337.9±16.0 | (301, 14) |
| | | | | ***Testis*** | | | |
| *BMAL1* | 0.3 | 0.876 | 0.472 | 100.00±13.74 | 24.40±19.43 | 331.1±45.6 | (0, 0) |
| *CLOCK* | 1.2 | 0.365 | 0.228 | 100.00±13.95 | 35.66±19.73 | 168.6±31.7 | (0, 0) |
| *PER1* | 1.0 | 0.446 | 0.566 | 100.00±21.77 | 33.46±30.78 | 297.2±52.7 | (0, 0) |
| *PER2* | 0.5 | 0.754 | 0.627 | 100.00±22.21 | 30.82±31.41 | 139.6±58.4 | (0, 0) |
| *CRY1* | 1.6 | 0.237 | 0.637 | 100.00±18.65 | 25.41±26.38 | 10.3±59.5 | (0, 0) |
| *CRY2* | 2.4 | 0.095 | 0.829 | 100.00±20.11 | 17.54±28.44 | 25.2±92.9 | (0, 0) |
| *REV ERBα* | 0.5 | 0.765 | 0.399 | 100.00±25.44 | 50.28±35.98 | 141.8±41.0 | (0, 0) |

*Using grouped data, overall fractional variations calculated on time qualified gene expression levels were analyzed for time-effect across the six time points by one-way analysis of variance (ANOVA) and Kruskal-Wallis one-way ANOVA on Ranks followed by all pairwise multiple comparison procedures (Student-Newman-Keuls method or Dunn's method) as indicated. Single Cosinor: fit of 24 h cosine to all data by least squares linear regression. Acrophase, the crest time of rhythm, is expressed in degrees.*

05:00h (p=0.002), 13:00h (p=0.008) and 17:00h (p=0.042), for *PER2* at 01:00h (p=0.011), 05:00h (p=0.002), 09:00h (p=0.050) and 17:00h (p=0.027), for *CRY1* at 05:00h (p<0.001), 09:00h (p=0.021), 17:00h (p=0.047) and 21:00h (p=0.047), for *CRY2* at 05:00h (p=0.032) and 13:00h (p=0.045), for *REV-ERBα* at 05:00h (p=0.021), 09:00h (p=0.037), 17:00h (p<0.001) and 21:00h (p=0.002).

No statistically significant difference was evidenced between kidney and testis for the expression of *BMAL1* at 17:00h (p=0.839) and 21:00h (p=0.064), *CLOCK* at 01:00h (p=0.791), 09:00h (p=0.180), 13:00h (p=0.751), 17:00h (p=0.614) and 21:00h (p=0.113), *PER1* at 01:00h (p=0.153), 09:00h (p=0.283), 17:00h (p=0.227) and 21:00h (p=0.129), *PER2* at 13:00h (p=0.089) and 21:00h (p=0.391), *CRY1* at 01:00h (p=0.088) and 13:00h (p=0.159), *CRY2* at 01:00h (p=0.642), 09:00h (p=0.217), 17:00h (p=0.648) and 21:00h (p=0.425), *REV-ERBα* at 01:00h (p=0.427) and 13:00h (p=0.080),.

*Fractional variations among single time point clock gene expression levels in kidney and testis*

As shown in Fig. 2, a statistically significant difference was evidenced between kidney and testis for the fractional variation of *BMAL1* at 07:00h (p=0.050) and 23:00h (p=0.001), *PER2* at 07:00h (p=0.034), *CRY1* at 23:00h (p=0.019), *CRY2* at 07:00h (p=0.010) and 15:00h (p=0.045), *REV-ERBα* at 23:00h (p=0.005) (7 over 42 time points = 16.7%)

No statistically significant difference was evidenced between kidney and testis for the FV of *BMAL1* at 03:00h (p=0.193), 11:00h (p=0.280), 15:00h (p=0.214) and 19:00h (p=0.915), *CLOCK* at 03:00h (0.076), 07:00h (p=0.332), 11:00h (0.541), 15:00h (p=0.770), 19:00h (p=0.268) and 23:00h (p=0.971), *PER1* at 03:00h (p=0.280), 07:00h (p=0.080), 11:00h (p=0.585), 15:0 (p=0.258), 19:00h (p=0.137) and 23:00h (p=0.377), *PER2* at 03:00h (p=0.209), 11:00h (p=0.558), 15:00h (p=0.284), 19:00h (0.382) and 23:00h (p=0.190), *CRY1* at 03:00h (p=0.133), 07:00h (p=0.064), 11:00h (p=0.598), 15:00h (p=0.149) and 19:00h (p=0.138), *CRY2* at 03:00h (p=0.296), 11:00h (p=0.583), 19:00h (p=0.572) and 23:00h (p=0.569), *REV-ERBα* at 03:00h (p=0.927), 07:00h (p=0.151), 11:00h (p=0.201), 15:00h (p=0.595) and 19:00h (p=0.734).

*Rhythm features of clock gene expression in kidney and testis*

Results from ANOVA and 24h cosinor analyses for circadian time-effects on original values of expression levels and fractional variations among single time points for each CG in each tissue are listed in Table I and Table II, respectively.

A time effect was evidenced by ANOVA for the original values of expression of *BMAL1, CLOCK, PER1, PER2, CRY1, CRY2* and *REV-ERBα* for the kidney and for *BMAL1, PER1, PER2, CRY1* and *CRY2* for the testis.

A time effect was evidenced by ANOVA for the fractional variations calculated on the time qualified original values of expression of *BMAL1, PER2, CRY1, CRY2* and *REV-ERBα* for the kidney and for no clock gene for the testis.

A significant 24-h rhythmic component was found for *BMAL1, CLOCK, PER1, PER2, CRY1, CRY2* and *REV-ERBα* in the kidney, whereas no core clock gene showed circadian rhythmicity in the testis.

Fractional variations provided significant circadian rhythms for *BMAL1, PER2, CRY, CRY2* and *REV-ERBα* in the kidney, whereas in the testis the calculations of fractional variation showed no circadian rhythmicity.

## DISCUSSION

Our data resulting from 24-h cosinor analyses for circadian time-effects on original values of expression levels showed a significant 24-h rhythmic component for *BMAL1, CLOCK, PER1, PER2, CRY1, CRY2* and *REV-ERBα* in the kidney, whereas no core clock gene showed circadian rhythmicity in the testis. Similarly, fractional variation calculations among single time points for each clock gene in each tissue provided significant circadian rhythms for *BMAL1, PER2, CRY, CRY2* and *REV-ERBα* in the kidney, whereas in the testis the calculations of fractional variation showed no circadian rhythmicity, but quantitatively the rates of change were comparable between the kidney and the testis.

These results are in agreement with previous reports that evidenced circadian rhythmicity of expression of clock genes and clock controlled genes in the kidney, suggesting that the transcriptional

machinery of peripheral clocks in renal tubular cells directly regulates the circadian expression of key functional output genes (20). Renal tubular NHE3, the Na(+)/H(+) exchanger, is a clock-controlled gene regulated directly by CLOCK:BMAL1 heterodimers in kidneys, and in rat kidney NHE3 mRNA level displays circadian kinetics. NHE3 is one of the Na+/H+ exchangers (NHEs) that catalyze the electroneutral exchange of one extracellular Na+ for one intracellular H+ across the plasma membrane, represents an output gene of the peripheral oscillators in the kidney, and is critical for systemic electrolyte and acid-base homeostasis. The transcription and translation product of this clock-controlled gene mediates bulk reabsorption of filtered Na+ in the proximal convoluted tubule, is required for maintenance of normal set point for Na+ fluid volume balance and plays a central role in the long-term control of arterial blood pressure (21).

Differently from other peripheral tissues, examination of oscillating expression of clock genes in the testis and in extratesticular ducts and accessory organs of different animal models has yielded discrepant results, suggesting tissue-specific patterns of endogenous peripheral clock expression (22-25). We did not find circadian rhythmicity in the expression of *BMAL1, CLOCK, PER1, PER2, CRY1, CRY2* and *REV-ERBα* in the mouse testis and the evaluation of periodicity in the rate of change of gene expression showed no time related differences. These results are in agreement with several mammalian studies, but it is worth interpreting them on the premise that in photoperiodic mammals reproduction is a peripheral activity that is strongly influenced by the circadian clock. Most mammals that exhibit a seasonal cycle are able to decode the daily changes in light across the year and to translate these in hormonal signals that regulate reproductive cycles. Expression of many clock genes has been revealed in mouse testis, although transcription of these genes seems to be constitutive in 24 h, suggesting that these genes may play a different role in the testis with regard to the central clockwork function. The internal clock gene machinery may regulate developmental and differentiation phenomena, while the environmental factors, such as photoperiod and temperature, affect the endogenous elements. Temperature signals have a direct influence on clock processes such as transcription, translation, protein phosphorylation and degradation, and the expression of circadian clock genes, such as *PER2*, is affected by length of photoperiod, so that the core clockwork may also decode seasonal information (26).

Clock gene expression likely plays a role in testicular steroidogenesis, as BMAL1 protein oscillates in mouse Leydig cells and *BMAL1* KO mice exhibit decreases in *StAR* expression and testosterone production with infertility (27, 28). Clock genes may play non-circadian roles in spermatogenesis, as several studies revealed constitutively elevated and non-rhythmic expression levels of *PER* and *CRY* in whole testes or within the seminiferous tubules (29, 30). The testis is composed primarily of differentiating cells and the circadian clock might be not operational in immature, differentiating cells, and may start ticking in mature cells upon receipt of an initiating signal (31)

The expression of clock genes in the testis is not circadian rhythmic, however the statistical analysis of variance shows a time effect and the dynamics of variation are quantitatively similar to those depicted in the kidney, since we have demonstrated statistically significant differences in less than 20% of the analyzed time points. These data may indicate a tissue-specific pattern of function of the clock gene machinery in the testis in respect to other peripheral tissues or organs and in particular to the kidney. The circadian clock system drives genes that gate rate-limiting steps of organ functions and may control post-translational processes in the regulation of gene product activity, so that first order clock-controlled genes in the peripheral organs may be mediators of circadian information (32). In the testis the core feedback loop could transduce its signal to downstream effectors in a tissue-specific pattern and clock genes may play a different role in the testis with regard to other peripheral tissues and organs, maybe in relation to the presence of developmental and differentiation phenomena.

In conclusion, we have demonstrated a circadian rhythmicity in the oscillation and in the dynamics of variation of clock gene expression in the kidney, whereas in the testis the pattern of clock gene expression is not circadian rhythmic, but the statistical analysis of the rate of change showed quantitative similarities in the dynamics of variation.

The clock gene machinery in the kidney drives the circadian expression of key functional ouput genes, whereas in the testis the presence of differentiating cells may impinge on a tissue-specific pattern of function of the biological clockwork, independently from the circadian timing system.

## ACKNOWLEDGEMENTS

This study was supported by a grant from the Italian Ministry of Health through Department of Medical Sciences, Division of Internal Medicine and Chronobiology Unit (RC1203ME46), IRCCS Scientific Institute and Regional General Hospital "Casa Sollievo della Sofferenza", Opera di Padre Pio da Pietrelcina, San Giovanni Rotondo (FG), Italy.

## REFERENCES

1. Takahashi JS, Hong HK, Ko CH, McDearmon EL. The genetics of mammalian circadian order and disorder: implications for physiology and disease. Nat Rev Genet 2008; 9:764-75.
2. Mazzoccoli G. The timing clockwork of life. J Biol Regul Homeost Agents 2011; 25:137-43.
3. Schibler U, Sassone-Corsi P. A web of circadian pacemakers. Cell 2002; 111:919-22.
4. Hastings MH, Reddy AB, Maywood ES. A clockwork web: circadian timing in brain and periphery, in health and disease. Nat Rev Neurosci 2003; 4:649-61.
5. Filipski E, King VM, Etienne MC, Li XM, Claustrat B, Granda TG. Persistent twenty-four hour changes in liver and bone marrow despite suprachiasmatic nuclei ablation in mice. Am J Physiol Regul Integr Comp Physiol 2004; 287:844-51.
6. Reppert SM, Weaver DR. Molecular analysis of mammalian circadian rhythms. Annu Rev Physiol 2001; 63:647-76.
7. Nagoshi E, Saini C, Bauer C, Laroche T, Naef F, Schibler U. Circadian gene expression in individual fibroblasts: cell-autonomous and self-sustained oscillators pass time to daughter cells. Cell 2004; 119:693-705.
8. Young MW, Kay SA. Time zones: a comparative genetics of circadian clocks. Nat Rev Genet 2001; 2:702-15.
9. Yu W, Nomura M, Ikea M. Interactivating feedback loops within the mammalian clock: BMAL1 is negatively autoregulated and upregulated by CRY1, CRY2, and PER2. Biochem Biophys Res Comm 2002; 290:933-41.
10. Eide EJ, Vielhaber EL, Hinz WA, Virshup DM. The Circadian Regulatory Proteins BMAL1 and Cryptochromes Are Substrates of Casein Kinase Iε. J Biol Chem 2002; 277:17248-54.
11. Lee C, Etchegaray JP, Cagampang FR, Loudon AS, Reppert SM. Posttranslational mechanisms regulate the mammalian circadian clock. Cell 2001; 28:855-67.
12. Sahar S, Zocchi L, Kinoshita C, Borrelli E, Sassone-Corsi P. Regulation of BMAL1 Protein Stability and Circadian Function by GSK3b-Mediated Phosphorylation. PLoS ONE 2010; 5:1-9.
13. Liu AC, Tran HG, Zhang EE, Priest AA, Welsh DK, Kay SA. Redundant function of REV-ERBalpha and beta and nonessential role for Bmal1 cycling in transcriptional regulation of intracellular circadian rhythms. PLoS Genet 2008; 4:e1000023.
14. Preitner N, Damiola F, Lopez-Molina L, Zakany J, Duboule D, Albrecht U. The orphan nuclear receptor REV-ERBalpha controls circadian transcription within the positive limb of the mammalian circadian oscillator. Cell 2002; 110:251-60.
15. Ueda UR, Hayashi S, Chen W, et al. System-level identification of transcriptional circuits underlying mammalian circadian clocks. Nat Genet 2005; 37:187-92.
16. Fang Z, Carlson SH, Peng N, Wyss JM. Circadian rhythm of plasma sodium is disrupted in spontaneously hypertensive rats fed a high-NaCl diet. Am J Physiol Regul Integr Comp Physiol 2000; 278:R1490-R1495.
17. Yamamoto T, Nakahata Y, Soma H, Akashi M, Mamine T, Takumi T. Transcriptional oscillation of canonical clock genes in mouse peripheral tissues. BMC Mol Biol 2004; 5:18.
18. Liu S, Cai Y, Sothern RB, Guan Y, Chan P. Chronobiological analysis of circadian patterns in transcription of seven key clock genes in six peripheral tissues in mice. Chronobiol Int 2007; 24:793-820.
19. Mazzoccoli G, Giuliani F, Sothern RB. A Methodology to evaluate dynamics and periodicity

of hormone secretion. J Biol Regul Homeost Agents 2011; 25:231-8.

20. Tong Y, Guo H, Brewer JM, Lee H, Lehman MN, Bittman EL. Expression of haPer1 and haBmal1 in Syrian hamsters: heterogeneity of transcripts and oscillations in the periphery. J Biol Rhythms 2004; 19:113-25.
21. Saifur Rohman M, Emoto N, Nonaka H, et al. Circadian clock genes directly regulate expression of the Na(+)/H(+) exchanger NHE3 in the kidney. Kidney Int. 2005; 67:1410-19.
22. Gvakharia BO, Kilgore JA, Bebas P, Giebultowicz JM. Temporal and spatial expression of the period gene in the reproductive system of the codling moth. J Biol Rhythms 2000; 15:4-12.
23. Cermakian N, Pando MP, Cardone L, Yujnovsky I, Morse D, Sassone-Corsi P. On the communication pathways between the central pacemaker and peripheral oscillators. Novartis Found Symp 2003; 253:126-36.
24. Okamura H. Clock genes in cell clocks: roles, actions, and mysteries. J Biol Rhythms 2004; 19:388-99.
25. Bebas P, Goodall CP, Majewska M, Neumann A, Giebultowicz JM, Chappell PE. Circadian clock and output genes are rhythmically expressed in extratesticular ducts and accessory organs of mice. FASEB J 2009; 23:523-33.
26. Della Ragione F, Comitato R, Angelini F, D'Esposito M, Cardone A. Molecular cloning and characterization of the clock gene period2 in the testis of lizard *Podarcis sicula* and its expression during seasonal reproductive cycle. Gene 2005; 363:105-12.
27. Alvarez JD, Chen D, Storer E, Sehgal A. Non-cyclic and developmental stage-specific expression of circadian clock proteins during murine spermatogenesis. Biol Reprod 2003; 69:81-91.
28. Alvarez JD, Hansen A, Ord T, et al. The circadian clock protein BMAL1 is necessary for fertility and proper testosterone production in mice. J Biol Rhythms 2008; 23:26-36.
29. Bittman EL, Doherty L, Huang L, Paroskie A. Period gene expression in mouse endocrine tissues. Am J Physiol 2003; 285:561-9.
30. Morse D, Cermakian N, Brancorsini S, Parvinen M, Sassone-Corsi P. No circadian rhythms in testis: Period1 expression is clock independent and developmentally regulated in the mouse. Mol Endocrinol 2003; 17:141-51.
31. Alvarez JD, Sehgal A. The thymus is similar to the testis in its pattern of circadian clock gene expression. J Biol Rhythms 2005; 20:111-21.
32. Gumz ML, Cheng KY, Lynch IJ, et al. Regulation of αENaC expression by the circadian clock protein Period 1 in mpkCCD(c14) cells. Biochim Biophys Acta 2010; 1799:622-9.

**ERRATA CORRIGE**
**Journal of Biological Regulators Vol. 26 No. 1.**

Page 131: Corticosteroids provoke acute endothelial injury – an ideal ground for thrombosis in multiple sclerosis
The correct list of authors and affiliations should read as follows:
I. SOSA[1], I. STRENJA LINIC[2], S. BAJEK[3], D. CUCULIC[1], Z. CRNCEVIC-ORLIC[4], A. GRUBESIC[5], O. CVIJANOVIC[3] and A. BOSNAR[1]
[1]Department of Forensic Medicine and Criminalistics, University of Rijeka School of Medicine, Rijeka, Croatia [2]Neurology Clinic, Rijeka University Hospital, Rijeka, Croatia; [3]Department of Anatomy, University of Rijeka Medical School, Rijeka, Croatia; [4]Department of internal medicine, University of Rijeka Medical School, Rijeka, Croatia; [5]Rijeka Emergency Medicine Institute, Rijeka, Croatia

Page 51: Tissue distribution and metabolism of guanosine in rats following intraperitoneal injection.
The correct list of authors and affiliations should read as follows:
P. GIULIANI[1], P. BALLERINI[2], R. CICCARELLI[2], S. BUCCELLA[2], S. ROMANO[1], I. D'ALIMONTE[2], A. POLI[3], A. BERAUDI[4], E. PEÑA[3], S. JIANG[5], M.P. RATHBONE[6], F. CACIAGLI[2] and P. DI IORIO[1]
[1]Department of Human Movement Sciences, University of Chieti-Pescara, Italy; [2]Department of Biomedical Sciences, University of Chieti-Pescara, Italy; [3]Department of Evolutionist and Experimental Biology, University of Bologna, Italy; [4]Istituto Ortopedico Rizzoli, Bologna, Italy; [5]Department of Surgery, McMaster University, Canada; [6]Department of Medicine, McMaster University, Canada